Australian Journal of Earth Sciences (2002) **49**, 3–162

Regolith geology of the Yilgarn Craton, Western Australia: implications for exploration

R. R. ANAND* AND M. PAINE

CRC for Landscape Environments and Mineral Exploration, CSIRO Exploration and Mining, 26 Dick Perry Avenue, Technology Park, Kensington, WA 6151, Australia.

CONTENTS

*Corresponding author: ravi.anand@csiro.au

This paper presents and reviews the processes responsible for the distribution and formation of regolith and associated landscapes of the Yilgarn Craton and highlights their implications for mineral exploration. It provides an analysis of regolith geology investigations that were conducted in many districts of contrasting contemporary geomorphic and climatic conditions.

The Yilgarn Craton is composed of Archaean rocks, predominantly granitoids, that are crossed by north-northwest-trending belts of greenstones. It has an arid to humid climate at present. The gently undulating landsurface forms a partial etchplain and the topography is largely related to bedrock lithologies and a complex history of valley development and aggradation. Deep weathering has affected most lithologies and geological provinces across the craton. The depth of the weathered mantle may be as much as 150 m, but it varies considerably and rock outcrop may occur in any part of the landscape. The main factors influencing extent of weathering are rock type, mineralisation and deformation. Palaeomagnetic dating of deeply weathered regolith profiles suggest that they formed throughout the Phanerozoic.

An idealised profile commonly comprises fresh bedrock, grading upwards into saprock and saprolite, commonly bleached towards the top, especially on felsic or sheared mafic rocks. This is overlain by a clay-rich and/or quartz-rich zone, a mottled zone and a ferruginous, bauxitic or siliceous upper zone. These horizons are formed by a combination of weathering and landscape processes. Landscape processes would have been continuous throughout the weathering period, with major environmental changes triggering particular erosional and depositional events. Thus, upper horizons, mottled zone, ferruginous duricrust and silcrete have developed in residuum, colluvium and alluvium of various ages.

Weathering is the result of interaction between the hydrosphere, biosphere and lithosphere. During weathering some of the components of primary minerals are leached and secondary minerals are formed as residua. The pathways by which these minerals form are varied and complex. Biota were present in the regolith and it is likely that they and their associated chemical reactions played a significant part in the weathering process, as well as inorganic chemical processes. The final product of weathering of all rocks is a mineral assemblage of least soluble minerals (kaolinite, hematite, goethite, maghemite, gibbsite, anatase and boehmite) and the most resistant primary minerals (quartz, zircon, chromite, muscovite and talc), although neoformation of several generations of hematite, goethite, kaolinite and gibbsite may occur. Poorly crystalline minerals are an important constituent in surface or near-surface materials. In addition, the more soluble minerals, including carbonates, sulfates and halides, occur in arid environments.

The principal effects of weathering on element distributions relates leaching and retention of a range of elements to mineral transformations in the principal regolith profile horizons. However, the chemical patterns may not be consistent from profile to profile even for similar lithologies due to differences in groundwater regimes and topography. Minor and trace elements may be displaced from their primary host mineral. Thereafter, they may occur camouflaged in the newly formed secondary minerals, as major components of accessory new minerals, or in resistant minerals.

In the present landscape, deeply weathered profiles may be preserved or partly eroded and buried beneath a variety of sediments. Three major regolith–landform terrains were identified and the extents of these regolith–landform terrains vary across the Yilgarn Craton. The first is dominated, in its upper part, by sands, ferruginous gravels and duricrust that commonly overlie mottled zones and saprolites. Ferruginous duricrust is developed in weathered Archaean bedrock and younger sediments that have been extremely weathered and/or indurated by Fe oxides. A second regolith–landform terrain comprises saprolite with fresh rock in places. These may have been exposed by erosion of a pre-existing weathered material, or may represent the most weathered form of the parent rock, which had never been capped with a ferruginous duricrust. A third terrain is of sediment-dominated areas with fluvial, aeolian and/or lacustrine deposits, commonly several metres thick, that may be underlain by ferruginous duricrust, saprolite or bedrock. Sediments are highly variable in genesis, provenance, composition and thickness and were either derived from erosion of fresh and weathered Archaean bedrocks or the reworking of older pre-existing sediments. They vary according to region, topography and age.

Numerous buried palaeochannels occupy the lower parts of the landscape and are up to several hundreds of metres wide and many kilometres long. Drainage incision along palaeovalleys on the weathered landsurface resulted in development of channels that were subsequently filled with sand, lignite and kaolinite- and smectite-rich sediments with lenses of ferruginous gravel. Palaeochannels are younger than the palaeodrainage system of broad, shallow valleys in which they occur and were probably incised during the final stages of rifting between Australia and Antarctica during the Early–Middle Tertiary. Sediments were deposited under fluvial, lacustrine, estuarine and marine environments during the Middle–Late Eocene. Further deep weathering occurred in both sediments and bedrock. Mixing occurred between the accumulating sediments and the underlying saprolite, possibly as a result of the formation of palaeosols. The collapse features and associated nodular and pisolitic materials in the underlying saprolite were probably formed during this period. Hematitic megamottles have developed in sediments and the upper part of some palaeochannel sediments contain ferruginous nodules and pisoliths. All this indicates post-depositional weathering within the sedimentary sequence. The similarities in the nature and characteristics of palaeochannel sediments in the southern and northern regions suggest that similar conditions prevailed not only during the deposition of sediments, but also during their

subsequent weathering. Parts of the palaeochannel sediments were eroded prior to deposition of Quaternary colluvium and alluvium. Colluvial, alluvial and aeolian sediments unconformably overlie palaeochannel sediments, ferruginous duricrust or saprolite. These sediments have been derived from increased erosion following the change to a more arid climate during the Late Miocene–Pliocene, in part a result of instability caused by a reduction in the vegetative cover.

A variety of soils occur in the three major regolith–landform terrains, the nature of which is controlled largely by the parent material and erosional and depositional processes. There is a significant aeolian component in many soils, commonly in the finer fractions. Where these soils occur over basic or ultramafic rocks, the Ti/Zr ratio and quartz contents can be used to identify any aeolian contribution.

Duricrusts occur in many different associations. In places, duricrusts of Fe, Si and Ca occur together in a single profile. Inland, ferruginous duricrust did not form on a simple, extensive, peneplained surface, but as a discontinuous cover on a broadly undulating plateau. It is developed on all rock types, but is particularly well developed on mafic and ultramafic bedrocks. By contrast, in the humid region of the Darling Range of the western Yilgarn, ferruginous duricrusts of various morphologies form an almost continuous sheet on all rock types. Transported hematite–maghemite-rich gravels at the base of the palaeochannel sequence are evidence that ferruginous duricrust existed prior to deposition of palaeochannel sediments in the Eocene. Ferruginous duricrusts have formed in residuum, in colluvium and in alluvium of various ages and are not necessarily associated with deep weathering. Thus, it is unwise to assign a single age to all ferruginous duricrusts or imply a single extensive surface of planation of continental extent. Residual duricrust (lateritic residuum) has developed from bedrock by essentially residual processes. In contrast, transported duricrusts (ferricretes) develop by impregnation and cementation of sediments by Fe oxides precipitated from groundwater, so that ferricretes have little direct relationship with the underlying rocks. In places they now form low hills because of relief inversion. Evidence of ferruginisation from the pre-Eocene through to at least Pliocene can be seen in the arid parts of the Yilgarn Craton. However, this process is currently operating in humid regions of the Darling Range, where goethite-rich ferricrete is forming on the edges of valley floors. Recent overprinting of ferruginous duricrusts has continued both inland and in the Darling Range. In the Darling Range, degradation of bauxitic ferruginous duricrust continues by dissolution of gibbsite and goethite. In the Kalgoorlie region, ferruginous duricrust is extensively modified by precipitation of carbonates to form calcretes.

Inland with increased aridity, soil and groundwater-related processes became dominated by gypsification, silicification and calcification. Silicification and calcification have affected a wide variety of regolith materials; calcification post-dates silicification. There are at least two widespread episodes of silicification. One episode is related to silcrete formation and the other with red-brown hardpan formation. It is possible that red-brown hardpans were once more extensive, but were subsequently replaced by carbonates to form calcretes. The red-brown hardpans are formed by partial replacement and cementation of the matrix and clasts by amorphous Si and aluminosilicates with minor goethite and hematite, accompanied by clay illuviation. Silicification of hardpan is associated with weathering within and outside soil profiles and appears to be still active. Pedogenic and groundwater calcretes are end members of a continuum that varies according to landscape setting and origin. Pedogenic calcretes occur in soils in association with a variety of rock types, but are more abundant in soils developed on greenstones. Their thickness and forms are largely controlled by topographic setting and the nature of the host material. Airborne accession is an important source of calcium for the formation of pedogenic calcretes, but weathering of bedrock, lateral transport by soil creep and soil solutions, and redistribution by biological processes are equally important. Groundwater calcretes are linear, tabular bodies occurring at or close to the surface and forming gentle mounds. They are Ca- and Mg-cemented valley deposits that are up to tens of metres thick.

Many of the regolith types resulting from a complex array of processes of weathering, erosion and deposition have a distinctive pattern, and could be potential sampling media. However, a combination of a long weathering history and a variable degree of erosion have resulted in a landscape of highly variable and complex regolith. Thus, assessment of the nature and origin of the regolith, weathering history, geomorphological processes and regolith–landform relationships are essential in determining the optimum geochemical sampling medium applicable in a particular terrain. A regolith–landform framework and models of regolith evolution of the Yilgarn Craton provide a basis for exploration models and exploration strategy that, with appropriate modification, may be extended into similar terrain elsewhere.

KEY WORDS: duricrusts, exploration, landscape evolution, mineralogy, petrology, regolith, regolith–landform mapping, sediments, weathering, Yilgarn Craton.

INTRODUCTION

GENERAL

Deeply weathered regolith* profiles are widespread in the inter-tropical belt, particularly on the continental landmasses between latitudes 35°N and 35°S. Similar features are observed at much higher latitudes, although these are not regionally extensive. The thickness of regolith varies from a few metres to over 150 m, depending on the age of the landsurface, tectonic activity, climatic history and the nature of the bedrock. In parts of Australia, Africa, India and South America the regolith is considered to have been forming continuously for over 100 million years in a variety of climates and, hence, is an expression of the cumulative effects of this long weathering history (Tardy & Roquin 1992). Deeply weathered regolith profiles, consisting of weathered rock with a cover of transported overburden of various ages, are widely distributed in the Yilgarn Craton. Differential erosion, deposition and chemical modifications have added to their complexity. As a result, the various landscapes of the Yilgarn Craton have a variety of regolith materials, including lag, soil, sediment, duricrust and saprolite. The characteristics of the regolith are commonly very different from those of the rocks (including ore deposits) from which they were derived, affecting geological, geophysical and geochemical mapping and exploration techniques and constraining their use. Nevertheless, despite the many negative aspects, the effects of weathering can be used to enhance exploration, for example, by exploiting secondary dispersion haloes, some of which give targets many times larger than the primary deposit.

Research on regolith geology and exploration practice in Australia over the past three decades has concentrated on developing exploration procedures appropriate for regolith-dominated terrains. Increasingly, emphasis is placed on identifying and mapping regolith materials, assessing their geochemical and geophysical properties and where possible utilising these in exploration. An objective for geochemistry has been to develop sampling strategies for a variety of regolith terrains. Emphasis has also been placed on procedures to detect components of the primary deposit that are widely dispersed in groundwater or, more speculatively, as gases and vapours. An objective for geology has been recognising weathered lithologies based on the preservation of primary rock fabrics, mineralogy and geochemistry. Limitations of geophysical techniques, posed by responses directly related to specific properties of the regolith and sedimentary cover, were initially investigated to separate them from responses related to primary mineralisation or other basement features. It was discovered that these responses can be used for mapping the regolith. Consequently, understanding regolith–landscape evolution is directly relevant to geological, geochemical and geophysical techniques employed to discover ore deposits concealed within and beneath the regolith.

Understanding regolith materials, their characteristics and 3-D distribution is vital to the interpretation of the evolution of the regolith and landscape. Since the pioneering work of Woolnough (1918, 1927) and Jutson (1914, 1934), numerous workers have studied aspects of the regolith geology of the Yilgarn Craton. Woodall (1993) and Smith (1996) noted that since 1980 much of the research relating to regolith has been driven by mineral exploration. Some studies have emphasised the weathering and mineralogy of profiles (Grubb 1966, 1971; Gilkes *et al.* 1973, 1986; Sadleir & Gilkes 1976; Smith 1977; Davy 1979; Gilkes & Suddhiprakarn 1979; Butt 1981; Butt & Nickel 1981; Elias *et al.* 1981; Thornber 1982; Anand & Gilkes 1984a, b, c, 1987a; Anand *et al.* 1985; Davy & El-Ansary 1986; Ball & Gilkes 1987; McCrea *et al.* 1990; Lawrance 1991, 1996; Singh & Gilkes 1991; Monti & Fazakerley 1996); others have placed the regolith in a wider context (Teakle 1938; Mabbutt 1961; Bettenay 1962; Mabbutt *et al.* 1963; Bettenay & Hingston 1964; Prider 1966; Mulcahy 1967; Bettenay & Mulcahy 1972; Finkl & Churchward 1973; Playford *et al.* 1975; Churchward 1977; Finkl & Fairbridge 1979; Butt 1981; Glassford 1987; Brimhall *et al.* 1988; Ollier *et al.* 1988; Wyrwoll & Glover 1988; Chan *et al.* 1992; Anand & Smith 1993; Kern & Commander 1993; Clarke 1994a, b; Pringle 1994; Glassford & Semeniuk 1995; Anand 1997, 2000; Jones & Lidbury 1998; Krcmarov *et al.* 2000; Wildman & Compston 2000). Many have focused on the distribution and genesis of soils in the southern part of the Yilgarn Craton (Mulcahy 1960, 1967, 1973; Bettenay 1962; Bettenay & Hingston 1964; Finkl & Churchward 1973); others concentrated on specific materials such as Wiluna Hardpan (Teakle 1936; Bettenay & Churchward 1974), silcretes (Butt 1985), calcretes (Sanders 1974; Butt *et al.* 1977; Carlisle 1978; Mann & Horwitz 1979; Anand *et al.* 1997), bauxites (Tomich 1964; Grubb 1966; Baker 1972; Geidens 1973; Anand *et al.* 1991a; Hickman *et al.* 1992) and ferruginous duricrusts (Anand *et al.* 1989a; Anand 1995, 1998; Davy & Gozzard 1995). Several organisations including the Australian Geological Survey Organisation (AGSO), the Commonwealth Scientific and Industrial Research Organisation (CSIRO), the Geological Survey of Western Australia (GSWA) and the Cooperative Research Centre for Landscape Evolution and Mineral Exploration (CRC LEME) have mapped regolith and landforms at regional to local scales (Mabbutt *et al.* 1963; Churchward 1977, 1983; Anand *et al.* 1991b; Craig & Anand 1993; Kojan & Faulkner 1994; Craig & Churchward 1995; Craig 1995a, b, c; Kojan *et al.* 1996).

Palaeogeographical reconstructions indicate that some of Western Australia has been exposed to subaerial conditions since the Neoproterozoic (Daniels 1975; Playford *et al.* 1975; Butt 1989). It has been suggested that the present landsurface of the Yilgarn Craton is only a few metres

*The regolith is the weathered and transported blanket of material covering fresh rock. It may be defined as the entire unconsolidated and secondarily recemented cover that overlies more coherent bedrock, which has been formed by weathering, erosion, transport and/or deposition of older material. It includes fractured and weathered basement rocks, saprolites, soils, organic accumulations, glacial deposits, colluvium, alluvium, evaporitic sediments and aeolian deposits.

below the essentially flat-lying, sub-Proterozoic unconformity, and the overall flatness of the landscape suggests that the plateau may represent a Proterozoic erosion surface (Daniels 1975; Fairbridge & Finkl 1979; Finkl & Fairbridge 1979). King (1950) considered it to be one of the finest examples of a stable region and indicated that it has been a great plain at least since the Late Palaeozoic, although planation of the Archaean basement may have been accomplished long before this time. The drainages form one of the oldest features on this craton, which was suggested to be of Mesozoic or even Palaeozoic age (Beard 1973; Johnstone *et al.* 1973; Van de Graaff *et al.* 1977). The oldest dated sediments in the palaeodrainages are Early to Middle Eocene marine sediments deposited during two major Eocene transgressions, but the incision of the valleys may be much earlier (Ollier 1988). Glaciation occurred during the Late Carboniferous and Early Permian (BMR Palaeogeographical Group 1990), as evidenced by the wide scatter of glacigene sediments in the northern Yilgarn (Hobson & Miles 1950; Gower 1976; Van de Graaff *et al.* 1977; Mabbutt 1980). Glaciation in the Permian is likely to have removed any evidence of pre-existing regolith (Ollier 1978; Fairbridge & Finkl 1979).

Long periods of tectonic stability since the Permian glaciation have allowed a variety of climatic conditions and landscape forces to interact and develop various types of regolith and landscape (Ollier 1978; Ollier *et al.* 1988; Clarke 1994a). Two climatic regimes have been considered of particular significance in the evolution of the regolith (Johnstone *et al.* 1973; Beard 1973; Butt 1981). These were first, seasonally humid, subtropical to tropical conditions during the Cretaceous to Middle Miocene, and second, drier climates since the Miocene that have continued to the present. The former gave rise to extensive, deep lateritic weathering (Jutson 1934). Recent arid to semiarid climates (Bowler 1976) and some minor uplift have resulted in a general lowering of water tables, slowing chemical weathering and erosional modification of the landsurface (Mabbutt 1980; Butt 1981). Inland, erosional modification has been considerable, reflecting widespread and frequent landscape instability, but in the absence of an effective drainage system the resulting superficial deposits have been retained in the landscape (Mulcahy 1967). During the arid phase, soil processes became dominated by gypsification, silicification and carbonate precipitation. In general, only past regimes of long duration, extreme climates or recent regimes have had a significant effect (Butt 1981). Thus, the mineralogy and geochemistry of the regolith are related to the lateritic profile developed under humid climates with high water tables and generally acidic conditions, whereas others are due to late events related to arid, alkaline environments with lower water tables. These later events have modified the lateritic regolith and reflect concentrations of minor components (Bettenay *et al.* 1976).

Recognition and interpretation of ancient landsurfaces have been a major theme of Australian landscape studies. The low relief of much of the continent has promoted interpretations of the large parts of the Australian landsurface as palaeoplains within the context of various genetic models, including peneplains and pediplains. Many early geomorphological studies favoured the Davisian idea (Davis 1899) that a vast area of the Australian landscape has evolved through cycles of landscape lowering and relief reduction, punctuated by episodes of landscape rejuvenation. A notable example is the concept of the 'Great Peneplain', thought to be a single, regionally extensive landsurface found across much of the continent (Andrews 1903; Woolnough 1927).

In the Yilgarn Craton, the interpretations of regional peneplains have been suggested by Jutson (1914, 1934) who referred to gently undulating uplands as portions of 'Old Plateau' that are capped by deeply weathered profiles, sand and 'laterite'. Jutson perceived a 'New Plateau' developing as a consequence of the erosion of the 'Old Plateau' (Figure 1). In this case, the New Plateau would be free of 'laterite'. In reconstructing former lateritised landscapes, Jutson and others (Woolnough 1918; Stephens 1946; Prescott & Pendleton 1952) assumed former continuity of the now isolated, present-day ferruginous duricrust-capped mesas. Mulcahy (1960) and Bettenay and Hingston (1964), mapping soils on deeply weathered tracts in southwest Australia, recognised relatively stable and relict tracts characterised by sand, ferruginous gravel and duricrust that contrasted with adjacent tracts that had extensive saprolite or fresh rock exposure, and proposed that the relatively stable tracts were a complex of erosional areas dominated by ferruginous gravels and/or duricrust and adjacent sandy depositional areas. Mabbutt *et al.* (1963) relied extensively on a 'New Plateau – Old Plateau' model to interpret landform evolution in the Wiluna–Meekatharra area.

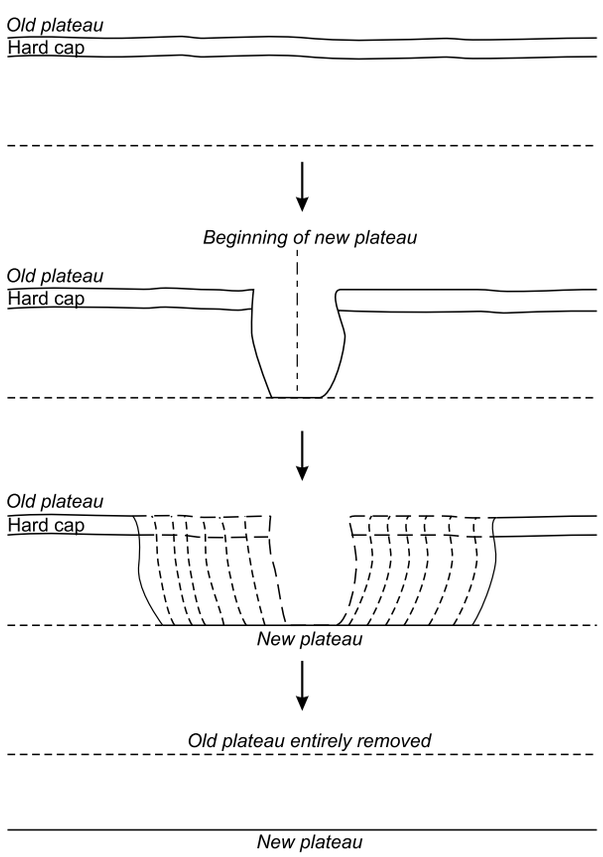

Figure 1 Jutson's diagrammatic explanation of the formation of the New Plateau from the Old Plateau (after Jutson 1934).

The etchplain concept (Wayland 1933) emphasises the formation of a deeply weathered mantle and its subsequent differential stripping. It was used by Thomas (1965) to classify weathered terrain in Africa and was applied to the southwestern region of Western Australia by Finkl and Churchward (1973). At the heart of this concept is the presumption that a continuous weathering profile covered the entire area now classed as etchplain. Differential degrees of stripping of the deeply weathered mantle are recognised by the use of such terms as incipient, partial, semi-stripped and stripped plains (Figure 2) (Finkl 1979). Stripping of regolith materials, as shown in Figure 2, progresses towards the interior in a stepped fashion from the north and south.

More recently, Ollier *et al.* (1988) suggested a very different interpretation of the evolution of the Yilgarn landscape. According to these authors, the landscape displays a recurring sequence of Old above New above Old Plateau and is essentially saw-toothed. The breakaways are not necessarily the edges of the plateau. They concluded that weathered material has been repeatedly deposited in valleys, after which the relief became inverted so that relics of alluvium occur as a ferruginous duricrust capping (Figure 3). A similar view on landscape evolution of the Mt Gibson and Darlot districts in the Yilgarn Craton has been presented by Jones and Lidbury (1998) and Krcmarov *et al.* (2000). Thus, these authors do not accept the concept of a former extensive lateritised duricrust-capped landsurface, and rather suggest that these deposits are relict valley-flanking sediments.

Duricrusts are some of the most characteristic and important features of the Yilgarn Craton and of similar

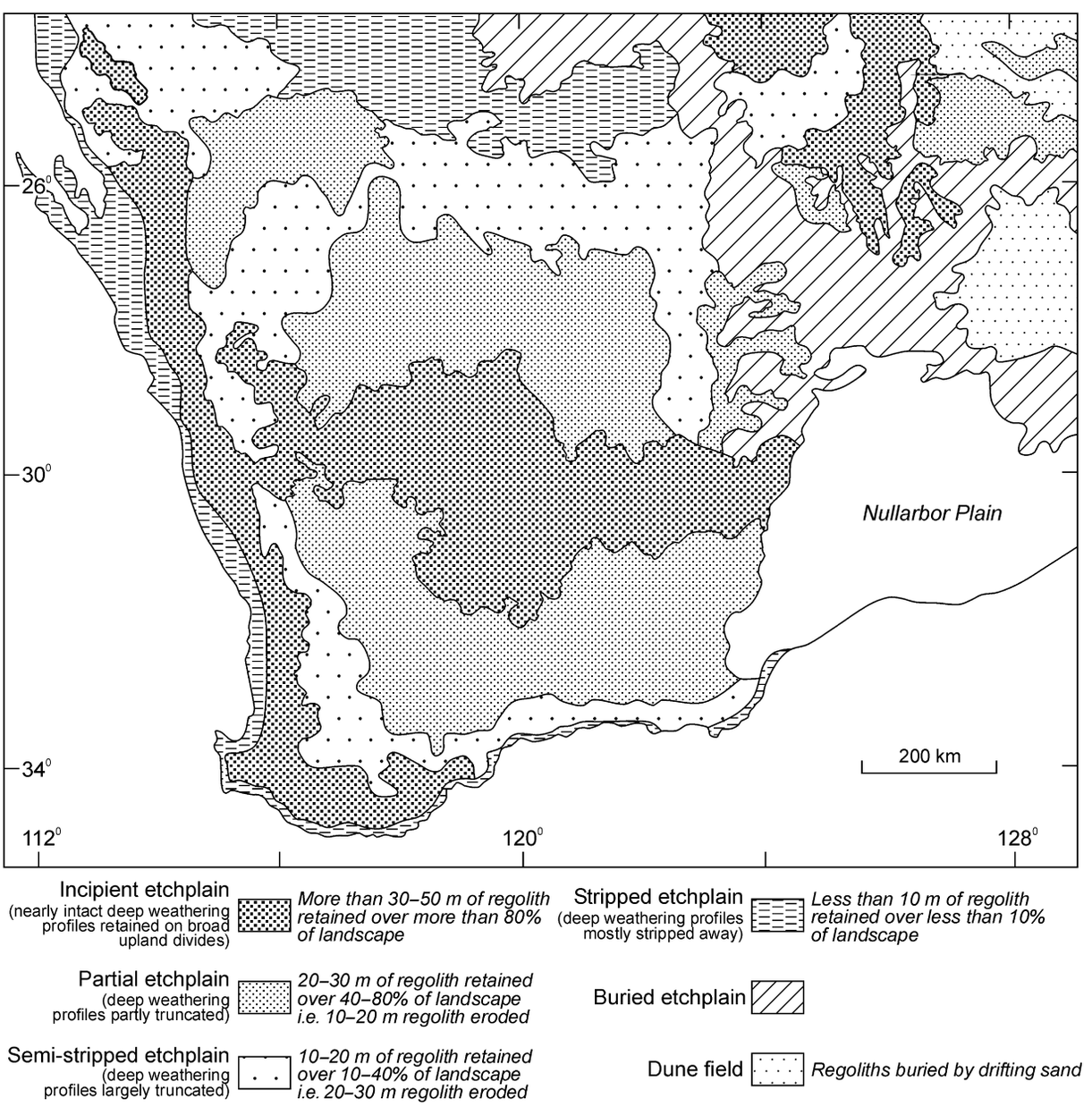

Figure 2 Distribution of etched surfaces in southwestern Australia (after Finkl 1979). Reproduced from Australian Geographical Studies, with permission from Blackwell Science Ltd.

deeply weathered terrains elsewhere: these include ferruginous duricrust, silcrete and calcrete. These deposits have at times been used as climatic indicators and as stratigraphic markers. Duricrusts may be residuum, colluvium, ferruginised, silicified or calcified sediment, or a mixture of these. A controversy exists over the origin of ferruginous duricrusts and, in particular, whether they have formed *in situ* from the weathering of underlying bedrocks or developed in sediments (Walther 1915; Jutson 1934; McFarlane 1976; Milnes *et al.* 1985; Nahon 1986; Bourman *et al.* 1987; Bardossy & Aleva 1990; Ollier & Galloway 1990; McFarlane 1991; Nahon & Tardy 1992; Bourman 1993; Anand 1995, 1998; Taylor & Howard 1999). On the Yilgarn Craton, ferruginous duricrusts are considered to have formed by the *in situ* weathering of bedrock (Walther 1915; Jutson 1934; Sadleir & Gilkes 1976; Davy 1979; Davy & El-Ansary 1986; Davy *et al.* 1988; Anand *et al.* 1991a; Hickman *et al.* 1992; Pringle 1994; Anand 1998), ferruginisation of fluvial (Grubb 1971; Ollier *et al.* 1988; Anand 1995, 1998; Davy & Gozzard 1995; Jones & Lidbury 1998; Krcmarov *et al.* 2000) or aeolian (Brimhall *et al.* 1988; Glassford & Semeniuk 1995) sediments. The distinction between the relative and absolute enrichment of Fe was stressed in the major pioneering works of D'Hoore (1954), Prescott and Pendleton (1952), Alexander and Cady (1962) and Maignien (1966). Relative accumulations owed their concentrations to removal of more mobile components. Absolute accumulations owed their concentrations to lateral transfer by convergent flow of groundwaters into valley floors and depressions. Recently, there have been more discussions on this topic (McFarlane 1976; Goudie 1983; Nahon 1986; Bardossy & Aleva 1990; Ollier & Galloway 1990; Bourman 1993; Thomas 1994; Eggleton & Taylor 1998; Jones & Lidbury 1998; Krcmarov *et al.* 2000). It is widely considered that relative enrichment predominates on interfluves with absolute accumulation more likely to occur in low catenary zones near discharge areas. However, agreement is not universal and some workers (Ollier & Galloway 1990; Ollier & Pain 1996; Jones & Lidbury 1998; Krcmarov *et al.* 2000) argued that, even on interfluves, absolute accumulation is the primary mode of duricrust formation. These workers follow the view that ferruginous duricrust formed in ancient alluvial channel systems and suggest that many duricrusts were formed in transported materials in low sites, but now occupy high ground by virtue of relief inversion.

Arguments about silcrete formation are similar to those concerning ferruginous duricrust and depend on the provenance of the silica and the conditions under which it has been mobilised. Extreme positions have been taken on both issues. Long-distance transport of silica from the humid environments of the eastern highlands of Australia into the interior basins was advocated by Stephens (1971), although Wopfner 1978) and Butt (1985) have proposed that silica is drawn mainly from the kaolinised profiles and toposequences within which it is found. Some authors assumed that silcrete indicates arid or semiarid conditions. Although some silcrete may form in this way, there is increasing evidence that it can also form in humid climates (Wopfner 1978; Taylor & Ruxton 1987).

The main objectives of this paper are to: (i) summarise the distribution and characteristics of regolith materials; (ii) present models of their evolution; and (iii) examine implications for exploration. The sites discussed or mentioned in the text are shown in Figure 4. All the figured thin-sections and samples are kept at CSIRO, Exploration and Mining, in Kensington, Western Australia.

BEDROCK GEOLOGY

The Yilgarn Craton comprises an area of approximately 657 000 km^2 and forms one of the largest intact segments of Archaean crust on Earth. The craton is situated in the central part of the Precambrian Western Shield of Australia, which comprises Archaean granitoids and greenstones of the Yilgarn and Pilbara Cratons, metamorphosed Archaean and Proterozoic granitoids, gneisses and volcanic rocks of the Paterson and Gascoyne Provinces and the Albany–Fraser Province. The shield also includes Proterozoic sedimentary rocks of the Nabberu, Bangemall and Hamersley Basins (Figure 5a on Plate 1).

Much of the Yilgarn Craton is a granite–greenstone terrain characterised by arcuate belts of metamorphosed sedimentary and volcanic rocks (greenstone belts) that lie between large areas of granitoid (Figure 4). The bulk of the craton is thought to have formed between 3000 Ma and 2600 Ma, with some gneissic terrains exceeding 3000 Ma in age (Myers 1993). The rocks and structures that comprise the craton are superficially similar over large parts of the craton and in detail can be subdivided into various terranes on the basis of pre-metamorphic lithological associations, geochronology and styles of tectonism and metamorphism (Gee *et al.* 1981; Myers 1993). These terranes, which include the Barlee, Gindalbie, Kalgoorlie, Kurnalpi, Laverton, Murchison, Narryer, Pinjin, Yellowdine and Southwestern composite terranes are thought to have undergone intense tectonic, volcanic, plutonic and metamorphic activity between 2780 Ma and 2630 Ma. This is interpreted as a period of major plate-tectonic activity that swept together and amalgamated a number of diverse crustal fragments, including volcanic arcs, backarc basins and microcontinents, to form the Yilgarn Craton (Myers 1993).

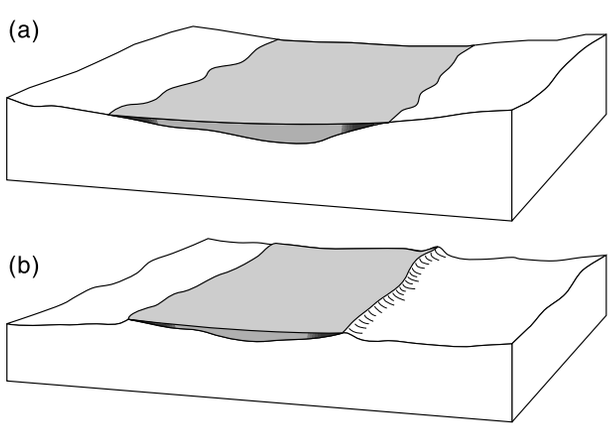

Figure 3 Ollier's model of landscape evolution (after Ollier *et al.* 1988 figure 13). (a) An old valley is eroded and the floor and lower slopes of the valley are partly covered with alluvium and colluvium, which are then cemented to form ferricrete. Ferricrete is especially prevalent on footslopes. (b) Later erosion attacks neighbouring weathered rock and the resistant ferricrete comes to occupy the edge of plateau. Reproduced with permission from Geoscience Australia.

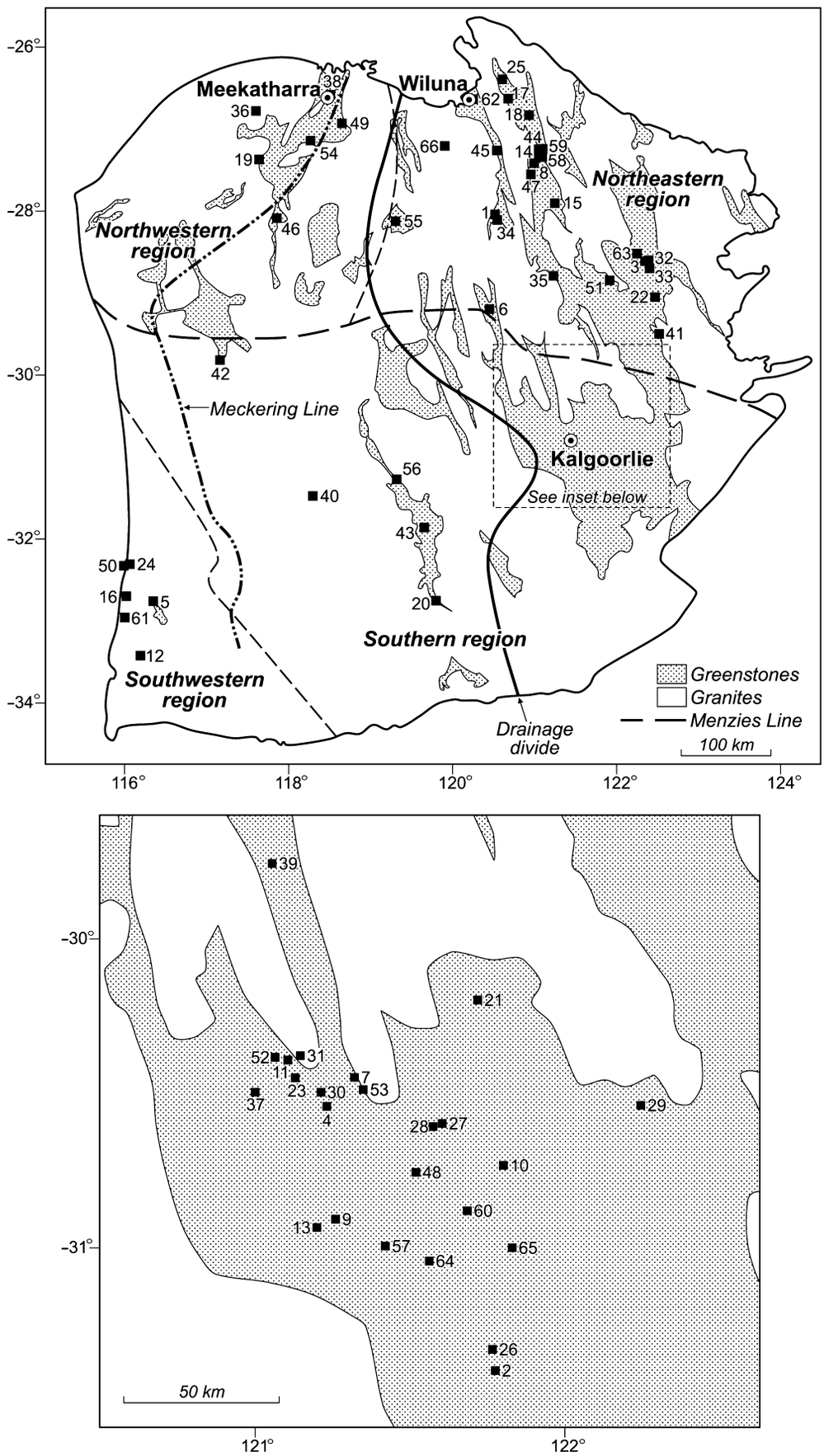

1 Agnew
2 Argo – Apollo
3 Beasley Creek
4 Black Flag
5 Boddington
6 Bottle Creek
7 Broad Arrow
8 Bronzewing
9 Brown Lake
10 Bulong
11 Cawse
12 Collie
13 Coolgardie
14 Cyclonic
15 Darlot
16 Del Park
17 Elliot, Gourdis
18 Empire
19 Fender
20 Forrestania
21 Gindalbie
22 Golden Delicious
23 Grants Patch
24 Jarrahdale
25 Jundee
26 Kambalda
27 Kanowna
28 Kanowna Belle
29 Kurnalpi
30 Lady Bountiful Extended
31 Lady Evelyn
32 Lancefield South
33 Laverton
34 Lawlers
35 Leonora
36 Madoonga
37 Matt Dam
38 Meekatharra
39 Menzies
40 Merredin
41 Mt Celia
42 Mt Gibson
43 Mt Hope
44 Mt Joel
45 Mt Keith
46 Mt Magnet
47 Mt McClure
48 Mt Percy
49 Mt Yagahong
50 Mundijong South
51 Murrin Murrin
52 Ora Banda
53 Paddington
54 Reedy
55 Sandstone
56 Southern Cross
57 Steinway
58 Sundowner
59 Ularri Hill
60 Waterfall
61 Willowdale
62 Wiluna
63 Windarra
64 Wollubar
65 Wombola
66 Yeelirrie

Figure 4 Location of the sites, regional subdivisions and features referred to in the text. The Menzies Line (after Butt *et al.* 1977), Meckering Line (after Mulcahy 1960) and Drainage Divide (after Morgan 1993) are also shown.

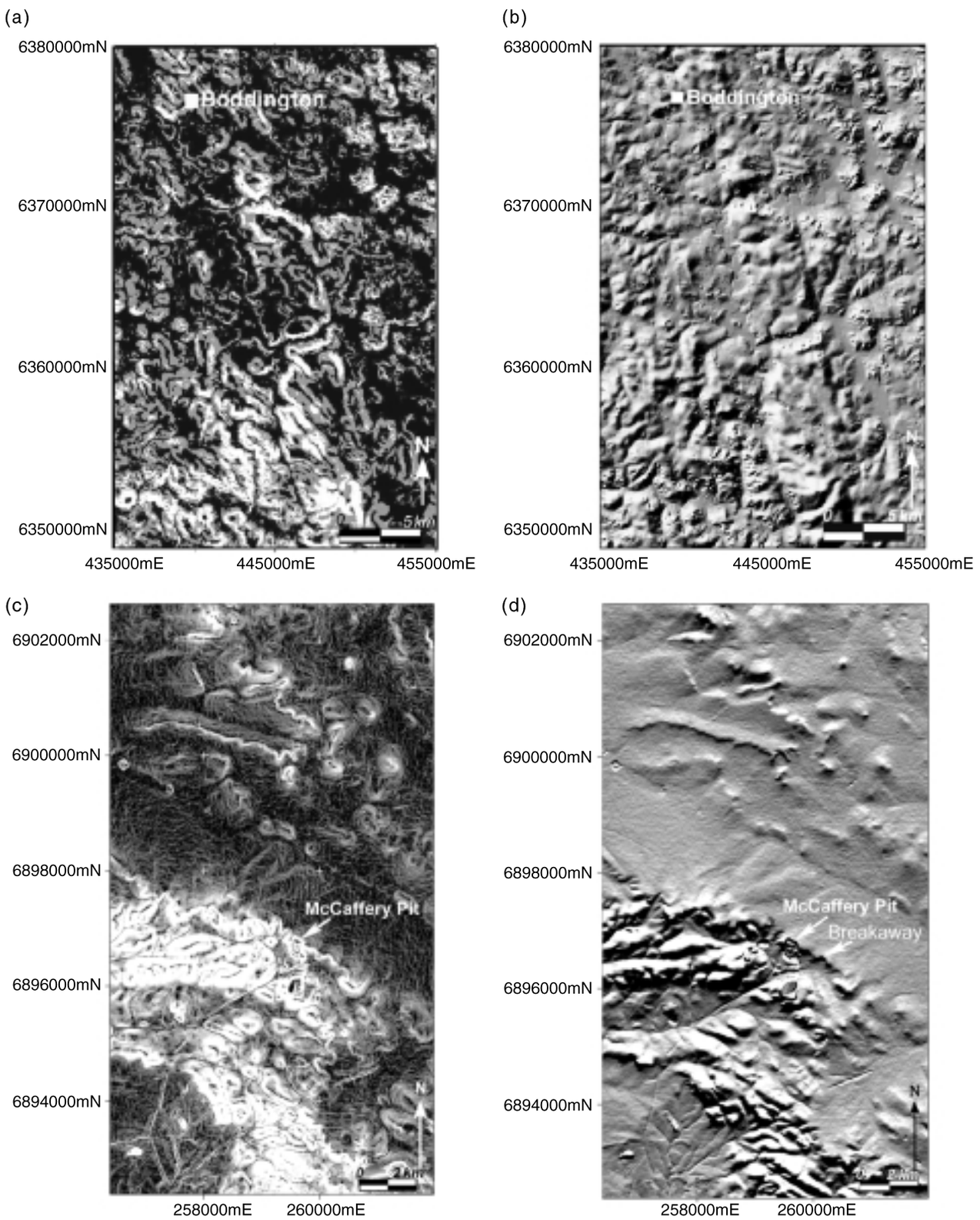

Figure 6 Geomorphic features of the Darling Range and Lawlers. (a) Intensity of slope about the Boddington district with slopes ranging from 0° to 35°. (b) Shaded digital elevation model about the Boddington district (data courtesy of the Australian Surveying and Land Information Group, Canberra, Australia. Crown Copyright ©. All rights reserved). (c) Intensity of slope about the Lawlers district with slopes ranging from 0° to 20°. (d) Shaded digital elevation model about the Lawlers district (source Tapley 1998).

The Southwestern composite terrane is characterised by a relatively high-grade (granulite to upper amphibolite facies) granite–greenstone complex (Myers 1993) and numerous dolerite dykes have intruded the predominantly granitic rocks of the area. The dykes are vertical or subvertical and range in thickness from less than 1 m to over 200 m, averaging approximately 10 m. The most significant greenstone sequence in the area occurs at Mt Saddleback and is referred to as the Saddleback Group (Wilde 1976). The Saddleback Group extends for 43 km north-northwest from near Boddington and is between 5 km and 12 km wide.

The terranes that occupy the remainder of the craton comprise greenstone belts (approximately 30%) within extensive granitoids (approximately 70%) that are typically metamorphosed to greenschist facies. The greenstones are characterised by ultramafic and mafic volcanic rocks formed as extensive submarine lava plains, and volcanic centres of felsic and mafic volcanic rocks developed more locally. Sedimentary rocks are mainly derived from felsic volcanics and banded iron-formation and form a prominent greenstone component. They appear to have formed in broad basins during tectonic and volcanic quiescence. Layered gabbroic sills are another major greenstone component. Widespread granite intrusion throughout the craton is thought to have occurred between 2700 Ma and 2600 Ma. The granites were emplaced as sheets into the pre-existing greenstone sequences (Myers 1993).

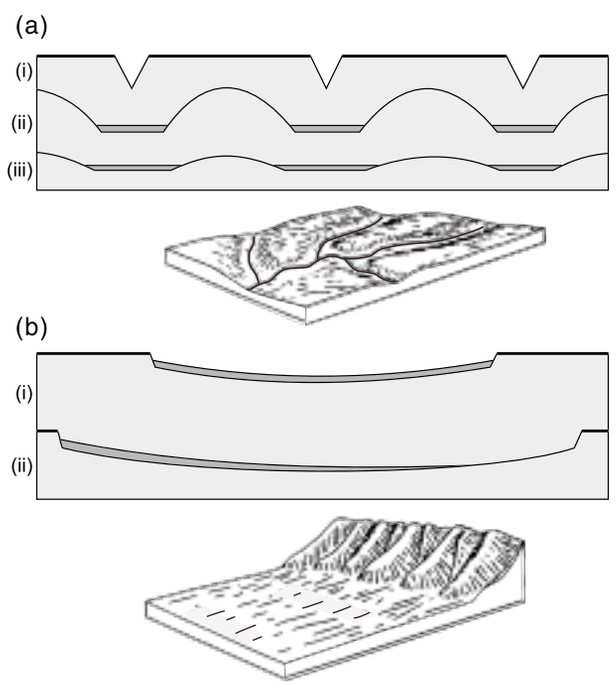

Figure 7 Peneplain and pediplain models of landscape evolution. (a) Peneplains are formed from the downwearing of a landsurface: (i) early stages in the dissection of an uplifted old landsurface (heavy horizontal line); (ii) advanced stages in development; the old landsurface has been removed and rounded hillslopes formed between broad, mature river valleys; and (iii) late stage, with initiation of a peneplain, which in time is still further reduced. (b) Pediplains are formed by scarp retreat: (i) formation of scarps and pediments with a thin cover of detritus; (ii) pediplain formed as scarps retreat further; in places, detrital cover is removed. Note: the total amount of vertical erosion is minimal against the formation of peneplain (modified after Thornbury 1954; Hills 1975).

GEOMORPHOLOGY

The Yilgarn Craton is a landscape distinct from the adjacent sedimentary basins and falls into the Western Plateau Division of Jennings and Mabbutt (1977). Dominant landforms in the Yilgarn Craton are sandplains, plateaux, breakaways, colluvial and alluvial plains, north-northwest-striking ridges of mainly metamorphic rocks (greenstones), granitic hills and rises with extensive debris fans, large salt lakes and dunes along broad valleys. The craton has a gently undulating, low relief, except along its western margin, where an escarpment (the Darling Range) separates it from the Coastal Plain. The position of the scarp closely corresponds to that of the Darling Fault, which separates resistant Precambrian rocks to the east from more easily eroded Phanerozoic sediments to the west. The elevation of the craton ranges from 0 m to 650 m above mean sea-level (Figure 5b on Plate 1) and is partitioned by a meridional continental divide. Large areas of the craton are underlain by granitic rocks and although there are many prominent granitic domes, inselbergs or monadnocks, in general, these areas are small and have low relative relief. Subordinate in the area to the granitic terrains are north-northwest-orientated linear belts of metamorphic rocks, parts of which form rocky ranges. The rocky ranges have the greatest positive relief on the craton (Jutson 1914). Extensive regolith-dominated plains separate the ranges.

In the southwest, the Darling Range is a broadly undulating plateau (e.g. Boddington district: Figure 6a, b) that has crests 250–400 m above mean sea-level and swampy valley floors set approximately 50–100 m below the crests. Several bedrock hills reach approximately 400 m and these are restricted to the central part of the area within a distance of 50 km from the Darling Scarp. Dissection of the plateau has created three distinct subdivisions: uplands, deeply incised valleys and wide valleys with intervening low hills. Inland, the landscape is gently undulating (e.g. Lawlers district: Figure 6c, d), interspersed with sheet flood plains, tributary to major regional valleys, which are in part occupied by extensive playas. Numerous playas, many large (up to several kilometres wide and tens of kilometres long), form chains generally trending southeast and occupy large parts of the drainages. The low relief of this landscape is broken by low breakaways, dunes, granite tors and greenstone strike ridges. Elevations are 300–600 m above mean sea-level, with most of the terrain being 350–550 m, and tend to decrease southwards.

The terminology used to describe landscapes in southwestern Australia have been summarised by Finkl and Churchward (1973), and it is from their work that the following summary has been derived. Two major concepts of peneplanation and pediplanation have frequently been invoked to describe landscapes in this region. Peneplains are formed from the downwearing of a landscape, whereas pediplains are formed by scarp retreat (Figure 7). Gregory (1861) and Brown (1873) were the first to comment on

the 'undulating tableland' or 'plateau' in southwestern Australia. Suess (1906) described the upland as the 'Great Plateau' and the escarpment flanking it to the west as the 'Darling Scarp'. David (1911) referred to the southwestern part of the Great Plateau of Western Australia as the 'Darling Range Peneplain'. Jutson (1914, 1934) called it both the Darling Peneplain and the Darling Plateau: the interior of the Great Plateau was referred to as the 'Old Plateau' and was considered to be part of the 'Great Peneplain of Western Australia'. By contrast, King (1950) suggested that the Great Plateau was part of 'The Australian Pediplain' and that it belonged to the 'Australian Cycle'.

Woolnough (1918) referred to a major erosional feature of the western part of the Great Plateau as a 'partial peneplain' having been 'carved out of the laterite covered plateau'. He also referred to this feature as the 'Mature Valley Level' and 'Meckering Level'; King (1950) termed it a 'partial bevel'. Jutson (1934) delineated the extent of the rejuvenation of the drainage due to uplift, which Mulcahy (1967) called the 'Meckering Line' (Figure 4). Erosional modification of inland parts of the 'Great Plateau' has resulted in the development of a younger surface (Finkl & Churchward 1973), which Jutson (1934) termed the 'New Plateau', generally separated from the Old Plateau above by prominent breakaways. In addition to these broad-scale terms, the landscapes of the Yilgarn Craton have been considered in terms of landscape zones (Mulcahy 1961), physiographic divisions (Jutson 1934), valley forms (Bettenay & Mulcahy 1972) and erosional–depositional surfaces (Mulcahy & Hingston 1961). Butt *et al.* (1977) recognised differences in the environmental and regolith characteristics between the north and south of semiarid regions of the Yilgarn Craton. These differences became the basis of the so-called 'Menzies Line' (Figure 4), an irregular east–west-trending transitional zone across the Yilgarn Craton through the town of Menzies. The boundary, which is gradational, has been informally recognised by numerous workers for many years. It is essentially that shown by Bettenay *et al.* (1976) defining landform zones 3 and 4 of southwestern Australia.

A land-system mapping approach was developed by Christian and Stewart (1953) and has been widely used to describe arid terrains (Mabbutt *et al.* 1963). The land system is essentially an area or group of areas throughout which a recurring pattern of topography, soils and vegetation can be recognised. A typical example is shown in Figure 8.

DRAINAGE

The drainage of the Yilgarn Craton is inherited from an ancient river system (Gregory 1914) radiating from the broad drainage divide that approximately bisects the craton (Figure 9). In southwestern Western Australia, the drainage follows two main directions, west-southwest and north-northeast, which are the predominant lineament patterns in the southwest part of the Western Shield of the Yilgarn Craton (Salama & Hawkes 1993). A well-preserved palaeodrainage (Van de Graaff *et al.* 1977) is present in the Yilgarn Craton and forms the extensive palaeodrainage system of the Australian continent (Morgan 1993). Ollier *et al.* (1988) and Clarke (1994b) proposed that incision of an extensive palaeodrainage system into weathered Archaean bedrock prior to the initial breakup of Gondwana in the Jurassic, resulting in the formation of the Cowan palaeodrainage near Norseman and further to the north, the Lefroy palaeodrainage. Relative uplift of the Yilgarn Craton occurred along the Jarrahwood Axis (Cope 1975) and this event was responsible for drainage reversal and formation of the coastward-sloping Ravensthorpe Ramp (Clarke 1994b). Consequently, the Cowan palaeodrainage

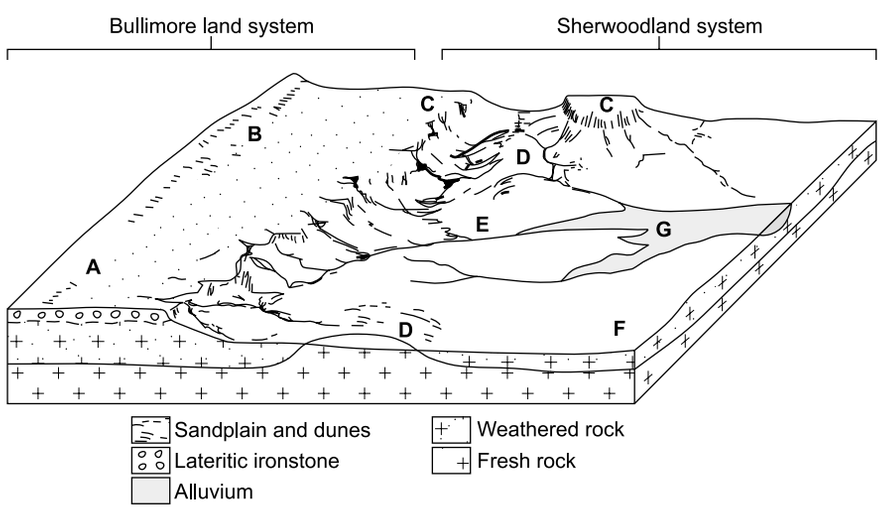

Landform
A Sandplain
B Dunes (mostly stable) and swales
C Partly stripped lateritie
D Low rock hills to 10 m
E Hill footslopes
F Plains
G Drainages

Surficial materials
Red clayey sands on colluvium
Red sands
Ironstones and saprolite
Lithosols
Lithosols and colluvium
Stony soils on weathered rock
Red earths on alluvium; valley calcrete

Figure 8 Examples of land systems and landforms from a partly stripped etchplain in the Wiluna–Meekatharra area (after Mabbutt *et al.* 1963; Butt & Zeegers 1992).

channel then flowed south towards the Bremer Basin, rather than north and east into the Eucla Basin. However, the pre-Jurassic palaeodrainage age and subsequent drainage reversal is disputed by Morgan (1993) who proposed that the existing palaeodrainages were incised during an Early Eocene erosional event. Downwarping of the southeastern craton due to separation from Antarctica developed short, deeply incised southward-directed rivers. Grimley (1995) argued that this model fails to account for the acute, north-flowing drainage pattern or the width of Lake Cowan palaeodrainage sediments at Esperance.

With the trend to aridity since the Miocene, the drainages have become clogged with sediments and most have no surface flow except after periods of exceptional rainfall. Inland, many of the drainages are essentially massive and represented by chains of salt lakes. These lakes become inundated during occasional, intense rainfall and in rare cyclonic events. For example, as a result of rainfall from Cyclone Bobby in 1995, Lake Raeside overflowed and discharged eventually onto the Nullarbor Plain (Allen 1996). Rejuvenated streams, with connected flow, occur in the wetter, near-coastal regions; some of the large rivers, such as the Avon, also tap the west-draining salt-lake systems. The upstream limit of rejuvenation is a subdued nick point, termed the Meckering Line (Mulcahy 1967).

CLIMATE

The Yilgarn Craton has a semiarid to Mediterranean climate with wide ranges in annual rainfall from 150 mm to 1400 mm (Figure 5c on Plate 1) and an annual evaporation potential of 2500–4100 mm (Bureau of Meteorology 1990). Rainfall may vary widely between different years and droughts and floods are features of the semiarid region. From the southwest to the northeast margin, there is a generally consistent and marked decrease in rainfall (Figure 5c on Plate 1) and an increase in temperature and potential evaporation. The reliability of the rainfall decreases progressively to the north, where summer

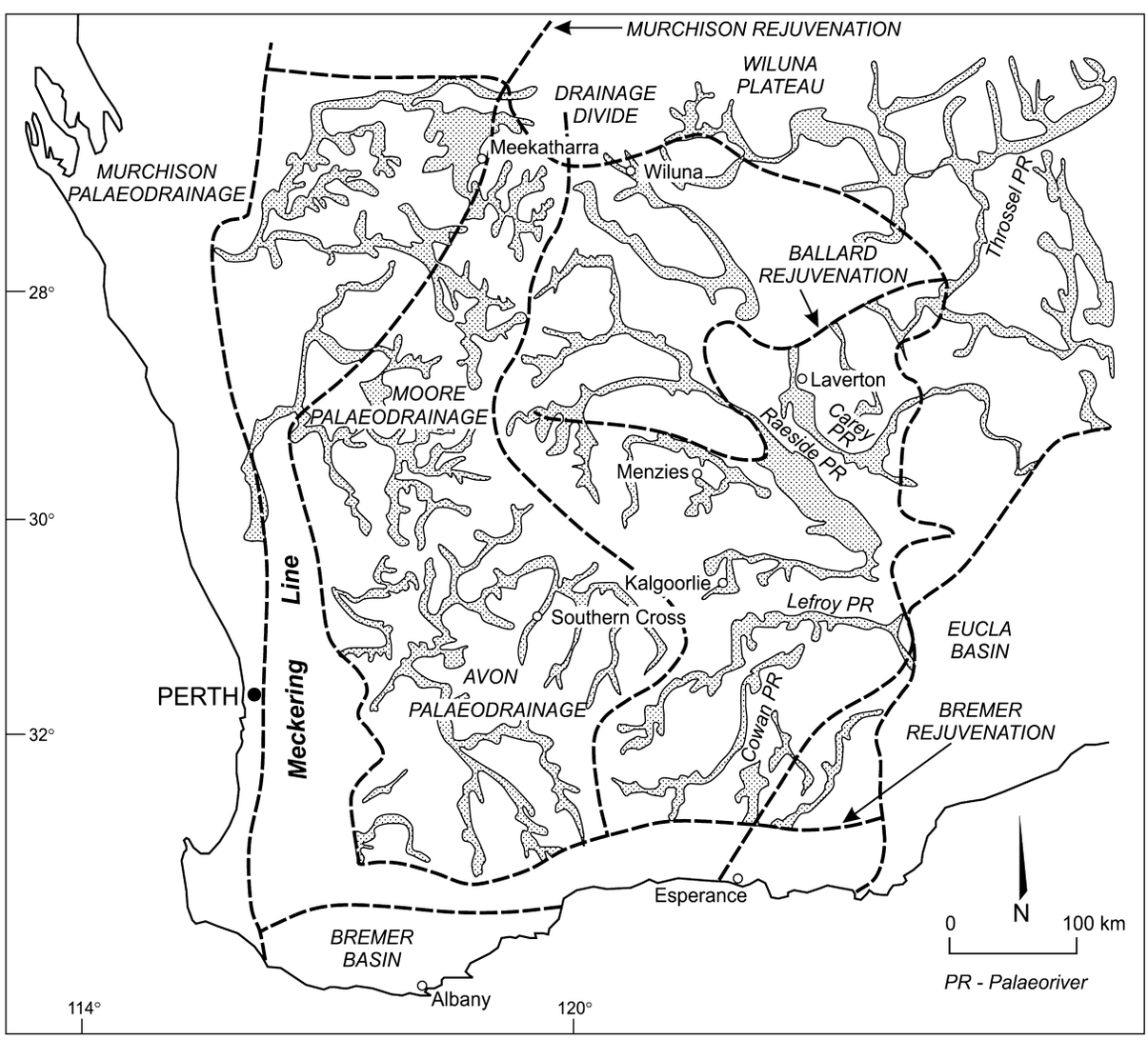

Figure 9 Palaeorivers and associated geomorphic features of the Yilgarn Craton (modified after Morgan 1993, pp. 637–656). Reproduced from Sedimentary Geology with permission from Elsevier Science.

cyclonic rains contribute significantly to the major rainfall and these storms can move south, causing irregular heavy falls.

VEGETATION

The flora of the Yilgarn Craton is quite diverse and shows marked regional changes based largely on climate, with local variations of geology, soils, topography and drainage affecting individual communities (Aplin 1975). The Darling Range in the high-rainfall area has open eucalypt forests of jarrah (*Eucalyptus marginata*) and marri (*Eucalyptus calophylla*). Paperbarks (*Melaleuca* spp.) occur in swamps. The Avon district of woodlands and savannah covers much of the wheatbelt and is characterised by eucalyptus such as wandoo (*Eucalyptus wandoo*), mallet (*Eucalyptus astringens*), York gum (*Eucalyptus loxophleba*), and yate (*Eucalyptus cornuta*). Farther east, in the Kalgoorlie region, there are open forests of salmon gum (*Eucalyptus salmonophloia*) and gimlet gum (*Eucalyptus salubris*) and shrublands of mulga (*Acacia* spp.), *Grevillea* spp., mallee eucalyptus (*Eucalyptus pumila*) and *Casuarina* spp. Spinifex grasses (*Triodia* spp.) are common on sandplains. Finally, the northeast region consists of arid shrublands dominated by mulga. Eucalypts, such as the river red gum (*Eucalyptus camaldulensis*) are common only along watercourses.

HYDROGEOLOGY

The depth to which groundwater occurs is controlled by numerous factors including topography, elevation, geology and the depth of the weathering front. Most of the groundwater occurs between 30 m and 60 m below the surface on divides and upper slopes (Allen 1994), but discharges at the surface in playas. Groundwater quality and quantity are related primarily to the geomorphic and climatic regimes and to the geochemical interactions with the surrounding rock. It varies widely in salinity with the lowest salinity generally occurring beneath catchment divides and the highest along the palaeodrainages. Where precipitation is confined to the summer months, the groundwater is less saline than comparable regions with winter rain. Thus, the occurrence of fresh groundwater increases northward in response to more effective rainfall recharge.

WEATHERING

LATERITIC PROFILE TERMINOLOGY

Introduction

The study of regolith materials spans many disciplines of the earth sciences. Thus, many of the terms are used in different senses by the different disciplines. Therefore, some terms used herein are defined from the perspective of regolith geology and their definitions may be found in Eggleton (2001).

The terminology of an idealised lateritic profile is summarised in Figure 10. A 'typical' deep-weathering lateritic profile (Figure 10) described by Anand and Butt (1988) comprises fresh bedrock grading upwards into saprock, saprolite, a clay-rich (plasmic) or sand-rich (arenose) zone, a mottled zone and a lateritic residuum. The terminology used by some other workers (Walther 1915; Millot 1964; Ollier & Galloway 1990; Nahon & Tardy 1992; Aleva 1994) is also shown in Figure 10, to demonstrate the equivalence between different profile terminology adopted in this paper and related literature. Nahon and Tardy (1992) have used the terms coarse and fine saprolite (lithomarge) as synonymous with saprock and saprolite, respectively, whereas others (Millot 1964; Ollier & Galloway 1990; Aleva 1994) have made no distinction (Figure 10). The scheme of Ollier and Galloway (1990) included the term 'pallid zone' to describe the pale part of saprolite. Saprolite was long called the 'pallid zone' by some earlier workers (MacLaren 1906; Walther 1915; Prescott & Pendleton 1952), because it has a light-coloured horizon, decolourised by loss of iron, and is generally located below the mottled zone. Use of the adjective 'pallid' indicates this zone has lost iron (Bourman 1993), yet there is no evidence that iron has been removed (McFarlane 1991). Pallid zone should, perhaps, be used as an informal term, but should not be used synonymously for saprolites because the latter may exhibit a wide variety of colours (Anand & Butt 1988). Although saprolites are commonly white over felsic rocks, they are not over some felsic and most mafic and ultramafic rocks; conversely, not all pale or white horizons are saprolites. The schemes of Nahon and Tardy (1992) also replace the pallid zone with fine saprolite and these authors have made a similar call to abandon the term pallid zone.

The term 'laterite' was originally applied to Fe-rich material in Kerala (India) by Buchanan (1807). It was hard enough to cut into building blocks, which hardened on exposure. However, the laterites of Kerala would now be regarded as vermiform mottled zone. The crust is a separate entity largely used in Kerala for dry-stone walling. The mottled material is soft enough to be cut by an axe. The extensive literature on 'laterite', since Buchanan, has produced a range of terms describing ferruginous duricrust. Ollier and Rajaguru (1991) observed that 'laterite' is used to refer to both the indurated, mottled saprolite, as well as to concretionary material and, in Africa, to nodular and pisolitic material. In some African dialects, surficial materials that are generally red are called (in translation) 'brick earth' (Maignien 1966) and the term 'laterite' refers to blocks used in construction (Prescott & Pendleton 1952).

McFarlane (1976) adopted the definition of Sivarajasingham *et al.* (1962): 'laterites are highly weathered material, depleted in alkalis and alkaline earths, composed principally of secondary oxides and oxyhydroxides of iron (goethite, hematite, maghemite) and hydroxides of aluminium (gibbsite)'. These oxides may incorporate other minerals including clays and other secondary minerals (kaolinite, anatase), resistant primary minerals (quartz, zircon) and weatherable primary minerals (ilmenite, muscovite). According to Schellmann (1983), laterites are products of intense subaerial rock weathering whose Fe and/or Al content is higher and Si content is lower than in merely kaolinised parent rocks: they consist of goethite, hematite, gibbsite, kaolinite and quartz. It is clear that Schellmann's definition embraces anything more weathered than saprolite. Aleva (1994) included only duricrust above mottled zone as 'laterite', whereas Millot (1964) grouped mottled zone and duricrust as 'laterite'. The term 'laterite' is used by some authors to refer to the whole weathering profile (ferruginous zone, mottled zone, saprolite), but the restricted usage, which only applies to the ferruginous/aluminous horizon of such a profile, is more common.

Recently, a new view of 'laterite' has emerged. For example, Ollier (1991) preferred to define 'laterite' as reddish mottled saprolite in a deep-weathering profile. Several authors (Milnes *et al.* 1985; Ollier & Galloway 1990; Ollier 1991; Bourman 1993) argued that the term 'laterite' should be abandoned, replacing it with 'ferricrete'. The term 'ferricrete' was originally used by Lamplugh (1902) to describe a ferruginous conglomerate of surficial sands and gravels cemented by Fe 'salts'. Subsequently, it has been extended to include all Fe-cemented and indurated surface crusts and subsurface horizons, but provides little information about the materials that have been ferruginised. Hence, this term is also very general and imprecise. Furthermore, some authors (Ollier & Galloway 1990) suggested that no relationship exists between the ferricrete and underlying saprolite zones, although these are generally considered to be genetically linked to the 'laterite' as part of a 'complete' laterite profile (McFarlane 1976; Nahon 1986; Bardossy & Aleva 1990; Nahon & Tardy 1992). Laterite is perhaps best considered as an informal term and used as a descriptor i.e. lateritic (Eggleton 2001).

'Typical' weathering profile

The 'typical' weathering profile consists of two major components, the saprolith and the pedolith, distinguished by their fabrics. The base of the saprolith is the boundary with fresh rock that forms the weathering front. The boundary between saprolith and pedolith is termed the pedoplasmation front (Figure 10).

The *saprolith* is generally the lower part of the regolith that has retained the fabric originally expressed by the arrangement of the primary mineral constituents of the parent material (Figure 11d–h). There are two major saprolith horizons, saprock and saprolite. *Saprock* is a compact, slightly weathered rock of low porosity (Trescases 1992) with less than 20% of the weatherable minerals

altered. Weathering effects occur along mineral boundaries and intra-mineral fissures, along cleavages, shears, joints and fractures or affect only a few minerals. The first signs of weathering are generally oxidation of sulfides and some easily weathered iron-bearing silicates or breakdown of plagioclase feldspar to clay. The upper and lower boundaries of saprock may be sharp or gradational; it may vary markedly in depth and thickness over short distances and with only minor lithological changes. For example, at the Jarrahdale railway cutting there is a very sharp contact between the saprolite and the adjacent fresh dolerite dyke at which the rock appears fully altered within 5 cm of the contact (Figure 12a on Plate 2) (Anand & Gilkes 1984b). By contrast, the contact is very gradual and diffuse on granite. It may not be possible to determine the upper boundary of saprock without petrographic study because it is difficult to determine the proportion of weatherable minerals in a hand specimen.

Saprolite is weathered bedrock in which the fabric (e.g. crystals, grains) of the parent rock, originally expressed by the arrangement of primary minerals comprising the rock, is retained. Compared to saprock, saprolite has more than 20% of the weatherable materials altered. The saprolite is a product of a nearly isovolumetric weathering process, which is also shown by quartz veins and corestones continuing undeflected from bedrock to the top of the saprolite (Figure 12b, c on Plate 2). The primary minerals are pseudomorphically replaced by weathering products (Figure 11d–h), retaining the fabric and structure of the parent rock. In the upper saprolite, most of the weatherable minerals have been altered to kaolinite, goethite and hematite; only quartz, zircon, chromite and other resistant minerals remain unaffected. Saprolite may progressively lose its fabric upwards as the proportion of clay increases and cementation by secondary silica, aluminosilicates and, especially by, Fe oxides increases. However, Fe oxides may also lock the fabric in place.

The *pedolith* is the upper part of the profile, above the pedoplasmation front, that has been subjected to soil-forming processes resulting in the loss of the fabric of the parent rock and the development of new fabrics through non-isovolumetric weathering (Figure 11a–c). In addition, processes such as illuviation, mixing and churning across the residual–transported unconformity can form a zone having chemical and mineralogical characteristics that reflect the underlying and overlying rocks. The principal horizons of the pedolith are the

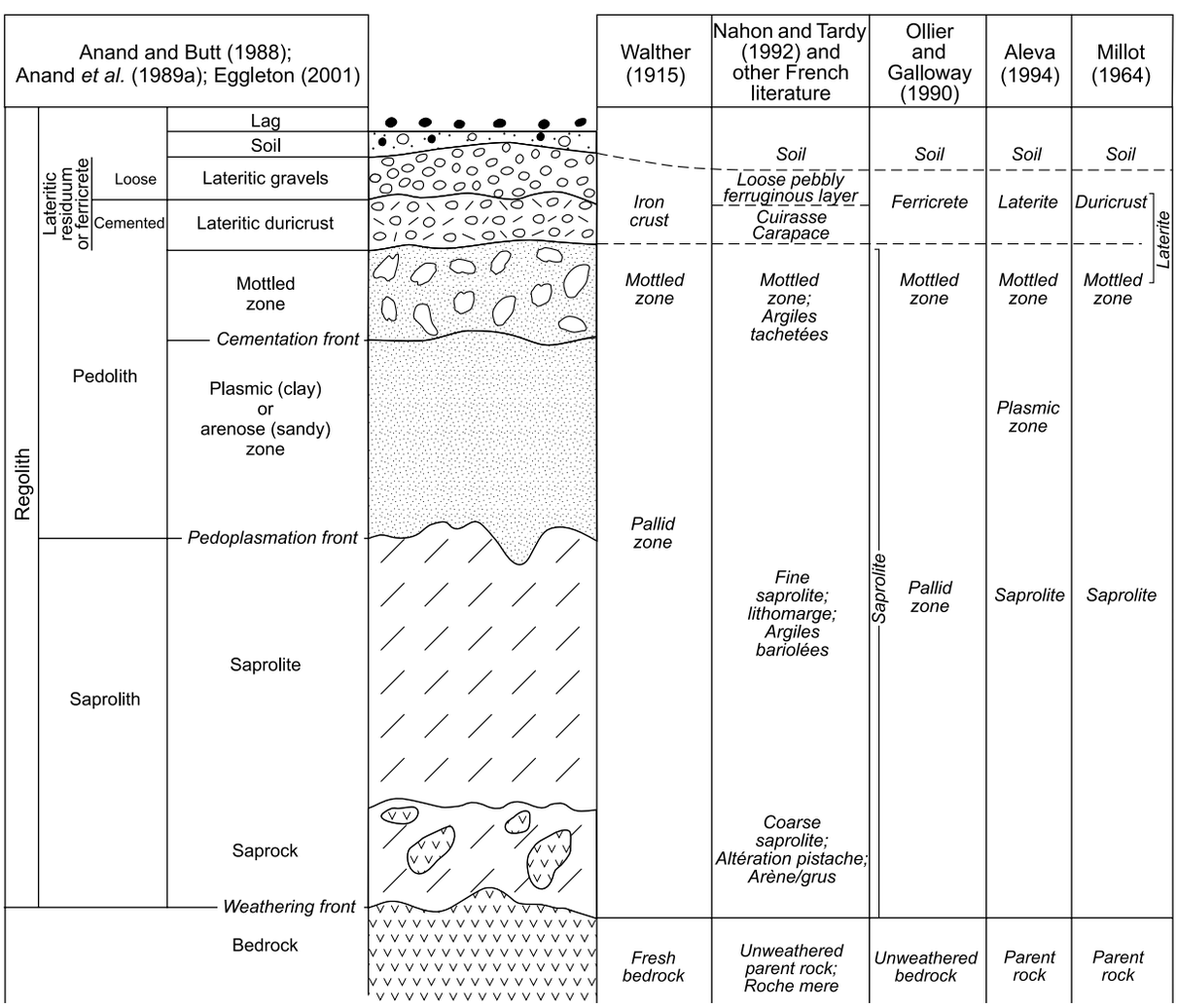

Figure 10 Comparisons of common terminology of a deeply weathered profile.

plasmic or arenose, mottled zone and lateritic residuum (lateritic duricrust and lateritic gravel). Particular elements are concentrated in some horizons (Fe and Al in ferruginous profiles; Si, Ti and Zr in silcretes) and some have secondary structures, such as collapsed structures, mottles, nodules and pisoliths.

The *plasmic horizon* is a mesoscopically homogeneous component of weathering profile developed on quartz-poor rocks. It is dominated by clay or silty clay that has neither the fabric of saprolite nor the significant development of secondary segregations such as mottles, nodules and pisoliths. It is a transitional zone of settling and consolidation produced between saprolite and mottled zone by a loss of fabric. The loss of lithic fabric is caused by solution and authigenesis of minerals and mechanical processes such as shrinking and swelling of clays and settling of resistant primary and secondary minerals through instability induced by leaching. Although lithological contacts may be preserved, there is generally some distortion. The equivalent horizon on granitic rocks is the arenose zone, which is composed of shardy or very angular quartz sand, with a grain-supported fabric. The loss of lithic fabric appears to be caused by solution and removal of kaolinite, and settling of resistant minerals, predominantly quartz. The plasmic and arenose horizons are not always present.

The *mottled zone* is the part of a weathering profile that has macroscopic segregations of subdominant colour that differ from the surrounding matrix (Figure 13a, b on Plate 3). The mottles may have sharp, distinct or diffuse boundaries; mostly there is a transition through a few millimetres of a goethite-rich halo (Figure 13c on Plate 3). They typically range in size from 10 mm to 100 mm, but may reach several metres in size. Mottles <10 mm have been termed minimottles and those >200 mm are megamottles (Eggleton 2001). Megamottles (Ollier *et al.* 1988; Anand & Smith 1993) are typically developed in transported palaeochannel clays (e.g. at Lady Bountiful Extended and Kanowna palaeochannel deposits), but have also developed in residual clays (e.g. Brown Lake; Kanowna Belle; Barton pit, Jundee; Bulong). At the Barton pit, the mottled zone is up to 15 m thick on basalt and gabbro and the mottles gradually become larger with increasing depth (Della Marta & Anand 1998). Megamottles may reach over 1 m in size and display a crude vertical orientation, possibly resulting from previous root structures. The mottled zone on felsic porphyry is relatively thin (4 m) and mottles were smaller and less dense than the mottles above mafic lithologies. This weak development of mottles is a result of the relatively low Fe content in the porphyry.

The terms ferruginous duricrust, lateritic residuum and ferricrete may be used to describe the upper part of the weathered ferruginous profile. *Ferruginous duricrust* may be used as a general term to describe regolith materials cemented by Fe irrespective of their origin. The term *ferricrete* is used as a conglomerate of surficial sands and gravels cemented by Fe oxides in the sense of Lamplugh (1902). *Lateritic residuum* is used as a collective term for the upper ferruginous zone of the lateritic profile and is composed predominantly of secondary oxides and oxyhydroxides of Fe (goethite, hematite, maghemite), hydroxides of aluminium (e.g. gibbsite, boehmite) and kaolinite, with or without quartz. It consists of loose lateritic gravels and/or lateritic duricrust (Figure 13d on Plate 3) that have developed essentially by residual processes and, therefore, have a broad genetic and compositional relationship with the substrate. Where both units are present, the gravels commonly overlie the lateritic duricrust. Lateritic residuum has evolved by partial collapse of mottled or ferruginous saprolite involving local vertical and lateral (generally 5–50 m) movement following chemical wasting, as well as the introduction and mixing of exotic materials through

Figure 11 Photomicrographs of fabrics from various horizons of a weathering profile. (a) Pisolitic duricrust and (b) mottled zone show replacement of rock fabrics by accumulation of Fe oxides as pisoliths and mottles. (a) Polished block taken in nrl showing concentric massive hematitic–maghemite-rich pisoliths (1) set in a goethite matrix (2): Lawlers (thin-section 07-0760). (b) Polished thin-section taken in ppl showing a red hematitic mottle (1) in a fine-grained kaolinitic matrix (2): Jundee (sample 05) (photo by J. Della Marta). (c) Polished thin-section taken in xpl showing a plasmic zone on granite: the fabric has been completely replaced by secondary, fine-grained kaolinite (1), which is set in a closely packed relict quartz (2): Jarrahdale (thin-section 07-4304). (d) Polished thin-section taken in nrl showing ferruginous saprolite retaining a schistose fabric: Bronzewing (thin-section 07-2680). (e) Polished thin-section taken in xpl showing saprolite on felsic porphyry: feldspars are completely replaced by fine-grained kaolinite (1) leaving muscovite (2) and quartz (3) unaltered: Jundee (sample 18) (photo by J. Della Marta). (f) Thin-section taken in xpl showing saprolite on granite: feldspars are replaced by kaolinite (1) leaving biotite (2) and quartz (3) unaltered: Jarrahdale (thin-section 07-4302). (g) Thin-section taken in ppl showing lower saprolite on ultramafic bedrock: preservation of relict spinifex fabric by pseudomorphism of original bladed olivine by goethite: Forrestania (thin-section 07-2927) (photo by A. Kelly). (h) Thin-section taken in xpl showing lower saprolite on gabbro: the plagioclase has been partly altered to kaolinite (1), leaving microcline (2) and slightly altered chlorite (3); the chlorite is turbid and has begun to alter to smectite: Jundee (sample 31) (photo by J. Della Marta). Photographs by authors unless otherwise specified; xpl, transmitted light with crossed polarisers; ppl, transmitted plane-polarised light; nrl, normally reflected light.

Table 1 Summary of the dataset used to calculate average weathering depths, showing the number of records for each lithology (after Ely 2000).

Lithology	Base of transported overburden		Base of complete oxidation		Top of saprock	
	Records	Mean depth (m)	Records	Mean depth (m)	Records	Mean depth (m)
Felsic	7620	7	5375	43	100	64
Basalt	27 544	7	21 911	37	1375	60
Granite	5445	6	4132	32	209	43
Dolerite	3293	6	2653	31	65	38
Ultramafic	1799	5	1498	29	97	37

soil forming and aeolian processes. The use of the term residuum is not meant to imply that all of the residuum is *in situ* because it has continually formed and been modified during weathering. Lateritic duricrust is the indurated component of lateritic residuum. It may be massive or, more commonly, contain various secondary segregations such as nodules, pisoliths and ooliths, and structures such as open and infilled vermiform voids. Lateritic gravels are the unconsolidated component of lateritic residuum, consisting of loose ferruginous segregations (nodules and pisoliths) and fragments, by convention in the size range 0.25–64 mm. The gravels are commonly grain-supported

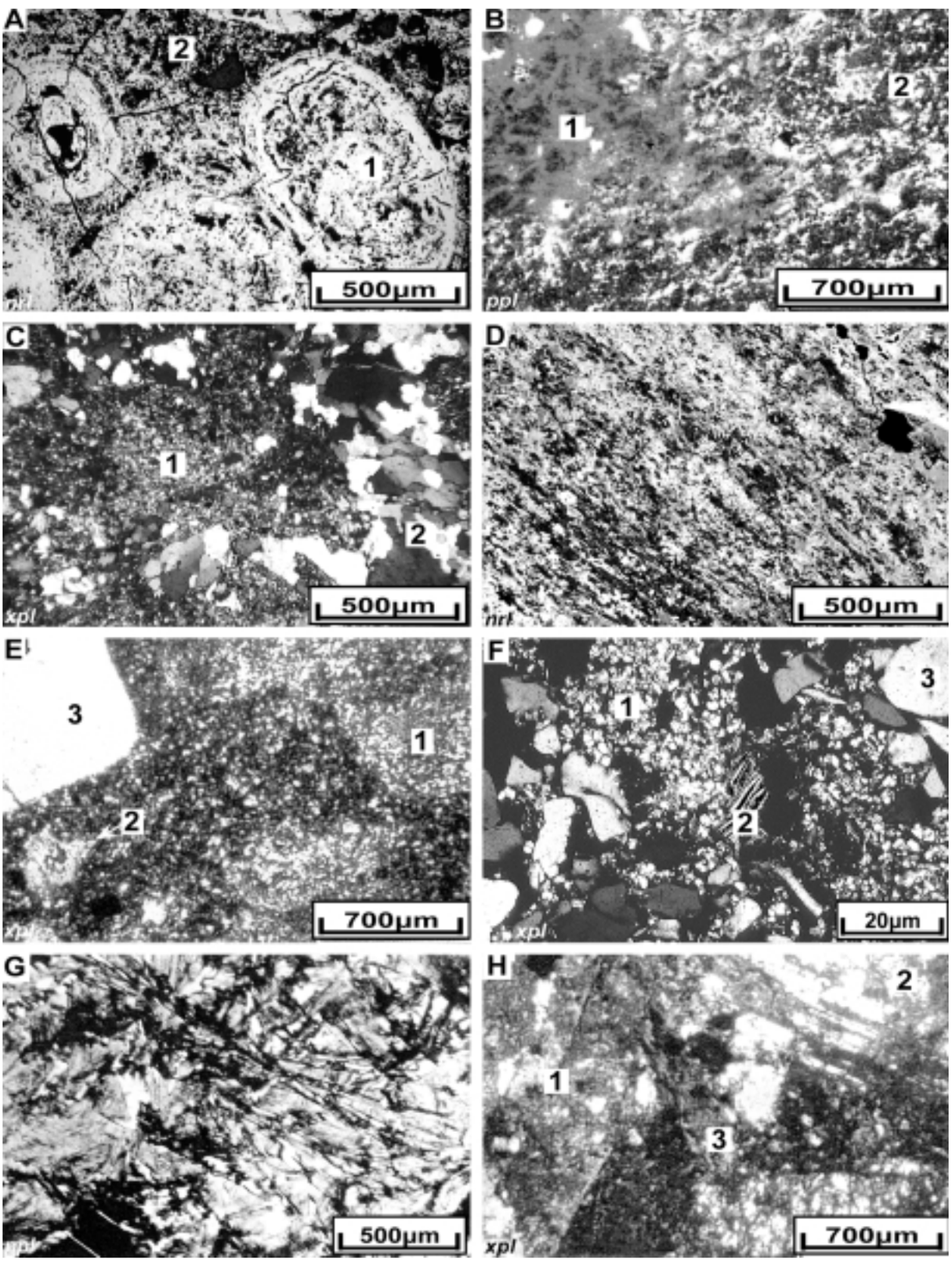

and may have a clay-rich or sandy matrix. Nodules are irregular with re-entrant features, whereas pisoliths are ellipsoidal or spherical. As the sphericity of nodules increases, they merge with pisoliths. Both nodules and pisoliths generally have an outer cortex or skin and the distinction between the two is based on shape rather than on the absence or presence of skins.

Few *soils* that had originally overlain the developing lateritic profiles are preserved. Most soils developed from, rather than with, the material they overlie. These may include the ferruginous zones of 'complete' profiles or the exposed horizons (e.g. mottled zone, saprolite or fresh bedrock) of truncated profiles.

Lag is the residual accumulation of coarse, usually hard, fragments that accumulate at the surface. It has been left as a residue after the physical and chemical dismantling of the upper horizons of the regolith and the removal of finer materials in solution, sheetwash or wind action.

Informal terms used

In regolith profiles, four major boundaries can be defined from exploration drilling. The boundaries include: (i) BOA—base of transported overburden (unconformity); (ii) BOCO—base of complete oxidation (oxide zone); (iii) TOSA—top of saprock (base of significant weathering); and (iv) TOFR—top of fresh bedrock (weathering front).

The base of complete oxidation is recognised in drill cuttings by the colour transition from red or yellow to green in residual clays or saprolite. The material above this boundary is dominated by clays, Fe oxides and oxyhydroxides, and resistant minerals. The top of saprock is the boundary between moderately weathered, low-density saprolite and the underlying compact, slightly weathered bedrock that has less than 20% of the weatherable minerals altered (saprock). Transition zone is referred to as a zone between the TOFR and BOCO.

FACTORS INFLUENCING DEPTH OF WEATHERING

Many Yilgarn Craton landscapes retain a deeply weathered mantle. Its preservation is generally favoured by long-term tectonic stability, low relief and protection by duricrust. Deep weathering has affected most rocks and geological provinces across the craton. The depth of weathering may be as much as 150 m (Figure 14 on Plate 4), but varies considerably and fresh outcrop may occur in any part of the landscape. Factors influencing extent of weathering are rock type, mineralisation and deformation (Davy 1979; Robertson & Butt 1993; Clarke 1994a; Brand *et al.* 1996), as shown by the Yandal greenstone belt in the northeastern goldfields (Anand 2000; Ely 2000). The Yandal greenstone belt consists of a wide variety of rocks including mafics, ultramafics, felsic volcanics, granite and sedimentary rocks. The large dataset formed the basis of calculating average weathering depths across the belt, and for comparing variation in these depths with other variables such as lithology (Table 1; Figure 15), mineralisation and deformation. Base of complete oxidation (BOCO) and top of saprock (TOSA) were chosen as the primary indicators of depth of weathering (Ely 2000). They illustrate a similar pattern with respect to the major lithologies. Fine-grained felsic rocks and basalt are the most deeply weathered. Granite, dolerite and ultramafic rocks weather to shallower than average depth. Although the variation is much smaller, average base of transported overburden (BOA) values also form a similar pattern to BOCO and TOSA. The variation in average BOA values indicates the tendency of dolerite and ultramafic rocks to form ridges in the landscape. On average, weathering is 30 m deeper in areas of high-grade Au mineralisation (Ely 2000).

Weathering of granitic rocks appears to be shallower, generally <40 m deep, except in mineralised areas and along shear zones. In the bauxitic province of the Darling Range, the depth of weathering on granite rarely exceeds 20 m (Sadleir & Gilkes 1976; Davy 1979; Anand *et al.* 1991a). However, the presence of deep shears has resulted in differential weathering producing a large area of kaolinitic clay (Hickman *et al.* 1992). Deep weathering in the mineralised areas is due to sulfides, intense shearing, and variation in competence of contiguous rocks. Joints and fractures act as permeable zones and as conduits for weathering fluids to flush away the soluble products of weathering. In the Kambalda district, Clarke (1994a) observed that depth of weathering is controlled by rock chemistry, with the following succession of increasing degree of weathering: mafic rocks and granite < ultramafic rocks < sedimentary rocks.

WEATHERING UNDER PALAEOCHANNELS

Numerous palaeochannels occupy the lower parts of the landscape. Most of the palaeochannels appear to be incised into pre-existing residual regolith (Clarke 1994b). Cross-sections through the palaeochannels reveal several very different weathering profiles. A typical section at Mt Joel, in the Yandal greenstone belt, illustrates deepening of weathering, which corresponds to the deepest section of the palaeochannel (Figure 16) and a weathering profile

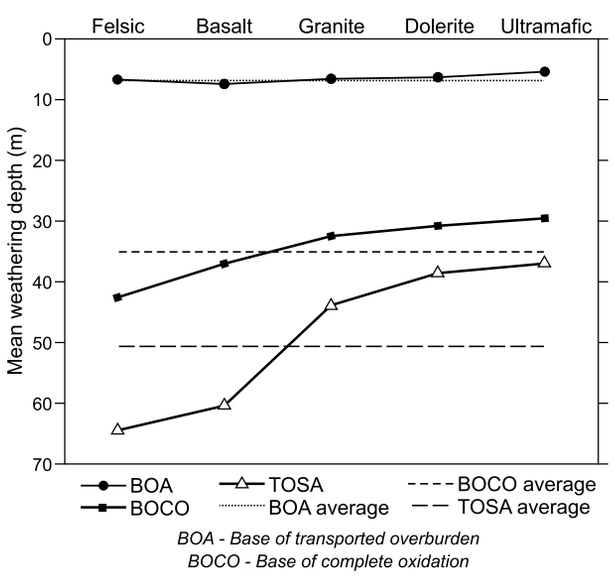

Figure 15 Mean weathering depths versus lithology for the Yandal greenstone belt (after Ely 2000).

occurs under the channel. The foliated basalt is deeply weathered underneath and adjacent to the channel. Weathering may have occurred after erosion of the channel, or the channel may have exploited weaknesses in a previously weathered landscape. This contrasts with a palaeochannel at Cyclonic that has little or no weathered material overlying the massive basalt (Anand *et al.* 1999a; Ely 2000). No completely oxidised material exists, and it is common for the top of fresh rock to be near the base of the channel (Figure 16). Very little weathering has occurred since the formation of this part of the channel. This example illustrates the variability of the depth of weathering underneath palaeochannels.

WEATHERING PROFILES AND LITHOLOGIES

Weathering leads to the formation of regolith profiles, which reflect the interplay of weathering, relocation of materials and erosion, generally over long periods. Walther (1915) summarised a combination of observations into a diagram showing a 'lateritic profile' as an iron crust with a mottled zone and a pallid zone overlying fresh rock (Figure 17). Examples of this can be seen in the Yilgarn Craton, but these deeply weathered profiles vary considerably depending on the nature of the parent rock, structures, topographic setting and present or past climates (Figures 18, 19). Weathering profiles on different lithologies reflect the bedrock. Saprolite is common to all the weathering profiles, but the nature of upper horizons may vary. The ferruginous horizon is commonly most strongly developed over mafic and ultramafic rocks. On some felsic rocks, duricrust may have never developed. A mottled zone occurs at the top of the profile, overlying a white, bleached plasmic zone. Over some mafic rocks, the mottled clay zone may be absent; instead, the saprolite becomes increasingly ferruginous and brecciated before merging into a lateritic gravel or duricrust. Silcretes occur over granitoids or felsic rocks (Butt 1985; Dell & Anand 1995) and massive, silicified saprolite, silcrete and silica veining occur on Al-poor ultramafic rocks (Butt & Sheppy 1975; Smith 1977; Butt & Nickel 1981; Elias *et al.* 1981; Anand *et al.* 1991b; Kelly & Anand 1995; Lawrance 1996; Monti & Fazakerley 1996). The massive silicification in lower saprolite results in a very impervious horizon and a perched water table may develop above it. This is commonly a site for the precipitation of Mn oxides and smectites. Similar silicification of ultramafic rocks is widely known (Melfi *et al.* 1980; Oliveria *et al.* 1992), resulting in prominent outcrops that are resistant to erosion. These are informally referred to as 'birbirites' and several have been described as being hydrothermal in origin, the true origin, i.e. weathering, not being recognised. In the high rainfall areas of the Darling Range, saprolite is overlain by a bauxite zone.

FABRIC CHANGES FROM BEDROCK TO REGOLITH

General

Fabric changes in a weathering profile are only one of the consequences of weathering reactions. Although some secondary minerals replace their precursors, pseudomorphing and, thus, preserving the fabric, others dissolve and reprecipitate elsewhere, causing the greatest fabric changes. Pseudomorphic replacements dominate the lower part of the weathering profile where original rock fabrics are well preserved (saprock and saprolite). Pseudomorphic replacement of feldspar by kaolinite or gibbsite, and pyroxene or amphiboles by goethite, leave the original rock fabric perfectly preserved or even accentuated. Fabrics are best preserved where the sizes of the elements of the original fabric are significantly greater than the crystal sizes of the replacing minerals.

Above the pedoplasmation front, where pedogenic processes are dominant, mineral dissolution and distant precipitation are important and fabric changes become more marked. Such changes involve dissolution and reprecipitation of clays, the formation of clay blasts, clay accordian structures and quartz segregation fabrics, the development of vesicular structures and channelways and the appearance of root casts, which become infilled with clays or fragments from higher levels in the regolith. Pedoplasmation tends to be incomplete and pockets of the saprolitic fabric may be found preserved very close to the surface (Robertson *et al.* 1998). The importance of these pedoplasmation processes increases into the mottled zone and lateritic residuum, where segregation, concentration and cementation by Fe oxides occur. The Fe oxides, chiefly goethite and hematite with some maghemite, replace and, thus, preserve the plasmic structures and any surviving saprolitic or primary structures.

Understanding the progressive fabric changes throughout the profile is essential to distinguish useful fabrics that may assist bedrock identification from those that have been imposed later. Four major processes are identified that can lead to the destruction or preservation of rock fabrics in

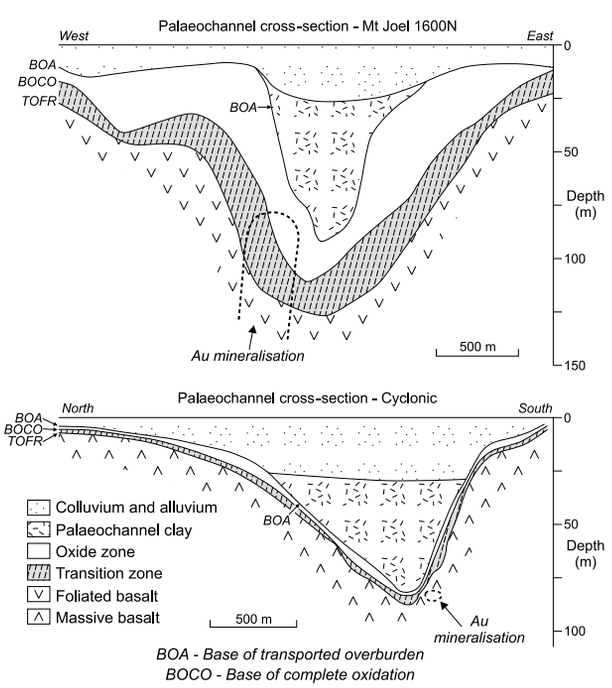

Figure 16 Cross-sections of palaeochannel profiles at Mt Joel and Cyclonic in the Yandal greenstone belt (after Ely 2000).

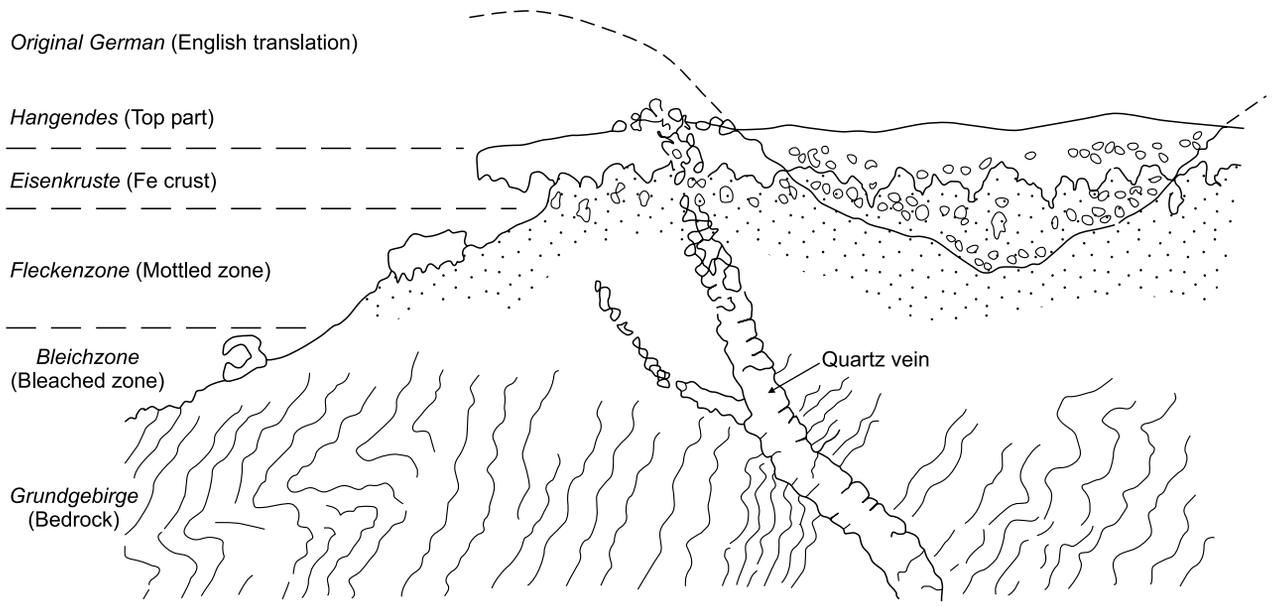

Figure 17 Lateritic profile of Western Australia as described by Walther (1915).

the near-surface horizons: (i) formation of clay blasts destroying primary rock fabric; (ii) primary fabric loss by collapse; (iii) formation of mottles destroying primary rock fabric; and (iv) mottling preserving primary rock fabric.

Formation of clay blasts destroying primary rock fabric

The formation of clay blasts destroying primary rock fabric is illustrated by weathering of a mafic schist from the Rand pit at Reedy (Figure 20) (Robertson *et al.* 1998). The mafic schist consists of granular quartz, untwined albite and lenticular patches of chlorite, cut by a strong foliation of muscovite and talc. The onset of weathering occurs at approximately 70 m, where white or cream turbidity in the albite indicates partial alteration to very fine-grained kaolinite. Complete kaolinisation of plagioclase occurs just above the base of the saprolite. Chlorite has altered to smectite and this, in part, has altered to kaolinite, but the schistose fabric remains. Near the top of the saprolite, the primary fabric is partly obliterated, quartz grains in vein quartz become separated, solution cavities and channelways occur and the saprolite grades upwards into the pedolith.

In the plasmic horizon, reorganisation of the schistose fabric, which consists of kaolinite, talc, chlorite and quartz of the saprolite, by recrystallisation of kaolinite, begins at 30 m depth, where patches of clay appear in the saprolite. This pedoplasmic process is virtually complete at 10 m, where remnant saprolitic fabrics are difficult to find. Initially, small, globular blasts of very fine-grained, secondary kaolinite have developed in the original, schistose, saprolitic fabric. This progressively becomes more marked with considerable reorganisation of the primary fabric. Large patches of very fine-grained kaolinite have developed and these have swept remnant quartz grains into clusters, destroying the foliation. The restructured plasmic minerals close to the surface (2–10 m) become increasingly more closely cut by channelways and voids, many of which are lined with kaolinite and completely or partly filled with mixed kaolinite and smectite.

Primary fabric loss by collapse

An example illustrating the primary fabric loss by collapse has been described from Waterfall near Mt Keith (Butt 1985). Kaolinitic granitic saprolite is exposed at the base of the profile, which passes gradually into sandstone at the top. The original granitic fabric is well preserved by kaolinite pseudomorphs after feldspar and primary quartz (Figure 21). Close to the surface there is a transition to an arenose horizon. A quartz vein may be traced upwards, where it becomes disjointed and terminates in a stone line. The fabric of the weathered granite is perfectly preserved at the base, but further up, where the quartz of the vein becomes disoriented, quartz grains in the saprolite become closely packed. Here much of the kaolinite has been removed, apparently by dissolution, leaving primary quartz (Figure 21). This settles and becomes concentrated into a residual sandstone or grit, now largely cemented by aluminosilicates. This arenose horizon is invaded by silica and minor titania to form silcrete, in which quartz grains are cemented by yellowish quartz, anatase and zircon.

Formation of mottles destroying primary rock fabric

Mottling may be developed in plasmic, arenose and saprolite horizons and results from either the accumulation of Fe-rich material (brown mottles) or the loss of Fe (white

Figure 18 Examples of commonly occurring weathering profiles on greenstone sequences and granite in the arid interior of the Yilgarn Craton. A, B, C, F, G and I are situated throughout the Yandal greenstone belt and are modified after Anand *et al.* (1999a) and Ely (2000); D (Lawlers) after Anand *et al.* (1991b); E (Mt Keith) after Butt (1985); H (Murrin Murrin) modified from Monti and Fazakerley (1996).

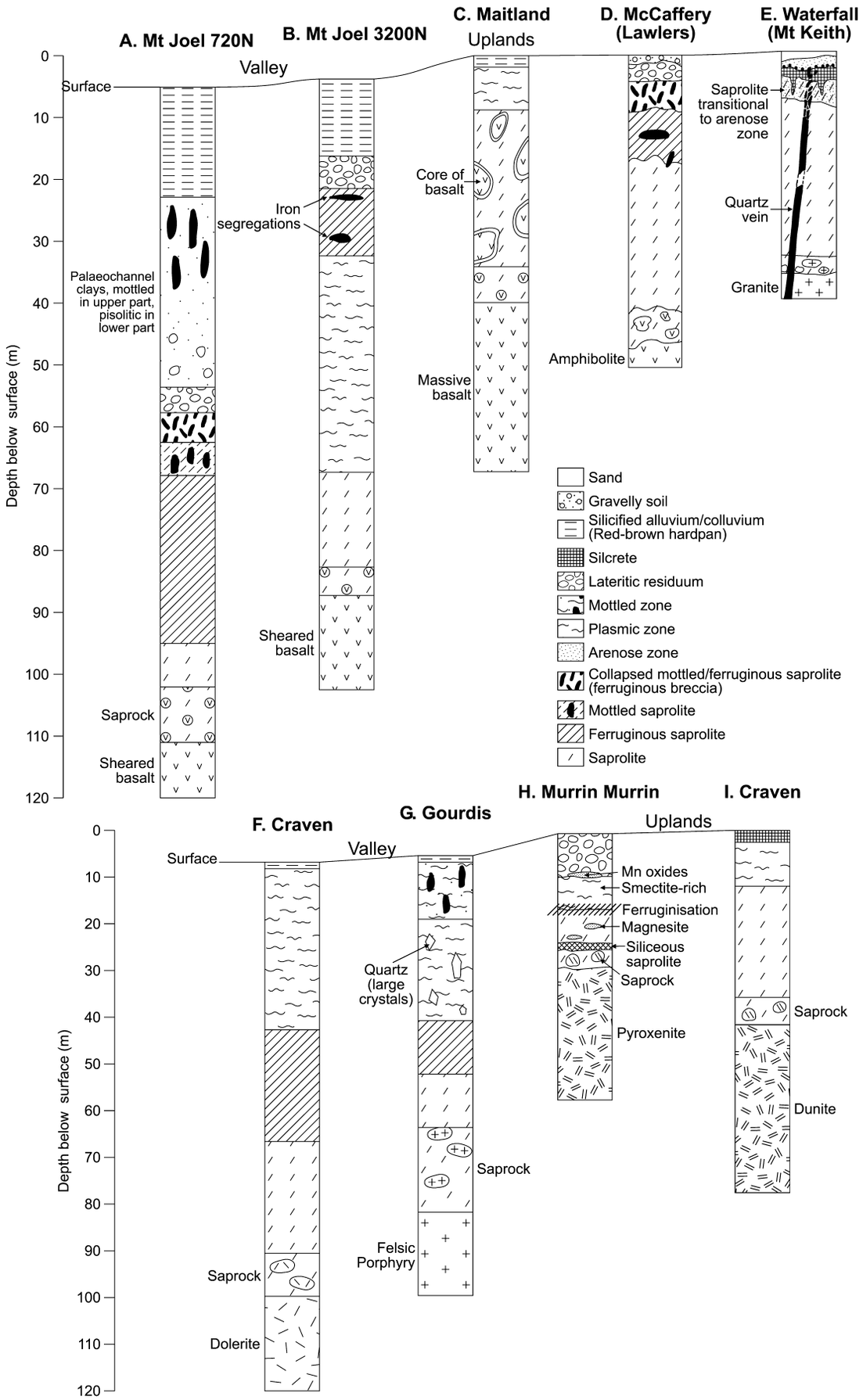
A. Mt Joel 720N
B. Mt Joel 3200N
C. Maitland
Uplands
D. McCaffery
(Lawlers)
E. Waterfall
(Mt Keith)
Valley
Surface
Depth below surface (m)
0
10
20
30
40
50
60
70
80
90
100
110
120
Palaeochannel clays, mottled in upper part, pisolitic in lower part
Saprock
Sheared basalt
Iron segregations
Sheared basalt
Core of basalt
Massive basalt
Amphibolite
Saprolite transitional to arenose zone
Quartz vein
Granite
Sand
Gravelly soil
Silicified alluvium/colluvium (Red-brown hardpan)
Silcrete
Lateritic residuum
Mottled zone
Plasmic zone
Arenose zone
Collapsed mottled/ferruginous saprolite (ferruginous breccia)
Mottled saprolite
Ferruginous saprolite
Saprolite
F. Craven
G. Gourdis
H. Murrin Murrin
I. Craven
Uplands
Valley
Surface
Depth below surface (m)
Quartz (large crystals)
Saprock
Felsic Porphyry
Saprock
Dolerite
Mn oxides
Smectite-rich
Ferruginisation
Magnesite
Siliceous saprolite
Saprock
Pyroxenite
Saprock
Dunite

mottles). Brown mottles developed in plasmic clays (e.g. Midway North pit, Mt Gibson) are marked by accumulation of Fe and Al oxides as spots, blotches and streaks (Figure 13a; see Plate 3) that may become segregated into secondary structures (nodules and pisoliths). They result from pedogenic activity and are formed by migration and accumulation of Fe oxides in the kaolinitic matrix or voids. Some of this kaolinite may be secondary, filling voids previously created in the bleached domains. Mottling and nodule growth progressively destroy pre-existing fabrics, although plasmic or arenose microfabrics may be preserved in the nodules and pisolith cores. Higher in the ferruginous duricrust, these mottles evolve into nodules as accumulation progresses: they are what Nahon (1976) has called argilomorphous nodules.

Where white mottles have formed, bleaching commonly extends down cracks, fissures and root channels, the latter accounting for near-vertical cylindrical bodies of bleached material (Figure 13e on Plate 3). The whole material was once oxidised and red or brown; bleaching is a later event.

Mottling preserving primary rock fabric

Mottling occurs without loss of the saprolitic fabric (e.g. Brown Lake: Figure 13b on Plate 3) in mottled saprolite. It is part of the saprolith rather than the pedolith. In mottled saprolite, mottles are iron accumulations in which the primary rock fabric remains. Some of the Fe required for mottling may have been derived, at an early stage, from patches of sulfides and ferromagnesian minerals. Cementation and Fe accumulation occur independently from pedoplasmation and, although ideally the former is depicted higher in the regolith than the latter, in reality cementation may overtake pedoplasmation (Figure 22). As ferruginisation has the ability to prevent the depredations of pedoplasmation, this overtaking of the fronts has a profound effect on preservation of fabrics. Where ferruginisation reaches the saprolitic fabric before pedoplasmation, there is a good chance of pseudomorphed primary fabrics surviving, even to the surface in lag (Robertson 1996).

The upper part of the mottled saprolite may be weathered by solution, resulting in a mesoscopic porosity as coarse, generally vermiform, voids. Some voids are lined with goethite and secondary silica. Progressive amalgamation of these voids leads to the ultimate collapse of the mottled saprolite (Anand *et al.* 1991b; Davy & Gozzard 1995). Collapsed mottled saprolite (ferruginous breccia), which although condensed is largely residual, is composed of fragments of mottled saprolite and incipient nodules, with voids filled by detrital matrix. In the collapsed mottled saprolite, individual fragments lose their original orientation. At Calista (Mt McClure), a ferruginous vein may be traced in the collapsed mottled saprolite where it becomes disjointed and terminates in a stone line (Figure 23). This vein is evidence of a residual profile. The base of collapsed mottled saprolite is very irregular, with cone-shaped pendants penetrating the mottled saprolite (e.g. Calista, Bronzewing) (Figure 13f on Plate 3). Very similar structures, sometimes referred to as 'Mukarra', ascribed to the differential loading caused by swelling smectite clays, are common in certain soil materials (Paton 1974). The absence of smectite in mottled saprolite beneath the pendants rules out the differential-loading process. The pendants appear to be a result of preferential removal of the kaolinitic matrix by chemical and physical processes. However, the exact controls on the shape of pendants are not clear, but the shape may be partly governed by the preferential access of tree roots, which enhances permeability. Further weathering, micro-fragmentation, coating and minor lateral transport of mottles may give rise to lithic nodules. Lithic nodules contain recognisable pseudomorphs after primary minerals (e.g. feldspars, mica, talc, or relics of gossan, amphiboles, banded iron-formation and mica). The angularity of the nodules tends to increase down the profile. Near the surface, nodules are dark-brown to black, but are yellowish brown in collapsed saprolite. As the sphericity of the nodules increases up the profile, by dissolution of irregular edges, some develop progressively into pisoliths.

Where Fe accumulation occurs without loss of the saprolitic fabric, the material is ferruginous saprolite. In places, particularly on some Fe-rich mafic and ultramafic rocks, the mottled saprolite is underlain by thick (5–15 m) ferruginous saprolite (uniform ferruginisation). Where exposed, for example, in the McCaffery pit at Lawlers, ferruginous saprolite (5–10 m thick) forms a continuous zone of several hundred metres on mafic and ultramafic rocks (Anand *et al.* 1991b). Ferruginous saprolite is a yellowish-brown, indurated mass, which was produced by infusion of goethite into clay-rich saprolite.

MINERALS IN WEATHERING PROFILES

Introduction

Weathering is the result of interactions between the hydrosphere, biosphere, lithosphere and atmosphere. During weathering, most primary minerals in the bedrock are broken down. Some components are leached and some are retained as secondary minerals. The final product is a mineral assemblage more stable in the regolith environment than their precursors. The mineral progression is towards greater relative stability in situations progressively near surface. In the final product, all bedrocks tend to produce similar assemblages of least soluble minerals. Thus, in the humid regions of the Yilgarn Craton, the upper horizons (ferruginous duricrust, mottled zone and bauxite), which have developed on a variety of rocks, now consist largely of the least soluble minerals (kaolinite, hematite, goethite, maghemite, gibbsite, anatase, boehmite and corundum) and the most resistant minerals (quartz, zircon, chromite, muscovite and talc) (Figures 24, 25). In addition, the more soluble minerals, including carbonates, sulfates and halides, occur in soils in arid environments; these generally form by dissolution, then precipitation upon evaporation.

The mechanisms and rates of weathering of primary minerals vary widely. Primary minerals may dissolve congruently to yield their components in solution in the same proportion in which they occur in the mineral. They may also dissolve incongruently, so that the solid residue has a different composition from the starting mineral.

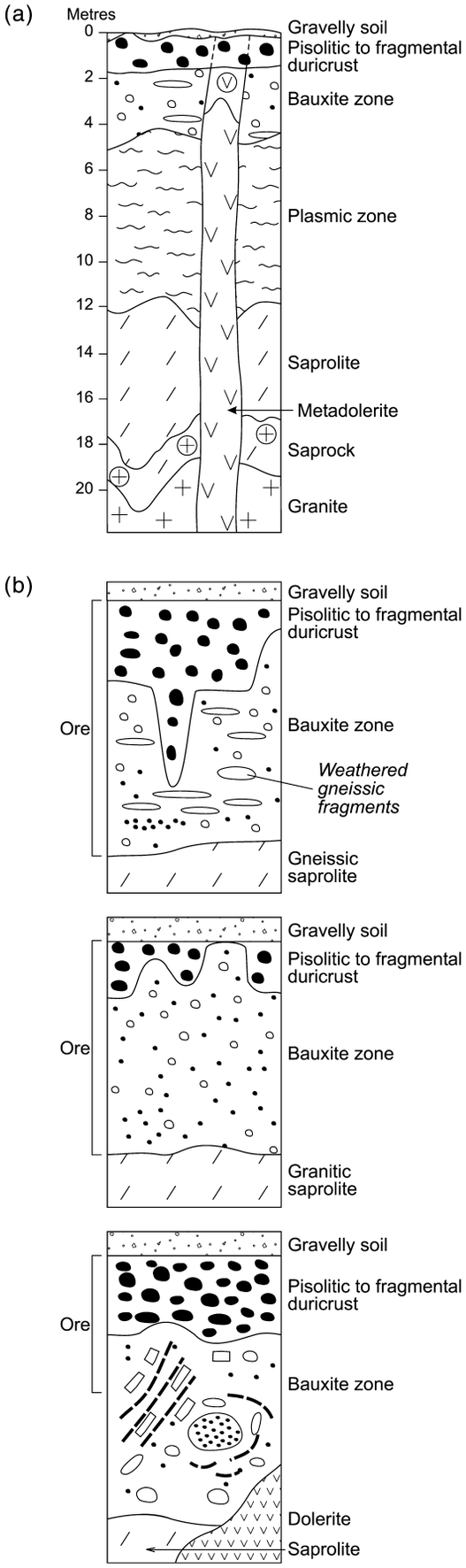

Mechanisms of weathering of primary minerals are not discussed here and readers should refer to Loughnan (1969), Ollier (1984), Gilkes and Suddhiprakarn (1979), Anand and Gilkes (1984a, b, c), Anand *et al.* (1985), Gilkes *et al.* (1986), Singh and Gilkes (1991), Robertson and Eggleton (1991), White and Brantley (1995), Eggleton (1998), Churchman (1999) and Taylor and Eggleton (2001). Most commonly, weathering leads to gradation of products in both space and time, resulting in weathering profiles in which there are variations with depth. However, neoformation of several generations of either hematite, goethite or kaolinite may occur within a hand specimen. There is also increasing evidence that two or more minerals (e.g. kaolinite and gibbsite) may be formed simultaneously in the same horizon, depending on the prevailing microenvironment (Anand *et al.* 1985). Furthermore, poorly crystalline materials can be present in significant amounts (Eggleton 1998). Commonly observed transformations of important minerals during weathering of granite, mafic and ultramafic rocks in the Yilgarn Craton are summarised in Figure 26.

Kaolinite, halloysite and smectite

Kaolinite, halloysite and smectite are generally the most common minerals in saprolite. However, their abundance varies according to the bedrock. For example, in profiles developed on Al-poor ultramafic rocks (e.g. dunite), halloysite and kaolinite can be much less abundant (<15%) compared to profiles developed on mafic and felsic rocks. Instead, quartz, secondary silica (opal CT: opal CT constitutes a disordered sheet-linkage of silica tetrahedra approximately 0.41 nm thick, which are stacked to yield randomly interstratified mixed layers of cristobalite-like and tridymite-like structures), Fe oxides and smectite are dominant minerals in these saprolites.

Smectite is generally a product of weathering under dry or poorly drained environments. Where present, it is most abundant at the base of the deeply weathered profile and largely results from weathering of amphibole, olivine, pyroxene, chlorite and, in places, talc. It generally occurs in small amounts in saprolite developed from granitic rocks, where amphibole and olivine are typically absent. However, smectite has also been reported to form from feldspars (Allen & Hajek 1989). The type of smectite in regolith is partially determined by the parent rock. Smectite formed by weathering is dioctahedral as a general rule (Borchardt 1989). Mafic rocks containing high Fe and low Al often weather to ferruginous smectite.

Smectite crystals are generally thin flakes with irregular outlines (Figure 27a), but when precipitated from solution they occur as rose-shaped crystals (Figure 27b). Higher in the saprolite, smectite generally alters to kaolinite and goethite.

Kaolinite and halloysite are major weathering products of feldspar and, to a lesser extent, muscovite (Figure 26). Feldspar may weather directly to kaolinite, or this stage

Figure 19 Examples of commonly occurring weathering profiles on granitic and doleritic rocks in the Darling Range, particularly highlighting the variations in the upper part of the profile. (a) after Anand *et al.* (1991a); (b) after G. Baker (pers. comm. 2000).

may be preceded by halloysite (Anand *et al*. 1985). Near the top of the profile, there may be secondary kaolinite. Kaolinite may also form hydrothermally and it may be difficult to distinguish these from those formed authigenically by weathering. Kaolinite crystals typically have platy morphology and are generally <0.5 μm (Figure 28a), although large accordian structures may occur (Figure 28b). Halloysite crystals are generally tubular (Figure 28c) and may be partly unrolled or platy especially higher in saprolite. Thus, distinction based on shape can be unclear. Kaolinite varies greatly in the degree of structural disorder. Iron commonly occurs in small amounts as an impurity in the structure of kaolinite and is generally correlated with its poor crystallinity (Calvert 1981). Similarly, halloysite exhibits a wide range of contents of structural Fe (Churchman 1999).

The proportion of halloysite generally decreases upwards in the profile, which may suggest a possible genetic relationship between halloysite and kaolinite (Eswaran & Wong 1978; Calvert *et al*. 1980). However, in places halloysite (1–3 μm) occurs in significant amounts in ferruginous pisoliths (e.g. at Ora Banda: Figure 28c). Churchman and Gilkes (1989) studied the pattern of appearance and disappearance of different forms of halloysite in weathering profiles at Jarrahdale. Hydrated halloysite dominated the clay fraction of the saprolite close to fresh dolerite. With further weathering, corresponding to distance from the rock up the profile, the halloysite progressively became more dehydrated, and finally fully dehydrated. Halloysite tubes tended to split and unroll as weathering continued. Kaolinite as platy particles appeared later than halloysite in the course of weathering. Halloysite tubes and kaolinite plates appeared to form by separate pathways (Churchman & Gilkes 1989). In other studies of Australian weathering profiles, both Robertson and Eggleton (1991) and Singh and Gilkes (1992b) showed clear

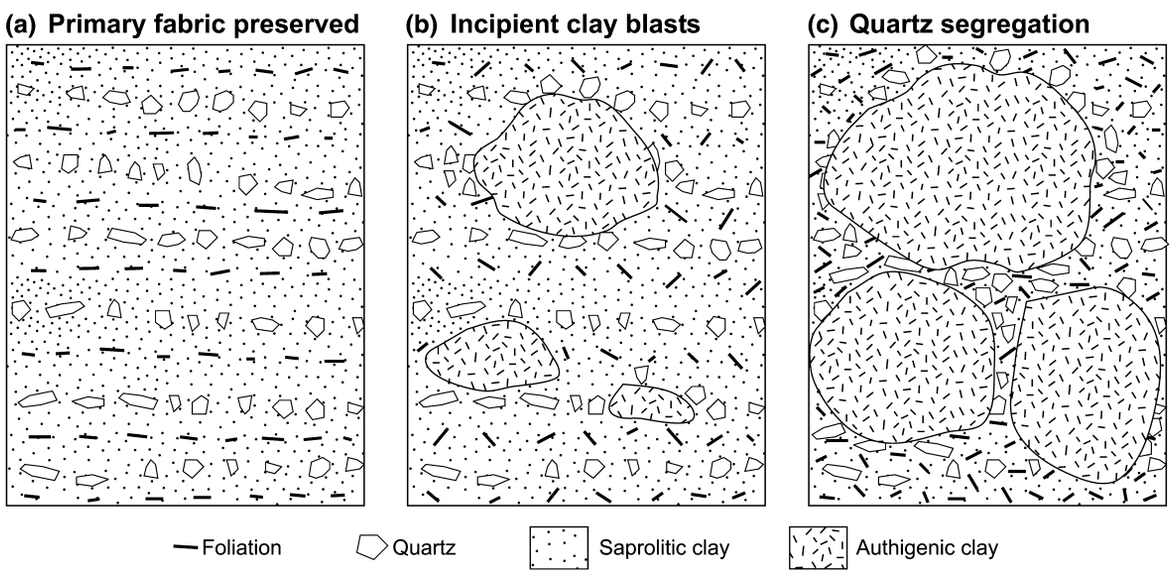

Figure 20 (a–c) Loss of schistose fabric by progressive development of blasts and secondary kaolinite around which remnant quartz becomes segregated (after Robertson *et al*. 1998).

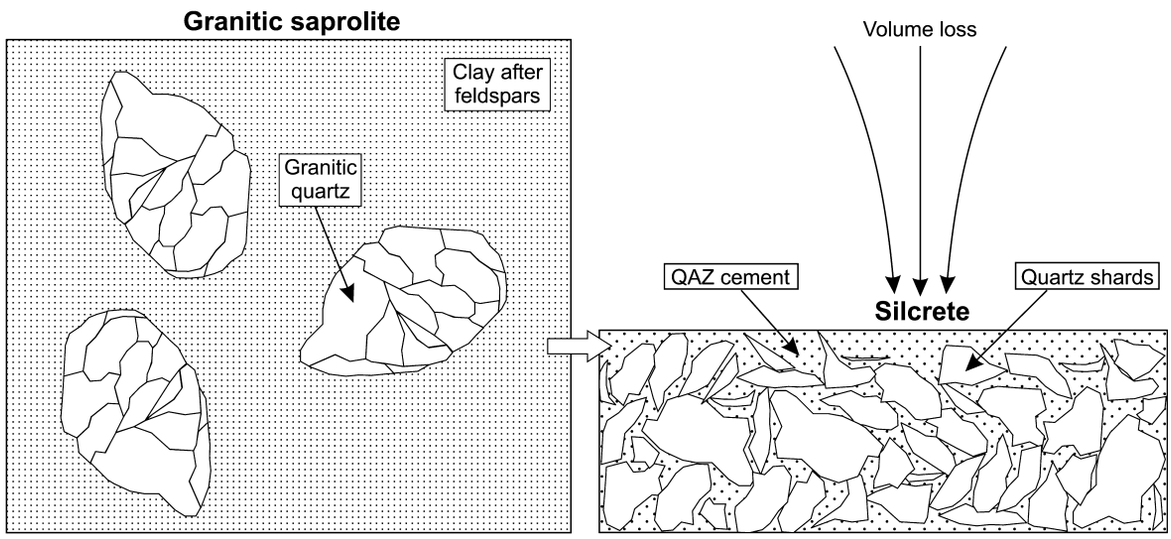

Figure 21 Transformation of granitic saprolite into sandy arenose material by disaggregation of quartz and loss of kaolinite, with resultant collapse (after Robertson *et al*. 1998). QAZ, quartz, anatase and zircon.

evidence for the transformation of kaolinite plates to halloysite tubes. Recently, Singh (1996) has provided a theoretical model to explain the observed transformation of kaolinite to halloysite, and Singh and Mackinnon (1996) tested this model by experimentally converting Georgia kaolinite to halloysite tubes. Churchman (1999) observed that different parent materials are involved in each case (plagioclase feldspars in Robertson and Eggleton's study, and micas in Singh and Gilkes' study), thus, the nature of the microenvironment is more likely to be the common feature. In both of these studies and those of the deeply weathered profiles, it is agreed that the essential requirement for the formation of halloysite is the incorporation of water into the interlayers. Hence, halloysite is generally most common in the lower, wetter parts of the weathering profiles (Churchman 1990).

Gibbsite, boehmite and corundum

Among the aluminium hydroxides and oxyhydroxides, gibbsite is the major aluminium mineral in the humid region of the Darling Range (Figure 24) (Grubb 1966, 1971; Sadleir & Gilkes 1976; Davy 1979; Anand *et al.* 1991a). Here, rainfall is more plentiful and drainage more effective, kaolinite dissolves and gibbsite is precipitated. Gibbsite reaches maximum concentrations in the bauxite zone, decreasing significantly as the bauxitic zone passes down into kaolinitic saprolite. However, some profiles (e.g. at Jarrahdale railway cutting) have two gibbsite horizons (M. Paine & R. R. Anand unpubl. data). The first is in the lower saprolite at the base of the profile close to the weathering front. The second is at the top of the profile close to the surface. A kaolinite-rich horizon separates the two. Inland, gibbsite is generally absent or present in small amounts (<5%). Under strong leaching conditions, feldspars weather directly to gibbsite. More commonly kaolinite is the precursor for gibbsite (Figure 26). Gibbsite consists mostly of 0.1–2 μm anhedral platy crystals (Anand *et al.* 1991a). Occasional subhedral to euhedral hexagonal gibbsite crystals occur and most gibbsite crystals are present as components of basally orientated aggregates.

Very small amounts of boehmite and corundum occur in the upper part of the ferruginous duricrusts and in overlying ferruginous gravels, but Grubb (1971) also recorded these lower in the profile in the Darling Range. Corundum is associated with maghemite-rich samples in ferruginous duricrust and gravels and is considered to have formed by the dehydroxylation of Al oxyhydroxides in bush fires (Anand & Gilkes 1987b).

Goethite, hematite and maghemite

DISTRIBUTION AND ORIGIN

The nature of Fe oxides (general term used here for goethite, hematite and maghemite) that are formed by weathering is generally dependent more on the environmental conditions than on the particular structures of the primary mineral from which the Fe was released (Cornell & Schwertmann 1996). Iron oxide abundances generally increase towards the top of the profile (Figures 24, 25), although they may be very heterogeneously distributed and may be absent in certain zones (Figure 25a), yet be dominant minerals only a few centimetres below. Goethite may occur anywhere in the profile, but is especially common in the upper parts; it is absent only in the pale clays. Goethite-rich bands, possibly related to redox fronts, commonly occur in saprolite (Lawrance 1991). In nodules and pisoliths, hematite is generally more abundant than goethite. However, in places hematite is much less abundant in ferruginous duricrust. Such is the case at the Turrett pit, Lawlers, where goethite is dominant in duricrust developed on ultramafic rocks (Anand *et al.* 1991b). The presence of high amounts of hematite in nodules and pisoliths has been

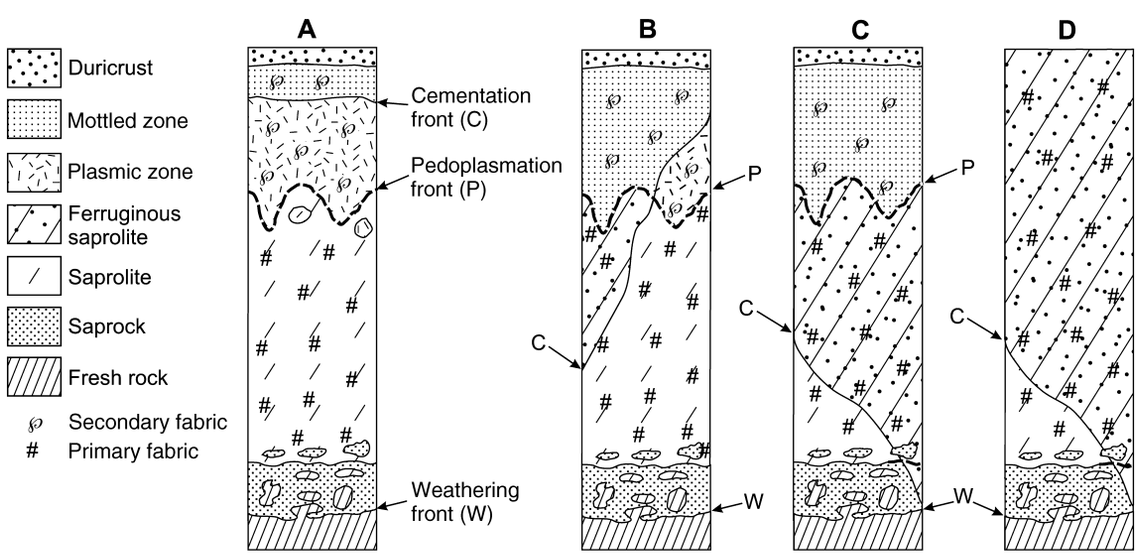

Figure 22 Fabric preservation by ferruginisation. A conventional profile (A) with progressive overlap of the pedoplasmation front by the ferruginisation front to preserve both pedoplasmic and saprolitic fabrics (mottled zone and mottled or ferruginous saprolite), leaving small patches of pedoplasmic fabrics unferruginised (B), to ferruginise all pedoplasmic fabrics and most saprolitic fabrics (ferruginous saprolite) (C) or to ferruginise most weathered materials, preventing pedogenesis (ferruginous saprolite and minor saprolite) (D) (after Robertson *et al.* 1998).

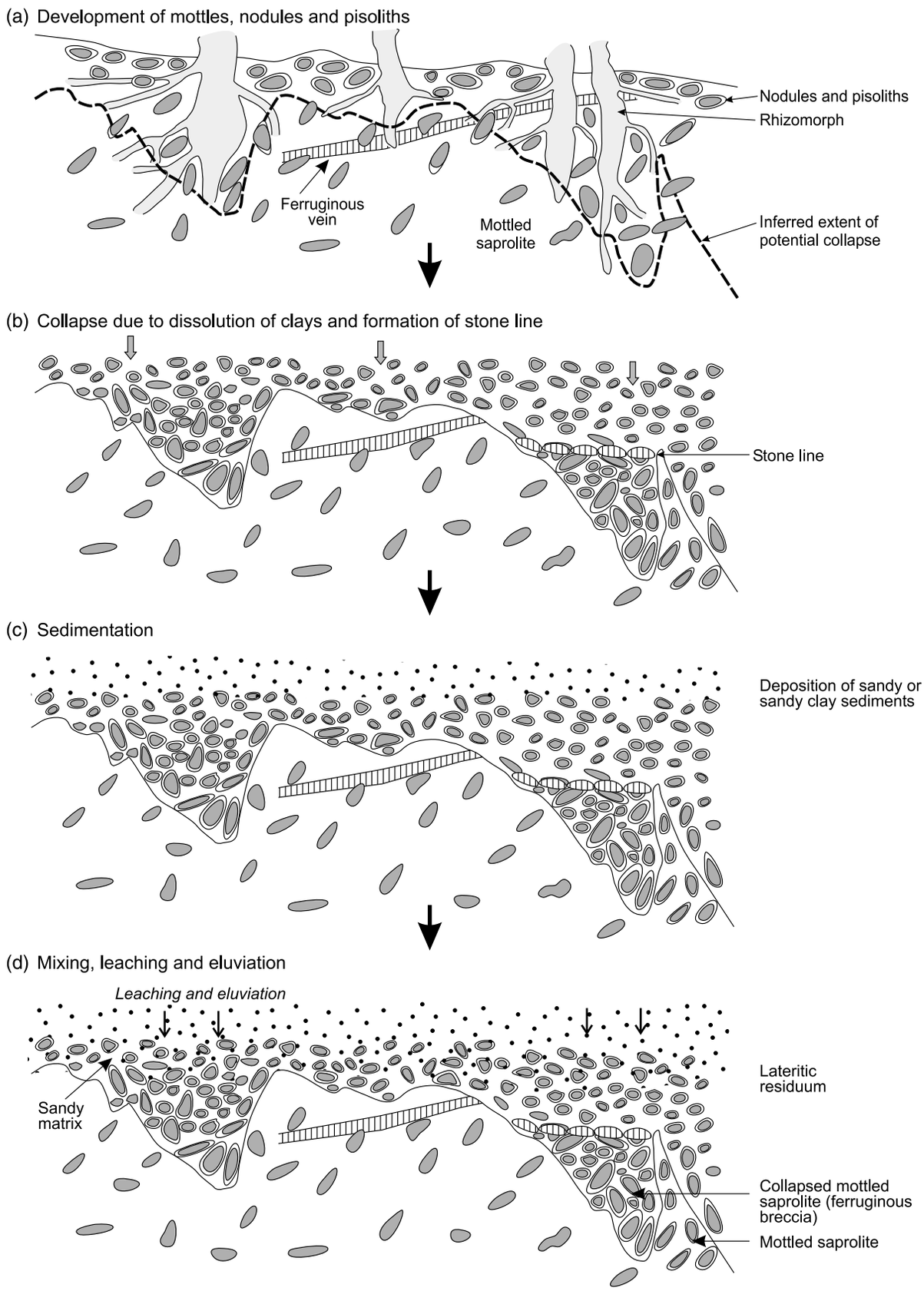

Figure 23 Interpreted model of formation of pendant-like structures and associated ferruginous materials. This is demonstrated by taking an example from the Calista deposit, Mt McClure.

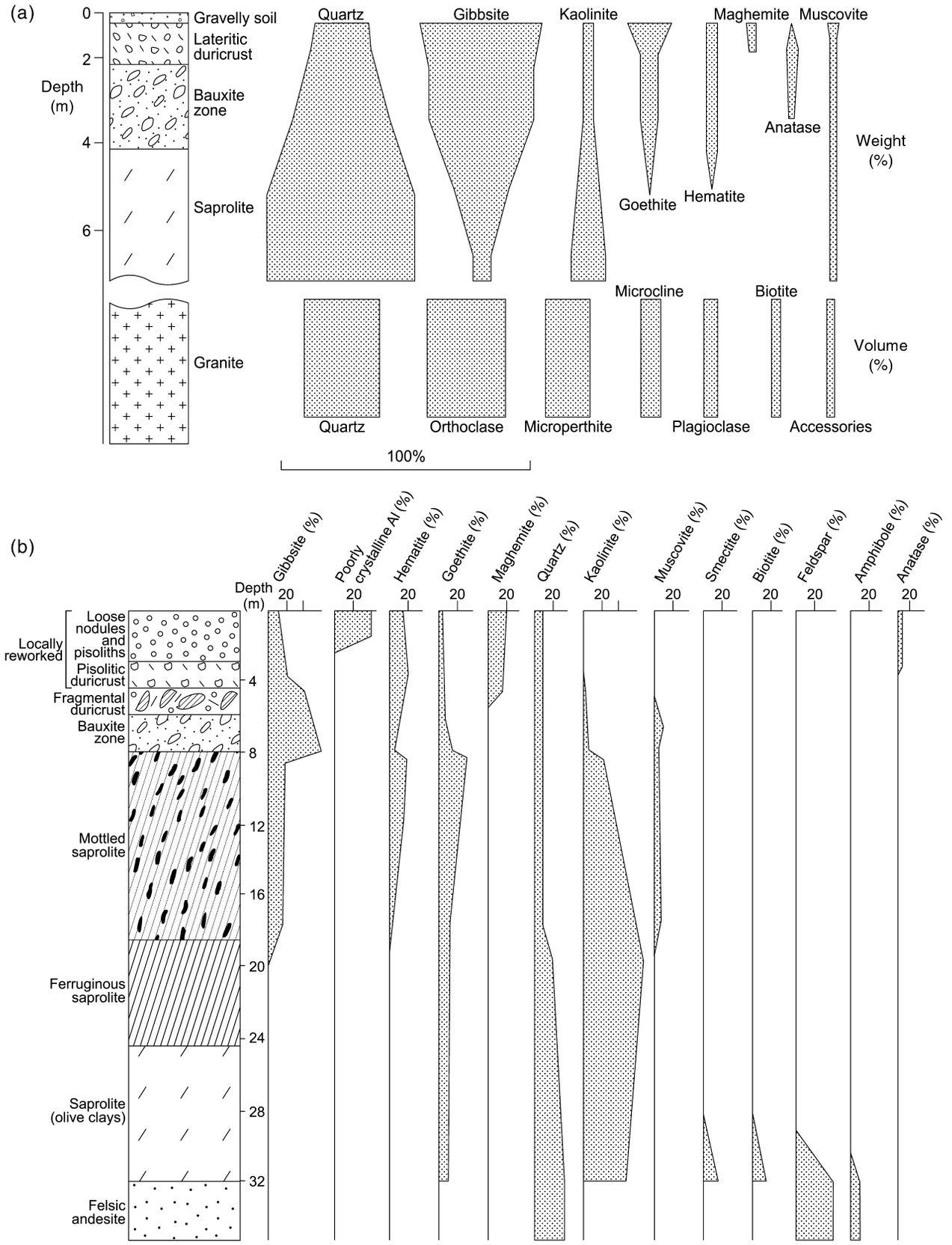

Figure 24 Mineralogy of the Darling Range bauxitic profiles. (a) On granitic bedrock: Jarrahdale (modified from Sadleir & Gilkes 1976). (b) On felsic andesite: Boddington (after Anand 1994).

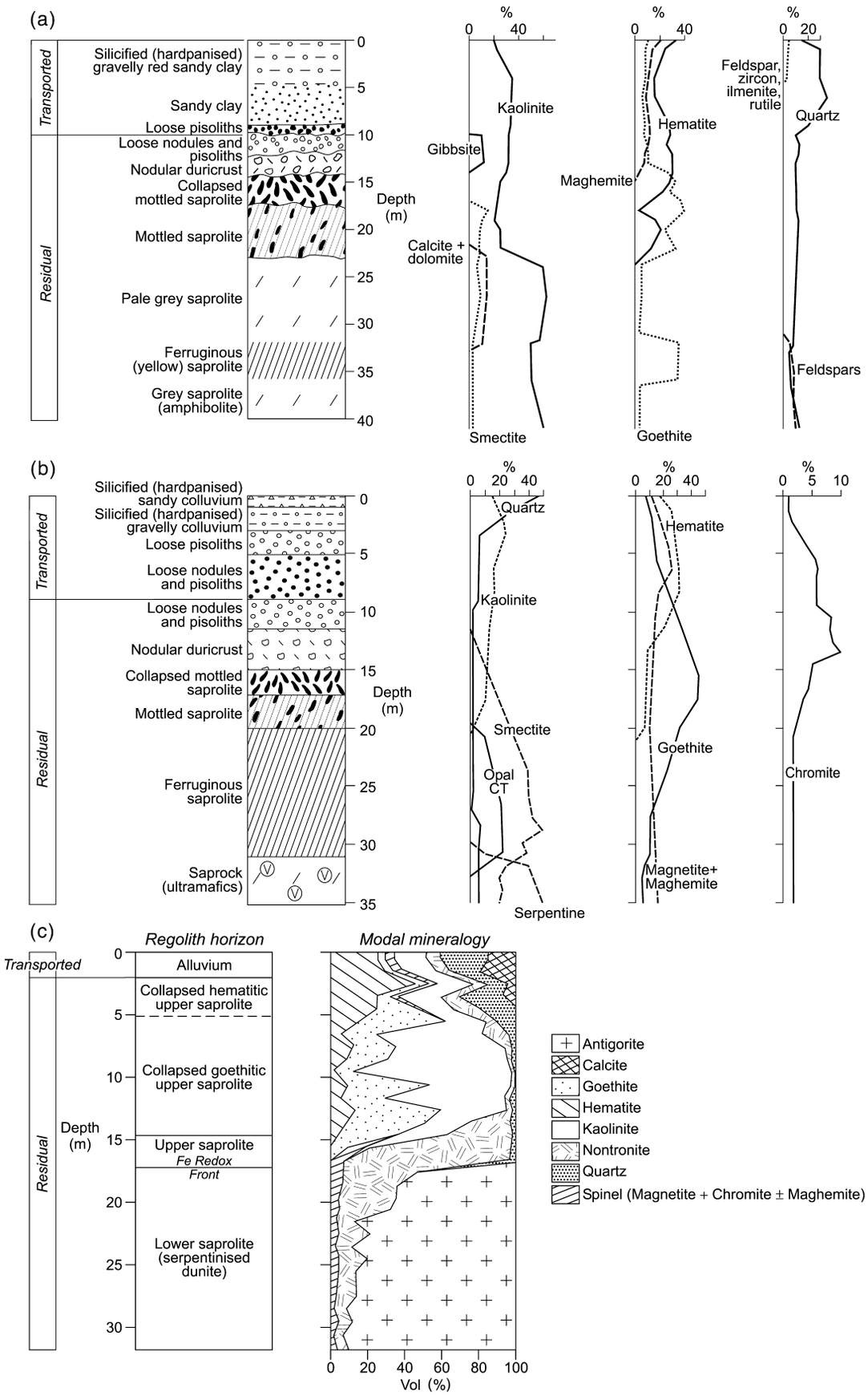

Figure 25 Mineralogy of inland kaolinitic weathering profiles. (a) On amphibolite: North pit, Lawlers. (b) On ultramafic rock: Turrett pit, Lawlers (after Anand *et al.* 1991b). (c) On serpentinised dunite: Bulong [after Elias *et al.* 1981 figure 2 (modified); Lawrance 1996]. Part (c) reprinted with permission from Economic Geology.

observed in several studies (Taylor & Schwertmann 1974; Anand & Gilkes 1987a).

Maghemite is generally present in near-surface loose pisoliths and duricrust (Figures 24, 25), but it may occur in saprolite developed on some ultramafic rocks (Figure 25). In the Darling Range, it is commonly associated with corundum (Anand & Gilkes 1987b). Maghemite may form on any rock type, but is more abundant on mafic and ultramafic rocks.

The crystal sizes of goethite and hematite are small. For example, in the Darling Range bauxitic duricrusts and soil goethite crystals range from 160 μm to 260 μm, whereas hematite ranges from 180 μm to 690 μm (Anand & Gilkes 1987a; Singh & Gilkes 1992a). Anand and Gilkes (1987a) observed that where both Fe oxides occurred in the same sample, hematite crystals were always approximately 60% larger than goethite crystals. Goethite and hematite crystals generally occur as platy, granular (Figure 29a) and in places as lenticular aggregates (Figure 29b). It is not possible to distinguish between goethite and hematite crystals because characteristic morphologies cannot be discerned. Goethite and hematite occur in soils as aggregates of very fine platy, subrounded or lath-like crystals rather than the acicular crystals, which are most commonly produced by laboratory synthesis (Torrent *et al.* 1980; Schwertmann & Kampf 1985).

The formation pathways of the different Fe oxides are complex. Iron oxides are the dominant products of weathering of Fe-bearing minerals (Figure 26). Under aerobic conditions and in the pH range of a normal weathering environment, the Fe^{3+} oxides are very stable and persist for a long time. However, in the anaerobic environment Fe^{3+} oxides may be reductively dissolved by microorganisms through the enzymatic transfer of electrons from the decomposing biomass. Because Fe becomes mobile by reduction, it can be redistributed over various distances: within a horizon, a weathering profile, a toposequence or even a landscape. Both hematite and goethite can form from ferrihydrite, and while ferrihydrite is believed to be a necessary precursor for hematite (Schwertmann 1988), goethite can precipitate directly from solution. Ferrihydrite has not been detected in ferruginous duricrusts of the Yilgarn Craton. Hematite certainly also forms by dehydroxylation of goethite and by oxidation of magnetite (Anand & Gilkes 1984c; Wells *et al.* 1989). In some cases, hematite is a relatively early weathering product, occurring either disseminated or segregated at depth in the profile. There, its coexistence with goethite is possibly the result of seasonally varying hydrological conditions that affect the ageing product of goethite. In the upper part of the profile, particularly in soils, hematite has commonly altered to goethite by rehydration (Tardy & Nahon 1985).

Maghemite tends to be associated with relatively high concentrations of hematite and low concentrations of kaolinite. Similar observations have also been made by Taylor and Schwertmann (1974) and Coventry *et al.* (1983) who explained this association on the basis of the inhibiting effects of aluminium in solution on the formation of maghemite and lepidocrocite. However, in the Darling Range, the maghemite-rich pisoliths contain large amounts of Al_2O_3 (40–50%), which indicates that maghemite may not have formed via solution, but by some other mechanism. Many hypotheses have been advanced for the formation of maghemite, for example, oxidation of magnetite, oxidation of green-rust at pH7–8 and transformation of other pedogenic oxides by heating at approximately 300–500°C in the presence of organic matter (Schwertmann 1988). Laboratory work suggests that dehydration of lepidocrocite is a possible source, but field relationships suggest that this transformation is unlikely in nature (Schwertmann & Taylor 1989). The most probable mechanism is heating of other Fe oxides between 300°C and 425°C. In particular, the association of hematite, maghemite and corundum in the near-surface horizons is probably evidence that they

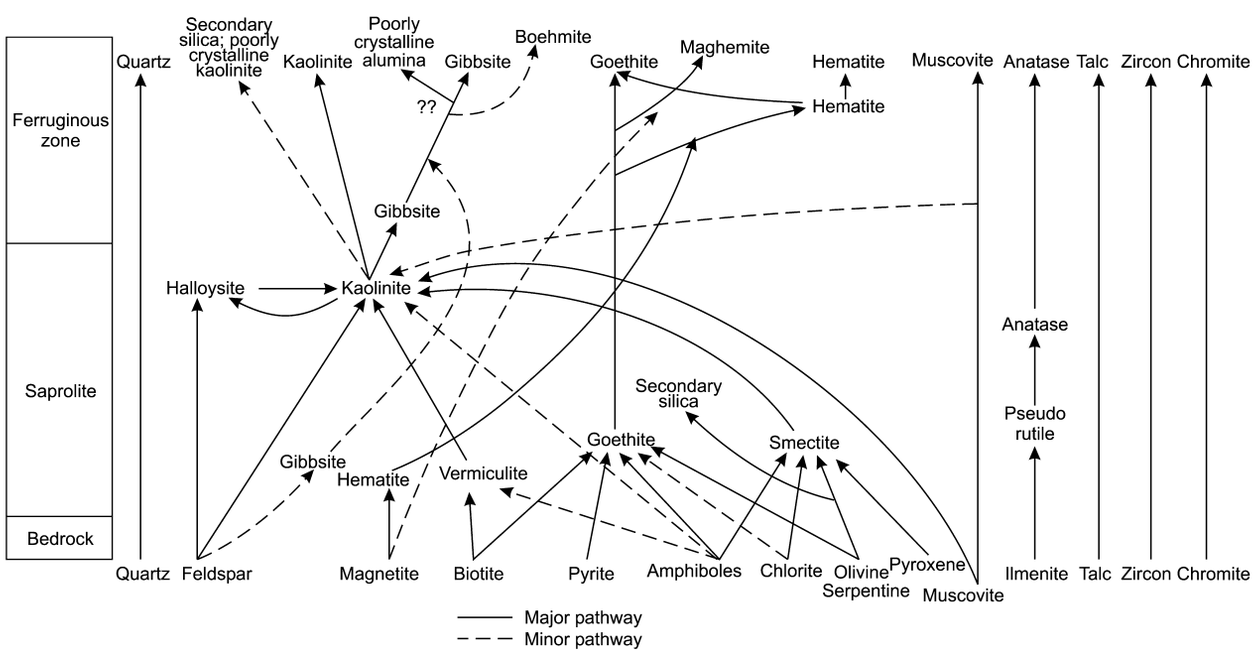

Figure 26 Pathways of formation of secondary minerals in weathering profiles (after Gilkes *et al.* 1973; Butt & Nickel 1981; Anand & Gilkes 1984a, b, c, 1987a, b, c; Anand *et al.* 1985; Singh & Gilkes 1991, 1992b; Robertson & Butt 1993).

have been exposed to fire. The maghemite and corundum contents are positively correlated, which may indicate a common origin due to dehydroxylation of Fe and Al oxyhydroxide (Anand & Gilkes 1987b). Ancient forest fires would have provided suitable conditions for the formation of maghemite from Fe oxides (Schwertmann & Fechter 1984; Milnes *et al*. 1985; Anand & Gilkes 1987b). However, the maghemite that occurs in saprolite developed on ultramafic rock cannot be explained by the heating mechanism. It may have formed through a topotactic reaction by the natural oxidation of primary magnetite (Fontes & Weed 1991).

ALUMINIUM SUBSTITUTION IN Fe OXIDES

Aluminium substitution for Fe is quite common in both goethite and hematite, and it affects unit cell size, particle size and crystallinity (Taylor 1987). The extent of Al substitution in goethite and hematite is a sensitive indicator of the pedogenic environment of Fe-oxide formation and is dependent on accompanying minerals (Fitzpatrick & Schwertmann 1982; Schwertmann 1988). The ranges and means of percentage of Al substitution in goethite indicate systematic differences for the various categories of materials and between regions (Table 2). Inland, substitution of Al ranges from 6 mole% to 28 mole% in goethites of lateritic residuum rich in kaolinite (Table 2) (Davy & Gozzard 1995; Anand 1998). This contrasts with Al substitution ranges of 22–35 mole% in goethites associated with gibbsite in bauxitic duricrusts in the Darling Range at Boddington (Table 2), Jarrahdale, Del Park, Huntly and Willowdale (Anand & Gilkes 1987a). These values are consistent with those for highly weathered materials in Australia and elsewhere (Fitzpatrick & Schwertmann 1982; Schwertmann & Kampf 1985). Values in excess of 33 mole%

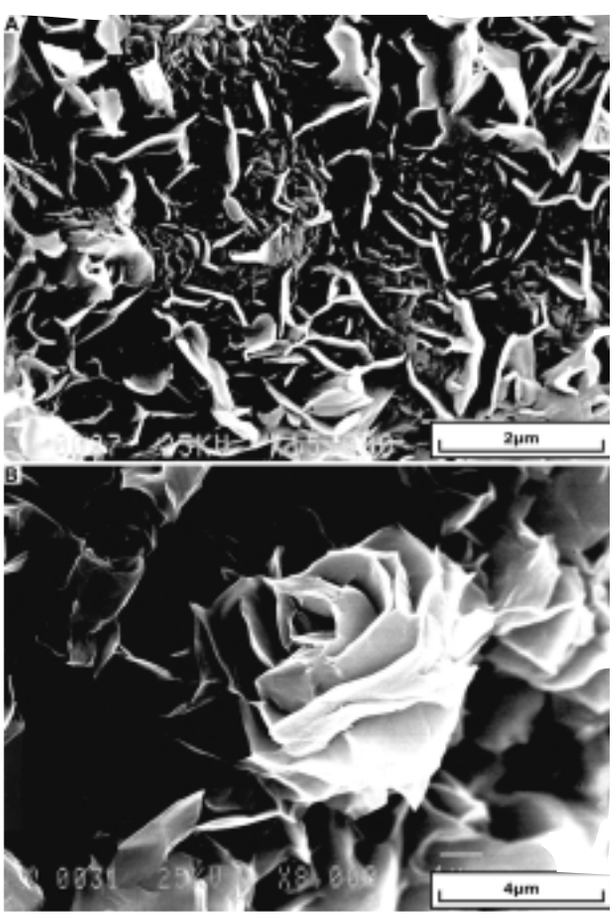

Figure 27 Scanning electron micrographs of lower saprolite formed from basalt showing different morphologies of smectite: Sundowner. (a) Thin flakes with irregular outlines. (b) Aggregates of rose shaped crystals. R. R. Anand unpubl. data.

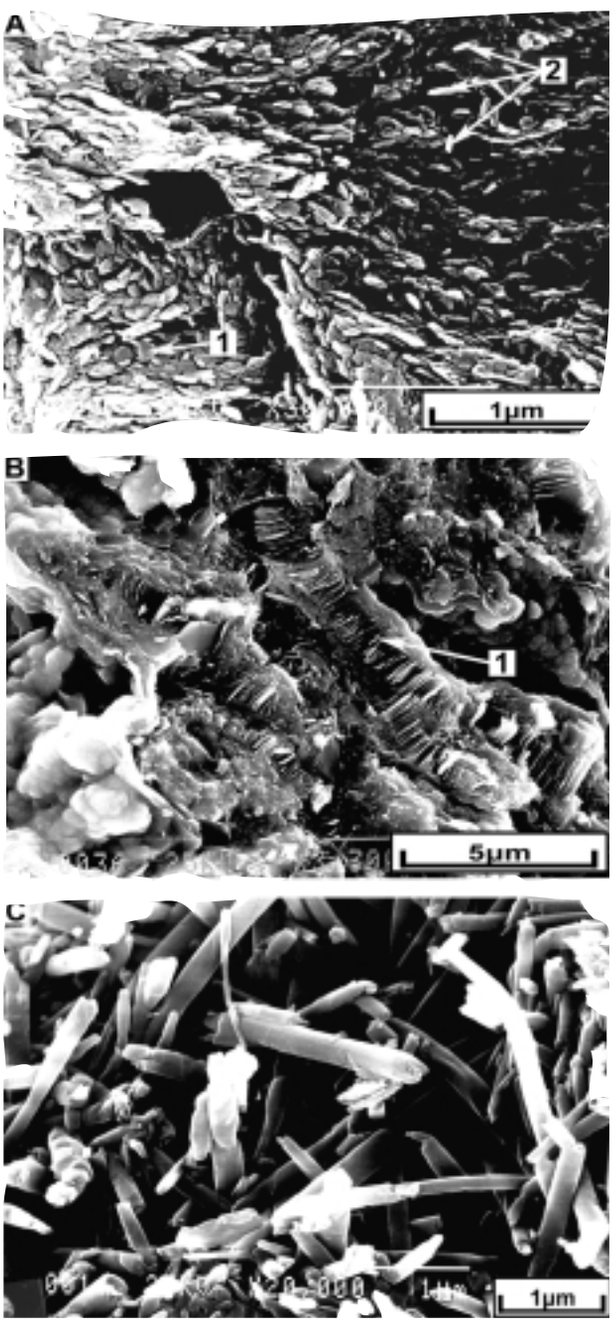

Figure 28 Scanning electron micrographs of upper saprolite formed from basalt. (a) Platy crystals of kaolinite (1) and tubular crystals of halloysite (2): Sundowner. (b) Accordian structure of kaolinite after mica (1): Sundowner. (c) Tubular crystals of halloysite in a ferruginous pisolith: Ora Banda. R. R. Anand, C. Phang and J. E. Wildman unpubl. data.

Al substitution do not occur in nature and a similar limit has been observed in laboratory synthesis experiments (Schwertmann 1985). The morphologically distinct materials (i.e. pisolith cores, matrix and cutans) separated from bauxitic duricrusts in the Darling Range showed that the levels of Al substitution in goethite and hematite in the matrix (mean 25 mole%) and pisolith cutans (mean 25 mole%) were systematically lower than for cores of pisoliths (29 mole%) (Anand & Gilkes 1987b). Fitzpatrick and Schwertmann (1982) also found that goethites in ferruginous bauxites from South Africa were highly substituted, containing between 20 mole% and 25 mole% Al and that the nodule rinds contained goethite with lower amounts of Al substitution (14–18 mole%) than in cores (20–27 mole%).

Anand and Gilkes (1987a) found no significant differences in levels of Al substitution in Fe oxides between lateritic residuum on granite and dolerite in the Darling Range. The two parent materials provide quite different amounts of Fe, Al and other ions, but these differences had no effect on Al substitution, which must reflect pedochemical conditions rather than the gross abundance of ions. By contrast, Singh and Gilkes (1992a) found that substitution of Al in goethite was higher for soils on felsic rocks (median value 26 mole%), compared to soils on alluvial (17 mole%) and mafic (19 mole%) parent materials. However, no reasons were given for these differences.

Goethites in ferricretes show the least Al substitution (1–11 mole%) (Davy & Gozzard 1995; Anand 1998). In conglomeratic and pisolitic ferricretes, the extent of Al substitution in the goethite cement is systematically lower than for ferruginous clasts (not shown in Table 2). Goethite in mottled zone and ferruginous saprolite has less Al substitution (8–23 mole%) than in overlying lateritic residuum.

The difference in Al substitution in goethite between the various types suggests different environments and/or mechanisms of formation. Minimal Al substitution in goethite of ferricretes suggests an environment almost lacking soluble Al. In ferricretes, Fe is probably derived hydromorphically by absolute accumulation (Fitzpatrick & Schwertmann 1982), or by Fe migration in strongly reducing conditions (organic complexes: Fitzpatrick 1988). In contrast, the goethite in lateritic residuum has formed in an Al-rich environment, indicated by the presence of kaolinite and gibbsite. On the basis of the differences in Al substitution between the cutans and cores of pisoliths, Fitzpatrick and Schwertmann (1982) believed that the two different goethites might have formed during different phases of profile development and that goethite in the cutans formed under reductomorphic conditions that resulted in lower levels of Al substitution.

Hematite has generally less Al substitution than coexisting goethite (Anand & Gilkes 1987a; Singh & Gilkes 1992a; Davy & Gozzard 1995), and this is consistent with the findings of Schwertman (1985) who found that hematite can accommodate about half as much Al as coexisting goethite. Aluminium substitution in maghemite is generally low (<5 mol%). These low levels of Al substitution may

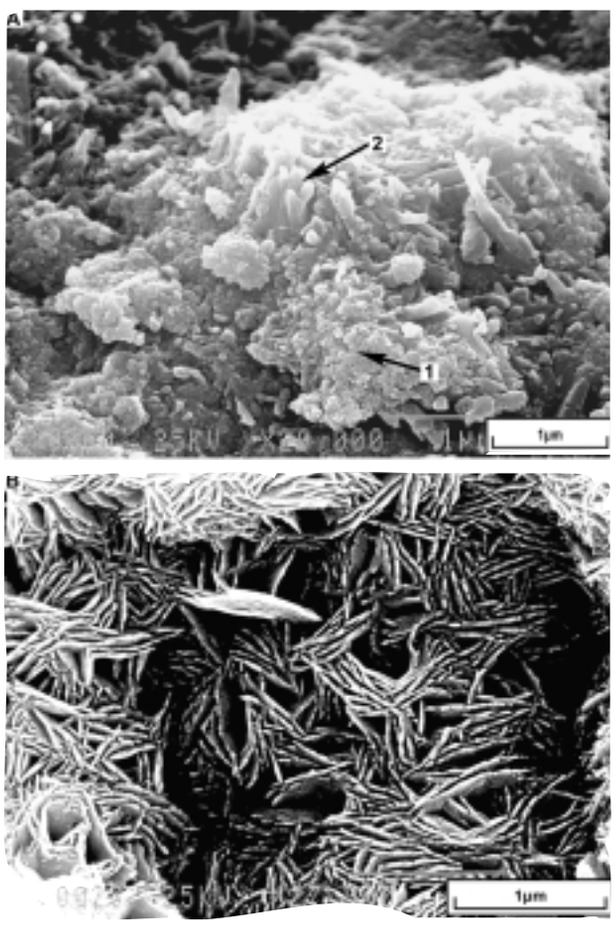

Figure 29 Scanning electron micrographs of ferruginous pisoliths showing different morphologies of goethite. (a) Aggregates of platy crystals of goethite and hematite (1) with a few tubular halloysite crystals (2): Ora Banda. (b) Lenticular goethite: Bronzewing. R. R. Anand, C. Phang and J. E. Wildman unpubl. data.

Table 2 Mole% Al substitution in goethite for various categories of regolith materials.

	Lateritic residuum		Ferricretes		Ferruginous saprolite and mottled zone
	Boddington (Darling Range)	Lawlers Mt Gibson (inland)	Lawlers Ora Banda Grants Patch (inland)	Leonora[a] (inland)	Lawlers Mt Gibson Bronzewing (inland)
Sample	$n = 25$	$n = 58$	$n = 19$	$n = 10$	$n = 23$
Range	22–35	6–28	1–10	2–11	8–23
Mean	28	19	4	4	13

[a]after Davy and Gozzard (1995); other data after Anand (1998).

not be significantly different from zero because the very small observed displacements in X-ray diffraction (XRD) peak position could, alternatively, be due to strain or the variation in structure factor over broad reflections (Schulze 1984). Substitution of Al in maghemite has been found to vary from 2% to 15% in a range of highly weathered soils (Schwertmann & Fechter 1984), but values significantly different from 0% are generally uncommon.

Poorly crystalline minerals

Recent examination of regolith materials by transmission electron microscopy and differential XRD has allowed mineralogical characterisation of these materials, and their importance in regolith mineralogy and geochemistry is gradually being recognised (Anand 1994; Singh & Gilkes 1995; Tilley & Eggleton 1996; Eggleton 1998). Poorly crystalline minerals occur in various forms and abundances in the weathering profile. Two main types are observed.

(1) Poorly crystalline minerals formed directly from primary minerals at the base of the weathering profile. These may be only temporary phases that generally alter to more crystalline phases. Banfield and Eggleton (1990) conducted transmission and analytical electron microscope (TEM and AEM) studies on weathering of granodiorites and found protocrystalline material forming an alteration layer <1 mm thick on feldspar surfaces. However, this was not found to be a significant constituent in weathering feldspars in the Darling Range (Anand *et al.* 1985). Although hisingerite [$Fe_2Si_2O_5(OH)_4$] is generally thought to be a rare amorphous alteration product of Fe sulfides, carbonates

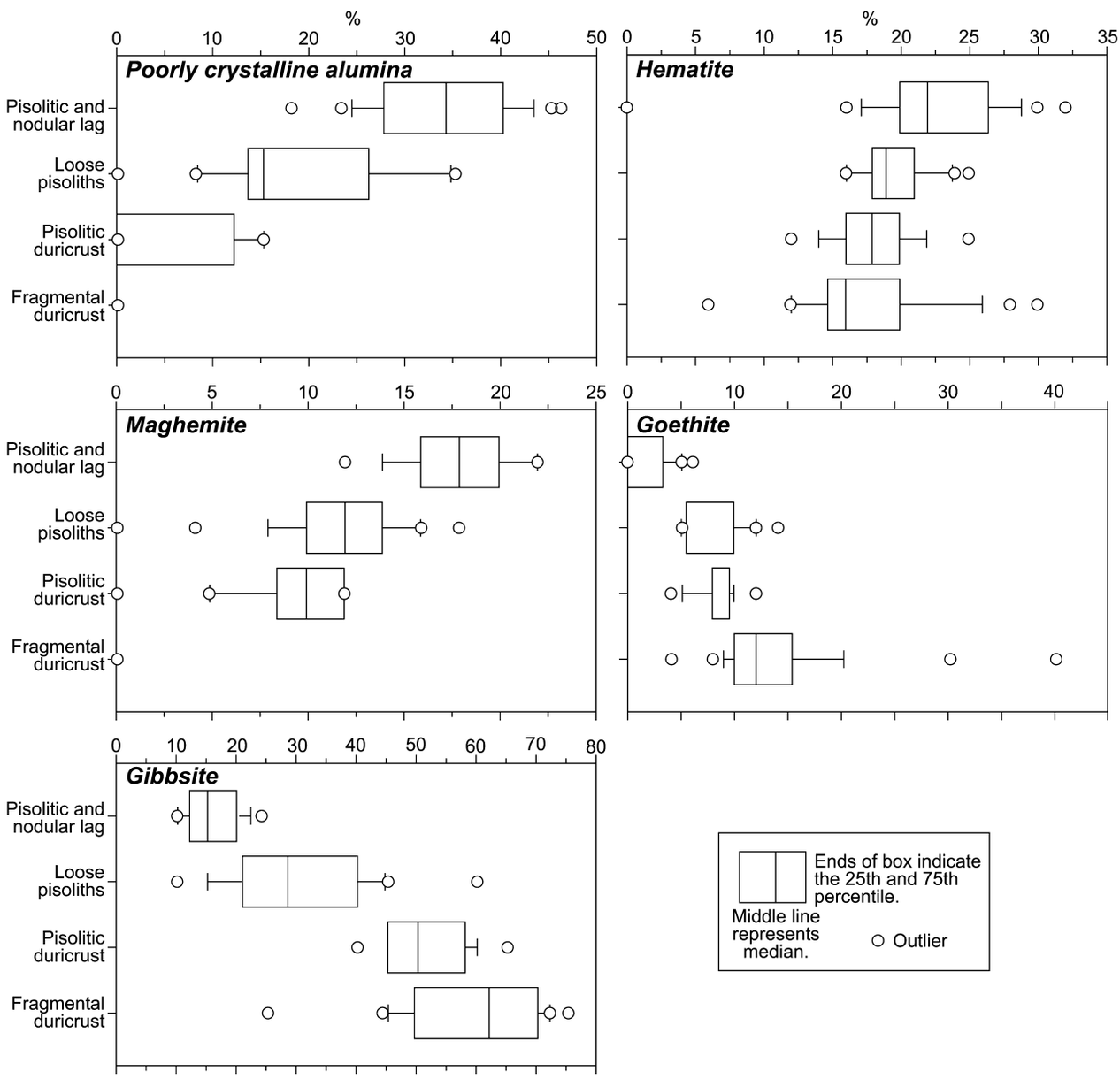

Figure 30 Distribution of poorly crystalline alumina, hematite, maghemite, goethite and gibbsite in the ferruginous zone of bauxitic weathering profiles from the Boddington gold deposit (after Anand 1994).

and silicates, it has been recently shown to be a ferric form of spherical halloysite. Transmission electron microscope studies of weathering of amphibole (Wang 1988) and chlorite (Aspandiar 1992) suggest that hisingerite may be a common first alteration product.

(2) Poorly crystalline minerals that form at or near the surface. The upper part of the weathering profile, particularly ferruginous pisoliths and nodules and sediments, commonly yield very weak XRD patterns. X-ray diffraction studies of pisoliths from the Darling Range suggest that some poorly crystalline alumina (PCA) is also present in addition to crystalline Al minerals (gibbsite, corundum and boehmite). The PCA appears to be a major constituent in near-surface magnetic pisoliths and nodules and decreases markedly or disappears in subsurface fragmental duricrust (Figure 30) (Anand 1994). The trend in PCA distribution in the profile is similar to that of hematite and maghemite, but is opposite to goethite and gibbsite. Indications of PCA also come from the relationship between Al_2O_3 and loss on ignition. Poorly crystalline alumina has low loss on ignition. The loss on ignition is essentially an indirect indication of gibbsite, goethite and kaolinite contents. Figure 31a shows two distinct populations for Al_2O_3 and loss on ignition, one with a positive correlation and one with a negative correlation. For the same level of Al_2O_3, the fragmental duricrust and bauxite samples show much higher loss on ignition than the pisolitic and nodular lag. This suggests that most Al in the pisolitic and nodular lag is present as PCA, not gibbsite. Singh and Gilkes (1995) subsequently demonstrated that this unaccounted alumina is χ-alumina, one of the several poorly crystalline forms of anhydrous alumina. χ-alumina produces a broad, but distinctive, XRD pattern that is unrecognisable in the presence of maghemite and hematite. This relationship was not observed for inland pisoliths and nodules (Figure 31b), where PCA is either absent or present in small amounts. Here, most Al is present as kaolinite. The reasons for this distribution between the two regions are not clear and further research is required to understand this variability. Tilley and Eggleton (1996) have also shown from Weipa bauxites that near-surface regolith materials may contain PCA (η-alumina).

Amorphous to poorly crystalline aluminosilicates have been suggested to occur as cementing agents in saprolites, red-brown hardpans and silcretes, particularly in granitic terrains in the Yilgarn Craton (Brewer & Bettenay 1973; Killigrew & Glassford 1976; Butt 1983; A. Mahizhnan pers. comm. 2000). This suggestion was supported by observations of the active precipitation of allophane from groundwaters in a broadly similar environment in Western Australia (Thornber *et al.* 1987). These are novel occurrences because amorphous aluminosilicates typically occur in immature soils developed from volcanic glass (Wada 1989). This aluminosilicate cement may have originally been amorphous allophane, but high-resolution electron microscopy shows that it has now recrystallised, on a submicrometre scale, to a mixture of kaolinite and opaline silica (Singh *et al.* 1992).

X-ray diffraction patterns of sediments generally show disordered kaolin compared to the underlying *in situ* regolith. The crystallinity of kaolin can be determined by the Portable Infrared Mineral Analyser (PIMA-11) (Gray & Cudahy 1996; Pontual & Merry 1996; Phang & Anand 2000). Several authors have shown that transported overburden (Quaternary colluvium and alluvium and Tertiary palaeochannel clays) and residual regolith can be discriminated by differences in kaolinite crystallinity. Pontual and Merry (1996) indicated that kaolinite

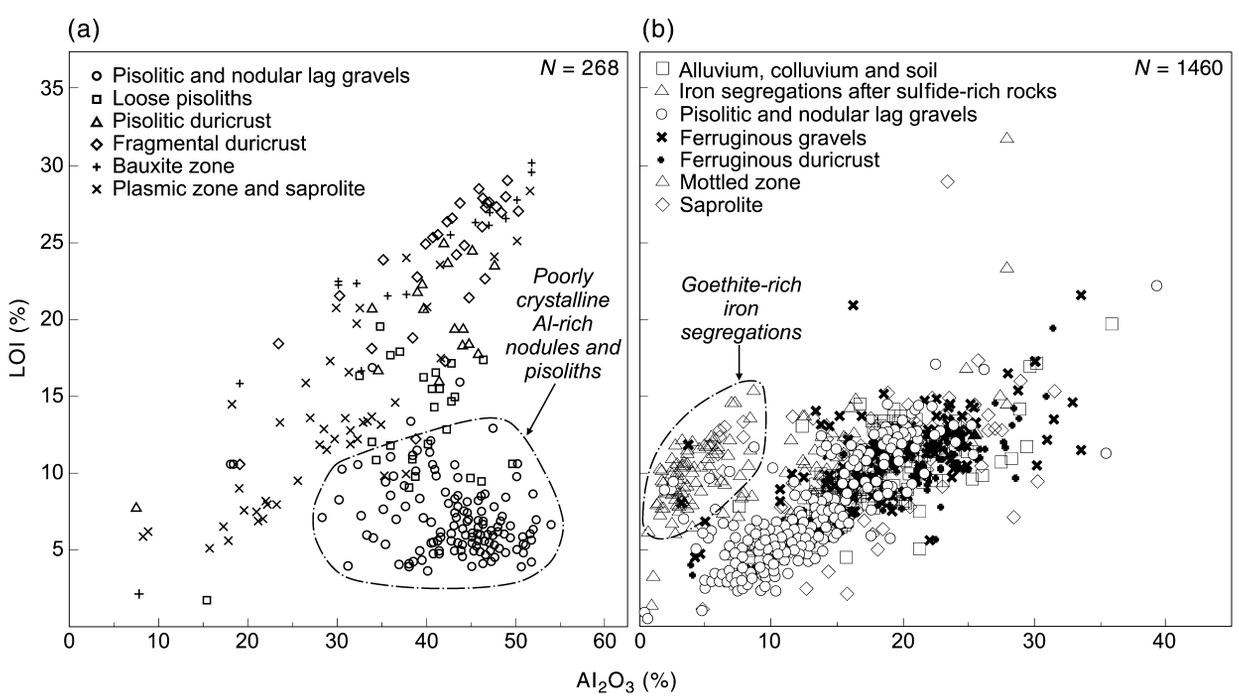

Figure 31 Relationship between Al_2O_3 and loss on ignition (LOI) in regolith units from (a) Boddington gold deposit (after Anand 1994) and (b) Inland (R. R. Anand unpubl. data).

crystallinity is best depicted using the reflectance ratio (r) of 2160/2177 nm. A similar result was obtained by Phang and Anand (2000), but they also found that 2164/2181 nm gave a similar result (Figure 32). The higher the r value, the less ordered the kaolinite. Based on 16 drillholes at Bronzewing, it was observed that higher r values are associated with palaeochannel clays. A ratio of r = 1 is a suitable threshold value to separate transported from residual regolith for most samples (Figure 33). However, samples containing muscovite/illite from felsic intrusives have an absorption peak at 2200 nm, which interferes with this calculation.

Variations in the degree of 'order–disorder' of kaolinite group minerals were recognised many years ago (Brindley & Robinson 1946) and have been attributed to genetic factors (profile drainage, vegetation, parent material and profile depth) that might influence the environment in which the kaolinite crystallised. The reasons for poorly crystalline kaolinite in sediments are unclear, but it appears that crystallinity of kaolinite in sediments has been modified during transportation, diagenesis or post-depositional weathering.

Quartz and opal

Quartz contained in the regolith may be either residual or transported, having resulted from the weathering of the underlying bedrocks and/or a variety of sedimentary processes. There is also evidence of abundant crystalline secondary quartz in silcretes over a variety of rocks (Butt & Nickel 1981; Butt 1985).

Muscovite, fuchsite and talc

The weathering of muscovite and talc to kaolinite is well documented (Singh & Gilkes 1991; Eggleton 1998), although they may persist throughout the weathering profiles (Anand & Gilkes 1987c; Robertson & Butt 1993). Flakes of muscovite, partly altered to hydromuscovite, may occur even in the ferruginous duricrust and overlying lag, where they are set in, and apparently protected by, goethite. Apart from being rock-forming minerals, micas (muscovite or fuchsite) are important components of phyllic alteration haloes around mineralisation and their survival has exploration implications. Talc, for example, is a useful indicator of ultramafic rocks.

Titanium and zirconium minerals

Anatase is a common mineral in the upper regolith. It can form authigenically (Milnes & Fitzpatrick 1987), but commonly forms from the weathering of silicates containing Ti. Ilmenite oxidises and then hydrolyses to form pseudorutile. Pseudorutile, which may contain Fe^{2+} and Fe^{3+} and Mn in addition to Ti in oxide form (Grey & Reid 1975; Anand & Gilkes 1984a), can then dissolve to give either rutile (Grey & Reid 1975) or anatase (Anand & Gilkes 1984a). In the weathered beach sands studied by Grey and

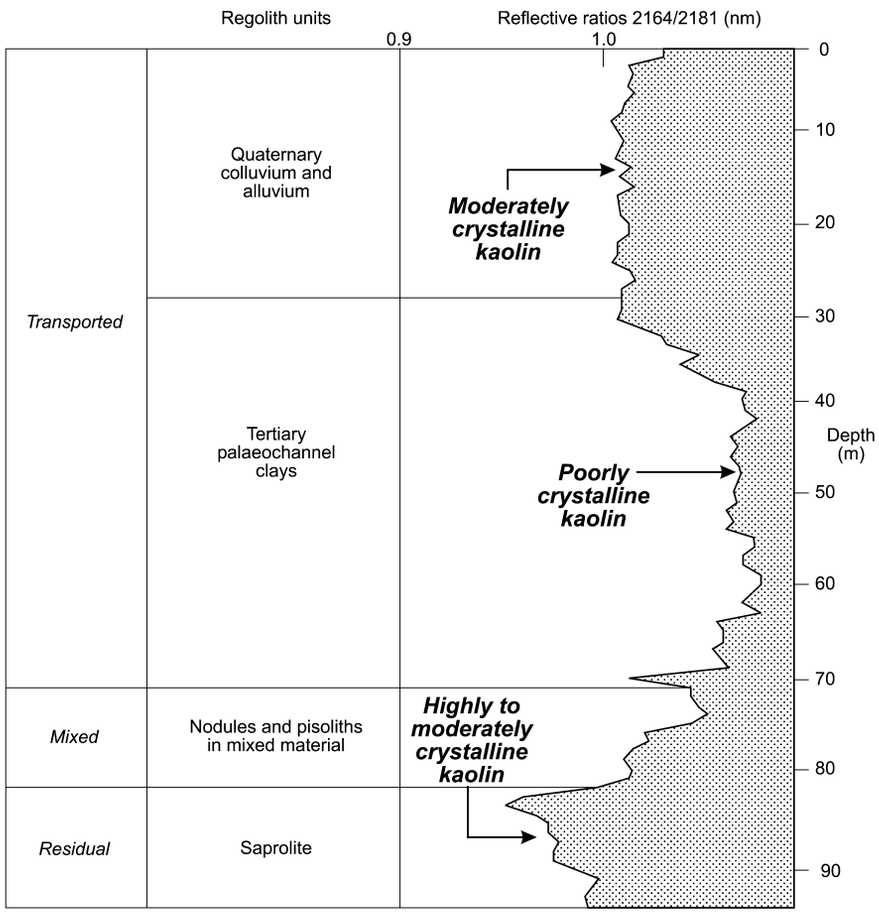

Figure 32 Ratio of reflective intensities in drill cuttings, Sundowner. 2164/2181 nm reflectance ratio measured by the Portable Infrared Mineral Analyser (PIMA) gives the most appropriate parameter for measuring the overall disorder of kaolin (after Anand 2000).

Reid (1975), hematite formed with rutile, whereas in the saprolite zone of the lateritic weathering profile studied by Anand and Gilkes (1984a), Fe oxides were lost, but halloysite, kaolinite and gibbsite crystallised out in pores with the anatase. According to Anand and Gilkes (1984a), the lower density of anatase compared to rutile may have enabled it to crystallise in the presence of other ions in soil solution within the weathering profile, while the low concentrations of other ions in solutions from beach sands would allow the denser rutile to form there.

Zirconium and titanium are very widely used as immobile elements, mainly because they occur in most rocks only as the minerals zircon, anatase and rutile, which are considered to be very resistant to weathering. The immobile element approach assumes that one or more elements have not been affected by weathering, undergoing neither dissolution or physical translocation, or that their mobility is restricted to a region smaller than the sample size. With this assumption, the ratio of the immobile element content in a weathered sample to its content in the parent rock is a measure of the overall loss suffered by the rock during weathering. Provided there is no mechanical movement of zircon in or out of the profile, Zr is probably the least mobile of the common elements (Eggleton 1998). Nonetheless, the presence of leached, skeletal zircons (e.g. in silcretes: Butt 1985) and, conversely, reports of the presence of overgrowths on zircon, indicate that even Zr can become mobile under certain circumstances. Braun *et al.* (1993) showed clear evidence for zircon dissolution during the weathering of a syenite from Cameroon. Furthermore, zircon can be added by aeolian action. For example, in Jarrahdale, two populations of zircons were identified by Brimhall *et al.* 1988). The euhedral grains were interpreted as having been derived from the granitic bedrock, whereas the rounded grains were regarded as having been introduced by translocation of exotic aeolian material from the surface. Foo (1999) determined the concentrations of Zr in different parts of pisoliths at Boddington and found that Zr is higher in the cutans of pisoliths, which may support its derivation from external sources during the formation of the cutans.

Titanium occurs in rocks largely as rutile, ilmenite and sphene, or in the structure of micas, amphiboles and pyroxenes. The susceptibility of these minerals to weathering increases from micas through to pyroxenes. Titanium is, therefore, released early in the weathering of igneous rocks and continues to be released as weathering proceeds. Its mobility during weathering in solution is poorly understood because of its extreme solubility at regolith pH (Eggleton 1998). If Ti precipitates immediately on release from its parent material as anatase, it becomes fixed in the weathering profile and may be effectively immobile. Presumed physical migration of anatase particles (Milnes & Fitzpatrick 1987) and chemical precipitation of Ti as anatase (Butt 1985) have been documented particularly in silcretes.

Hallberg (1984) showed that the major groups of igneous rocks could be distinguished even in the moderately weathered state by the Ti/Zr ratio. Basalt has a Ti/Zr ratio >60, andesite ranges from 60 to 12, dacite from 12 to 14 and rhyolite is generally <4. Inevitably, the fields show some overlap. This method of distinction works well for moderate to severe weathering in the saprolite and the plasmic zone (Figure 34). However, some of these near-

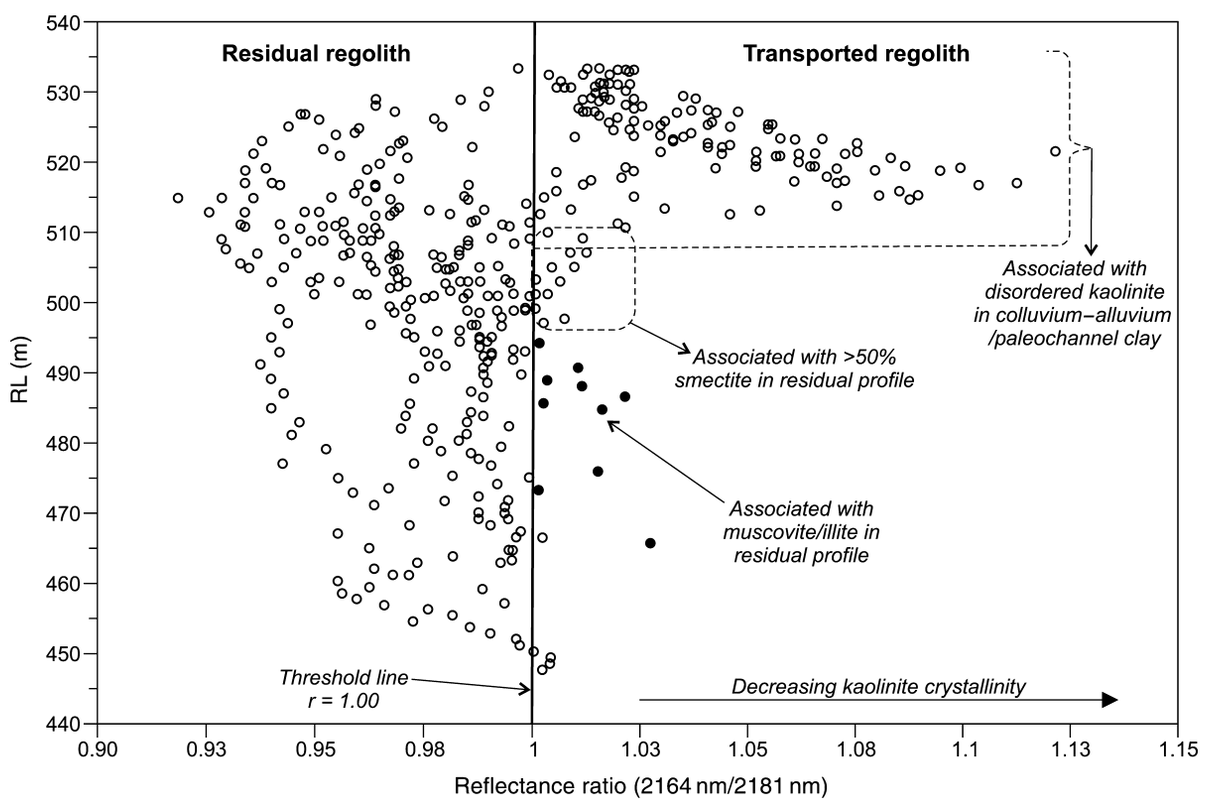

Figure 33 Overall reflectance ratio 2164/2181 nm for 16 drill-cutting samples versus depth in RL (m) (after Phang & Anand 2000).

surface materials (mottled zone and duricrust) have abnormally low Ti/Zr ratios (Robertson & Butt 1993; Anand 1994; Davy & Gozzard 1995; Anand 2000). Thus, this method has limited application in the mottled zone and in the duricrust.

Carbonates and sulfates

Primary carbonates occur near the base of the profile where they may either form part of the alteration halo or be due to widespread greenstone carbonation. Because they weather and dissolve so readily, carbonates are absent from all but the top of the profile, where they reappear as secondary carbonates. Under arid conditions, carbonate precipitation is widespread in the regolith (this topic is dealt with in detail below under the heading: Calcrete). These carbonates may include calcite, dolomite (Figure 35a, b, e) or magnesite or mixtures of these. Dolomite and magnesite are commonly developed over ultramafic rocks. Sulfur-bearing minerals, such as sulfides, are consumed at the base of the profile, but sulfates (barite, gypsum and alunite) appear within the regolith. Deposition of secondary carbonates and sulfates, except for some barite, is not linked to a particular part of the weathering profile and deposition appears to be a late event.

Palygorskite and sepiolite

Palygorskite and sepiolite tend to occur in arid regions (Allen & Hajek 1989). It has been noticed in some sites that samples rich in dolomite also contain some palygorskite, which occurs as dense mats up to 1 μm wide and 8 μm long (Figure 35b, e) (Anand *et al.* 1997). Palygorskite is common in calcretes and its genesis has been ascribed to *in situ* weathering or lacustrine environments (Arakel 1986). At Mt Gibson, palygorskite occurs in residual calcareous soils overlying mafic bedrock (Figure 35e), whereas at Bronzewing it occurs in dolocrete formed in palaeochannel sediments (Figure 35b). At Mt Gibson, its formation appears to be controlled by the bedrock, whereas at Bronzewing its genesis is related to lacustrine environments. Authigenic sepiolite is abundant in groundwater calcretes (Butt 1988).

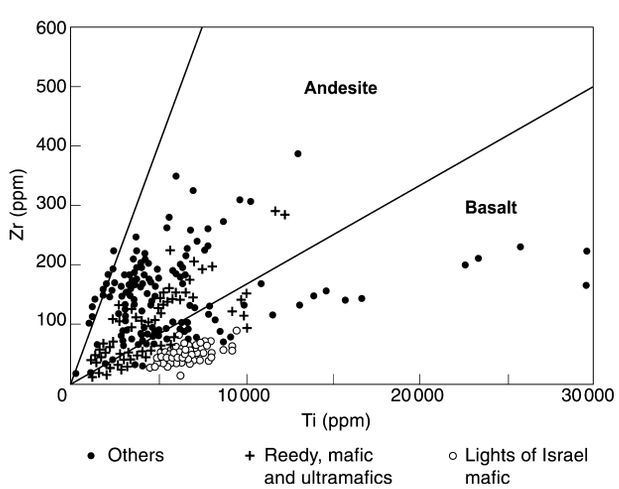

Figure 34 Ti–Zr 'Hallberg' plot of the database comparing the basaltic trend of amphibolites from Lights of Israel and the 'andesitic' trend of rocks from Reedy (after Robertson & Butt 1993). 'Others' refers to samples from Ora Banda and Mt Percy.

BIOLOGICAL WEATHERING

In general, literature on the weathering of primary minerals and the formation of secondary minerals in the regolith has considered the processes to be governed wholly by inorganic chemical reactions, mineral stability fields and the concept of equilibrium chemistry. In practice, processes such as diffusion, adsorption/desorption and modification of the regolith in the rhizosphere play major and commonly dominant roles in determining the nature and rate of weathering reactions (Gilkes 1998). The role of biota in regolith formation can be observed both on macro- and micro-scales, particularly in the upper parts of weathering profiles. The morphology of the regolith may also reflect these processes. Some of the main features of biological weathering are briefly described below.

(1) The coarse reticulate or vermiform pattern of pale grey mottles that commonly occurs in the clay zone and in some ferruginous duricrusts appears to be biogenic, related to an environment created by tree roots (Figure 13e on Plate 3).

(2) Scanning electrom microscope (SEM) analysis of regolith materials reveals fabrics and materials that have formed by replacement of biological materials by minerals. For example, deposition of biogenic carbonate has a profound effect on regolith morphology (Figure 35a, b). At Mt Gibson, needle-fibre calcite (Figure 35a) and micro-rod calcite in pedogenic carbonates are probably calcified remains of fungi, algae, root hairs and bacteria (Klappa 1979). The needles are 20–160 μm long, straight or gently curved, and vary in diameter from 0.2 μm to 2.0 μm (Anand *et al.* 1997). Radial dolomite (Figure 35b) from dolocrete of palaeochannel sediments at Bronzewing is probably bacterial in origin (Vasconcelos & McKenzie 1997).

(3) Plant materials are commonly replaced by goethite or hematite in ferruginous duricrust (Anand *et al.* 1991b; Robertson & Butt 1993; Davy & Gozzard 1995; Anand 1998). Figure 35c shows the replacement of stromatolitic layers by goethite in cutans of concentric pisoliths in palaeochannel sediments.

(4) Examination of SEM images of the red-brown hardpans show areas of silicified root remnants (Figure 35d). These are similar to the vegetative hyphae of actinomycetes. Actinomycetes are known to colonise root cells extensively subsequent to cell lysis (Mayfield *et al.* 1972).

(5) Although the enrichment of Fe and Al in the regolith is largely due to the accumulation of insoluble constituents, the role of vegetation in the cycling of elements is also regarded as an important mechanism. For example, Rose *et al.* (1993) observed that in addition to mobile elements (K, Na, Mg, P and S), Si, Al, Fe and Mn cycled through the vegetation are an appreciable fraction of the amount in the soil for the Igarape Bahia Au deposit in the Serra Carajas mining region (Brazil). Rose

et al. (1993) proposed that over a period of 10^7 y, a major proportion of the Si, Al, Fe and Mn in the soil is picked up by roots and moved into above-ground vegetation, to be returned to the surface of the soil after the death of the vegetation. They argued that although much of this material is probably recycled repeatedly, the amounts are so large that vegetation-cycled material must be the source of at least part of the Fe- and Al-oxides that form pisoliths and nodules in tropical soils. However, they also noted that not all of the material is simply recycled, as roots commonly extend to depths of at least 10 m below the surface, indicating that some trees obtain nutrients from that depth and not just from the shallow soil.

It is clear that organisms were present in the regolith and it appears likely that they and their associated chemical reactions took part in the weathering process, in addition to simple inorganic chemical processes.

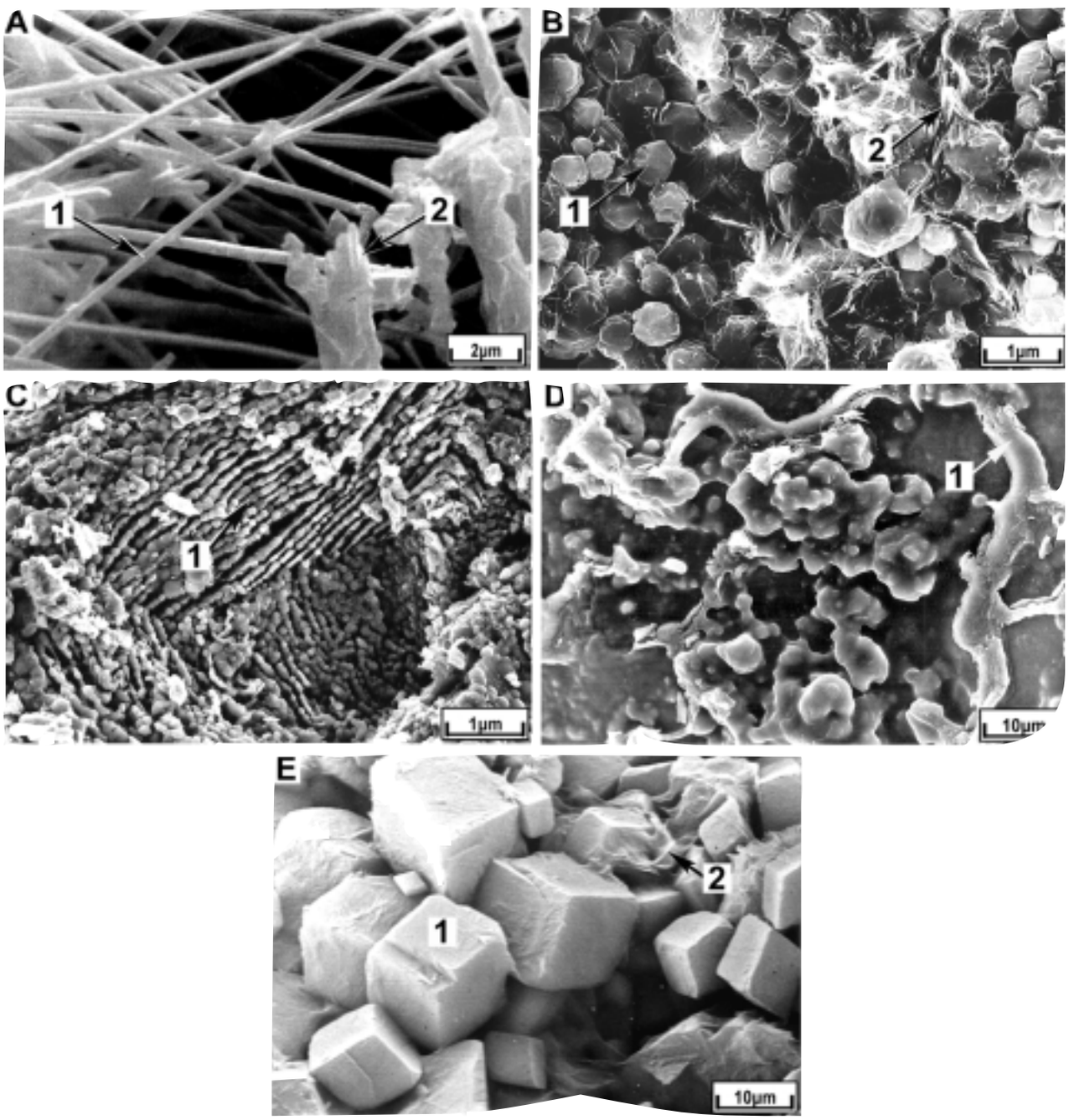

Figure 35 Scanning electron photomicrographs of broken surfaces of regolith materials showing mineral replacements of once-living organisms. (a) Calcrete nodule showing calcified fungal hyphae, now needle-like fibres of calcite (1), some with saw-tooth edges (2): Mt Gibson (after Anand *et al.* 1997). (b) Bacteria replaced by radial dolomite (1) and fibrous palygorskite (2): Bronzewing (J. E. Wildman & C. Phang unpubl. data). (c) Cutan on a ferruginous pisolith showing cyanobacteria replaced by aggregates of goethite (1): Sundowner (R. R. Anand unpubl. data). (d) Silicified root remnants (1): Lawlers (R. R. Anand unpubl. data). (e) Euhedral–rhombohedral dolomite crystals (1) and fibrous crystals of palygorskite (2): Mt Gibson (after Anand *et al.* 1997).

Table 3 Summary of the behaviour of the chemical components in each profile, Boddington gold deposit (after Davy & El-Ansary 1986).

Profile	WBR 9 (Over felsic rock)	WBR 10 (Over mafic rock)	WBR 12 (Over mafic? rock)	WBR 14 (Over felsic rock)
Group A: Generally leached				
(i) Components leached at or near bedrock–saprolite boundary	Sr, Ta, Zn, CaO, Na2O	Co, La, Mn, Rb, Sr, W, Y, Zn, CaO, K_2O, MgO, Na_2O	–	Sr, CaO, Na_2O
(ii) Components leached within clay zone, no surface enrichment	Ba, (Cu), Li, (Ni), Rb, (Ta), K_2O, MgO	Ba	Ce, Cu, La, Li, Ni, Rb, Sr, Ta, Y, Zn, CaO, K_2O, MgO, Na_2O	Ba, Cu, La, Ni, Rb, Zn, K_2O, MgO
(iii) Components leached at top near bedrock–saprolite boundary	Ce, Co, La, Mn, Y	Cu	Co, Mn	Co, Mn
Group B: Mobilised and reprecipitated				
(i) Components reduced in or absent from central clay zone, but with values in ferruginous duricrust or upper clay zone similar to those in bedrock.	Cu[a], Ni[a]	Ba[a], Ce, Cr[a], Li, Ni, TiO_2, (Y), (Fe_2O_3)	Cr, Mo	Au, Ca, (Cu), Li, Sn, Y
(ii) As in (i), but enriched in ferruginous duricrust–bauxite zone relative to bedrock	Au, Cr, Mo, Fe_2O_3	(Mo)	Au, Sn, V, Fe_2O_3	Mo, (TiO2), (V), W Fe_2O_3
Group C: Components generally residually concentrated				
	Nb, Sn, Th, V, Zr Al_2O_3, TiO_2	(Au), (Cr), (Sn), (Th), Zr	Th, Zr, Al_2O_3, TiO_2	(As), Cr, Mo, (Sb), Th, V, Zr, Al_2O_3, TiO_2
Group D: Components enriched in clay				
	–	V	Ba, (Pb)	–
Group E: Components with no consistent behaviour				
	(Au), W	(TiO_2)	Nb, (Sn), W	(Pb)

[a]Upper clay zone only.
Parentheses indicate either low levels of component or a secondary, less certain behaviour pattern.

EFFECTS OF WEATHERING ON ELEMENT DISTRIBUTIONS

Introduction

The behaviour of major and minor elements during lateritic weathering is illustrated on the Yilgarn Craton by several workers (Sadleir & Gilkes 1976; Smith 1977; Davy 1979; Butt & Nickel 1981; Elias *et al.* 1981; Davy & El-Ansary 1986; Ball & Gilkes 1987; Anand *et al.* 1991b; Butt *et al.* 1991, 1997a; Lawrance 1991; Butt & Zeegers 1992; Robertson & Butt 1993; Anand 1994). Principal geochemical trends observed in regolith in the Darling Range bauxitic profiles and inland kaolinitic profiles are summarised in Tables 3 and 4.

Bauxitic profiles: Darling Range

The major chemical components of bauxitic duricrust profiles are Al, Si and Fe, whereas Ti, V and Zr are minor, but important, constituents. The concentrations of these various elements are a function of bedrock geology and the modifying influences of weathering. Each element exhibits a particular pattern of enrichment or depletion through the profile horizons according to these factors. Davy and El-Ansary (1986) determined element patterns in bauxitic lateritic profiles at Boddington. Table 3 presents a summary of element patterns. There are five main groups: (i) group A—components mobilised in the lateritic profile, but not reprecipitated and, therefore, depleted in the upper parts of the profile; (ii) group B—components depleted in clay zone relative to either bedrock or ferruginous duricrust; (iii) group C—components generally residually concentrated towards the surface; (iv) group D—components enriched in the clay zone in certain profiles; and (v) group E—components with irregular behaviour.

Groups A and B are subdivided in Table 3 on the basis of the part of the profile in which the greatest changes have taken place. Table 3 reveals that although all profiles are essentially residual in character, the chemical patterns are not entirely consistent from profile to profile.

No component that features in any part of group A also features in group C. However, some elements appear in groups A and B, while others appear in groups B and C. Components with the most consistent behaviour are: Sr, CaO and Na_2O, leached at the bedrock/saprolite interface; Ba, Rb, K_2O and MgO, leached close to the interface of the clay zone with overlying ferruginous duricrust; Th and Al_2O_3, concentrated upwards; and Mn and Co, enriched at the base of the clay–saprolite zones.

Some components (in parentheses in Table 3) do not fit into any simple pattern. Copper and Ni, for example, tend to be very low in the ferruginous duricrust, but are locally concentrated at the bottom of the duricrust or in the upper clay zone. They are less abundant in the lower clay zone. Copper, in particular, then tends to be enriched in the saprolite along with Co and Mn. The position of its maximum enrichment in the upper part of the profile either coincides with, or is slightly below (by 2–3 m), the equivalent enrichment for Ni.

Non-bauxitic profiles: inland

The principal effects of deep lateritic weathering (non-bauxitic) on element distributions are summarised by Butt *et al.* (1997a). This distribution relates leaching and retention of a range of elements to mineral transformations in the principal regolith profile horizons (Table 4). In compiling this table, Butt *et al.* (1997a) noted that this summary is a gross simplification and emphasised that no mineral is entirely unaffected by weathering, no element is entirely leached from any regolith horizon and no element is entirely immobile. Many of the geochemical characteristics of regolith can be related to the development of the lateritic profile under humid tropical to (possibly) temperate climatic conditions of higher water tables, whereas others are due to later events related to more arid environments with lower water tables and may still be active (Butt *et al.* 1997a). The features produced by these

Table 4 Element mobility during deep weathering under humid conditions.

Host minerals	Leached	Partly retained in secondary minerals
Released at weathering front		
Sulfides	As, Cd, Co, Cu, Mo, Ni, Zn, S	As, Cu, Ni, Pb, Sb, Zn (Fe oxides)
Carbonates	Ca, Mg, Mn, Sr	
Released in the lower saprolite		
Aluminosilicates	Ca, Cs, K, Na, Rb	Si, Al (kaolinite); Ba (barite)
Ferromagnesians (pyroxene, olivine, amphiboles, chlorite, biotite)	Ca, Mg	Fe, Ni, Co, Cr, Ga, Mn, Ti, V (Fe and Mn oxides)
Released in the upper saprolite		
Aluminosilicates (muscovite)	Cs, K, Rb	Si, Al (kaolinite)
Ferromagnesians (chlorite, talc, amphibole)	Mg, Li	Fe, Ni, Co, Cr, Ga, Mn, Ni, Ti, V (Fe oxides)
Smectites	Ca, Mg, Na,	Si, Al (kaolinite)
Released in the mottled and ferruginous zones		
Aluminosilicates (muscovite, kaolinite)	K, Rb, Cs	Si, Al (kaolinite)
Iron oxides	Trace elements	
Retained in stable minerals (all horizons)	B, Cr, Fe, Hf, K, Nb, Rb, REE, Th, Ti, V, W, Zr	

Data derived from Butt *et al.* (1991); Butt and Zeegers (1992) and references therein.

later events appear as modifications of the pre-existing lateritic profile and tend to be reflected more by the minor components of the regolith.

Five general trends can be identified.

(1) Sulfides are some of the most unstable minerals in humid, oxidising environments and typically persist in the profile only if preserved within vein quartz or resistant lithorelicts. This is consistent with observations that S has been strongly leached from the deepest levels of the regolith and appears to be the element most susceptible to weathering. Many elements hosted by sulfides (e.g. Cd, Co, Cu, Mo, Ni, Zn) are commonly leached deep in the saprock, although a proportion is retained in Fe oxides derived from the sulfides. Carbonates are similarly highly susceptible to weathering, hence elements dominantly or significantly hosted by them, such as Ca, Mg, Mn and Sr, are strongly leached. Calcium and Sr, for example, are commonly reduced to very low concentrations throughout most of the regolith.

(2) Weathering in the lower saprolite causes destruction of feldspars and ferromagnesian minerals. Sodium, Ca and Sr are leached from the former, with Si and Al retained as kaolinite and halloysite. In addition, K, Rb and Cs will be lost if hosted by orthoclase or biotite but, if present mainly in muscovite, concentrations are maintained or residually increased throughout much of the regolith. Barium, commonly hosted by feldspars, is released early during weathering, but is reprecipitated as barite, which remains stable through the regolith and is only partly leached in the ferruginous duricrust. Weathering of less-stable ferromagnesian minerals (pyroxene, olivine, amphibole and biotite) results in the formation of Fe oxides, partial retention of minor and trace elements such as Ni, Co, Cu, Mn and Ni, and progressive loss of Mg and Si, except where retained in smectite (Mg, Si), kaolinite (Si) or quartz (Si). Brand (1997) observed that in ultramafic rocks the Mg discontinuity marks the top of the Mg-saprolite and is characterised by the loss of Mg-bearing phases (silicates and carbonates), a sharp decline in Mg concentration and a coincident relative increase in Fe oxides and silica. The 2:1 layer of smectites can include a variety of cations having comparable size to the major octahedrally coordinating cations Mg^{2+}, Al^{3+} and Fe^{3+}. Paquet *et al.* (1987) detailed the involvement of smectites as early hosts for selected trace elements during the development of the weathering profile. Trace elements accommodated in the octahedral sheet include Zn, Mn, Co, Ni and Cu. A similar relationship was also observed by Kelly and Anand (1995) in weathering profiles developed on ultramafic rocks at Forrestania. On the basis of electron microprobe analysis of ferruginous saprolite, they suggested that, initially, Ni is associated with smectite but, with further weathering, the association with Fe oxides increases. Brand (1997) suggested that Ni is hosted by eight different phases in the regolith with Mg silicates, magnesite and Fe oxides being the dominant control on its distribution.

(3) The alteration of all but the most resistant primary minerals occurs in mid to upper saprolite zones; in addition, less stable secondary minerals, such as smectite, are also destroyed. Serpentine, magnetite, ilmenite and chlorite are progressively weathered through the zone, but talc and, in particular, muscovite may persist through to the mottled clay zone and, in places, to the ferruginous duricrust. Ferromagnesian minerals are the principal hosts for transition metals, such as Ni, Co, Cu and Zn, in sulfide-poor mafic and ultramafic rocks and are retained higher in the profile than sulfide-hosted metals. Nevertheless, they become leached from the upper horizons and reprecipitate with secondary Fe-Mn oxides in the mid to lower saprolite.

(4) Most remnant major primary minerals, except quartz, are commonly finally destroyed in mottled and ferruginous duricrust zones. These zones, in particular, demonstrate one of the principal characteristics of deeply weathered regolith profiles, namely domination by Si, Al and Fe, resident in kaolinite, quartz, Fe oxides (goethite, hematite, maghemite) and in places gibbsite. The abundances and distributions of Si, Al and Fe oxides broadly reflect their lithologies. The distributions of several minor and trace elements are controlled wholly or in part by the distribution of these major elements, due to substitution or coprecipitation. Thus, Cr, As, Ga, Sc and V tend to accumulate with Fe oxides; Cr, mainly derived from ferromagnesian minerals, is also associated with neoformed kaolinite. Many resistate and immobile elements also tend to concentrate with clay and Fe oxides in the ferruginous zones, although for most no chemical interactions are involved. Thus, the distributions of Cr, K, Hf, Th, Nb, Ta, W, Sn, REE, Ti and V relate wholly or in part to their inertness during weathering, which is due to their relative chemical immobility (e.g. V, Ti) and/or to the stability of primary and/or secondary host minerals (e.g. Zr and Hf in zircon; Ti in rutile and anatase; Cr in chromite; K in muscovite). Their abundances tend to increase upwards through the profile due to the gradual loss of other components, with marked accumulation in lateritic residuum, within which lateral dispersion by colluvial action can occur during the course of profile evolution.

(5) Characteristics commonly associated with weathering under arid conditions are those related to an excess of evaporation, which results in the accumulation in the regolith of weathering products that would otherwise be leached. Duricrusts, formed by the exposure and irreversible hardening of ferruginous residuum, or the later precipitation of Fe oxides, silica and carbonates, are important in armouring and protecting the regolith from erosion. In the southern Yilgarn Craton especially, enrichment of Ca, Mg, S and Sr in soils and upper horizons, commonly in the top 2 m, relates to the precipitation of secondary sulfates and carbonates (i.e. gypsum, calcite and dolomite in soils). In the north of the Yilgarn Craton, carbonates are much less common in soils and have only a sporadic occurrence. Sulfates may also precipitate in saprolite, as alunite, and halite is commonly present as a trace constituent throughout the regolith. Silica induration of various types is also a common feature of the regolith in semiarid areas. Although geochemical dispersion in arid environments is generally considered to be dominated by mechanical processes, it is evident that, particularly where there is an extensive deep regolith, there is significant chemical (hydromorphic) mobility of many ore-related trace elements in groundwater and soil environments, including U and V (Mann 1984; Gray & Lintern 1994) and rare-earth elements (Gray 1993).

REGOLITH MATERIALS

Differential erosion and chemical modification of the Yilgarn Craton landsurface has produced a variety of regolith materials and intricate regolith–landform relationships. The nature of regolith materials is strongly related to the landforms with which they are associated so that a framework of landforms provides a useful way of describing regolith materials. The salient regolith types and associated landform elements recognised in the region are shown in Table 5. Regolith materials include lag, soils, sediments, ferruginous duricrust and gravel, calcrete, silcrete and red-brown hardpan. These are discussed in the following sections.

LAG

Lag is the residual accumulation of coarse, usually hard, fragments that accumulate at the surface. They have been left as a residue after the physical and chemical dismantling of the upper horizons of the regolith and the removal of finer materials in solution or by sheetwash or wind, supplemented by particles moving upwards (e.g. by churning). The close relationship between lag, topography and parent material is illustrated in Figure 36. On crests, the surface is dominated by coarse (20–50 mm), irregular, fragments of mottled saprolite or hardened mottles with yellowish-brown cutans (Figure 37a on Plate 5). The lag becomes finer with fewer cutans, the lag colour darkens and magnetic pisoliths increase downslope from the crest. Thus, upper to mid backslopes are dominated by reddish-brown (generally 10–20 mm) hematite-rich pisoliths (Figure 37b on Plate 5). On lower slopes, a fine (<10 mm) lag of magnetic black, dense hematite–maghemite-rich pisoliths is dominant (Figure 37c on Plate 5); there is little or no quartz and lithic fragments are very rare. Pisoliths typically have a dark-brown to black surface and no cutans. It is here suggested that pisoliths with cutans were eroded from upslope and subsequently lost their cutans during transportation.

Polymictic lag mantles much of the plains on gently sloping, drainage floors. Much of it is dark-brown to black and it has a smooth, varnished appearance (Figure 37d on Plate 5). This lag comprises ferruginous pisoliths, saprolite and quartz. Fine lag is generally magnetic, whereas coarse lag is non-magnetic. On slopes below the breakaway scarps and on hills, saprock outcrops and lag derived from saprolite are extensive. Most of the lag is ferruginous and lithic (Figure 37e on Plate 5). Veins of ferruginous masses related to sulfide-rich rocks occur as low, narrow ridges and are flanked by a lag of coarse, black, iron segregations (Figure 37f on Plate 5).

The relative abundance of kaolinite, goethite and hematite varies between the lag types. In a sequence of yellowish-brown fragments of mottled saprolite to reddish-brown pisoliths and to black pisoliths, the goethite/(goethite + hematite) ratio decreases (Figure 38a), whereas kaolinite content decreases slowly. This relationship suggests replacement of kaolinite by goethite and dehydration of goethite to hematite. This is consistent with the Fe content, which increases from yellowish-brown fragments of mottled saprolite to black pisoliths (Figure 38b). Iron segregations related to sulfide-rich rocks are dominated by goethite with variable amounts of hematite (Figure 38a). Kaolinite is absent or present in traces. These mineralogical differences between the lag types are due to the differences in origin and the degree of weathering. Goethite in iron segregations is derived mainly from Fe released into solution by the weathering of sulfides,

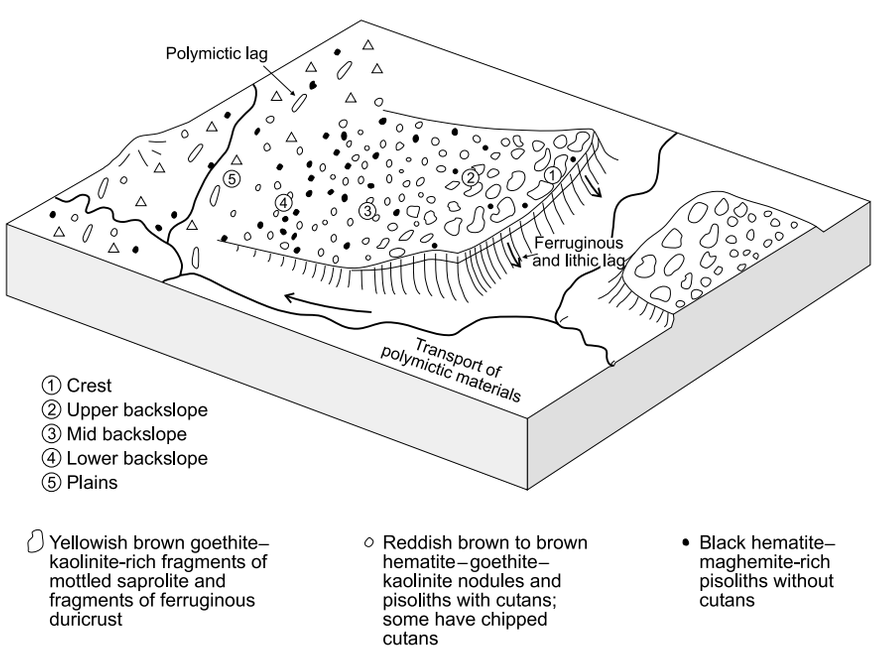

Figure 36 Block model showing the general relationships between lag and topography. Lag type is related to the nature of substrate and geomorphic processes. Nodular and pisolitc lag occur on backslopes, ferruginous lithic lag on pediments and erosional plains, and polymictic lag on depositional plains.

although there may also be contributions from other Fe-bearing minerals. Goethite has been reported to be the dominant mineral in gossans by several workers (Nickel 1984). Fragments of mottled saprolite have experienced a lesser degree of weathering compared with that of brown and black pisoliths as is shown by the large amounts of goethite and kaolinite. Black pisoliths are 'older' and are hematitic. Although hematite has largely formed by the dehydration of goethite, it can also form directly by internal dehydration of ferrihydrite.

SOILS

Introduction

It has often been said that Australia has an old landsurface, the implications of this being that the soils and the underlying materials have been strongly weathered. While many areas of Australia have been exposed to weathering for many millions of years, many of its soils and landscapes, particularly in eastern Australia, are quite young. Even in those parts of Australia (western and northern Australia)

Table 5 Salient features of landforms and regolith on greenstone terrain.

Landform	Regolith type	Description
Crest	Lag	Mainly coarse (20–50 mm) fragments of yellowish-brown mottled saprolite; few fragments of ferruginous duricrust (<100 mm); fine(<10 mm) to medium (10–20 mm) reddish-brown to black ferruginous nodules and pisoliths.
	Outcrop	Blocks of ferruginous duricrust and/or ferruginous saprolite. On some crests saprock is exposed.
	Soil	Shallow, light stony, friable, brown, fine, sandy loam.
	Ferruginous duricrust and/or ferruginous gravel	Patchy, indurated nodular, pisolitic or massive duricrust.
	Red-brown hardpan	Moderate
Slopes		
Upper to mid slopes	Lag	Lag becomes finer downslope from crest; lag colour darkens downslope; magnetic lag increases downslope; also there are less cutans. Fine to medium (10–20 mm) brown to black nodules and pisoliths (<10 mm).
	Outcrop	None
	Soil	Gravelly, light brown to red, fine, sandy loam. Coarse, gravelly at depth.
	Transported regolith type	Widespread gravelly, sandy loam colluvium to 3 m thick, on mid slope.
	Ferruginous duricrust and/or ferruginous gravel	Indurated patchy, ferruginous nodules and pisoliths with yellowish-brown cutans. Ferruginous nodules and pisoliths can be continuous substrate on upper to mid slopes.
	Red-brown hardpan	In the colluvium and ferruginous nodules and pisoliths at ~1 m; 1–3 m thick.
Lower slopes	Lag	Fine (<10 mm), dark brown to black nodules and pisoliths.
	Outcrop	None.
	Soil	Brown to red, fine sandy clay loam to light clay.
	Transported regolith type	Colluvium continuous, 2–5 m sandy clay loam to light clay with fine, black ferruginous gravels of mixed origin. In places, thick (2–5 m) sheets of detrital pisolitic gravels.
	Ferruginous duricrust and/or ferruginous gravel	Patchy, partially to strongly indurated, ferruginous nodules and pisoliths with yellowish-brown cutans. Ferruginous nodules and pisoliths can be continuous substrate to lower slopes.
	Red-brown hardpan	At ~1 m and thence to ~3–4 m.
Plains (includes flat gently inclined plains; alluvial tracts)	Lag	Fine (dominant) to medium (10–20 mm) polymictic. Quartz always present. On some alluvial tracts, no lag.
	Outcrops	None.
	Soil	Red, friable, fine, clay.
	Transported regolith type	Sandy, silty; gravelly sandy clay alluvium; sandy clay with lenses of ferruginous gravels; and palaeochannel deposit.
	Ferruginous duricrust and/or ferruginous gravel	Partially to strongly indurated, patchy ferruginous nodules and pisoliths, saprolite, or rarely bedrock.
	Red-brown hardpan	At ~1 m, and extending to a maximum depth of ~10 m. Generally well developed from 1 m to 4 m.
	Calcrete	Scattered pockets.
Breakaway scarps, **pediments**, **erosional plains**	Lag	Fragments of ferruginous saprolite; Fe-stained saprock and lithic fragments; very rare pieces of ferruginous duricrust.
	Outcrop	Patchy-subcrop of saprolite.
	Soil	Shallow, stony, friable, sandy loam to sandy clay loam colluvium; residual soils underneath colluvium.
	Transported regolith type	Shallow, stony colluvium on slopes. Local, alluvial trains; 1–2 m thick.
	Ferruginous duricrust and/or ferruginous gravel	Absent.
	Red-brown hardpan	Occasionally on local, gently sloping pediments.

where there has been intensive and deep weathering, older landscapes have been dissected and progressively younger soils have been developing in the older weathered materials (Finkl & Churchward 1973; Churchward & Gunn 1983). Simultaneously, new surfaces have been developing on the sediments eroded from the old landsurfaces and these sediments have in turn been reworked by the action of water and wind. Thus, the Australian landscape consists of old and young soils, very often in close proximity; in some cases old soil materials have been incorporated into young soils. These variations can have a profound effect on the surface geochemical expression of mineralisation.

General patterns

Because of the high proportion of granitic rocks, and in particular because of the widespread occurrence of leached, weathered parent materials, the soils of the Yilgarn Craton do not show the clear climatic zonality that is characteristic of many other continental landmasses (Bettenay *et al.* 1976). Thus, in one area, soils may be present that are developed from fresh rock, saprolite or a variety of alluvial, colluvial or aeolian materials derived from saprolite and/or bedrock. In addition, there has been considerable vertical and lateral transport in solution, followed by precipitation, particularly in sump areas in the landscape. Thus, there are only limited areas in which soils are both *in situ* and relatively unweathered and, hence, where there is a close correlation between soil and bedrock geochemistry.

There are, however, broad systematic changes in soil characteristics over the Yilgarn Craton (Bettenay *et al.* 1976) (Figure 39). The legend for Figure 39 gives the broad characteristics of the dominant and associated soils of each region. Among the most notable differences between regions are: (i) the dominance of sands with ferruginous gravels (60% of soil material is between 2 mm and 77 mm in diameter) in region A; (ii) the change from acid and neutral reaction trends in region B to alkaline reaction trends in the dominant soils of region C; (iii) the dominance of soils with large amounts of pedogenic calcrete throughout the profile in region D; (iv) the change from yellow earthy sands in the western part, to red earthy sands in the eastern, drier, part of region E, and the absence of yellow earthy sands in the zones to the north and east of this; (v) the dominance of alkaline red non-calcareous earths in region F; (vi) the dominance of earthy loams with red-brown hardpan in region G (hardpan is also common in soils of regions F and H); (vii) the presence of saline calcareous and siliceous loams in the main drainage lines of regions C–H, with powdery calcareous loams formed on calcretes in drainage lines of regions G and H; and (viii) the dominance of acid and neutral red non-calcareous earths in region H.

The effect of erosional modification of the weathered mantle and landscape processes on the pattern of soils on the Yilgarn Craton has been well documented by a number of workers (Mulcahy & Hingston 1961; Bettenay 1962; Bettenay & Hingston 1964; Northcote *et al.* 1967; Stace *et al.* 1968; Finkl & Churchward 1973; Churchward & Dimmock 1989). One group of soils is formed on ferruginous duricrust and mottled saprolite on broad crests and backslopes. A second group of soils is formed from less-intensively weathered *in situ* and colluvial materials on hills, pediments and erosional plains, with a third formed in alluvium, lacustrine and aeolian sediments on plains and salt lakes. Topography affects the depth of the soil, depending on whether the soil is receiving material from upslope or losing it downslope. It may also affect the drainage status of the soil profile which may, in turn, determine the nature of Fe oxides and clay minerals.

On crests, where present, are shallow (10–30 cm), stony, light-brown, very friable, kaolinitic fine sandy loams that commonly contain abundant ferruginous nodules and pisoliths on a substrate of duricrust and mottled saprolite (Figure 40a on Plate 6). On backslopes, the soil is gravelly,

Table 5 (cont.)

Landform	Regolith type	Description
Hills		
Low hills and intervening	Lag	Iron-stained fresh and weathered rocks; patches of coarse lateritic cobble related to massive sulfide lodes and quartz.
narrow alluvial	Outcrop	Patchy, extensive subcrop of saprock and bedrock.
tracts	Soil	Shallow, stony, grey-brown to red sandy loam to sandy clay loam.
	Transported regolith type	Shallow, stony colluvium on slopes, local alluvial trains; 1–2 m thick.
	Ferruginous duricrust and/or ferruginous gravel	Rare Fe-rich ferruginous duricrust.
	Red-brown hardpan	Rare.
High hills	Lag	None.
	Outcrops	Bedrock.
	Soil	Where developed, stony grey-brown sandy loam.
	Transported regolith type	None.
	Ferruginous duricrust and/or ferruginous gravel	Absent.
	Red-brown hardpan	Absent.

Soils in all landscape positions contain variable amounts of aeolian materials. Ferruginous duricrust is developed in residual and transported materials.
In the southern region, pedogenic calcrete occurs on all landscape positions. In contrast, in the northern region, calcrete occurs as scattered patches to extensive on pediments, erosional plains and hills. On plains, it may occur as laminated calcrete coatings on red-brown hardpan surfaces. Groundwater calcretes are extensive in the north.

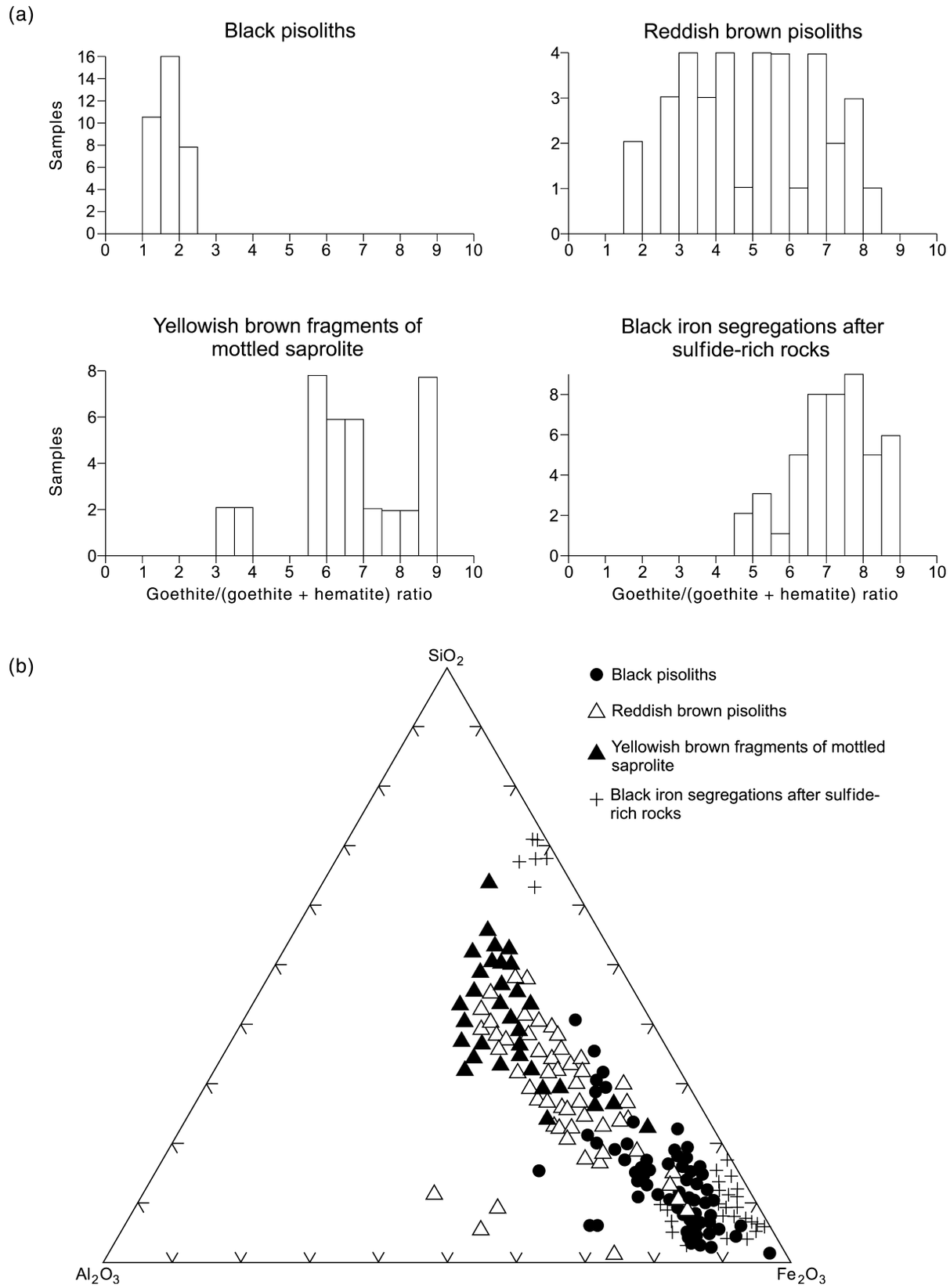

Figure 38 (a) Histograms of goethite/(goethite + hematite) ratio for four types of lag. These are black pisoliths, reddish-brown pisoliths, yellowish-brown fragments of mottled saprolite and black iron segregations after sulfide-rich rocks. (b) Ternary diagram showing compositions of lags in terms of Fe, Al and Si content. In a sequence of yellowish-brown fragments of mottled saprolite to reddish-brown pisoliths and to black pisoliths, hematite increases. Maghemite (not shown) commonly occurs in reddish-brown and black pisoliths. This is consistent with the iron content, which increases from yellowish-brown fragments of mottled saprolite to black pisoliths. Iron segregations are goethite-rich (R. R. Anand unpubl. data).

friable, light-brown to red, kaolinitic fine sandy loam to sandy clay loam, with moderate, fine reddish-brown to black pisoliths. The upper part of the soil has developed in a colluvium, in which the gravel fraction is predominantly fine, ferruginous gravels of a similar composition to the lag. On plains, red-brown sandy loam to sandy, light clay soils are developed in the top 0.5–1 m of alluvium (Figure 40c, d on Plate 6). The soil consists of sand, silt and clay with polymictic gravels similar to those of the lag. Faceted and polished sand- to silt-sized surficial quartz grains indicate an aeolian component to the soil. Some drainage foci in areas of low relief are characterised by heavier soils, including cracking clays. On playas, gypsum dunes accumulate around the lee margin of the lake edge.

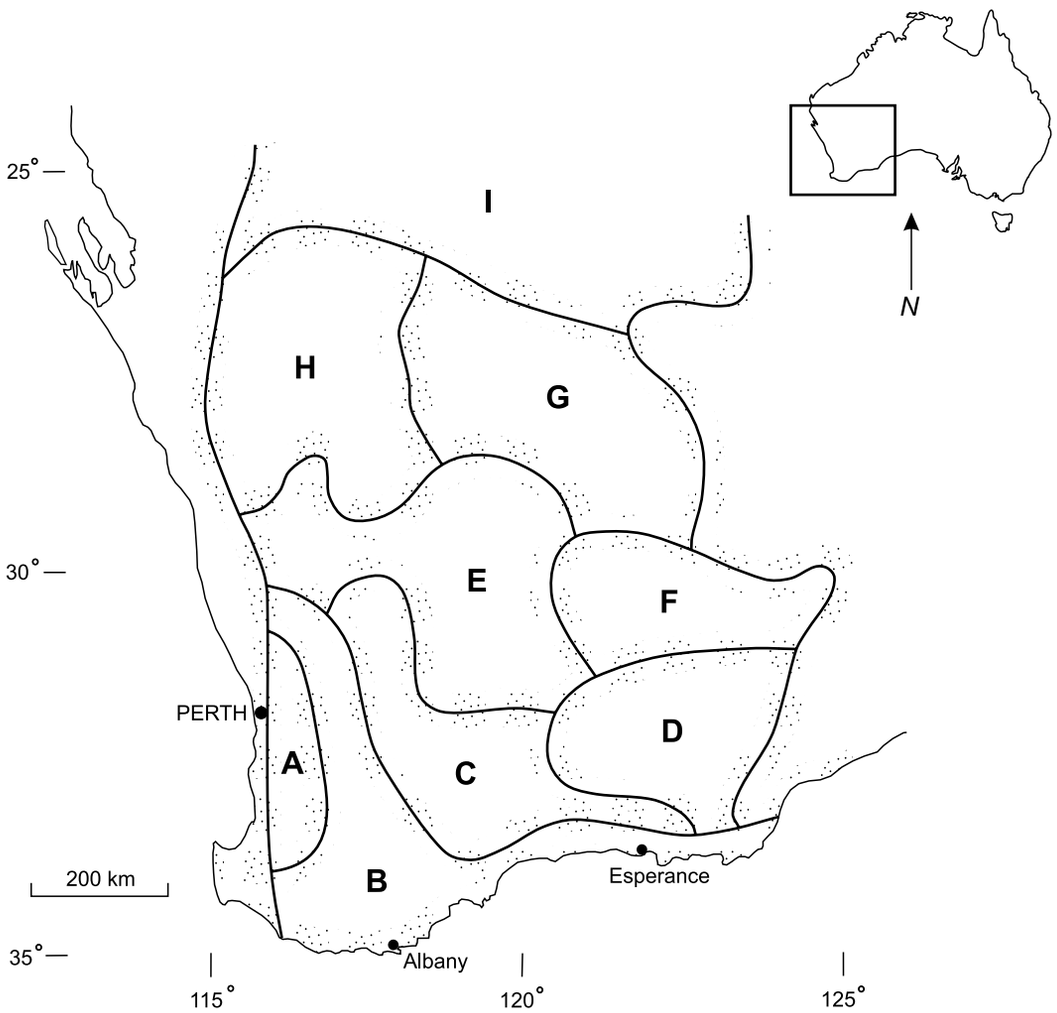

Region	Dominant Soil	Associated Soils
A	Sands with ironstone gravels	Non-calcareous massive earths and hard acid mottled-yellow duplex soils.
B	Hard acid and neutral mottled-yellow duplex soils	Hard neutral and alkaline red duplex soils and bleached sands.
C	Hard alkaline mottled-yellow duplex soils	Acid yellow non-calcareous earths, hard alkaline red duplex soils and saline calcareous and siliceous loams.
D	Grey-brown calcareous earths	Crusty alkaline red duplex soils and saline calcareous and siliceous loams.
E	Yellow earthy sands	Red earthy sands and neutral and alkaline non-calcareous earths.
F	Alkaline red non-calcareous earths	Earthy loams with hardpan and saline calcareous and siliceous loams.
G	Earthy loams with hardpan	Acid and neutral red non-calcareous earths, red earthy sands, hard alkaline red duplex soils, saline calcareous and siliceous loams and powdery calcareous loams.
H	Acid and neutral red non-calcareous earths	Earthy loams with hardpan, hard alkaline red duplex soils and powdery calcareous loams.
I	Red earthy sands with red-brown hardpan	

Figure 39 Soil zones in southwestern Australia (after Bettenay *et al.* 1976).

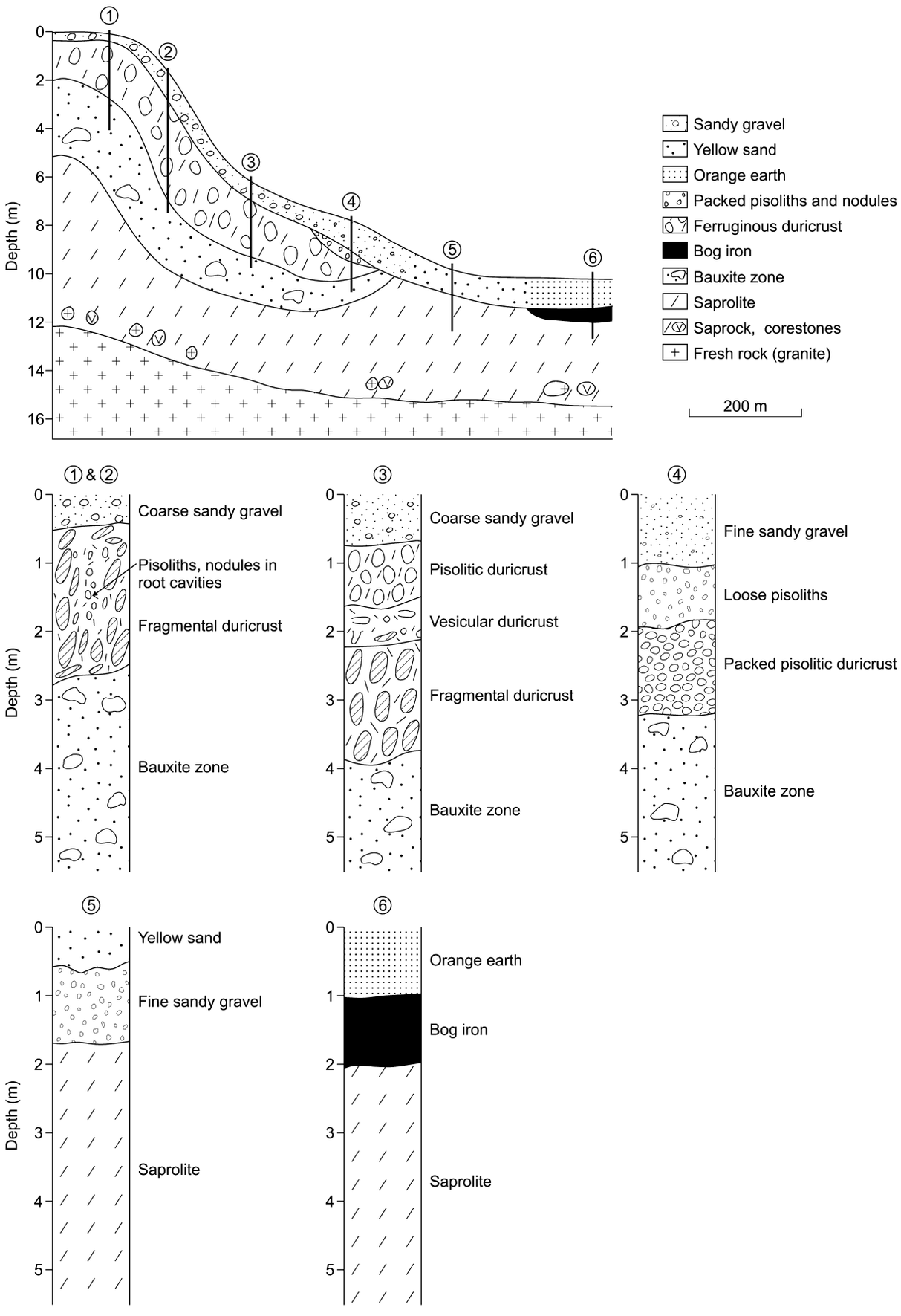
Depth (m)
0
2
4
6
8
10
12
14
16
1
2
3
4
5
6
Sandy gravel
Yellow sand
Orange earth
Packed pisoliths and nodules
Ferruginous duricrust
Bog iron
Bauxite zone
Saprolite
Saprock, corestones
Fresh rock (granite)
200 m
1 & 2
Coarse sandy gravel
Pisoliths, nodules in root cavities
Fragmental duricrust
Bauxite zone
3
Coarse sandy gravel
Pisolitic duricrust
Vesicular duricrust
Fragmental duricrust
Bauxite zone
4
Fine sandy gravel
Loose pisoliths
Packed pisolitic duricrust
Bauxite zone
5
Yellow sand
Fine sandy gravel
Saprolite
6
Orange earth
Bog iron
Saprolite

Lunettes vary in texture from coarse sand to clay and are carbonate-rich (Bettenay & Hingston 1964). Clayey parna derived from playas has been deposited in extensive sheets. Soils on lunettes are either podsolised sands, in which the materials are coarse, or primary solonchaks that form finer and more saline deposits.

Deeper units of the weathered mantle, as well as country rock, are exposed on pediments and low hills and are the parent materials of soils (Figure 40e–g on Plate 6). Pediments that extend from the base of low breakaways are mantled by acid to calcareous red earths in fine, sandy, light clay residual soils or colluvium that overlies saprolite or saprock to a depth of less than 1 m. Colluvial deposits can be silicified (hardpanised) at depths of 30–50 cm. In granitic terrain, a complex pattern of duplex soils and red and yellow earths occurs, which is controlled largely by the nature of colluvium and the exposed weathered material. Duplex soils have a strong textural contrast between the major surface soil horizons and the subsoil horizon. These soils also show the development of secondary ferruginous soft mottles and pisoliths in the subsoil horizon.

There is very little soil on breakaway scarps. On low hills, the dominant soils are shallow (20–50 cm), friable to stony, calcareous, grey-brown to red sandy loam or sandy clay loam (Figure 40g on Plate 6), but some are non-calcareous. They contain mainly smectite, unweathered primary minerals, calcite and/or dolomite, with small amounts of kaolinite. These soils show close association with weathered or subcropping rock and result from *in situ* weathering of bedrock and its interaction with water, biota and the atmosphere. Fresh bedrock or saprock is exposed on some of the high hills and there is little soil development. Where soil does occur it is a stony, grey-brown, sandy loam.

Examples of soil catena

Examples given below typify the importance of parent material, landscape processes and present climate in determining the nature and distribution of soils.

JARRAHDALE, DARLING RANGE

Undissected areas

On the Darling Range in undissected terrain, with its shallow valleys and gentle slopes, a relatively simple picture of soil distribution emerges. In general, the solum thickness increases with distance from crests toward the valley floor. Sandy gravel materials are predominant on slope and crest positions, whereas sandy soils increase in thickness towards the valley floor and become best expressed in the middle of the valley floor. Figure 41 typifies these relationships from the Jarrahdale area. Uplands show a toposequence of very gravelly soils (sandy gravels) and ferruginous duricrust on the crests to mid slopes. Sandy gravels increase in thickness to more than 1 m in mid-slope and lower slope positions, where they overlie various forms of ferruginous duricrust, which in turn overlies bauxite zone. The gravels become finer downslope. On lower slopes, the gravels merge with sand and the profile shows a layered sequence, being interleaved with sand. 'Orange earths' dominate the valley floor, but in some situations yellow-brown sand may extend on to them. Podzolic soils (Figure 40b on Plate 6) and cracking clays also dominate some valley floors. Pockets of goethite-rich 'bog iron', formed by chemical or biochemical precipitation of hydromorphically dispersed Fe, may occur in valley floors. In such areas, duricrust is absent and the soils overlie saprolite. Fresh rock outcrops are rare.

Figure 41 Soil catena from the humid region of the Darling Range showing trends in soil following a sequence from crest to valley floor at Jarrahdale (modified from Anand *et al.* 1989a; Churchward & Dimmock 1989). Sandy gravels on crest and mid-slope give way to yellow sandy soils on the lower slopes and 'orange earths' in the valleys. The gravels become thicker and finer downslope.

Dissected areas

On long steep slopes in dissected terrain, the soil pattern is complex. Rock outcrops are common, and slump features and infilled valley-side depressions indicate a prior geomorphic environment more dynamic than on the Darling Plateau. Orange earths dominate the surface with saprolite an important substrate, although fresh rock is not uncommon. Local convexities are associated with a greater thickness of soil materials.

MT GIBSON, INLAND

Figure 42 shows an east–west cross-section through the N2 pit at Mt Gibson. The upland area to the west is characterised by red clay soils overlying saprolite, with sporadic fresh subcrop of amphibolite. These soils largely consist of smectite, calcite and lithorelics with small amounts of kaolinite and hematite. Red clays are formed *in situ* from the weathering of underlying rocks. The abundance of smectite and calcite in red clays suggest that they have formed in a low-leaching environment. This is in contrast to the mid-slope, which is characterised by kaolinitic, red calcareous gravelly sandy clay underlain by nodular sandy and gravelly silicified colluvium and alluvium (red-brown hardpan). These soils typically contain detrital black, hematite–maghemite-rich, ferruginous pisoliths without cutans, which have formed in colluvium. The colluvium itself is derived from erosion of the regolith interpreted to have previously covered the adjacent upland area. Red, sandy clays merge laterally, downslope, with acid, orange to yellow sandy clay or sandy soils that contain nodules and pisoliths with goethite cutans similar to the underlying nodular duricrust. The abundance of nodules and pisoliths decreases towards the top of the soil profile. The underlying duricrust is crumbly and forms an essentially *in situ* loose gravelly soil horizon. The kaolinite–goethite-rich duricrust matrix is being broken down by dissolution, permitting separation of nodules and pisoliths and producing a highly porous horizon of nodules and pisoliths dispersed in a goethitic, sandy clay matrix. Fine dissolution cracks and voids that split hematitic nodules into fragments are visible in the duricrust. Further dissolution of Fe oxides produces a residual quartz-rich sand (Anand *et al.* 1989b).

Differences in soil colour can be attributed to differences in the hydrology of the soil cover. Red soils occur in well-drained upper slopes, whereas orange earths occur in

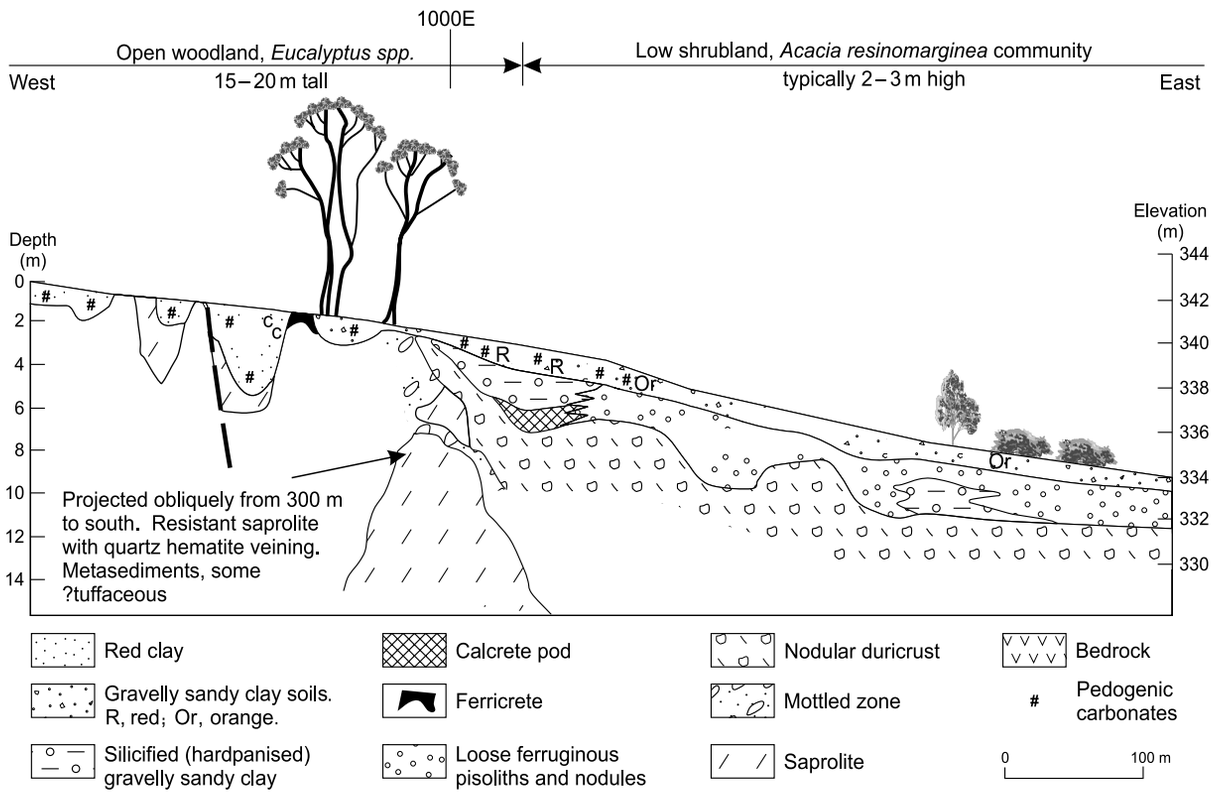

Figure 42 Soil catena at Mt Gibson showing variations in soil type with parent material and position in the landscape (after Anand *et al*. 1989b).

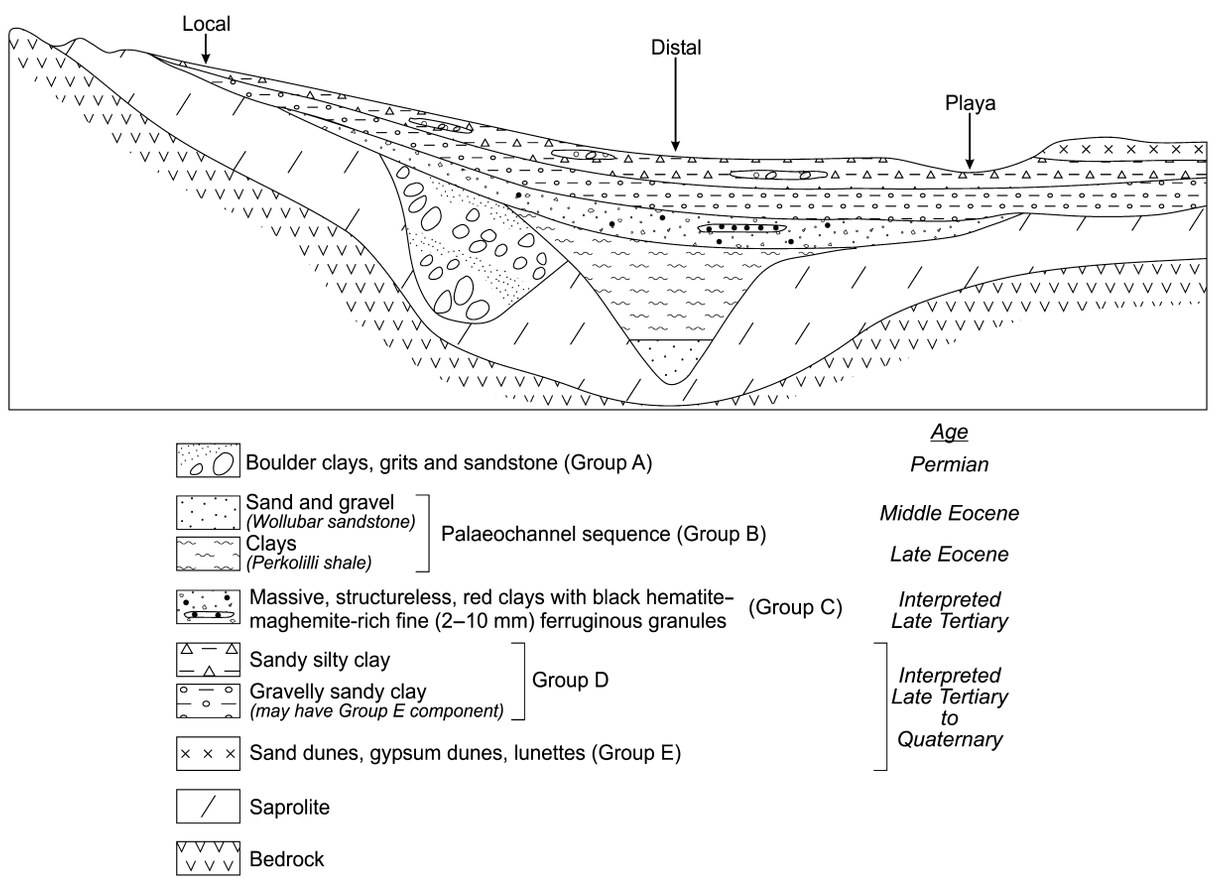

Figure 43 A schematic section showing the relationship between landscape and the major groups of sediments identified.

relatively poorly drained environments. These colours are due to different degrees of hydration of Fe oxides.

SEDIMENTS

Introduction

Sedimentary cover is common on the Yilgarn Craton and ranges in age from Permian to Holocene and in thickness from a few centimetres to many tens of metres. There are no known occurrences of Mesozoic sedimentary rocks on the Yilgarn Craton. Cretaceous marine sediments of the Madura Formation (Lowry 1968) are widespread in the Officer and Eucla Basins, but do not appear to have been deposited beyond the current basin margins. Permian and Cretaceous sedimentary rocks in the Collie and Wilga Basins (Le Blanc Smith 1993) are not considered as regolith and are not included in the classification below. Unlike the Permian deposits further inland, these sediments are thick and lack any known significant weathering overprints. The sediments include glacial, glaciofluvial, colluvial, alluvial, lacustrine, estuarine, marine and aeolian types and several may occur in the sequence at a given site. They may overlie ferruginous duricrust, saprolite or bedrock. There are five principal sedimentary units: (i) group A (Permian)—boulder clays, grits and sandstone; (ii) group B (Early to Middle Tertiary)—palaeochannel sediments [sand and gravel (Wollubar Sandstone, Middle Eocene); clay (Perkolilli Shale, Late Eocene)]; (iii) group C (interpreted Late Tertiary)—massive, structureless, red clays with black hematite–maghemite-rich fine (2–10 mm) ferruginous granules; (iv) group D (interpreted Late Tertiary – Quaternary)—sandy, silty clay, and gravelly, sandy clay units; and (v) group E (interpreted Late Tertiary – Quaternary)—aeolian materials [dunes (sand dunes, gypsum dunes), lunettes; aeolian materials in soils; and aeolian materials in ferruginous and bauxitic duricrusts].

Group D sediments are the most widespread and variable. They may overlie not only fresh and weathered basement, but also the sediments of the other groups, and consist of their physical and chemical weathering products. The relationship between landscape and sediments is shown in Figure 43. The detailed stratigraphy of the sediments is presented diagrammatically in Figure 44.

Group A

Excluding remnants of the mid-Proterozoic Glengarry Formation, which overlap the northern margin of the Yilgarn Craton and occur as outliers such as Mt Yagahong, 40 km south-southeast of Meekatharra, and Kaluweerie Hill, 40 km east-northeast of Agnew, the only known sediments of this type are glacial sediments of the Paterson Formation (Lower Permian). These occur near Laverton and Lawlers, and become increasingly abundant to the north and east. Sediments at Laverton consist of boulder clay, grit and sandstone and are interpreted to be glacial and fluvioglacial deposits (Clarke 1920; Hobson & Miles 1950; Gower 1976). The boulder clays consist of rounded, smooth boulders, cobbles and pebbles of chert, quartzite, granite, gneiss, metavolcanics, gneiss and banded iron-formation in a clay matrix. The deposits occur predominantly in channels, commonly following ultramafic rocks, some over 80 m deep; one shallow channel is exposed in the wall of the Beasley Creek pit. Some of the deeper deposits are unweathered and carbonaceous material within them has been dated palynologically as Permian (J. Hronsky *in* Butt *et al.* 1997b). In many places, the sediments have been deeply weathered after deposition. Boulder clays exposed in the Lancefield South pit, for example, have clay-rich saprolites in which the fabrics of the boulders and matrix are well preserved (Figure 45a on Plate 7). These are overlain by megamottled horizons in which the fabric is partly or wholly destroyed. In the Agnew–Lawlers district, flat-lying sediments, which are locally over 12 m thick, are thought to be Permian fluvioglacial sediments that occupy shallow, erosional hollows developed over steeply dipping Archaean bedrock (Westaway & Wyche 1988). The basal unit is a boulder clay, with granitic, ultramafic and quartz clasts in a clay-rich matrix, and is overlain by laminated siltstone and claystone. A thin cover of these sediments is present above the Genesis pit, west of Agnew (Anand *et al.* 1991b).

Group B

INTRODUCTION

Group B consists of palaeochannel sediments that include clay, sand and gravel (Figure 44) that, in places, contain lignite. The presence of palaeochannels ('deep leads') has long been recognised as a feature of the regolith on the Yilgarn Craton (Blatchford 1899; Maitland 1919; Balme & Churchill 1959; Bunting *et al.* 1974). In places, palaeochannels overlie mineralisation or occur adjacent to the deposits. Palaeochannel sediments generally occupy the lower parts of the landscape and some are exposed as mottled clays at the edges of lakes and breakaways (e.g. Black Flag). Tributary drainages, however, may follow quite different courses and may occur in the higher parts of the landscape (e.g. Mt Percy pit, Kalgoorlie; Ora Banda, Bronzewing).

An important feature of the channels and their sediments is their relationship with the deeply weathered regolith developed on the basement rocks. Most of the channels appear to be steeply incised into deeply weathered surfaces and major Mesozoic valleys initially developed prior to the Jurassic breakup of Gondwana (Ollier *et al.* 1988; Clarke 1994b). Major incision/re-incision occurred in the Eocene and was followed by local erosional quiescence, aggradation of the channels and infilling with sands and overlying clays during the Middle to Late Eocene (Van de Graaff *et al.* 1977; Commander *et al.* 1991; Clarke 1994b). Some channel sediments overlie ferruginous gravels or duricrust [e.g. Bronzewing (Varga *et al.* 1997); Sundowner (Wildman & Compston 2000)], fresh bedrock [e.g. Cyclonic prospect near Bronzewing (Ely 2000)] or more commonly saprolite [e.g. Kanowna (Dell 1992; Ladhams 1994) Mt Magnet (Robertson *et al.* 1994)]. Lower units may contain detrital pisoliths and nodules (Ladhams 1994; Anand 1995). In addition, the sediments themselves have been weathered since deposition. They have strongly leached lower horizons (saprolite after reduced clay-rich sediment) and strongly mottled upper horizons, which contain pisoliths

formed *in situ*. In places, ferricretes have developed in palaeochannel sediments in which Fe oxides have invaded gravels, sand and clay. They may be buried or, following exposure, form low hills due to relief inversion (this is discussed in more detail under the heading: Ferruginous materials).

SOUTHERN (KALGOORLIE) YILGARN PALAEOCHANNELS

In the Kalgoorlie region, segments of the palaeochannel system have a northeast trend parallel to a regional bedrock fracture direction, which cuts the general north-northwest strike of the Archaean greenstone belts. These northeast structures are also considered as important controls on Au mineralisation in the greenstone belts (Vearncombe 1997). The stratigraphy of palaeochannel sediments in the Kalgoorlie region has been documented by Playford *et al.* (1975), Smyth and Button (1989), Jones (1990), Dell (1992), Kern and Commander (1993), Gardiner (1993), Clarke (1993, 1994b), Anand *et al.* (1993a), Ladhams (1994), Dusci (1994), Woolrich (1994) and P. de Broekert (unpubl. data). Sediments from the Roe palaeochannel were first described by Playford *et al.* (1975). The name Rollos Bore Beds was proposed by these authors, later amended to the Rollos Bore Formation by Cockbain and Hocking (1989). Kern and Commander (1993) rejected these names on the grounds that palaeochannel sediments at Coolgardie are not representative and are any case unrealistically thick. Instead, they proposed their own classification based on an extensive drilling program aimed at assessing the groundwater resources of the palaeochannel sediments in the Kalgoorlie region. Clarke (1993, 1994b) established a formal stratigraphy for the Lefroy and Cowan palaeochannels; the correlation of stratigraphy of the Roe, Cowan and Lefroy palaeochannels with that of the Bremer and Eucla Basins is summarised in Figure 46. The Lefroy and Cowan palaeochannels are characterised by marine sediments and widespread reduced, commonly lignitic units. The sediments in the Roe palaeochannel are non-marine.

Roe palaeochannel system

The formal stratigraphy of the Roe palaeochannel system consists of two formations; the underlying Wollubar Sandstone and the overlying Perkolilli Shale, which equate to the sand and clay-rich units, respectively (Kern & Commander 1993). The Wollubar Sandstone is at the base of the sequence and rests unconformably on weathered Archaean rocks throughout the Kalgoorlie region, and is typically conformably overlain by the Perkolilli Shale. The contact between the Wollubar Sandstone and Perkolilli Shale may be gradational, but is generally sharp. The Perkolilli Shale may in turn be unconformably overlain by groups C–E sediments. The Wollubar Sandstone comprises sand with minor conglomerate, clay, pisolitic gravel, carbonaceous siltstone and lignite and has been dated palynologically as Middle Eocene (Backhouse 1989). It is a continental fluvial deposit with minor lower energy lacustrine and paludal components (Kern & Commander 1993). At many sites, the sediments are weathered and all pre-existing organic matter has been destroyed. The Perkolilli Shale is an Upper Eocene grey to white clay with minor sandy clay and believed to be freshwater, lacustrine and was deposited when the drainage systems were impeded by a distant marine transgression (Kern & Commander 1993).

Recent openpit mining has allowed for more detailed studies of palaeochannel sediments at Lady Bountiful Extended, Kanowna QED deposits, Steinway, Wollubar and Kurnalpi (Dell 1992; Gardiner 1993; Dusci 1994; Ladhams 1994; Lintern & Gray 1995a, b). The stratigraphic and sedimentological features of the Lady Bountiful Extended and the Kanowna QED deposits presented by Dusci (1994), Dell (1992) and Ladhams (1994) typify those of the other sites. The palaeochannels at Lady Bountiful Extended were incised into granitic saprolite. They form a dendritic system of third- to fourth-order channels that vary from 90 m to 400 m wide, with a depth of up to 40 m and a gradient of approximately 30 m in 1500 m (Dusci 1994). The generalised stratigraphy is shown in Figure 44a. The sediments are sandy (Figure 45b on Plate 7) compared to most palaeochannels in the Kalgoorlie region and have been sourced from a proximal weathered granitic terrain, as evidenced by the detrital nature of the kaolinitic matrix in the clay-supported sand and the angular nature of quartz grains (Dusci 1994). The Kanowna channels were incised into a weathered greenstone sequence and form a dendritic system of third-order channels approximately 30 m deep (Dell 1992; Ladhams 1994; Dell & Anand 1995). They are more clay-rich than Lady Bountiful, largely due to the provenance of the sediments, and their stratigraphy is similar to the other channels in the Kalgoorlie region (Figure 44b). The uppermost unit consists of 1–4 m of red to pale, orange calcareous soils overlain by medium to fine polymictic lag comprising abundant ferruginous gravel, vein quartz and lithic fragments. The unit consists of multiple lenses of bedded and graded alluvial deposits in channels cut into the underlying clays. An acid, massive, structureless clay unit forms a sharp, but irregular, lower boundary with the overlying calcareous alluvials. The 2–5 m thick red clay contains small, magnetic, subangular to rounded magnetic, black, ferruginous granules, detrital quartz and lithic fragments. Bleaching and incipient mottles develop within the basal Fe-rich clays and mark the transition into the megamottled zone. Megamottles are commonly developed in the clay unit. The megamottled zone is characterised by increased bleaching and the development of evenly spaced hematite–goethite-rich mottles. Two zones are recognised in the mottled zone, the mini-mottled (4–8 m thick) zone and the megamottled (6–10 m) zone, the boundary between the units is marked by a larger crack within the clays. Magnetic, black, ferruginous granules are abundant in the mottled zone. The transition from the mottled zone to the underlying clay unit is marked by a gradual decrease in mottles until the clays are totally bleached. The clay unit, 4–6 m thick, is characterised by sub- to well-rounded ferruginous pisoliths in a matrix of grey clay with minor detrital quartz. The underlying sandy unit comprises angular to subangular, bipyramidal, quartz-rich alluvial sediments. Bedding and grading within the basal units of the 'deep leads' are enhanced by fine, black, organic-rich material forming bands along with the gravels. Saprolite forms the lowest unit of the weathering

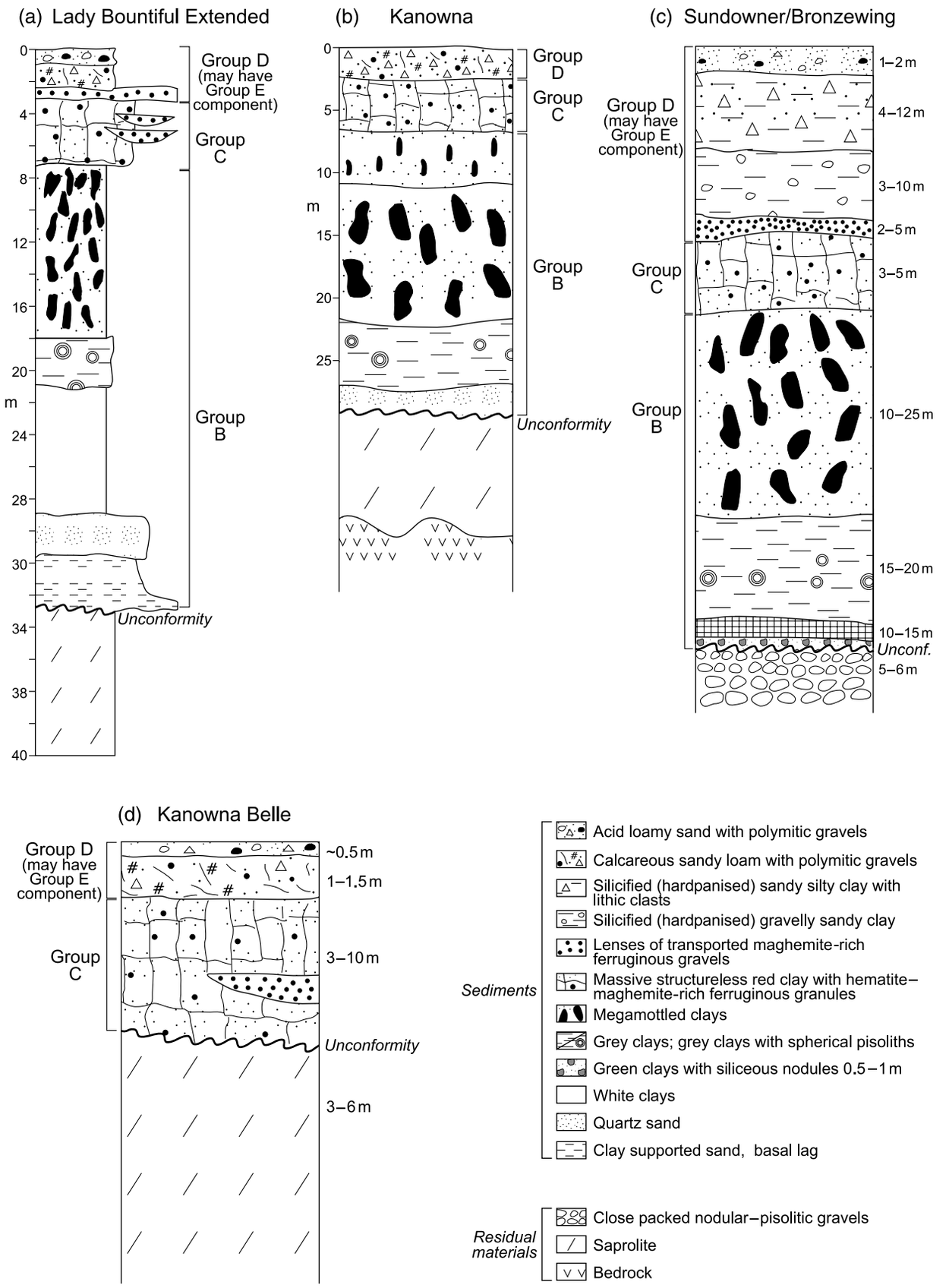

Figure 44 Examples of some sediment groups. These are typified by (a) Lady Bountiful Extended (after Dusci 1994), (b) Kanowna (after Dell 1992), (c) Sundowner/Bronzewing (after Varga *et al.* 1997; Wildman *et al.* 1998; Anand 2000) and (d) Kanowna Belle (after Dell 1992; Dell & Anand 1995).

profile with variably green, orange to white clays overlying bedrock.

The classification of sediments by Dell (1992), Dusci (1994) and Ladham (1994) broadly corresponds to the stratigraphy established by Kern and Commander (1993) for the Roe palaeochannel system. However, at the Lady Bountiful Extended and Kanowna QED deposits, a sandy clay facies within the mottled clay facies sequence has been identified (Dusci 1994; Ladhams 1994). This sequence differs from that of the type description of the Perkolilli Shale and the clay facies sequence due to the presence of ferruginous granule lenses. The sandy clay facies was deposited in a shallow, low-energy setting (possibly a semipermanent lacustrine environment), as indicated by the dominance of clay. Episodes of arid climatic conditions are characterised by erosion and deposition of gravel lenses, which are believed to have been deposited by fluvial processes (Dusci 1994). The sandy clay facies may be tentatively correlated with the Revenge Formation of the Lefroy and Cowan palaeochannels (Clarke 1993). A more extensive study of the palaeochannels and their fills in the Kalgoorlie region by P. de Broekert (unpubl. data) shows that the lithofacies composition of the Wollubar Sandstone, in particular, is strongly dependent on basement rock type and position within the palaeochannel network.

Description of megamottles and pisoliths

Post-depositional weathering, in particular, strong mottling of the clays has obliterated much of the primary sedimentary fabric. However, in the coarser sediments at Lady Bountiful Extended, many more sedimentary features have survived post-depositional weathering (Dusci 1994). Megamottles (>200 mm) (Ollier *et al.* 1988) are well developed and are thicker in the middle of the palaeochannel than at the edges. At Kanowna, a zone in transported clays contains evenly spaced, irregular, vertical, hematite- and goethite-rich megamottles (Dell 1992). Many of the megamottles have a grey kaolinite-rich zone around their margins.

Ferruginous pisoliths occur in some palaeochannel clays (Figure 47a on Plate 8). These pisoliths are well- to sub-rounded and most are 1–15 mm in diameter. Some have a single thin cutan (<1 mm), but most have multiple cutans and a variety of cores including hematite–maghemite fragments, ferruginous lithic fragments, clay, organic debris, quartz or a mixture of these (Figure 47b–g on Plate 8). Some nuclei are simple (a single particle) or complex (composite particles) (Figure 47c on Plate 8). Nuclei may be either regular or irregular and are surrounded by concentric goethite- or hematite-rich cutans, which are more and more circular in section (Figure 47g on

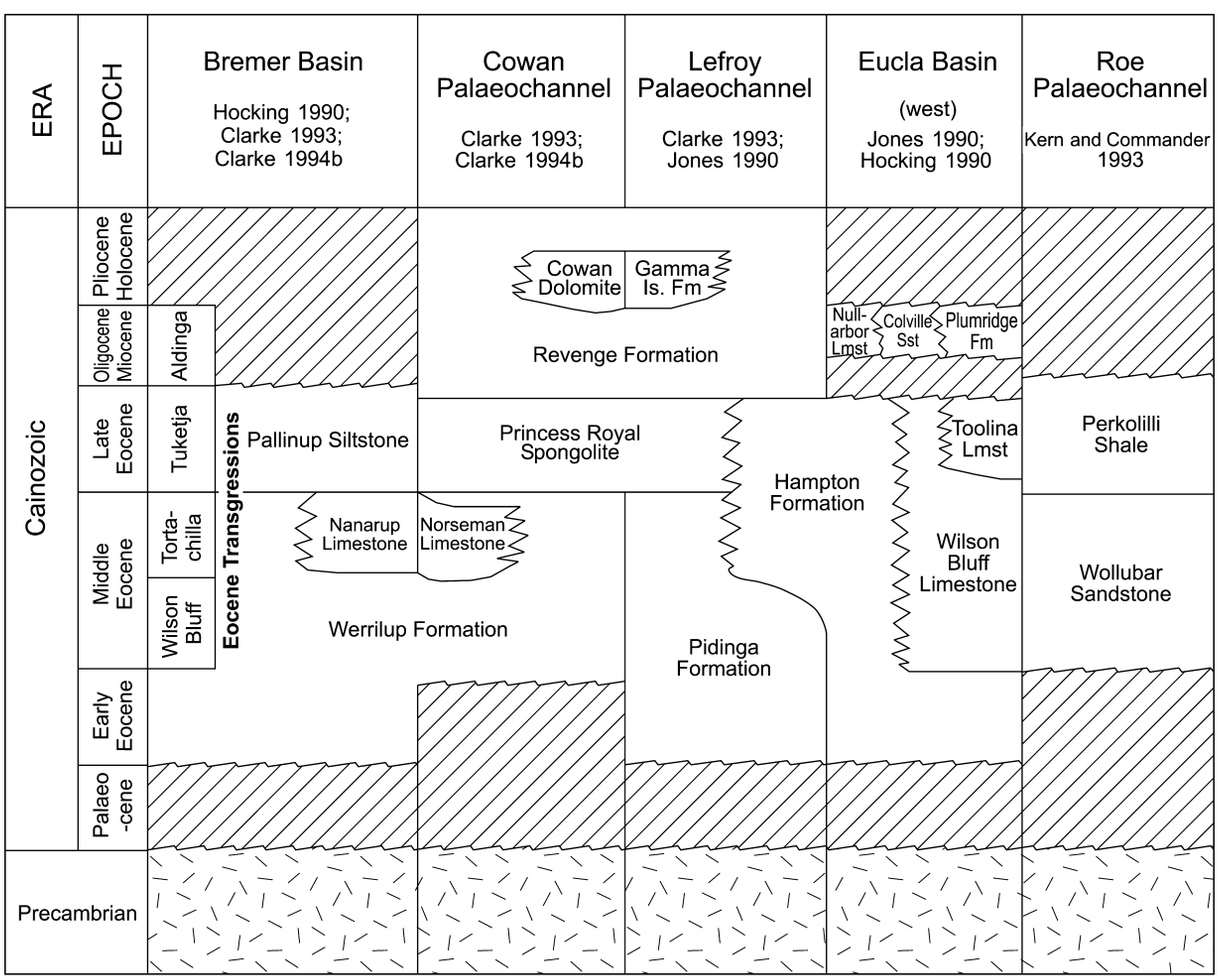

Figure 46 Diagrammatic section illustrating the stratigraphic relationships and nomenclature of the main palaeochannels of the south-eastern Yilgarn Craton and correlation with the Eucla and Bremer Basins. Fm, formation; Lmst, limestone; Sst, sandstone.

Plate 8). Only the first few cutans closely follow the small external irregularities of the nucleus; the cutans further from the nucleus become more and more regular and circular. Whatever the shape of the nucleus, the external shape of such composite pisoliths appears to be circular, or very nearly so, in the plane of a section. Cutans show different levels of dehydration. In general, the cutans show increasing dehydration (maturity) towards the nucleus, although a few outer cutans can be more dehydrated than an inner cutan. Rarely, a band of quartz may be sandwiched between two concentrically banded zones. The number of laminae in the cutans of pisoliths varies greatly, depending on grainsize, but generally there are 10 or more laminae. In places, there are two sets of cutans; broken hematitic cutans are encased by *in situ* concentric goethitic cutans (Figure 47d on Plate 8).

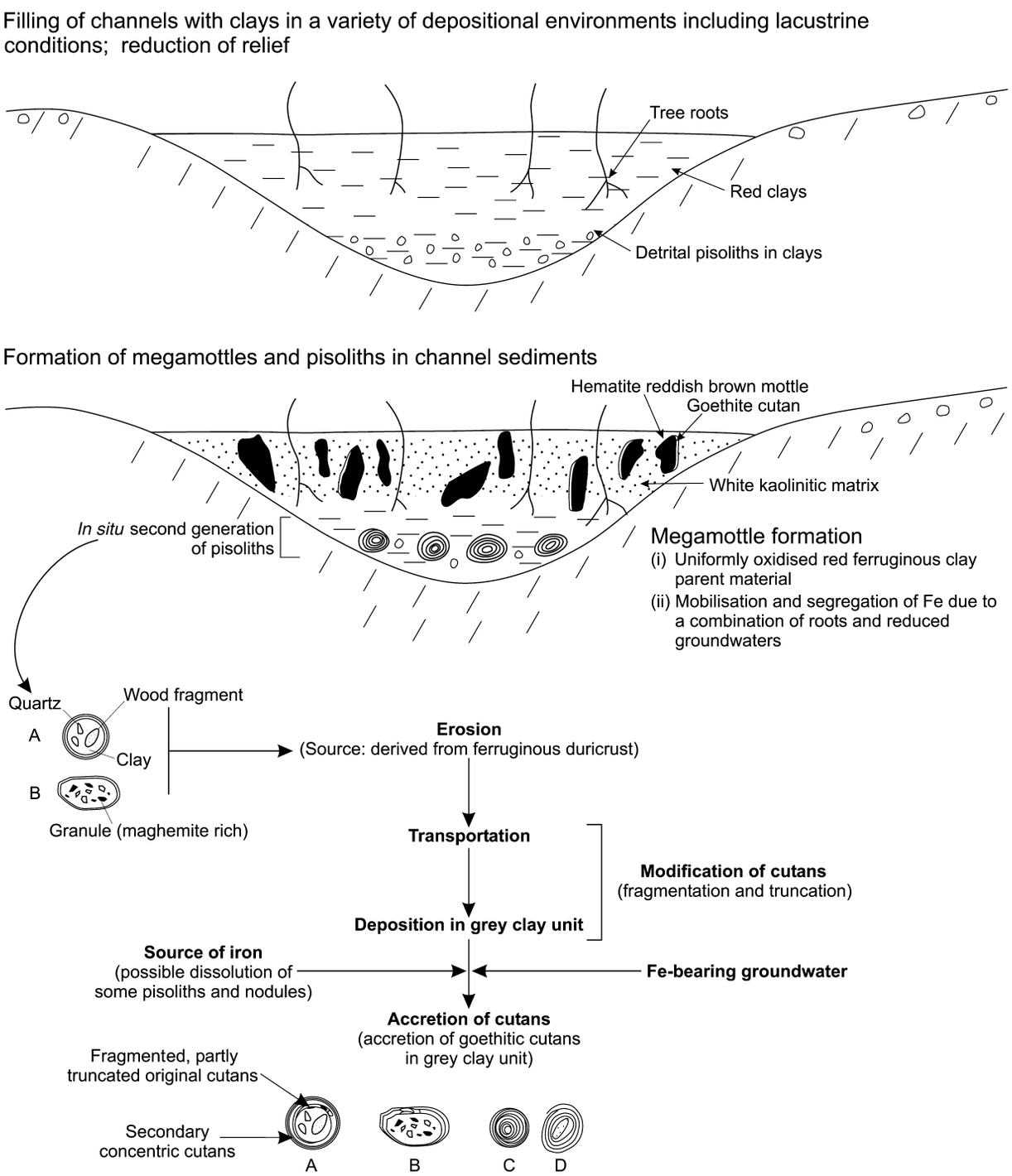

Figure 48 Interpreted pathways for the formation of megamottles and pisoliths in palaeochannel sediments. Pisoliths formed in palaeochannel environments are formed by an accretionary process and are typically concentric with multiple cutans (after Anand *et al.* 1993a; Dusci 1994).

Formation of megamottles and pisoliths in palaeochannel sediments

The likely pathways of formation of megamottles and pisoliths in palaeochannel sediments are shown in Figure 48. Megamottles in palaeochannel sediments are formed by mobilisation and segregation of Fe by a combination of roots and reduced groundwaters. Root systems penetrate mottled sediments and show an intimate relationship with Fe accumulations as these palaeochannels would have once supported abundant vegetation (Dell & Anand 1995; Anand 1998). Fine-grained red clays, presumably derived from the erosion of an old red soil profile, may have been a source for the hematite of the megamottles of the palaeochannel sediments. In fact, these clays may have been a uniform red-brown and became white on reduction below the water table and mottled in the vadose zone.

Concentric pisoliths in palaeochannel clays have a complex history. Calcareous, pisolitic and oolitic structures are common in the sedimentary record, having been described from a variety of marine and non-marine sequences. Theories of formation of pisoliths and ooliths are numerous (Pettijohn 1975) and include: (i) accretionary growth by precipitation of new material on the grain surface in a free-rolling environment as in many modern-day marine oolite shoals; (ii) concretionary growth by replacement of nucleus materials; and (iii) *in situ* precipitation of new material in a relatively static environment, such as soils. Pisoliths in palaeochannel sediments appear to have formed in the static environments described below.

(1) In the palaeochannel environments, pisoliths originally developed within the upper part of the relict profile have been eroded and deposited within the grey clay facies of the channel sediments. This is indicated by incomplete or broken cutans, compound pisoliths, the presence of maghemite-rich fragments within cores, and a different quartz grain distribution between these nodules and pisoliths and that of the grey clay.

(2) Some of these pisoliths may have been partly dissolved in an originally reducing environment.

(3) Subsequently, however, a second generation of pisoliths has formed *in situ* either without a nucleus or around a detrital nucleus of fine quartz, organic debris, hematite–maghemite-rich fragments or clay. Accretionary growth may have been proceeded by either inorganic or biogenic mechanisms. Ostwald (1990) attributed fine layering to organically mediated growth in a fluid medium. Pisoliths containing fossil wood exhibit a stromatolitic pattern of cyanobacteria and it is possible that some concentric pisoliths in palaeochannel sediments formed in this way. However, in places, it is difficult to decipher which process (inorganic or biogenic) is dominant.

Cowan and Lefroy palaeochannel systems

The Lefroy and Cowan palaeochannel systems contain up to 100 m of sediments, the stratigraphy of which is described by Clarke (1993) (Figure 46). The Lefroy palaeochannel drained east into the Eucla Basin, whereas the Cowan palaeochannel drained south into the Bremer Basin. Sediments deposited from two marine incursions, which are thought to have occurred in the Middle and Late Eocene, are preserved in the palaeochannel sediments (Figure 46). The Middle Eocene incursion, which is correlated with the Tortachilla Transgression, resulted in the deposition of the Hampton Sandstone/Pidinga Formation and the Norseman Formation in the Lefroy and Cowan palaeochannels. The Hampton Sandstone/Pidinga Formation has a coarse- and fine-grained lignitic and siliciclastic composition and was deposited in a transgressive sequence of fluvial to estuarine sediments, respectively. The Norseman Formation is a fossiliferous marine

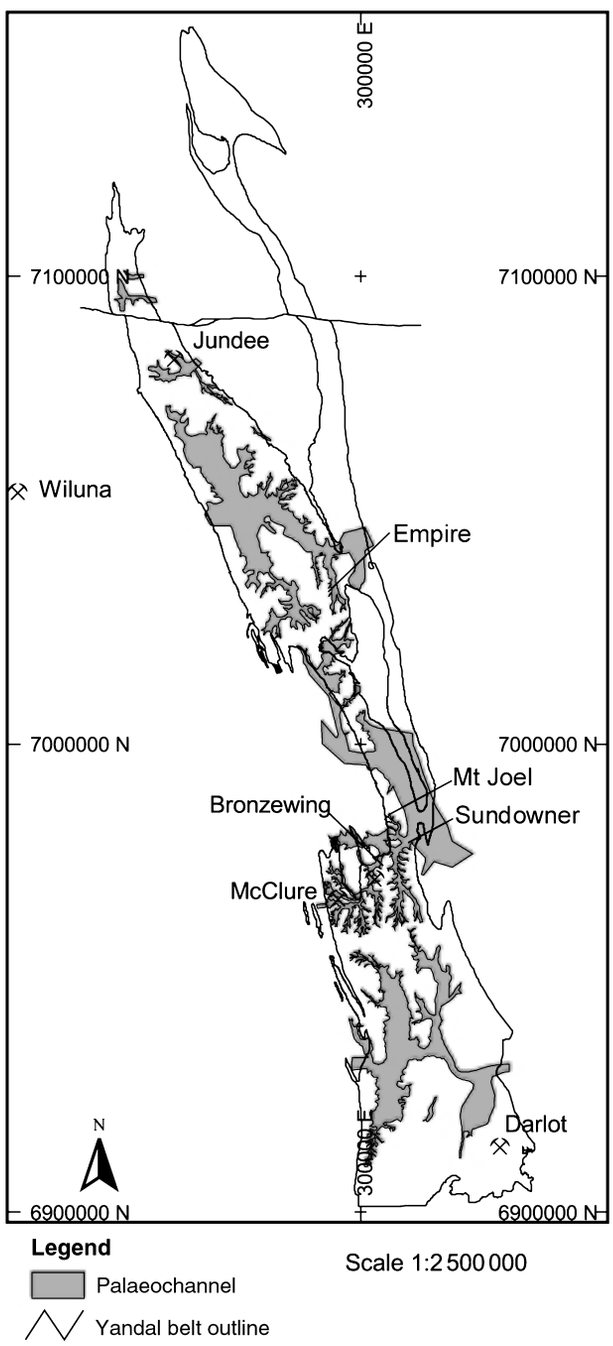

Figure 49 Distribution of palaeochannels in the Yandal greenstone belt based on the interpretation of magnetic images and drilling showing >5 m of cover (after Wildman & Compston 2000). Magnetic images were provided by Great Central Mines Limited, now Normandy Yandal Limited.

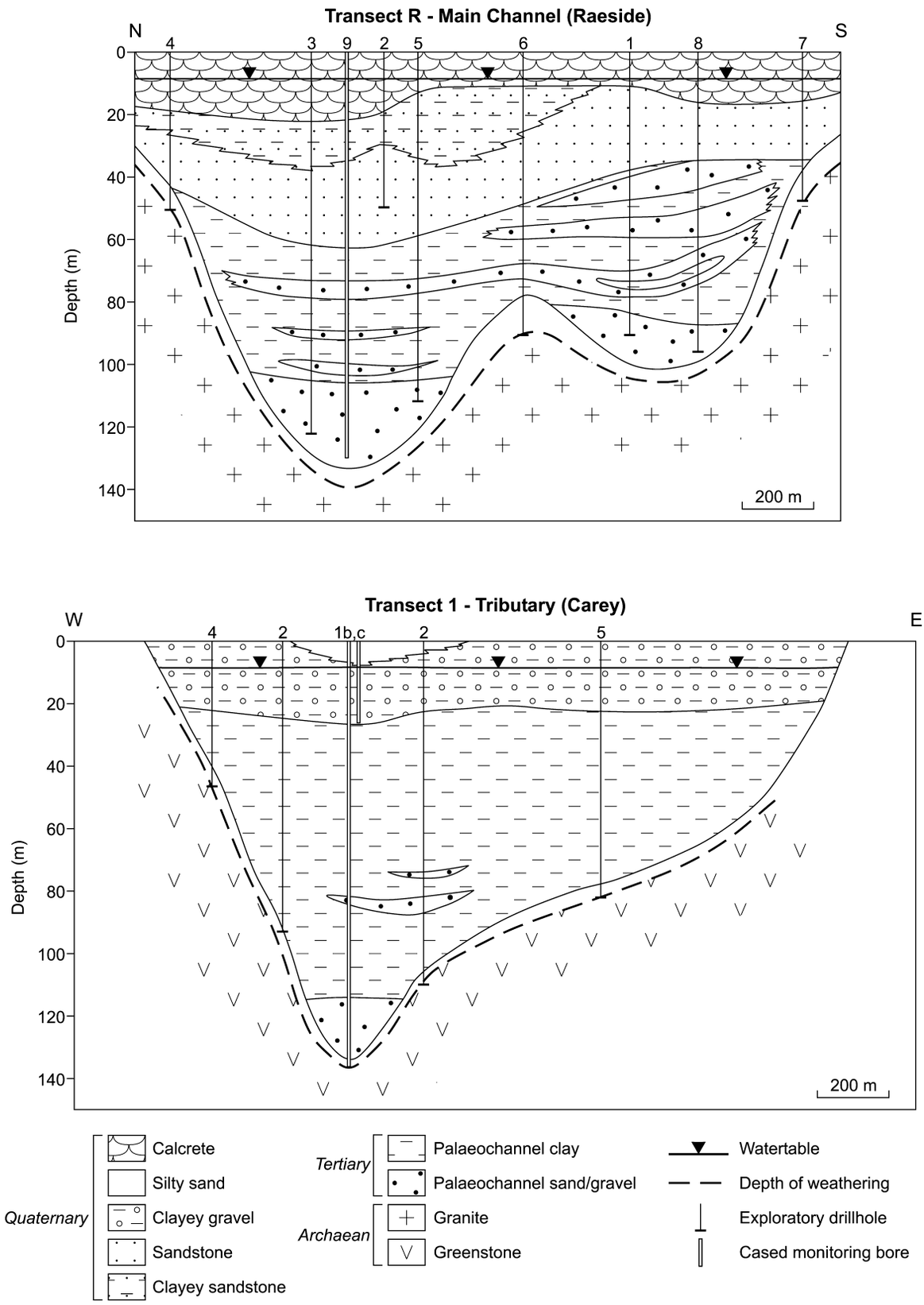

Figure 50 Cross-sections showing the stratigraphy of the Raeside and Carey palaeochannels sediments (modified after Johnston *et al.* 1999).

carbonate deposited in a shallow, cool-water environment (Clarke 1993).

The Tuketja Transgression resulted in the deposition of the second transgressive sequence. Deposition was initially lignitic sediments before the deposition of the Princess Royal Spongolite, containing up to 90% sponge spicules that can be observed in the Lefroy and Cowan palaeochannel systems. Investigations at Argo (Lefroy palaeochannel: Woolrich 1994) have largely confirmed the stratigraphic relationships established in the Lake Lefroy system by Clarke (1993).

NORTHERN YILGARN PALAEOCHANNELS

Numerous palaeochannels occupy the lower parts of the landscape in the northern Yilgarn (Anand *et al.* 1991b, 1999a; Robertson *et al.* 1994; Varga *et al.* 1997; Johnston *et al.* 1999; Wildman & Compston 2000), for example, in the Yandal greenstone belt (Figure 49). The stratigraphy and post-depositional weathering is broadly similar to that described by Kern and Commander (1993) for the Roe palaeodrainage in the Kalgoorlie region, namely a lower basal sand in the axis of the channel, overlain by a thick sequence of clay-rich sediments, strongly overprinted by ferruginous mottling. The sediments in the studied palaeochannels are non-marine. In the Raeside and Carey palaeodrainages, the sediments comprise a basal sand overlain by an interbedded sequence of dense, plastic clay with minor interfingering sand lenses (Figure 50) (Johnston *et al.* 1999). The palaeochannel sand at the base of the sequence occurs as a sinuous stringer sand unit, bounded by relatively steep topography, on the underlying Archaean bedrock surface. Palynological analysis of lignitic material in bore NER-3 indicates an Eocene age (Milne 1998) and is equivalent to the Wollubar Sandstone in the Roe Palaeodrainage (Kern & Commander 1993). The sandy unit may be up to 40 m thick and from 100 m to 1000 m in width. The thickness and presence of the palaeochannel sand is related to its origin, with the thickest sequences of sand occurring in granitoid catchments, which are capable of providing more quartz-rich, clastic material than the predominantly greenstone catchments (Johnston *et al.* 1999). The overlying clay rests on the basal sand with a gradational contact comprising several metres of dark-grey clayey sand. The unit reaches a maximum thickness of 78 m in bore NED-9 (Johnston *et al.* 1998) and grades downward from sandy clay to a uniform, light-grey plastic clay.

At Sundowner and Bronzewing (Varga *et al.* 1997; Wildman *et al.* 1998; Wildman & Compston 2000), the palaeochannel sediments are up to 45 m thick and are unconformably overlain by up to 26 m of sandy silts and gravels (Group D) [Figures 44c; 45c on Plate 7]. Elsewhere, the sediments are approximately 80 m thick and directly overlie fresh bedrock. The sediments consist of massive kaolinitic clays with extensive megamottling and pisoliths, grey clays and clays with concentric pisoliths (1–5 mm), directly underlain by ferruginous nodules and pisoliths formed from the weathering of basalt. The basal clays contain fine-grained quartz, but the unit of basal sand is absent at these sites. There is a small proportion of quartz sand grains in the grey clays, which are rounded and water worn; these are generally approximately 1 mm in size.

At the Discovery pit (Bronzewing), a layer of green smectite with siliceous nodules occurs at the base of the palaeochannel sediments (Figure 44c) (Varga *et al.* 1997; Anand *et al.* 2000). There is a lens of dolocrete up to 15 m thick in the palaeochannel sequence above the nodular green clay. The dolomite is of biogenic origin formed in lacustrine environments. There is evidence of extensive vegetation growing over the dolocrete as abundant root holes, now filled with green smectitic clay, are found in its upper part. The dolomite is formed from 2 μm to 8 μm spherules and is very pure (90%), with the main contaminants being smectite and Mn oxides, which occur on the faces of slickensides. The upper surface of dolomite is close to horizontal, except towards the centre of the channel where some collapse has occurred. A similar stratigraphy in palaeochannel sediments has been observed in a number of sites, including Stellar (Mt Magnet) (Robertson *et al.* 1994) in the northwest. At Stellar, the palaeochannel sediments are up to 18 m thick and consist of a grey, plastic clay and minor sandy clay (smectite and kaolinite). Hematitic brown mottles occur as vertically elongate aggregates up to 400 mm long. Creamy, grey clays become more prominent with increasing depth and contain elongate, columnar cracking structures that expose roots, commonly sheathed in Fe-rich accumulations. Detrital hematite–maghemite-

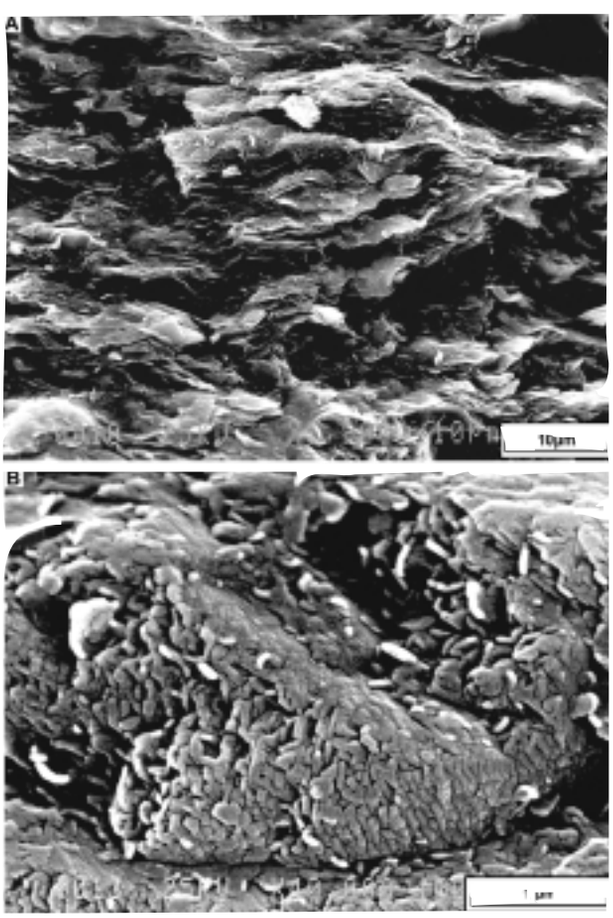

Figure 51 Scanning electron micrographs of palaeochannel clays from Sundowner showing parallel fabric of smectite (a) and vermicular fabric of kaolinite and halloysite (b) overprinting primary sedimentary fabric (R. R. Anand, J. E. Wildman & C. Phang unpubl. data).

rich ferruginous granules occur towards the base of this unit, whereas an irregular zone of sepiolite masses occurs towards the top of the palaeochannel. Sepiolite has been reported in both marine and lacustrine environments and is abundant in some valley calcretes in the Yilgarn (Butt *et al*. 1977). It is generally associated with aquatic, alkaline conditions, with high activities of Si and Mg (Allen & Hajek 1989).

MINERALOGY OF PALAEOCHANNEL CLAYS

The palaeochannel sediments consist mainly of varying proportions of clays, quartz, hematite, goethite and maghemite. The clays are commonly a mixture of smectite, kaolinite and halloysite or only kaolinite and halloysite, with no systematic distribution trend in the profile. In places, the smectite overlies the kaolinite (e.g. Kanowna) and in others kaolinite overlies smectite. Although the original sedimentary features are destroyed on a mesoscopic scale, they may be preserved as oriented layers of smectite, kaolinite and halloysite on a microscale (Figure 51). Kaolinite is generally poorly crystalline, probably due to comminution during transport. One of the characteristic features of the clays is that they are plastic. The reasons for the plasticity are not clear, but it may be due to the presence of Na on the exchange complexes of kaolinite. Hematite is the dominant Fe oxide species, although goethite is locally abundant. Rutile, zircon and ilmenite are common accessory minerals, particularly in the basal sand unit. Manganese oxides and dolomite may occur as lenses.

CORRELATION BETWEEN SOUTHERN (KALGOORLIE) AND NORTHERN YILGARN PALAEOCHANNELS

The two broad groupings of distinct sedimentological units (sand and clay), as discussed above, can be correlated with the stratigraphic nomenclature for the Kanowna and Lady Bountiful Extended palaeochannels (Roe palaeodrainage channel system) (Figure 52). The white to grey clay upper unit correlates with the Perkolilli Shale and the lower clayey sand with the Wollubar Sandstone. The sediments have very similar post-depositional weathering features, such as mottling, pisoliths and dolocrete. Thus, the similarity in the nature and characteristics of palaeochannel sediments between the regions suggests that similar conditions prevailed not only during the deposition of sediments, but also during their subsequent weathering. Several authors (Clarke 1994b; Dusci 1994; Ladhams 1994) suggested that the change from an active channel erosion to low energy deposition may be explained by a rise in base-level related to the Tortachilla Transgression during the Middle Eocene, as observed in the sediments of the Lefroy and Cowan palaeodrainage systems. This may be true in the Kalgoorlie region, but the effect of this transgressive event for areas such as Bronzewing and Lawlers, which are topographically higher than the Kalgoorlie region, remains unclear. It is possible that climate may have had a larger

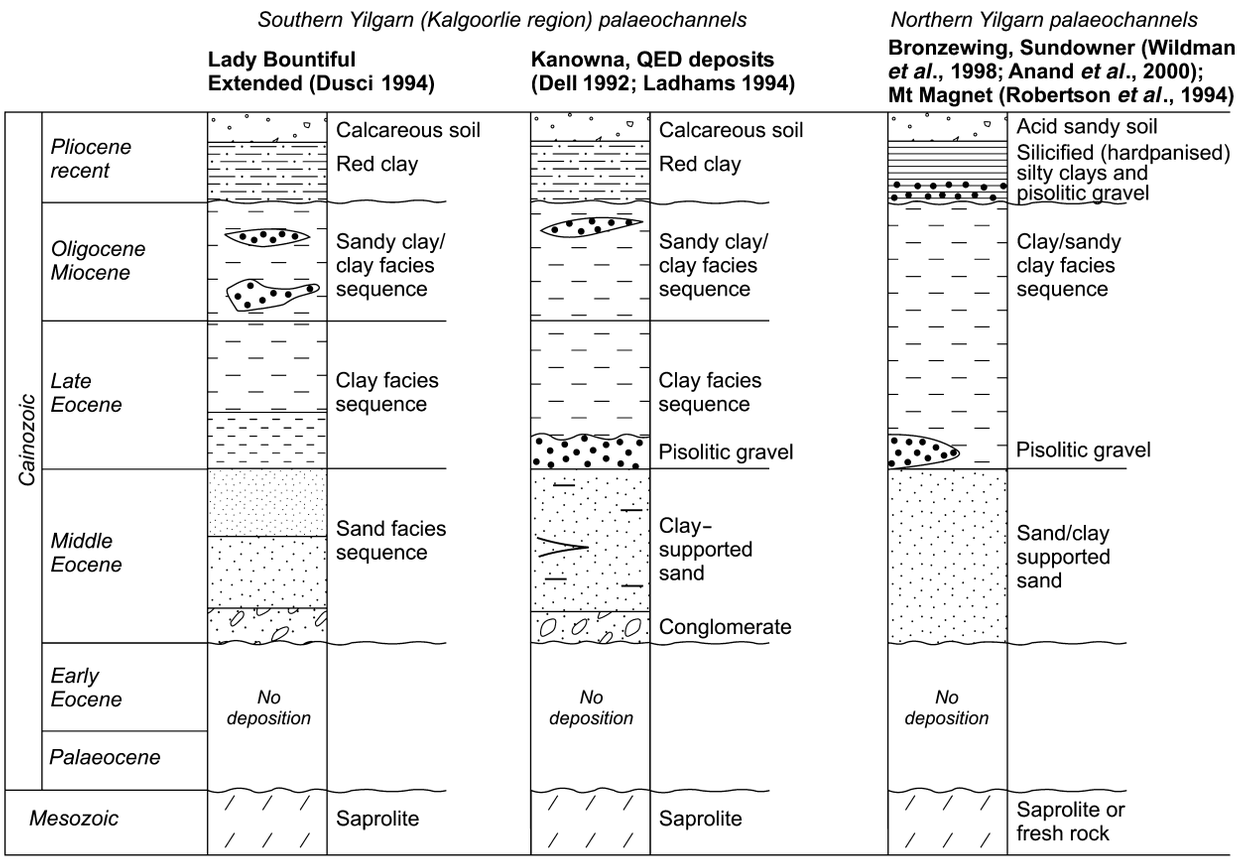

Figure 52 Correlation of the generalised stratigraphy of the northern Yilgarn palaeochannels (Bronzewing and Sundowner palaeochannels) and southern Yilgarn palaeochannels (Lady Bountiful Extended, Kanowna and QED deposits).

control on sea-level variations or that the northern portion of the craton has undergone post-depositional uplift.

MAGNETIC SIGNATURE OF PALAEOCHANNELS

The extensive occurrence of maghemite-rich gravel in the palaeochannel sediments is coincident with some dendritic patterns visible in aeromagnetic surveys (Figure 53). As discussed earlier, maghemite can form by the heating of goethite during bush fires over Fe-rich rocks that need not contain magnetic primary minerals. Primary magnetite and Fe sulfides generally weather to goethite or hematite; some magnetite may survive, although it will be a relatively small component of the total magnetism observed. Detailed stratigraphy and distribution of magnetic minerals in the palaeochannel environments at Bronzewing (Varga *et al.* 1997), Sundowner (Wildman & Compston 2000) and logging in general in the Yandal belt have provided sufficient detail to enable the mapping of dendritic patterns of the buried drainage systems (Anand *et al.* 1999a; Wildman & Compston 2000). With current aeromagnetic technology (with a line spacing of 50 m and terrain clearance of 25 m), data indicate that a bed of magnetic gravels needs to accumulate to more than 1 m to show on the aeromagnetic images. This excludes the large areas of thin ferruginous transported material less than 10 cm thick that often covers greenstone terrain. The channel boundaries are poorly defined magnetically in areas of felsic bedrocks. This is due to the paucity of ferruginous gravels because of their low Fe content and, therefore, erosion of regolith derived from felsic rocks is likely to be dominated by sandy colluvium. These observations are very similar to those reported by Ford (1996) for the Cobar region in New South Wales.

The beds of magnetic gravels at the palaeochannel margins may be up to 15 m thick, depending on the catchment area of the sheetwash adjacent to the channel and the Fe content of adjacent rock. The channels defined by the magnetic gravels vary in width from 1.5 km to less than 100 m (e.g. Empire pit: Figure 54) and may be traced for up to 20 km. On the modern surface, for example in the Yandal belt, tributaries of the palaeochannels are being stripped from the upper landscape in transect T1 (Figure 55) (Wildman & Compston 2000). The remnants of small creeks appear on the magnetic image as linear features produced by ferricretes containing magnetic gravels, fossilised wood fragments and detrital vein quartz. These ferricretes occur over 500 m above sea-level at the heads of some of the present drainages in an inverted stratigraphy. The wider channel on the transect T1 has a continuous bed of residual and transported magnetic gravels across its width and less than 10 m of channel clays. Where the channel is 300 m or more wide and over 20 m deep (T2), the magnetic gravels are mainly restricted to the edges, the channel clays are 15 m or more thick and are mottled towards the base. The wider drainages (>1 km: T3) may be up to 100 m deep with no gravels across the deeper 300 m, where saprolitic clays meet channel clays. The magnetic gravels are restricted to the edges, but may still

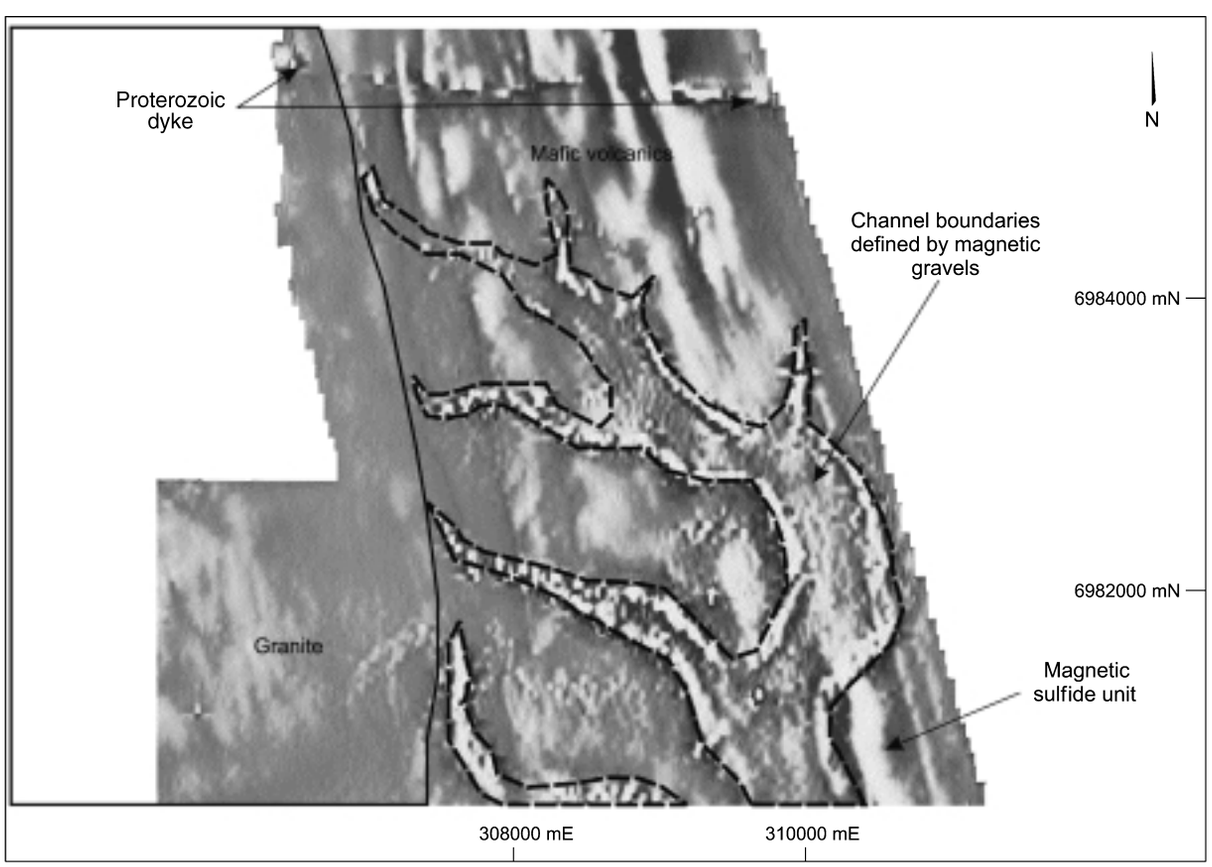

Figure 53 Magnetic image showing the delineation of palaeochannel boundaries by magnetic gravels, Mt Joel (after Anand *et al.* 1999a; Wildman & Compston 2000).

be buried by 15–20 m of colluvium and alluvium of group D. Some channels have more than one magnetic edge feature, which may represent episodic accumulation or the reworking of magnetic gravels from higher in the drainage.

The infilling of these palaeochannels with sediments produces an alluvial plain above the geological features that once constrained the watercourse. At Bronzewing, the flow direction indicated by the dendritic magnetic pattern is much the same as the modern drainage. At the 4800N area at Mt Joel, the palaeodrainage direction indicated by magnetic gravels is to the south, whereas modern drainage as indicated by satellite imagery is to the east (Figure 56). The evidence from these studies suggests that in greenstone terrain, magnetic data can be used for the mapping of palaeochannels and their flow direction and the discrimination of primary and secondary magnetism.

Group C

Group C consists of red, massive clays that may contain fine (2–5 mm), hematite–maghemite-rich ferruginous granules, either uniformly distributed or as lenses (Figures 44; 57a, b on Plate 9). In profiles, this may show little variation. However, in places the lower part of this unit may be mottled or pisolitic (e.g. the Calista deposit, Mt McClure). Group C is very extensive in the southern (Kalgoorlie) Yilgarn and less common in the northern Yilgarn, but has similar characteristics in both regions. In the Kalgoorlie region, the red clays are overlain by thin (0.5–2 m) calcareous soils and unconformably overlie saprolite (Figure 57a

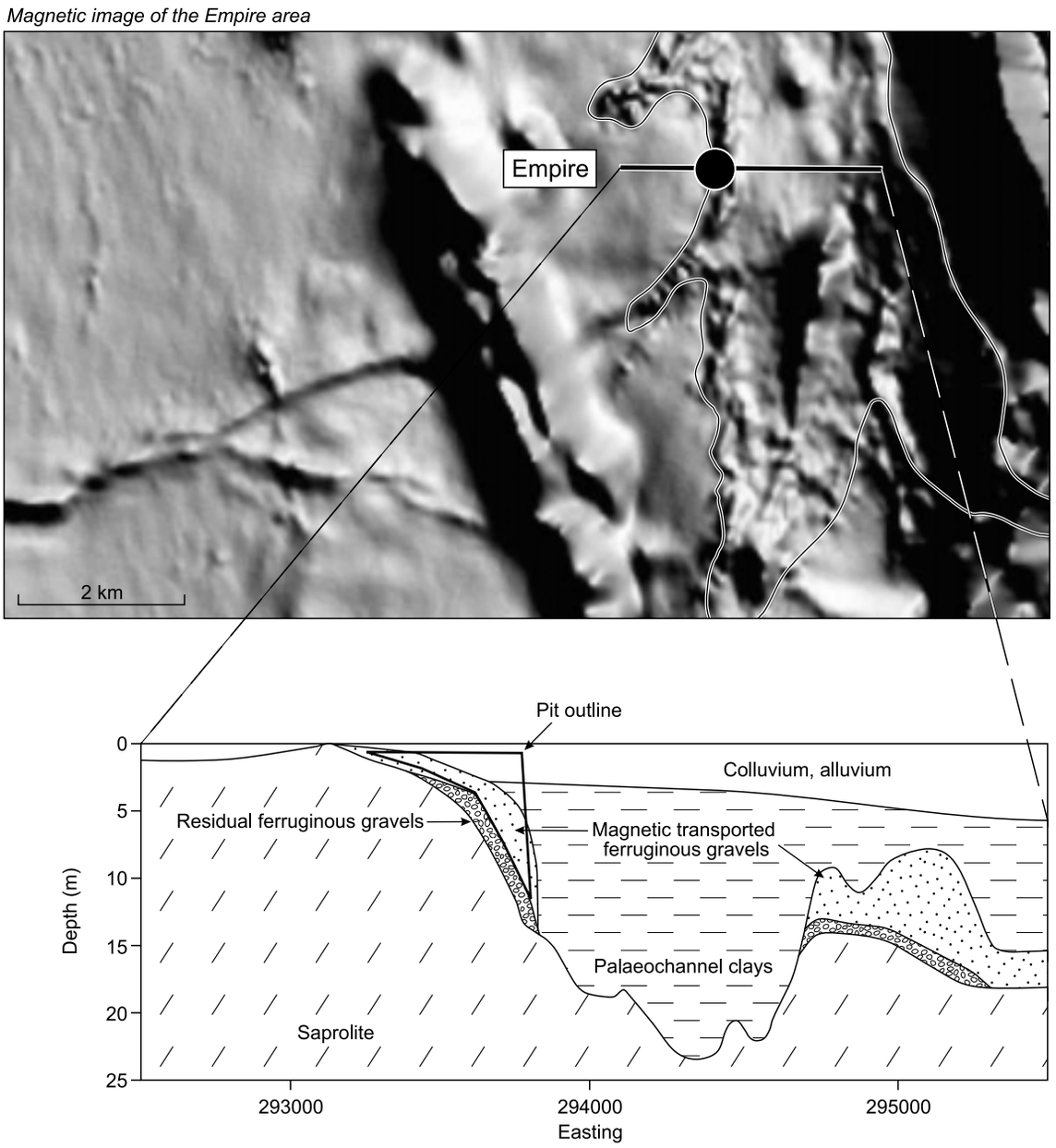

Figure 54 Comparison of the magnetic image for the Empire palaeochannel and a transect showing the distribution of the magnetic gravels that outline the palaeochannel boundary (after Anand *et al.* 1999a; Wildman & Compston 2000).

on Plate 9) or group B sediments. This unit occupies most topographic positions except hills and crests. The thickness increases down slope, varying from 3 m to 20 m (generally 3–5 m). Where present, in the north, the clays are 3–8 m thick and underlie the sandy silty or gravelly unit of group D (Figure 57b on Plate 9) (e.g. Mt Gibson, Central Zone, Bronzewing; Calista deposit, Mt McClure).

The matrix consists largely of poorly crystalline kaolinite with quartz and minor smectite. However, smectite can be abundant particularly towards the base. At Kanowna Belle and Matt Dam, granules extracted from the red clay samples are remarkably uniform, black, hematite–maghemite-rich, sub- to well-rounded and are 2–15 mm in size (Dell 1992; Anand *et al*. 1993a). Typically, the granules have an earthy to submetallic lustre; thin earthy clay cutans are developed around rare spherical granules.

Petrographic examination of the granules suggests that they are largely of detrital origin, but some have formed *in situ* in red clays. Fabric variations have identified four major granule groups.

(1) Granules developed within soils. These are textureless granules formed by the replacement of clays by hematite. Polished sections of these granules show brown, ferruginous clay pervasively replaced by hematite along cracks and voids. Quartz grains are common in the nucleus.

(2) Granules derived from ferruginisation of bedrock or saprolite fragments. These granules are identified by the preservation of relict rock fabrics and pseudomorphs after rock-forming minerals (e.g. hematite pseudomorphs after carbonate rhombs) preserved within the interiors of the granules.

(3) Ferruginised plant matter. Some of the granules represent ferruginised plant fragments that are clearly identifiable by the intricate preservation of individual cell walls, now totally replaced by hematite.

(4) Concentrically zoned granules. These granules have cutans developed around a nucleus of the cellulose, quartz, clays and saprolite fragments. Quartz fragments are commonly incorporated into the concentric bands, indicating multiple periods of development.

The nature and occurrence of this unit implies deposition in broad, flat-lying drainages, with the gravels laid down from small alluvial channels, probably during infrequent storm water flow.

Group D

Group D consists of talus, alluvial deposits and detrital sheets (Figures 44; 45c on Plate 7; 57b on Plate 9) deposited during occasional flooding and sheetwash events. The sediments have been derived from increased erosion following the change to more arid climates, in part a result of instability caused by a reduction in the vegetative cover. Although certain regolith units have been indurated by introduced cements, much of the regolith is soft and unconsolidated and, hence, susceptible to erosion by water (and wind) even in areas of low relief. Because of the reduced rainfall, much of the drainage is incompetent and sediments remain in the landscape further reducing the relief.

Sheetwash is a dominant process of erosion on surfaces of low relief, in all but thickly vegetated regions. This process is able to transport clay, silt and fine sand, even in rainforests, and in arid areas during heavy rainstorms, gravel and small coarser fractions, as a traction load. Water flow is discontinuous, changing with surface irregularities, rainfall intensity and wind. Networks of braided rills and wash channels can develop and, depending on the local topography, may converge into larger washes or diverge across flatter depositional areas. Such networks are temporary but, from season to season, the whole surface is affected. The resultant sedimentary sequence consists of a series of discontinuous, mostly poorly sorted, beds, commonly cross-cut by infilled scours and channels. These sediments are commonly referred to as colluvium (or colluvium–alluvium), and are the most widespread and abundant type of sedimentary cover on the Yilgarn Craton. Better sorted and mostly finer grained sediments (silty clay and clay), generally associated with more defined drainages, valley axes and floodplains, are referred to as

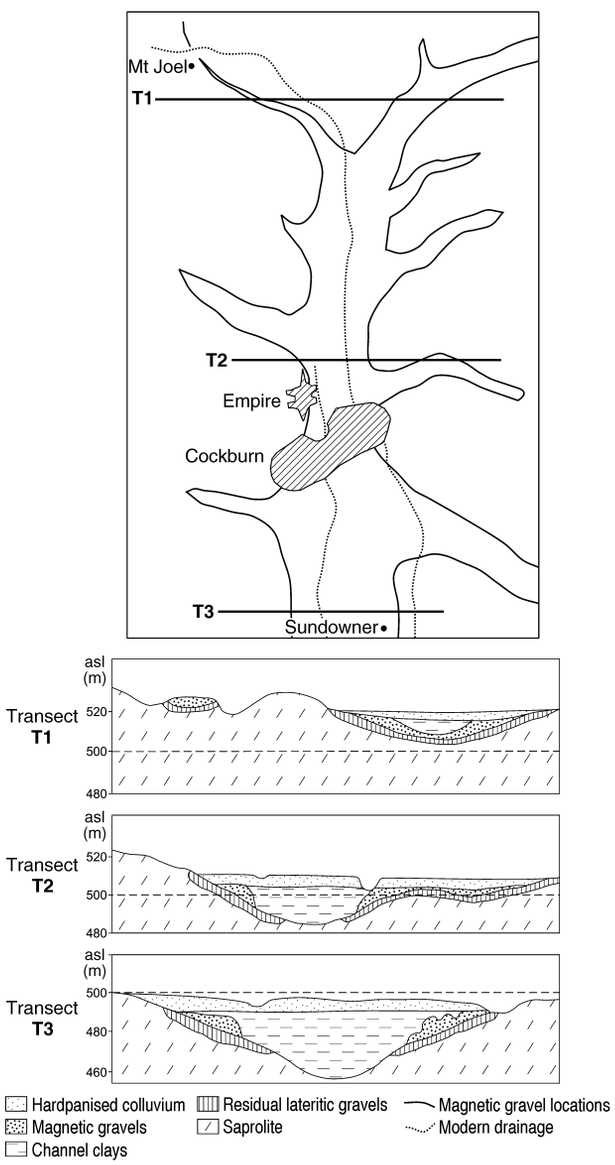

Figure 55 Schematic model for magnetic gravel distribution in the Yandal greenstone belt. Sections T1, T2 and T3 have been taken through various parts of the palaeochannel (after Wildman & Compston 2000).

alluvium. Around playas, these merge with mostly clay-rich lacustrine sediments that have a strong evaporitic component at the surface, predominantly gypsum and halite. Groundwater or valley calcretes are present as narrow, lenticular units, 5–30 m thick, in a drainage axis north of the Menzies Line (Butt *et al.* 1977).

The sediments may overlie not only fresh and weathered basement, but also the sediments of the other groups, and consist of their physical and chemical weathering products. The composition of sediments broadly reflects that of the catchment regolith. Thus, at Highway pit (Mt Gibson) and at Fender, the colluvium–alluvium is quartz–kaolinite-rich, contains abundant feldspars, and is derived from deeply eroded granitic rocks approximately 1 km to the west. Ferruginous materials are a small component of these sediments. Where sediments are derived predominantly from greenstone rocks they generally contain ferruginous clasts. The upper parts of these sediments are generally modified by silicification and/or calcification, forming red-brown hardpan and calcrete, respectively. At many sites, the colluvium–alluvium is composed of two major sedimentary units: yellowish to red sandy, silty clay and red, brown, gravelly, sandy clay. Each unit may also consist of several facies. Viewed together, the sandy, silty clay and gravelly, sandy clay units appear to have developed an inverted stratigraphy in relation to the residual regolith profile. Materials derived from the upper, ferruginous parts of the residuum occur at the base of the sediments.

SANDY, SILTY CLAY UNIT

The sandy silty clay unit varies from 2 m to 5 m in thickness, but can reach up to 15 m (Figure 44). In the north, it overlies ferruginous duricrust (Stellar, Mt Magnet), saprolite or, more commonly, a gravelly sandy clay unit; the latter relationship is exposed at many locations (e.g. S Pits, Mt Gibson; Central Zone, Bronzewing; North pit, Lawlers; Calista deposit, Mt McClure). In the Kalgoorlie region, it overlies saprolite or, more commonly, the red clays of group C (e.g. Kanowna Belle, Wombola). This unit has been studied from exposures in the Stellar pit, Mt Magnet (Robertson *et al.* 1994). Here, there are three facies, with each being laterally continuous across the pit face. Facies 1 consists of red-brown silty clay, up to 3 m thick, and is dominated by kaolinite and quartz, with small amounts of goethite, hematite, feldspars and mica. It is considered to be derived from erosion of saprolite and saprock. Facies 2 is 1–2 m thick and occurs as lenses of well-rounded, reddish-brown to black, hematite–maghemite-rich ferruginous gravels without cutans, and rounded pebbles of vein quartz within the sandy silty clay facies, and consists of transported ferruginous debris. These lenses are thinner than those of the fine-grained, sandy silty clay materials. A sharp boundary separates these two facies and they probably represent different environments of deposition. Facies 3 comprises sandy clay to silty clay, up to 1 m thick. The <75 μm fraction consists largely of smectite, kaolinite and quartz with small amounts of goethite and hematite. The pale, clay-rich, subvertical structures, possibly related either to roots or burrowing action, cut through this unit, but do not penetrate the underlying duricrust to any significant depth. The sediments of this facies also appear to have been derived from the erosion of saprolite.

GRAVELLY SANDY CLAY UNIT

The gravelly unit is approximately 3–5 m thick, but can reach up to 15 m, for example, at the Calista deposit. It

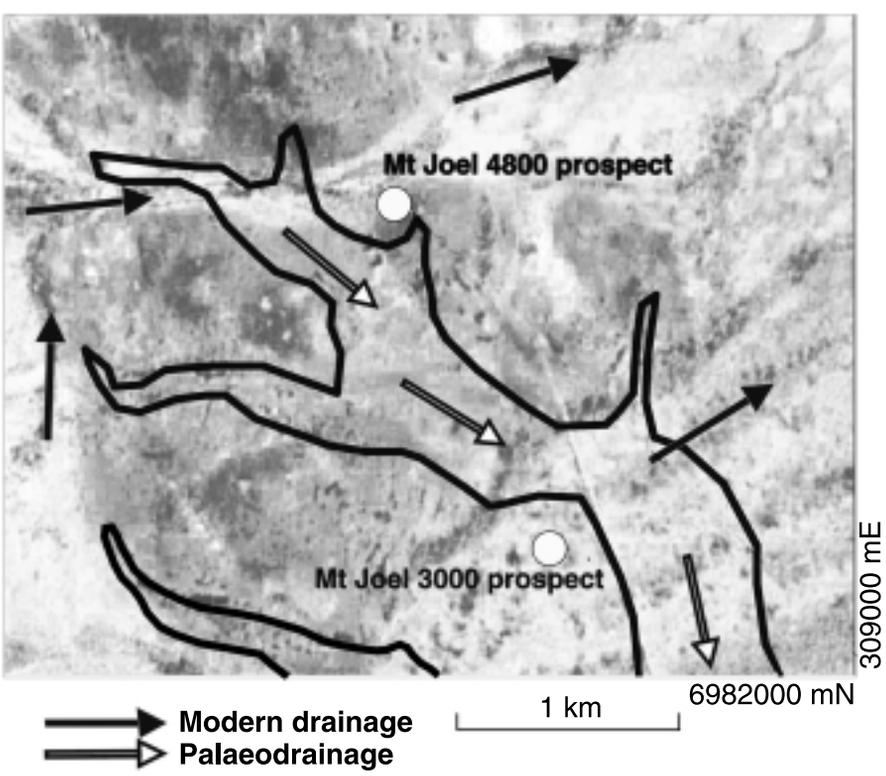

Figure 56 Landsat TM composite showing contemporary drainage (black arrows). The discordant palaeodrainage system is outlined in black (white arrows) (after Wildman & Compston 2000).

appears conformable with the overlying sandy, silty clay unit and lies unconformably on underlying ferruginous duricrust or saprolite. The gravels comprise magnetic and non-magnetic fractions, largely composed of subrounded to rounded ferruginous clasts without cutans, fragments of ferruginous saprolite, vein and detrital quartz, and lithic fragments in a red-brown, sandy clay matrix. The polymictic nature of clasts indicates diverse origins, including the breakdown of ferruginous duricrust and saprolite. The fine matrix largely consists of poorly crystalline kaolinite and quartz, with small amounts of goethite, hematite, zircon and mica. Similarities in the nature and mineralogy of the ferruginous clasts and those of the buried or exposed lateritic residuum in a number of areas (e.g. Mt Gibson, Bronzewing, Calista) suggest that the former are probably derived from ferruginous duricrust up slope in the palaeolandscape.

Group E

INTRODUCTION

The movement of aeolian material has been a significant process in Australia over the past several hundred thousand years (Butler & Churchward 1983). The mantle of aeolian deposits across the Yilgarn landscape is a common regolith type in the region. There has been some debate as to the origin of the sandplain; many regard it as sedentary with or without a transported component (see below under the heading: Regional distribution and patterns of regolith on the Yilgarn Craton). However, where sand occurs as dunes, there can be little doubt as to its transported nature. Plains of aeolian sands are extensive in the Laverton area (Gower 1976) and commonly overlie granitic rocks, but there is some encroachment over greenstones.

SCHEMATIC SECTION	DESCRIPTION	INTERPRETATION
5 to 7 / 4	7. Gypseous sands and muds (= Darlot Formation).	Lacustrine playa-lake, aeolio-lacustrine playa, aeolian dunes and sheets
	6. Lithoclast and quartz gravel, and sand and clayey quartz sand (= Nuendah Formation).	Channel, overbank, fan and unconfined-wash sub-aqueous deposits
	5. Red quartz sand (= Wirraway Formation).	Aeolian dunes and aeolian sand sheets
	4. Siliciclastic sand, massive yellow to red (= Gibson Formation)	Aeolian linear dunes and aeolian sand sheets in dryer areas; fluvially reworked aeolian sand sheets in wetter areas
2	2. Pisolitic, nodular, labyrinthoid sandy silt-clay rock and silt-clay sandstone (= Mulline Formation)	Altered, partly or wholly aeolian sediment; sandy duststone
	3. Red sandy silt-claystone (= Menzies Formation)	Mainly aeolian valley fill with lesser intercalations of playa, playa-lake, and ephemeral fluvial deposits
3 / 1	1. Grey sandy clayrock with lesser clayrock, sandstone and conglomeratic facies (= Westonia Formation)	Granitic-saprolite derived fluvial, lacustrine and aeolian deposits
b	b. Granitic saprolite of gravel and sand-sized quartz supported in a matrix of kaolin phases	Deeply weathered granitic rock
a	a. Granitic and gneissic rock	Archaean intrusive rocks

Figure 58 Schematic summary of the Cenozoic regolith stratigraphy of the southwestern margin of the Gibson desert, northeastern Yilgarn Craton (after Glassford and Semenuik 1995, pp. 131–166). Reproduced from Palaeogeography, Palaeoclimatology, Palaeoecology with permission from Elsevier Science.

Table 6 Chemical composition of soil profiles on gabbro and talc–chlorite schist (after Anand *et al.* 1997).

Depth (cm)		Fe_2O_3 (%)	SiO_2 (%)	Al_2O_3 (%)	MgO (%)	CaO (%)	Na_2O (%)	K_2O (%)	TiO_2 (%)	LOI (%)	Si/Ti ratio	Ti/Zr ratio	Cr (ppm)	Ni (ppm)	Co (ppm)	Zr (ppm)
Profile 1																
0–20	Soil	4.6	45.2	8.5	4.97	14.10	0.47	0.80	0.39	20.2	104.3	26.4	538	100	22	87
20–35	Soil	4.9	47.0	9.8	4.83	12.30	0.50	1.23	0.40	17.7	104.1	29.2	488	108	26	82
35–50	Soil	5.2	44.9	10.9	3.50	18.80	0.40	1.30	0.37	19.2	108.6	39.2	348	87	20	56
50–65	Soil	8.2	51.5	8.9	8.76	7.44	0.23	1.92	0.43	11.3	105.3	96.2	557	163	43	27
65+	Gabbro	6.8	47.8	15.4	9.82	14.40	1.08	0.30	0.51	2.6	81.9	310.0	307	170	36	10
Profile 2																
0–30	Soil	6.8	53.4	9.2	4.60	9.50	0.47	0.59	0.57	14.1	83.5	29.5	572	112	34	115
30–45	Soil	5.4	42.4	8.9	5.80	15.30	0.31	0.67	0.41	19.2	90.4	33.7	330	91	29	74
45–55	Soil	7.1	42.6	10.6	9.10	12.00	0.21	1.04	0.36	16.6	103.1	48.8	143	96	34	45
55+	Gabbro	7.2	47.7	17.7	8.40	14.30	1.17	0.26	0.59	2.6	72.5	233.3	108	123	37	15
Profile 3																
0–12	Soil	16.2	46.2	9.1	10.40	0.94	0.33	0.21	0.41	14.8	98.4	46.2	3130	1090	88	54
12–25	Soil	13.3	47.9	8.4	12.30	1.33	0.27	0.47	0.34	14.5	127.5	51.2	2670	1190	98	39
25–40	Soil	10.9	48.3	7.3	15.00	1.38	0.23	0.76	0.29	14.8	151.1	60.7	2370	1420	116	28
40+	Talc chlorite schist	10.2	52.9	6.4	17.60	0.39	0.10	BD	0.43	11.1	108.0	325.0	2590	1740	103	8

BD, below detection limit; LOI, loss on ignition.

The individual clasts are mostly silt to fine-sand size, consisting of quartz coated with Fe oxides, rounded pelletal aggregates of clay, carbonates and other minerals derived from local bedrock sources (e.g. feldspar, amphibole, muscovite, zircon, epidote, magnetite). The dunes may be partly stabilised by spinifex with scattered mulga, but some of the sand is mobile. Vestiges of cross-bedding can be seen in section, where the sand is slightly cemented by clay. Dunes commonly fringe playas. Aeolian modification of the major Tertiary river systems has resulted in the formation of playas connected by salt flats or salinas (Bettenay & Hingston 1964). Associated with these features are gypsum dunes, lunettes and lake parnas, the genesis of which has been discussed by Bettenay (1962).

The impact of wind-blown dust on regolith materials in the region is, however, not well known. Glassford and Semeniuk (1995) suggested that the upper part of the weathering profiles are in fact variously altered desert–aeolian sediments that unconformably overlie saprock or saprolite. The sediments include sandy clayrock facies, lateritic or bauxitic lithofacies, and siliciclastic sand facies (Figure 58) (Glassford & Semenuik 1995). Brimhall *et al.* (1991) also advocated significant aeolian accession to the bauxitic profiles of the Darling Range. Recent work at a number of sites in the Yilgarn Craton suggests that there is a significant component of aeolian material in soils (Anand *et al.* 1993a; Robertson 1999). Such components may be difficult to recognise in the field where soil overlies granitic bedrock. Grainsize distributions show a high proportion of fine material.

AEOLIAN MATERIALS IN SOILS

Examples from Ora Banda, Cawse Find and Forrestania

The influence of aeolian accession on soil composition is best illustrated on hill tops, to avoid effects due to colluvial transport. At Ora Banda, hills flanked by steep slopes, rise above the ferruginous duricrust-capped surface and exposed fresh rock. Here, the soil profiles consist of 55–65 cm thick moderately to strongly calcareous, red clay directly overlying fresh gabbro. At Cawse Find, the soil profile on low hill is approximately 40 cm thick above talc–chlorite schist (Anand *et al.* 1993a). The chemical compositions of these profiles are given in Table 6. Fresh gabbro inherently contains more Al, Ca, Na and K and less Fe, Mg, Cr, Ni and Co than fresh talc–chlorite schist. This difference is reflected in the composition of the soils which, over the talc–chlorite schist, are richer in Fe, Mg, Cr and Ni. However, despite the similar abundance of Si in soils and the underlying bedrock, it occurs in different forms. Silica occurs as plagioclase and amphiboles in gabbro, whereas it is present as quartz, kaolinite and smectite in soils. The soils on gabbro have 87–115 ppm Zr and a Ti/Zr ratio of 26/96. In contrast, the underlying gabbro has low Zr (10–15 ppm) and a Ti/Zr ratio of 233/310. The concentration of Zr increases up the profile. Similarly, the abundance of K is much greater in soils than in the underlying gabbro (Table 6). A similar relationship of Si, Zr and K was observed for the Cawse Find profiles.

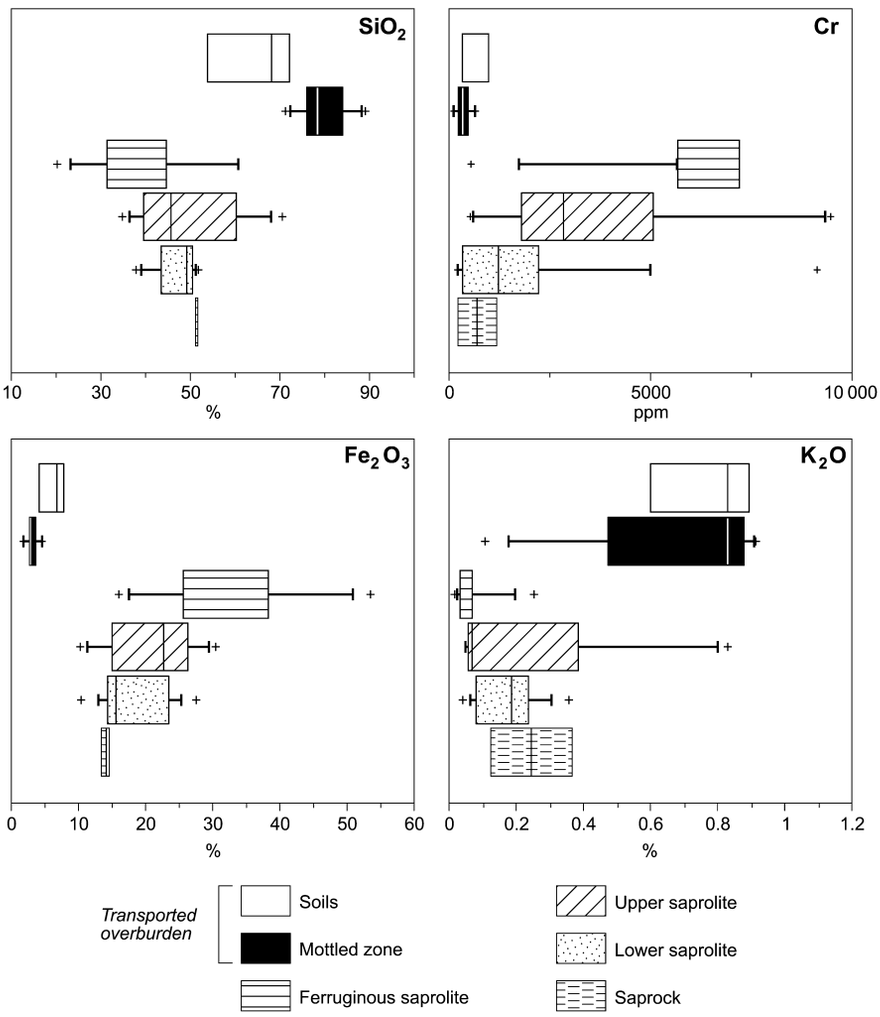

Figure 59 Distribution of SiO_2, Fe_2O_3, Cr and K in six regolith materials from Forrestania (after Kelly 1994). Potassium, Fe, Si and Cr discriminate transported overburden (soils and mottled zone formed in aeolian sediments) from the residual profile developed on ultramafic rocks.

The higher concentrations of Si, Zr and K are not consistent with *in situ* weathering of gabbro and talc–chlorite schist. Thin-sections, XRD data and particle-size analysis show moderate amounts of quartz and muscovite in soils over non-quartz–muscovite gabbro. Sieving of the soil indicates that angular to rounded quartz is concentrated in the finest (75–710 μm) fractions (Anand *et al.* 1993a). This is consistent with the chemical data, which reveal geochemical breaks between the bedrock and the overlying soil.

As all the soils were collected on the crests of hills, it is likely that this is the result of aeolian transport. These data suggest that most of the Si, Zr and K are externally derived from granitic terrain, whereas Fe, Cr and Ni are residual. Many soils in the Kalgoorlie region are commonly considered to be derived from greenstone rocks. However, it appears that these soils are partly residual and partly aeolian. Where these soils occur over mafic and ultramafic bedrocks, the Ti/Zr ratio and quartz readily identify any aeolian contribution.

Kelly and Anand (1995) investigated the nature of soils at Forrestania and found that the uppermost 8 m of regolith is quartz-rich material over greenstone sequence. Potassium, Fe, Si and Cr discriminated the aeolian component (granitic-derived) from the residual profile developed on ultramafic (Figure 59).

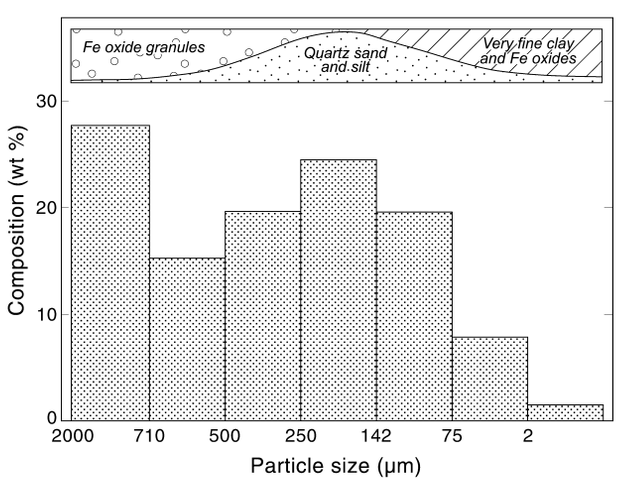

Figure 60 Relationship between particle size and mineralogical composition in a typical soil from Beasley Creek (after Robertson 1999).

Example from Beasley Creek

The Beasley Creek deposit subcrops beneath soil in a small window of deeply weathered bedrock, surrounded by extensive colluvial–alluvial plains. Regolith overlying

the mineralisation and its host sequence is comprised of ferruginous saprolite and some ferruginous duricrust, overlain by red-brown soil that is strewn with residual ferruginous lag (Robertson 1999). Soils consist of a coarse, ferruginous, granular, residual component (>710 μm), an intermixed aeolian, sandy component, and a very fine clay component (<5 μm). Size fractionation of the soils showed a bimodal distribution (Figure 60). Ferruginous granules with minor quartz dominate the coarse fractions. Quartz becomes particularly abundant at 200 μm; some of this quartz is aeolian. Clays and Fe oxides dominate the fine fractions, but quartz is still important even below 75 μm. The large quartz grains are rounded, but the smaller grains tend to be angular. Rounded, fresh microcline grains are less common than quartz. The quartz-rich fraction (75–710 μm) is remarkably similar to the materials of nearby linear dunes of sand (angular to rounded, hematite-coated quartz with minor microcline), which overlie granites and onlap greenstones 5 km to the west (Robertson 1999).

AEOLIAN MATERIALS IN FERRUGINOUS AND BAUXITIC DURICRUSTS

As discussed below (under the heading: Ferruginous materials), some ferruginous duricrusts are developed in sandy sediments. Very fine spherites (Killigrew & Glassford 1976) of poorly ordered kaolinite, generally <1 mm diameter, are common in the matrix and nodules of the duricrust in a number of locations [e.g. Mt Gibson and Bottle Creek: see Killigrew and Glassford (1976) for locations]. They become less abundant at depth. Electron microprobe analyses of these spherites from Mt Gibson indicate that they are largely kaolinitic. Similar kaolinitic spherites have been reported from the sandplains (Teakle 1936; Prider 1966; Brewer & Bettenay 1973) and are thought to have formed by concentric deposition of clay particles around a central core of isotropic kaolinite. Killigrew and Glassford (1976) suggested that they are aeolian.

Titanium and Zr, are generally considered to be residual elements, have higher concentrations in many ferruginous duricrusts than in bedrock, and tend to increase progressively from bedrock to the surface. However, Brimhall *et al.* (1988) concluded that both rutile and zircon have been introduced into the Jarrahdale bauxitic lateritic profile from above. Rutile grains were extremely rounded and restricted to the near-surface zone extending into the duricrust, but not the bauxite zone; no rutile was identified in the granitic bedrock of the profile studied. The rounded grains of zircon in duricrust were regarded as having been introduced by translocation of exotic aeolian material from the surface. Recently, Foo (1999) observed that there are significant differences in the abundance of Zr between the different parts of the pisoliths at Boddington. He found that Zr occurs in much higher concentrations in cutans than in cores of the pisolitic duricrusts. This may suggest that Zr is externally derived, possibly through aeolian action, and was available during cutan formation.

FERRUGINOUS MATERIALS

Introduction

Ferruginisation is an inherent feature of deeply weathered regolith and, although present over all lithologies, it is most strongly developed over more Fe-rich rocks. Ferruginous materials are abundant and widespread in the Yilgarn Craton and are developed in residual and transported materials of various ages. These take the form of crusts, gravels and impregnations of diverse character. There are four general types of ferruginous materials in the landscapes of the Yilgarn Craton: (i) ferruginous duricrust and gravel; (ii) ferruginous mottles; (iii) ferruginous saprolite; and (iv) iron segregations after sulfide-rich rocks (Figure 61). They may occur as outcrop or subcrop, as loose surface aggregates or lag, or buried beneath sediments. The relationships between these materials and the landscape are illustrated in Figure 62.

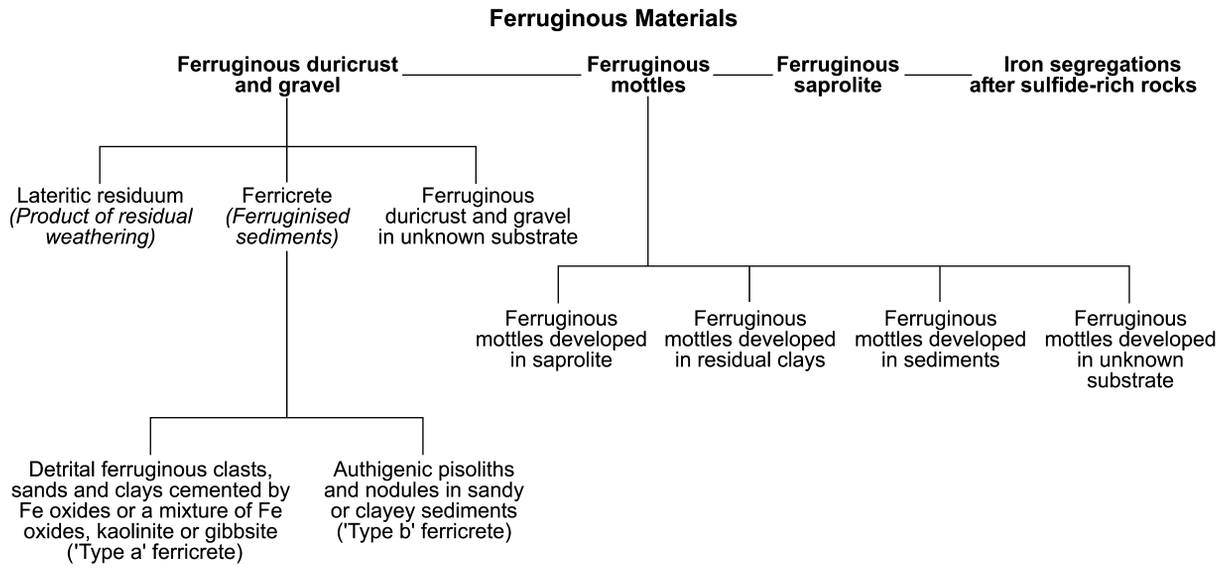

Figure 61 Broad subdivisions of ferruginous materials.

Ferruginous duricrust and gravel

DISTRIBUTION

Ferruginous duricrust and gravel are abundant in the high rainfall zone of the Darling Range, but are not a continuous feature of the deeply weathered, gently undulating plateau of the arid interior (Anand 1998). In the Darling Range, they occupy gently sloping to horizontal upland areas with an elevation of 280–325 m (Figure 63). Several granite hills reach approximately 600 m and duricrust occurs on the slopes of these crests at approximately 500 m (Hickman *et al*. 1992). There is little duricrust or gravel below 250 m. On a local scale, the 'topography' of the weathering front is much more irregular than that of the top of the duricrust. Pinnacles of bedrock and isolated corestones occur high in the weathered profile, locally lessening its thickness. Ferruginous duricrust and gravel are less common inland than in the Darling Range. They occur on all rock types, but are more common on mafic and ultramafic rocks. This is exemplified by the Mt McClure district (Figure 64 on Plate 10). In the northern Yilgarn (e.g. Lawlers, Mt McClure, Bottle Creek, Bronzewing, Mt Magnet and Madoonga), ferruginous duricrust and gravel occur in the higher parts of the landscape as mesas and are also widespread beneath colluvium and alluvium on the valley margins.

CLASSIFICATION

The terminology of ferruginous duricrusts was discussed above (under the heading: Weathering). Attempts at classification have been confusing because the term 'laterite' has tended to be used alone without describing the detailed characteristics of these ferruginous materials (Bourman 1993). Various morphological and genetic classification schemes of 'laterite' are summarised in Table 7.

Chemical classification

Chemical classification schemes of 'laterite' (Martin & Doyne 1932; Dury 1969; Schellman 1981) have been reviewed by Bourman (1993). Martin and Doyne (1932) were among the first to advocate a chemical classification of 'laterite'. They proposed silica–alumina ratios to measure varying degrees of lateritisation, but the values of this ratio were disputed by several workers. Schellman (1981) classified 'laterite' by the degree of lateritisation as indicated by positions on ternary chemical composition diagrams (Figure 65). He considered samples with high iron and/or aluminium to be strongly lateritised. Bourman (1993) questioned the indiscriminate use of the term laterite to describe a diverse range of materials. Furthermore, ferruginous duricrust may have formed in various ways

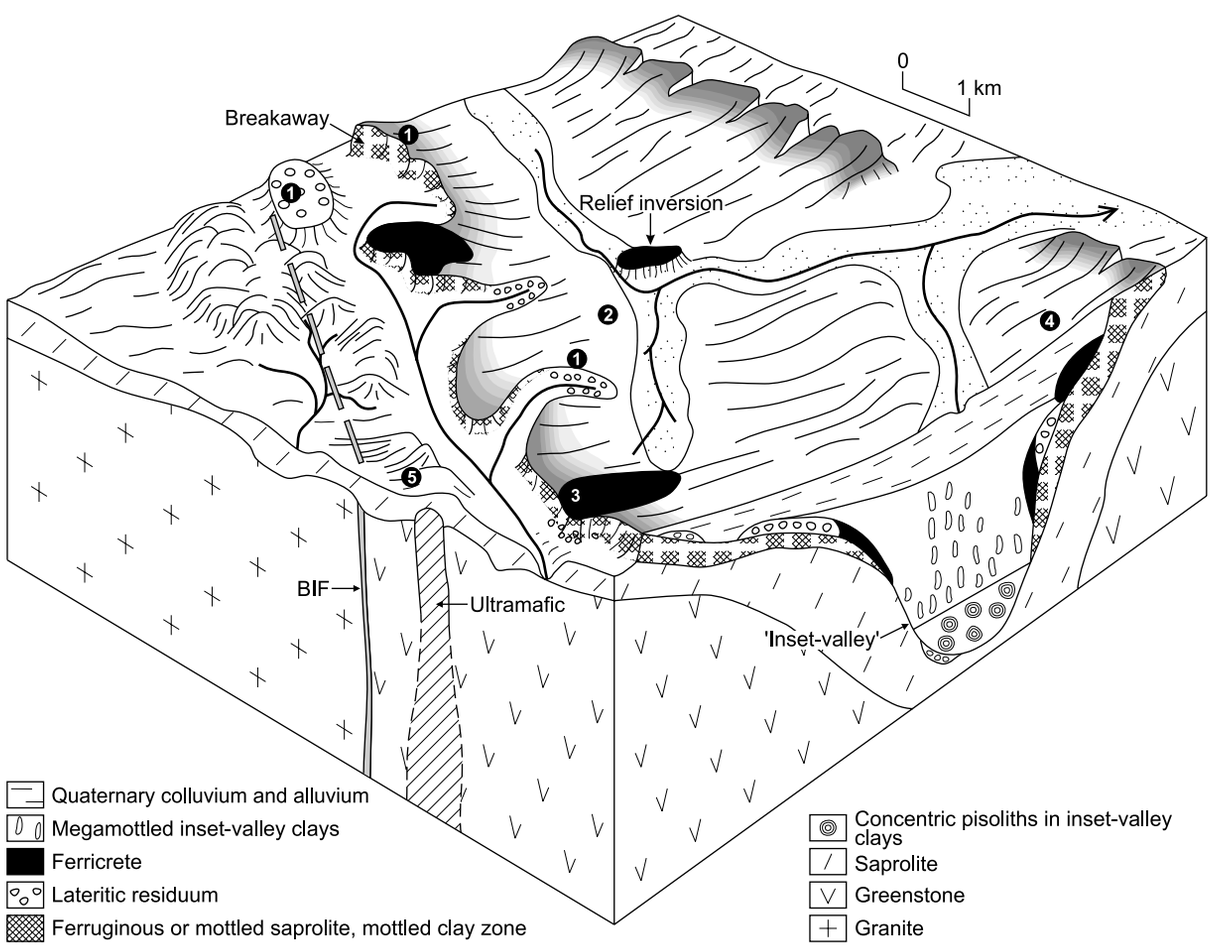

Figure 62 Block diagram showing the general relationships between landform and regolith in the arid parts of the Yilgarn Craton. The numbers 1–5 show the locations of the ferruginous profiles shown in Figure 69 (modified after Anand 2001).

Table 7 Classification systems of ferruginous duricrust and gravel ('laterite'/'ferricrete').

Morphological classification		Morphological–genetic classification		Genetic classification	
Anand *et al.* (1989a)	Bourman (1993)	Pullan (1967)	Anand (1995, 1998)	McFarlane (1976)	Aleva (1986)
1. Lateritic gravel (loose)	**1. Simple ferricrete**	**1. Primary lateritic ironstone**	**1. Lateritic residuum**	**1. Groundwater laterite**	**1. Autochthonous**
Loose pisoliths	Ferricreted bedrock	Vermicular	Loose nodules and pisoliths	Spaced pisolitic	
Loose nodules	Ferricreted sediment	Vesicular	Nodular duricrust	Packed pisolitic	
Loose nodules and pisoliths	Ferricreted clastic sediment	Cellular	Fragmental duricrust	Massive (vermiform)	
Loose ooliths	Ferruginised organic sediment	Cellular–nodular	Mottled duricrust		
	Ferricreted iron-rich sediment	Nodular	Massive duricrust		
		Oolitic			
		Pisolitic			
2. Lateritic duricrust (cemented)	**2. Complex and composite ferricrete**	**2. Secondary lateritic ironstone**	**2. Ferricrete**	**2. Pedogenic laterite**	**2. Allochthonous**
Massive	Pisolitic	Recemented nodular	Conglomeratic	Spaced pisolitic	
Mottled	Nodular	Recemented conglomeratic	Pisolitic	Packed pisolitic	
Fragmental	Slabby	Recemented breccia	Vesicular	Massive (cellular)	
Nodular	Vermiform	Platy	Ferruginised palaeochannel sediments		
Pisolitic					
Pisolitic–nodular					
Oolitic					
Vermiform					
Vesicular					
Cellular					

(Anand *et al.* 1989a; Bourman 1993; Anand 1998); it may not be genetically related to the underlying bedrock and, therefore, will not simply reflect the intensity of weathering. Confusion may arise when the sample contains transported material. The chemical classification is not readily applicable to the field identification of weathered materials (Bourman 1993).

Morphological classification

Anand *et al.* (1989a) identified several types of lateritic duricrusts in the landscapes of the Yilgarn Craton (Table 7). They proposed a descriptive classification scheme based on the morphological characteristics of hand specimen rather than its chemical composition. They subdivided duricrusts according to their dominant secondary structures: massive, mottled, fragmental, nodular, pisolitic, oolitic, vermiform, vesicular and cellular. These structures are not mutually exclusive and varying proportions of each structure may occur within a single hand specimen, resulting in categories such as 'nodular–pisolitic'. Voids of various shapes are common in all the lateritic duricrusts, but they also vary in abundance. Thus, a subdivision was made on the basis of the predominance of either solid or void phase. The terms in this classification appear to be similar to those used by other workers (Pullan 1967; McFarlane 1976; Bourman *et al.* 1987; Bourman 1993).

Bourman (1993) from work in South Australia, has contributed a useful classification scheme of 'ferricrete', which is also based on hand-specimen description (Table 7). He believed that an individual 'ferricrete' reflects both the character of the original material that has been ferruginised as well as the accumulated effects of the subaerial processes. Bourman classified into simple (ferruginised bedrock, ferruginised clastic, organic and Fe-rich sediments) and complex (pisolitic, nodular, slabby and vermiform) ferricrete. He suggested that there is generally no genetic relationship between ferricrete and the underlying saprolite. This model does not entirely fit materials found on the Yilgarn Craton, where ferruginous duricrusts have formed both in residual and transported materials. A distinction between categories is essential.

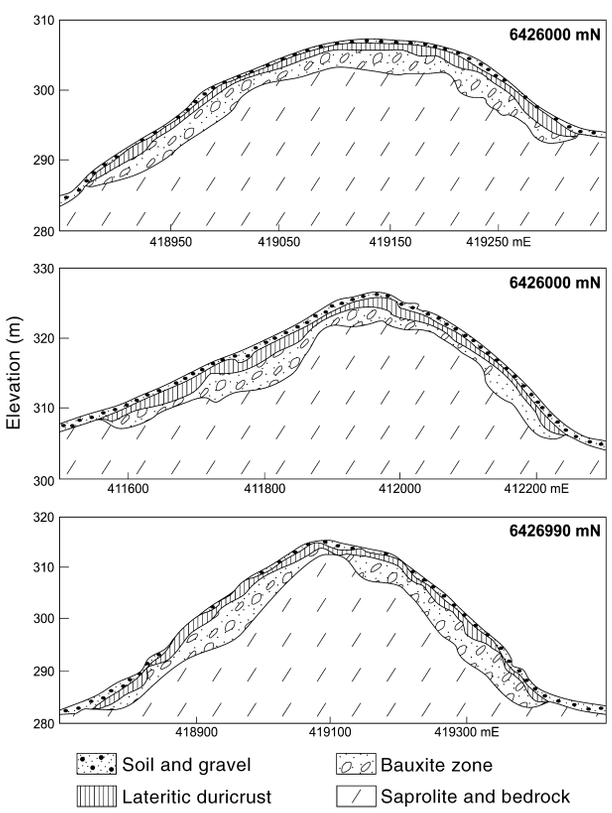

Figure 63 Relationships between lateritic duricrust, bauxite zone and landscape, Darling Range (P. Senini pers. comm. 2000).

Genetic classification

Several authors have proposed genetic classifications of 'laterite' based on its mode and mechanisms of formation. The morphological classification scheme of Pullan (1967), developed in Nigeria, recognised vermicular, vesicular, cellular, cellular–nodular, nodular, oolitic and pisolitic (primary forms), recemented nodular, recemented conglomeratic, recemented breccia and platy (secondary forms) lateritic ironstones as well as ferruginised rock and sediment. Primary ironstones are those developed *in situ* from different parent materials, without the introduction of externally derived Fe, whereas secondary ironstones are developed from the partial destruction of primary lateritic ironstones, transportation of fragments of the original ironstone, their subsequent deposition and recementation with iron compounds. On the basis of their morphological characteristics and mode of occurrence, Anand (1995, 1998) classified ferruginous duricrusts into two broad groups: lateritic residuum and ferricrete.

McFarlane (1976) distinguished two types of laterites in Uganda: pedogenic and groundwater laterites. Pedogenic laterites are considered to be formed in the unsaturated zone of the soil, whereas groundwater laterites are formed in the zone of fluctuation of the groundwater table, in both the soil (as a closely packed layer directly overlying the saprolite) and in the underlying saprolite (as more or less widely spaced pisoliths). A more comprehensive and complex classification of lateritic materials has been pre-

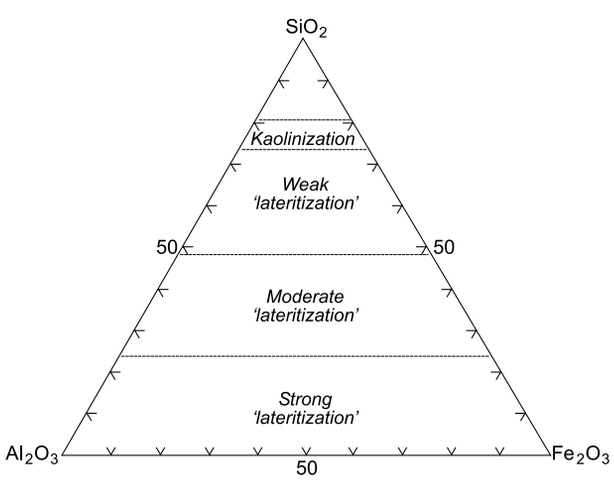

Figure 65 Triangular diagram showing the different degrees of lateritisation on granitic bedrock (after Schellmann 1981).

sented by Aleva (1986), which involves the mechanism of accumulation and mineralogical and chemical compositions. However, the first subdivision between autochthonous (relative accumulation) and allochthonous (absolute accumulation) is questionable, because it is often difficult to identify the source of iron (Bourman 1993).

In the Yilgarn Craton, morphological and genetic schemes have been continually modified and refined as further examples are added from new sites. For example, the classification of Anand *et al.* (1989a) does not include ferruginous materials formed in sediments, but this aspect was incorporated later (Anand 1995, 1998). Ferruginous duricrust and gravel have formed in a variety of materials but, more commonly, in residuum and in sediments of various ages. In the proposed classification the term ferruginous duricrust and gravel is used to describe regolith materials cemented by Fe irrespective of their origin (Figure 61). Based on origin, two major types of ferruginous duricrusts are recognised, namely lateritic residuum and ferricrete. Lateritic residuum has developed from bedrock by essentially residual processes. It has evolved by partial collapse of mottled or ferruginous saprolite, involving local vertical and lateral (generally 5–50 m) movement, following chemical wasting, as well as the introduction and mixing of exotic material through soil-forming and aeolian processes. The processes of Fe oxide precipitation, continued dissolution of clay, dehydration, nodule and pisolith development and the collapse of mottled saprolite has probably been repeated several times. The use of the term residuum is not meant to imply that all of the residuum is *in situ* because it has continually formed and been modified during weathering. Ferricrete is a product of cementation of sediments by introduced Fe oxides. The type of ferricrete formed is controlled by the nature of the sediments and the cement. The ferricretes have no genetic relationship with the underlying rocks (Anand 1998).

Lateritic residuum and ferricrete can be further subdivided according to their secondary structures (Figure 66). Similar structures can develop in different materials and, thus, morphology is not necessarily an indicator of the parent material in which the structures have developed.

Pisolith and nodules classification

Based on fabric, Anand *et al.* (1989a) subdivided pisoliths and nodules into four basic types (Figure 67): (i) homogeneous (no internal fabric); (ii) lithorelics (grains with relict rock fabrics and at least partial preservation of primary mineralogy); (iii) pseudomorphic (purely secondary minerals, but some preservation of primary fabrics); and (iv) concentric (with multiple cutans indicating concretion or accretion). Each of the four types could be modified by any of three additional terms: cutanic (thin outer layer or layers present, but not enough to impart a true concentric fabric); compound (several originally separate grains that have been cemented together); and syneresis (vuggy and fissured internal fabrics indicating dewatering of clay and oxyhydroxides). Clarke and Chenworth (1995) have proposed a four-level classification of lags, also based on fabric, expanding on the scheme of Anand *et al.* (1989a). The first level is based on the initial observation necessary to recognise the class of regolith materials to which ferruginous surface granules (FSG) belong, namely lags. The second separates FSG from other lag components, such as rock fragments and resistant mineral grains and, hence, requires more detailed observation of the sampled material. The third level of classification requires petrographic and mineragraphic examination—the main textural types being homogeneous, lithorelic, pseudomorphic, vesicular, sandy and oolitic. The fourth level of classification identifies modifying microfabrics, namely concentric, cutanic, compound, mottled and syneresis fabrics.

Homogeneous nodules and pisoliths (Figures 67a, 68a) are uniformly fine grained and composed of kaolinite or gibbsite impregnated with Fe oxides and may have thin, goethite-rich cutans. Pseudomorphic and lithorelic nodules and pisoliths (Figures 67b, c, 68b) can have a variety of internal fabrics depending on the nature of the host material. In pseudomorphic nodules, the internal fabric is very closely related to the fabric of primary minerals, which have been pseudomorphed. Pseudomorphic fabric relationships are seen best in the cores: examples are gibbsite pseudomorphs after feldspars in fragmental duricrust (Boddington), kaolinite and goethite after mica

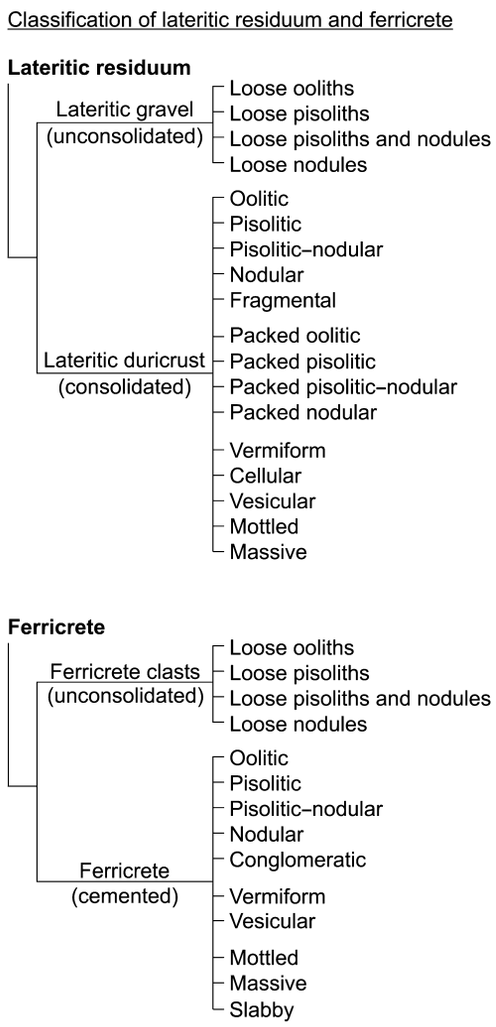

Figure 66 Classification of lateritic residuum and ferricrete (modified from Anand *et al.* 1989a; Anand 1998).

(Mt Gibson), goethite after talc (Lawlers) and fine, kaolinite booklets after amphiboles (Lawlers). Pseudomorphs are not readily seen in hand specimen, although a few larger grains may be visible under a hand lens; they are best recognised by microscopy. Lithorelic pisoliths are characterised by preservation of rock fabrics in their cores. Thus, at Madoonga, pisoliths of former banded iron-formation are layered, with the layers still composed largely of Fe oxides and quartz (Von Perger 1992). Relics of former schist retain a schistose fabric.

Well-developed concentric pisoliths (Figures 67d, 68c) are more common in the bauxitic province of the Darling Range than inland. They may have a variety of cores. In places, pisoliths are entirely banded without any obvious core. Where alternate darker and lighter cutans are seen under the microscope, the lighter cutans gave higher Al and lower Fe contents and are kaolinite–gibbsite-rich. Concentric cutans may include microlenses of detrital quartz grains, suggesting a complex history of their formation.

MODE OF GENESIS

Lateritic residuum

Profiles capped with lateritic residuum may include, from top to base, a lag of nodules and pisoliths, nodular, fragmental or massive duricrust or closely packed nodules and pisoliths, collapsed mottled saprolite (ferruginous breccia), mottled saprolite, ferruginous saprolite, saprolite, saprock and bedrock (Figures 69a; 70a–c on Plate 11; 71a–f). At Boddington, a bauxite zone occurs beneath fragmental duricrust. Lateritic residuum is not necessarily associated with deep saprolite (e.g. Agnew: Figure 69a) where massive duricrust overlies ferruginous saprolite on bedrock. Lateritic residuum may be exposed or buried beneath sediments. The top 1–3 m of lateritic residuum is composed of lateritic nodules and pisoliths of 5–20 mm diameter. The angularity of nodules increases down profile. The main characteristic of ferruginous materials is their

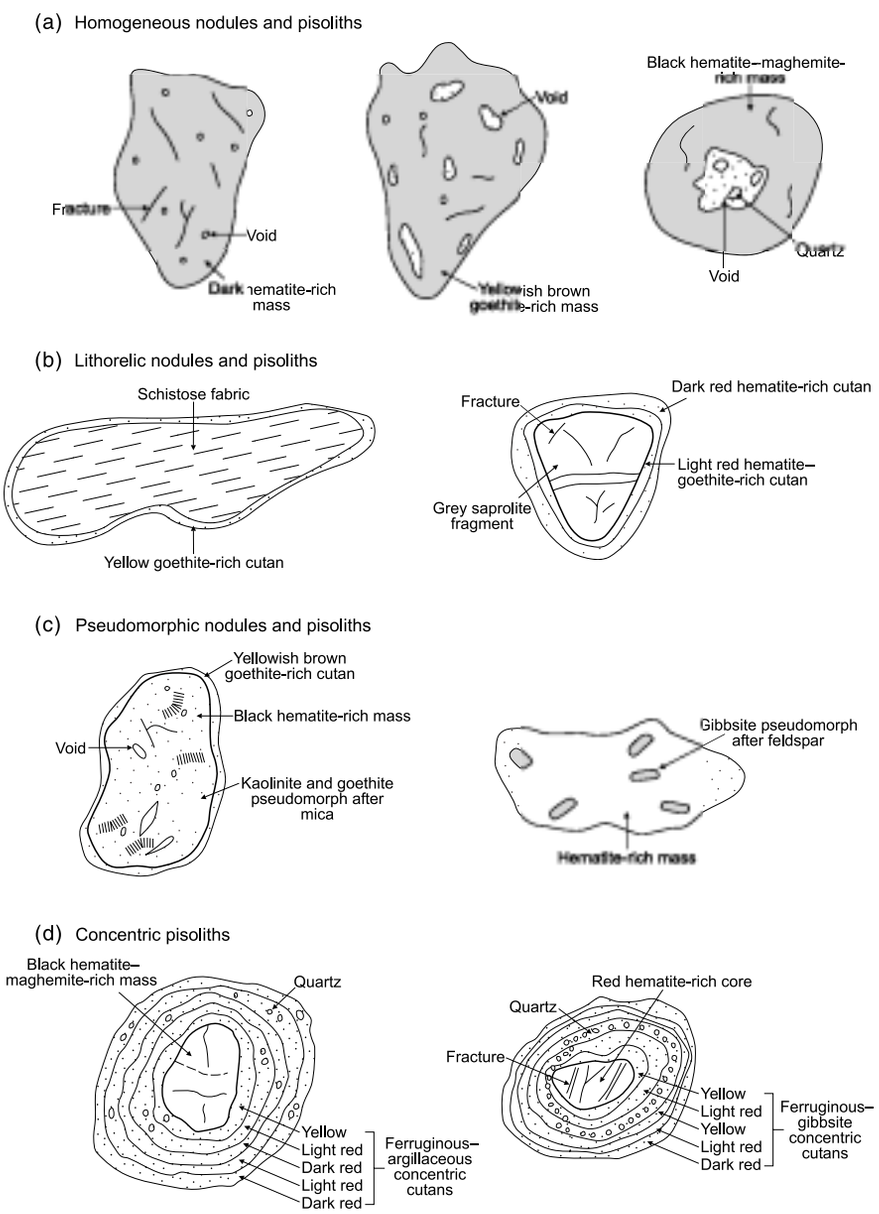

Figure 67 Classification of ferruginous nodules and pisoliths (modified after Anand *et al.* 1989a). (a) Homogeneous nodules and pisoliths, commonly 5–20 mm in diameter. (b) Nodules and pisoliths having lithorelics as their core, typically 10–40 mm in diameter. (c) Pseudomorphic nodules and pisoliths, 5–15 mm in diameter. (d) Concentric pisoliths, 2–10 mm in diameter.

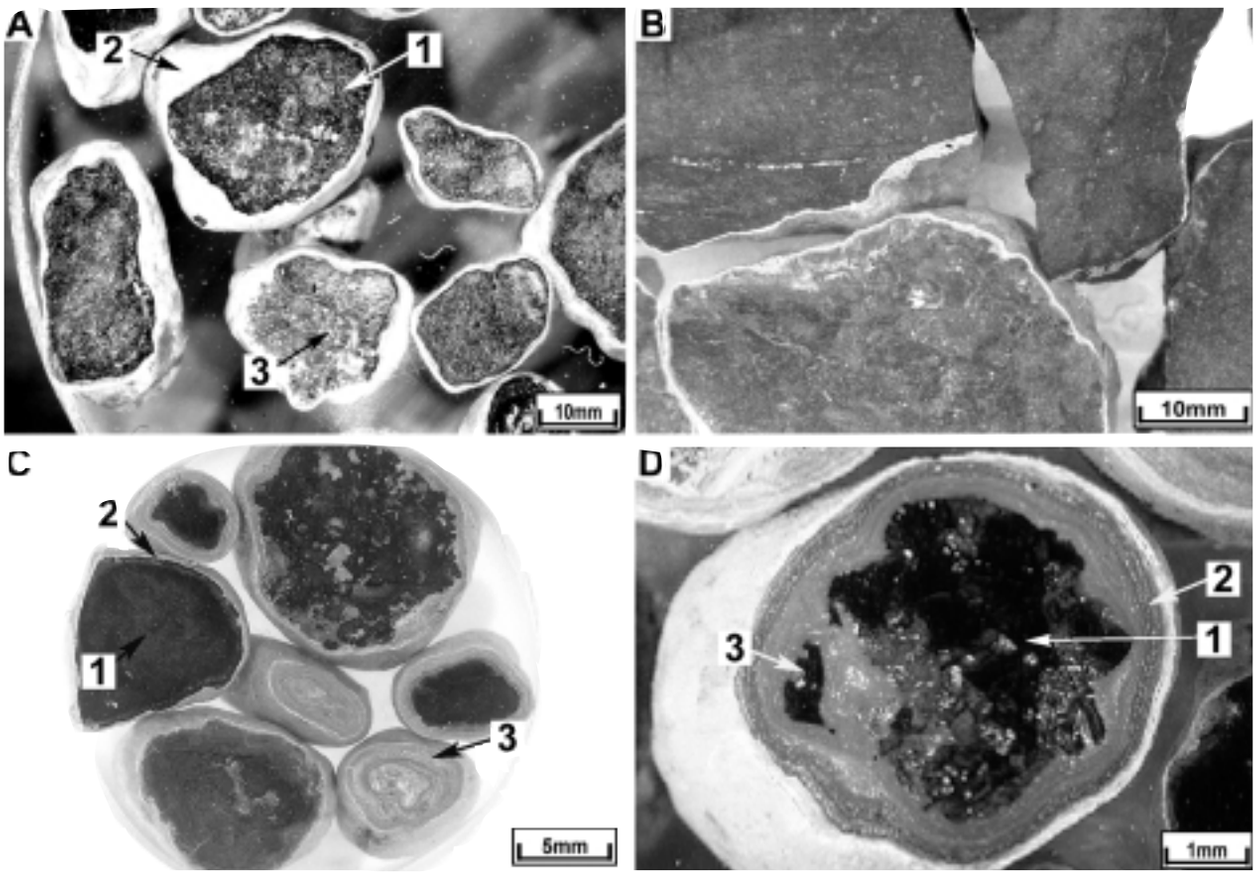

Figure 68 Photographs of homogeneous, lithorelic and concentric nodules and pisoliths. (a) Pisoliths from the near surface showing a homogeneous pisolith (1) with a thin, yellowish-brown cutan (2), some pisoliths also contain clay spherites (3): Mt Gibson. (b) Irregular, angular goethite–kaolinite-rich lithic nodules with yellowish-brown cutans formed in saprolite: Bronzewing. (c) Pisoliths from the near-surface showing a homogenous pisolith (1) with a thin, yellowish-brown cutan (2) and a concentric pisolith with multiple cutans (3): Jarrahdale. (d) Concentric pisolith from Boddington showing a partially replaced hematite-rich core (1) with finely laminated cutans (2) with islands of hematite-rich core (3). Photographs by the authors.

homogeneity. They consist of lithic and non-lithic nodules (Davy *et al*. 1988; Anand *et al*. 1989a). Lithic types preserve the original rock fabric (Figure 71a–d), whereas non-lithic types have one or more generations of Fe oxides disseminated through a clay- or sand-rich matrix. In the Darling Range (e.g. Jarrahdale), the location of subsurface dykes can be mapped from the overlying duricrust, which suggests that duricrust has formed *in situ* (Sadleir & Gilkes 1976; Davy 1979). Over the dolerite dyke, the duricrust is red-brown and contains very little quartz. Over the granitoid, the duricrust is light-brown, with abundant visible quartz (Davy 1979). Elsewhere, for example north of Bronzewing, the continuity of quartz veins through the massive duricrust illustrates its largely residual origin (Figure 70 on Plate 11). A similar feature was illustrated by Walther (1915) in his classic description of laterite in Western Australia.

The thickness of lateritic residuum is largely controlled by the nature of the parent bedrock. Thus, in the Lawlers area lateritic residuum is thin (0.5–1 m) on Waroonga gneiss, but thicker (3–5 m) on ultramafic bedrock (Anand *et al*. 1991b; Twomey 1992). Similarly, at Mt McClure lateritic residuum on mafic and ultramafic bedrock is approximately 2–4 m thick compared to 1 m on felsic bedrock (Williamson 1992). At Kanowna Belle lateritic residuum on ultramafic rock is 2–3 m thick, whereas it is absent on felsic andesite. These differences are probably due to the amounts of Fe available during weathering being considerably greater in mafic and ultramafic rocks than in felsic rocks.

The chemical composition of lateritic residuum formed on various rock types is given in Tables 8 and 9. Aluminium, Fe, Ti, Cr, V and Zr are the constituents of lateritic residuum that tend to remain as residual components (Davy 1979). The abundance of these elements varies broadly according to the bedrock from which the lateritic residuum has developed. Based on the study in the Darling Range, Davy (1979) found that there are systematic differences in the abundances of Si, Fe, Ti, V, K and Cu in lateritic residuum developed on felsic and mafic rocks (Table 8). The abundance of Fe, Ti, V and Cu are much higher over duricrusts developed over dolerite than on granite. Similarly, Murray (1979) observed that Fe in duricrust in the Darling Range reflects the nature of the bedrock, with less Fe in duricrust over granitoids than over dolerite (Figure 72). Thus, there are pronounced changes in Fe concentration where duricrust derived from granitoid passes into duricrust derived from

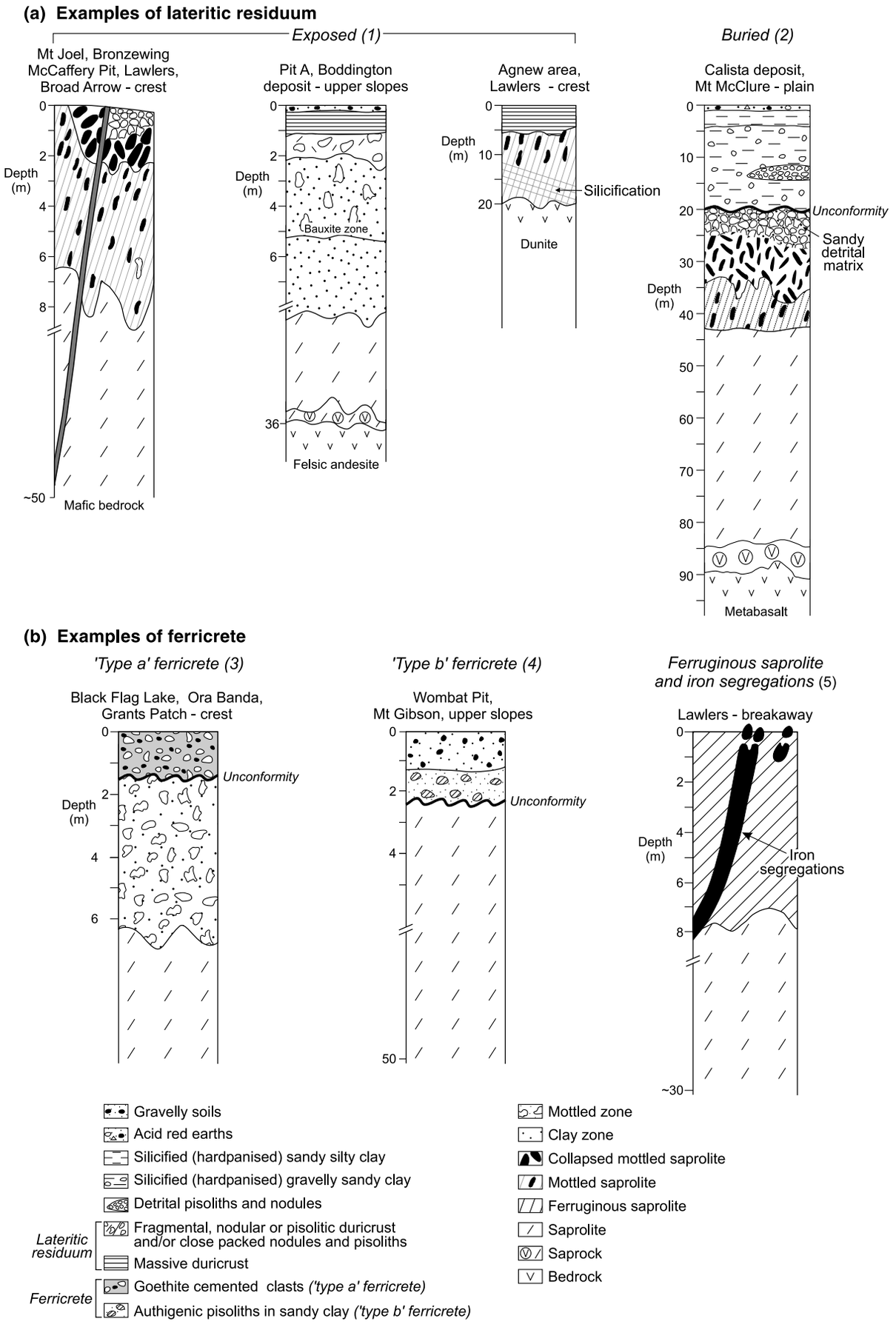
(a) Examples of lateritic residuum
Exposed (1)
Buried (2)
Mt Joel, Bronzewing
McCaffery Pit, Lawlers,
Broad Arrow - crest
Pit A, Boddington
deposit - upper slopes
Agnew area,
Lawlers - crest
Calista deposit,
Mt McClure - plain
Depth (m)
Bauxite zone
Silicification
Dunite
Unconformity
Sandy detrital matrix
Mafic bedrock
Felsic andesite
Metabasalt
(b) Examples of ferricrete
'Type a' ferricrete (3)
'Type b' ferricrete (4)
Ferruginous saprolite and iron segregations (5)
Black Flag Lake, Ora Banda,
Grants Patch - crest
Wombat Pit,
Mt Gibson, upper slopes
Lawlers - breakaway
Iron segregations
Gravelly soils
Acid red earths
Silicified (hardpanised) sandy silty clay
Silicified (hardpanised) gravelly sandy clay
Detrital pisoliths and nodules
Lateritic residuum
Fragmental, nodular or pisolitic duricrust and/or close packed nodules and pisoliths
Massive duricrust
Ferricrete
Goethite cemented clasts ('type a' ferricrete)
Authigenic pisoliths in sandy clay ('type b' ferricrete)
Mottled zone
Clay zone
Collapsed mottled saprolite
Mottled saprolite
Ferruginous saprolite
Saprolite
Saprock
Bedrock

Figure 69 Examples of (a) lateritic residuum and (b) ferricrete (modified after Anand *et al*. 1991b; Twomey 1992; Williamson 1992; Anand 1994; R. R. Anand unpubl. data). Bracketed numbers 1–5 refer to locations on the block diagram in Figure 62.

mafic rocks. Further major changes occur where residual duricrust passes laterally into lower slope transported gravels, although these changes are not systematic, but rather depend on the nature of the duricrust uphill and on effects related to the transport of Fe (Hickman *et al*. 1992).

Lateritic residuum overlying felsic andesite has less Fe (mean 25.3% Fe_2O_3) due to low original abundance (mean

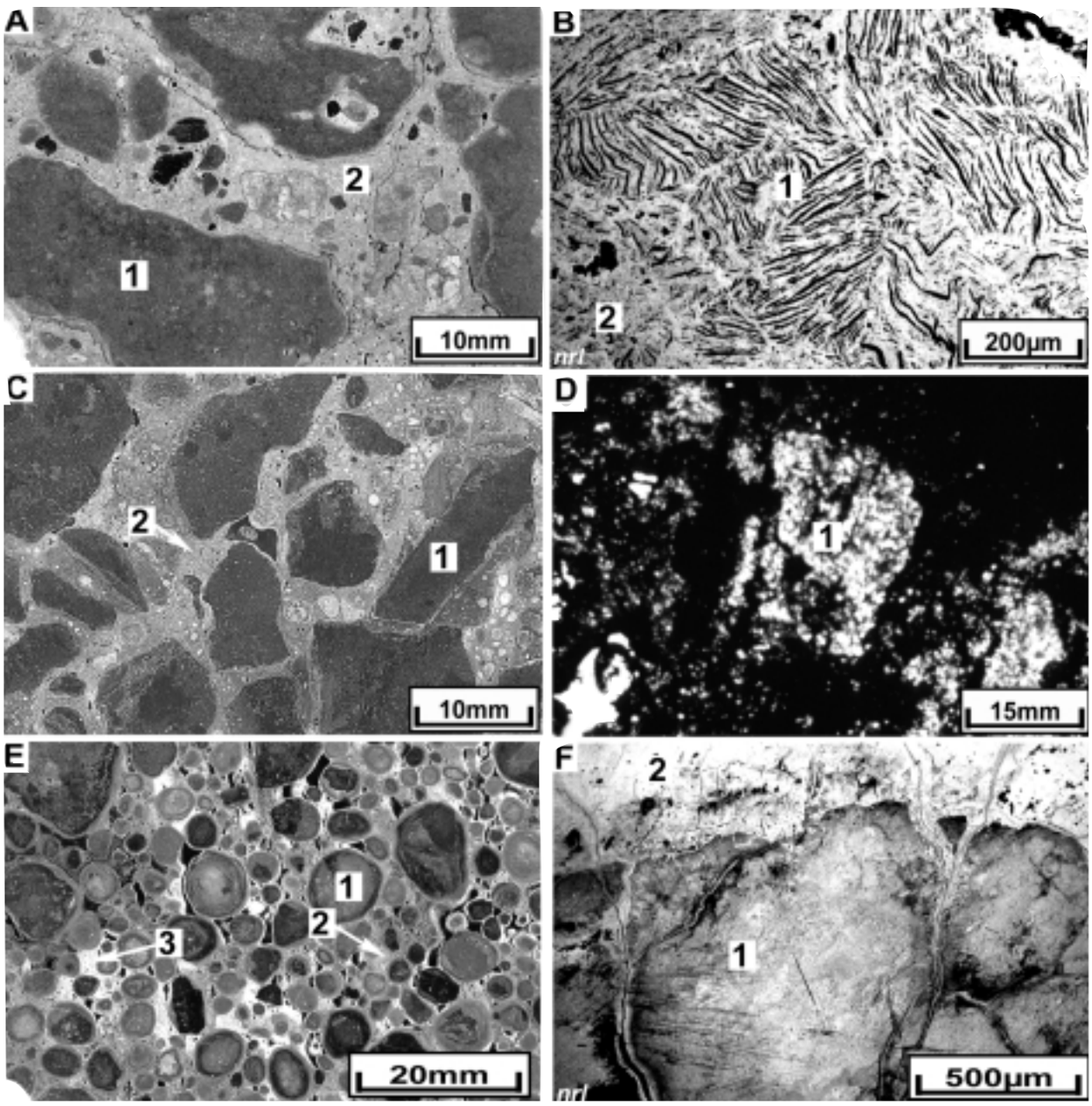

Figure 71 Examples of lateritic residuum. (a) Fragmental duricrust formed from mica quartz schist showing hematite-rich subangular to angular large (1) to small fragments set in a kaolinite–goethite-rich matrix (2): Mt Gibson (sample 07-0523). (b) Photomicrograph of a polished block taken in nrl showing a fragment with mica relics (1) set in a goethite matrix (2). Goethite has, in part, wedged the mica apart along cleavages resulting in exfoliation: Mt Gibson (thin-section 07-2045) (c) Fragmental duricrust formed from felsic andesite showing hematite–gibbsite-rich fragments (1) set in a gibbsite-rich matrix (2): Boddington (sample 07-1106). (d) Photomicrograph of a polished thin-section taken in xpl showing gibbsite pseudomorphs after feldspars (1): Boddington (thin-section 07-1106). (e) Pisolitic duricrust showing pisoliths (1) in a goethite-rich matrix (2): Kalgoorlie (sample 07-0769). Note the pale areas (3) from where Fe is interpreted to have been removed. (f) Photomicrograph of a polished block taken in nrl showing hematite and goethite (1) surrounded by hematite cutan (2): Kalgoorlie (thin-section 07-0769). Photographs by the authors; xpl, transmitted light with crossed polarisers; nrl, normally reflected light.

6.1% Fe_2O_3), whereas lateritic residuum formed from Al-poor ultramafic rock (mean 6.3% Al_2O_3) is richer in Fe (mean 63.1% Fe_2O_3) than that formed from dolerite and basalt (Table 9). Mean concentrations of Zr (405 ppm) and V (431 ppm) are greater in lateritic residuum associated with felsic andesite than lateritic residuum in dolerite (240 ppm), basalt (138 ppm) and ultramafic rocks (55 ppm). However, lateritic residuum over ultramafic rocks is richer in mean Cr (9588 ppm), Ni (550 ppm) and Co (35 ppm), which may be used to distinguish felsic and mafic from ultramafic-derived lateritic residuum. Thus, at Waroonga the concentration of Cr is much greater in lateritic residuum associated with ultramafic rocks than that in Waroonga gneiss (Figure 73a). Similarly, at Mt McClure, the abundance of Cr distinguishes mafic from ultramafic-derived lateritic residuum (Figure 73b). The close relationships between the chemical composition of bedrock and that of lateritic residuum suggest that it is developed in areas where the lateral accumulation of materials and Fe has been minimal.

Ferricrete

Ferricrete may develop in seepage zones, palaeodrainages and in the subaqueous environment in which Fe oxides have impregnated and invaded sediments of various ages (Figures 69b; 70e–f on Plate 11; 74) (Anand *et al.* 1991b; Butt *et al.* 1992; Davy & Gozzard 1995; Anand 1998; Jones & Lidbury 1998; Krcmarov *et al.* 2000). It commonly marks former lakes, swamps, discharge sites (seepages), valley floors, aquifers or groundwater-mixing zones and may be buried or, following exposure, possibly form low hills due to local relief inversion. There is no genetic relationship between the ferricrete and the underlying mottled and saprolite horizons.

Ferricrete may overlie or develop on a variety of substrates (Figure 69b). For example, near Grants Patch, Ora Banda and at Black Flag Lake in the Kalgoorlie region, ferricrete overlies mottled saprolite (Figure 70d, e on Plate 11), whereas at Wombat pit (Mt Gibson) and Madoonga, pisolitic ferricrete unconformably overlies saprolite or saprock (Figure 70f on Plate 11). Ferricrete is formed either by: (a) the cementation of detrital clasts, sands and clays by Fe oxides or a mixture of Fe oxides, gibbsite or kaolinite; or by (b) authigenic hematite and goethite-rich pisoliths and nodules in sediments. It includes conglomeratic, slabby, massive, pisolitic, vermiform and vesicular types, which have variable mineralogy.

Table 8 Chemical composition (summary) of ferruginous duricrusts developed on mafic and felsic rocks (after Davy 1979).

Element	Mafic	Felsic
SiO_2 (%)	<15	>20
Fe_2O_3 (%)	>25	5–20
TiO_2 (%)	>2	0.5–1
K2O (%)	<0.02	>1
V (ppm)	>700	<500
Cu (ppm)	>30	<10

Examples of 'type (a)' ferricretes

Conglomeratic and pisolitic ferricretes have a variety of ferruginous clasts derived from the erosion of pre-existing ferruginous duricrust and ferruginous saprolite. They consist of a dark-brown to reddish-black, hematite–maghemite-rich nodular or pisolitic, clast-supported masses in a dark-brown, detrital, goethite-rich matrix (Figure 74a–d). The clasts are composed of Fe oxides; some are lithorelics, others lack fabric. Some pisoliths and cutans formed on them have been broken and recemented, suggesting several detrital phases, interspersed with cycles of Fe oxide cementation. Some pisoliths are ferruginised wood (Anand *et al.* 1991b; Butt *et al.* 1992; Von Perger 1992; Davy & Gozzard 1995; Anand 1998). Massive or vesicular ferricretes are goethite-cemented ferruginised sand (Figure 74e, f). Slabby ferricrete (Bourman 1993) occurs at the edge of the breakaway and forms massive, horizontal plates of clay-rich material, impregnated by goethite (Figure 70e on Plate 11). It may also contain detrital hematite–maghemite-rich pisoliths. The characteristically narrow, linear distribution of some 'type (a)' ferricretes coincides with dendritic palaeodrainage patterns revealed by shallow, high-frequency maghemite signals in aeromagnetic data (Anand 2000; Krcmarov *et al.* 2000).

Conglomeratic and pisolitic ferricretes at Grants Patch, Ora Banda and Lawlers are characterised by high mean concentrations of Fe (76.9% Fe_2O_3) and low concentrations of Si (6.5% SiO_2) and Al (4.9% Al_2O_3) (Table 9) (Anand 1998). Electron microprobe analysis of clasts and matrix shows that both are similar in composition and are Fe-rich. Minimal Al corresponds with minimal Al substitution in goethite. These ferricretes typically show high mean concentrations of Ti (5.7% TiO_2), V (1826 ppm) and Cr (4500 ppm); Ti occurs as anatase, rutile and ilmenite, Cr as chromite and in Fe oxides. Some Ti-rich ooliths (2–40 μm) with goethite coatings occur in the matrix, apparently having crystallised from solution, which suggests mobility of Ti. These ferricretes are Ti- and Cr-rich, possibly because of sorting during transport. A similar composition of ferricretes near Leonora was described by Davy and Gozzard (1995) (Table 9). The ferricrete is distinguished by a lack of Al and a very marked mean enrichment of TiO_2 (8.5%), V (3283 ppm) and Zr (322 ppm) occur.

Examples of 'type (b)' ferricretes

'Type (b)' ferricretes are sandy clay or clayey sediments that have been more commonly modified by the *in situ* formation of hematite- and goethite-rich pisoliths or vermiform fabrics, the internal structure of which is controlled by original sediments. At the Wombat pit (Mt Gibson) and Forrestania, pisolitic ferricretes have a fine-grained, massive, ferruginous sandy clay or sandy structure (Figure 74g, h) and are formed by replacement of sediments (Kelly 1994; Jones & Lidbury 1998). Pisoliths consist of quartz, kaolinite, goethite and hematite. The matrix and nodules of these ferricretes may contain very fine clay spherites and are interpreted to be aeolian sediments (Killigrew & Glassford 1976; Glassford & Semeniuk 1995). Ferricretes are commonly overprinted by later bleaching. The bleached areas are commonly cylindrical and are cored by tubes that may be filled with secondary kaolinite or

Table 9 Chemical composition (mean) of ferruginous materials and their underlying rocks.

	Lateritic residuum								Ferricretes		Fe segregations after sulfide-rich rocks
	Boddington (Darling Range)[a]				Lawlers (inland)[a]				Grants Patch, Ora Banda, Lawlers (inland)[a]	Near Leonora[b] (inland)	Lawlers (inland)[a]
	LR on felsic andesite	Fresh felsic andesite	LR on dolerite	Fresh dolerite	LR on basalt	Fresh basalt	LR on ultramafic	Fresh ultramafic	Pisolitic/ conglomeratic ferricrete		
	$n = 12$	$n = 4$	$n = 5$	$n = 2$	$n = 10$	$n = 4$	$n = 6$	$n = 2$	$n = 26$	$n = 10$	$n = 74$
%											
SiO_2	1.5	63.1	0.4	50.7	24.1	50.3	14.2	21.2	6.5	10.6	15.5
Al_2O_3	43.7	16.3	30.6	14.2	23.8	15.6	6.3	0.7	4.9	8.6	3.8
Fe_2O_3	25.3	6.1	41.6	12.0	41.0	12.1	63.1	10.6	76.9	60.2	69.9
MgO	0.02	2.24	0.02	7.82	0.14	7.48	0.57	33.00	0.04	0.07	0.15
CaO	0.03	5.02	0.03	11.70	0.21	9.24	0.07	0.72	0.09	0.08	0.08
Na_2O	0.00	2.79	0.00	1.96	0.03	2.45	0.02	0.02	0.01	0.17	0.03
K_2O	0.02	2.00	0.02	0.62	0.08	0.40	<0.02	<0.02	<0.02	0.03	0.02
TiO_2	1.97	0.58	5.47	1.40	0.97	1.08	1.36	0.02	5.69	8.56	0.33
LOI	25.30	1.50	21.50	1.00	9.60	0.50	11.10	32.10	5.90	6.20	9.90
ppm											
Cr	349	59	435	110	656	245	9588	1880	4500	250	48
V	431	76	791	320	658	259	872	46	1826	3283	335
Zr	405	98	240	85	138	36	55	14	79	322	26
Ni	9	60	20	110	48	125	550	1780	320	7	176
Mn	36	522	75	1370	142	1360	149	1164	590	215	2300
Zn	9	88	13	80	10	98	18	86	32	21	321
Co	1	22	2	60	10	36	35	100	67	31	82

LR, Lateritic residuum.
[a]Anand (1998); [b]Davy and Gozzard (1995).

silica. Widespread preservation of such tubes, presumably fossil root/solution cavity systems, attests to high permeability around the residual and transported regolith boundary (Jones & Lidbury 1998).

Ferricretes can often be difficult to distinguish from lateritic residuum. However, they can be identified by their geomorphic relationships, the presence of an unconformity, preserved sedimentary structures, the presence of rounded quartz grains, transported clasts, broken cutans and abundant low Al (<10 mol%) substituted colloform goethite.

Summary

In conclusion, field and laboratory studies reveal that not all ferruginous duricrusts developed *in situ*, neither are they all transported. The fabric and mineralogical characteristics of the materials suggest that they have formed in diverse materials.

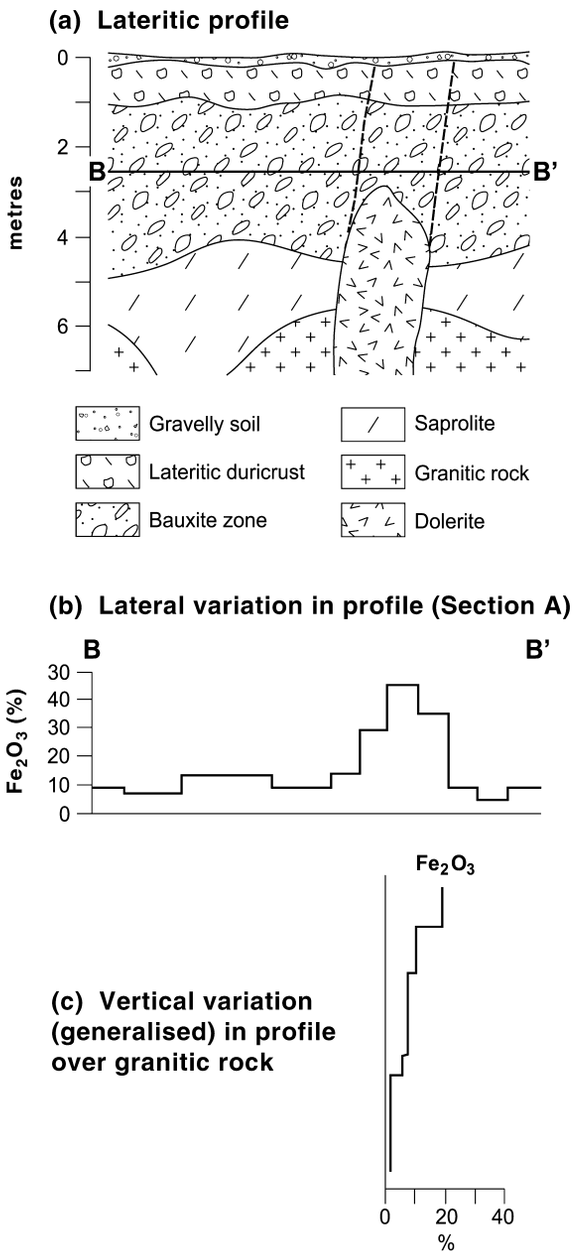

Figure 72 (a–c) Bauxite profile composition variations above granitic bedrock intruded by a dolerite dyke, Darling Range (after Murray 1979).

SOURCES OF Fe IN FERRUGINOUS DURICRUSTS AND GRAVELS

It is frequently found that duricrust in a profile contains more iron than could be derived from the underlying saprolite (Ollier & Galloway 1990). The presence of an Fe-depleted horizon or 'pallid zone', led to the theory of upward enrichment. Suggestions included seasonal fluctuation of the water table and/or capillary action brought about by simultaneous depletion of the lower and enrichment of the upper horizons. Some workers have explained the extra amounts of Fe in relation to the underlying saprolite by general landscape lowering (Trendall 1962; Mann & Ollier 1985; Tardy & Roquin 1992), others (Bourman 1993; Ollier & Pain 1996; Pain 1998) by lateral and oblique movement of Fe. Trendall (1962), using the Fe content of granite and the 'laterite' over it in Uganda, calculated that 14 m of granite would be required to produce 0.3 m of 'laterite' and proposed an overall process of ground-surface lowering to account for a surface covered with 'laterite'. Up to 3 km of surface lowering has been calculated by Tardy and Roquin (1992) for Madagascar. Nahon (1991) gave an average rate for surface lowering of 20 m per million years, but suggested that mafic rocks might be lowered at two–threefold this rate. Ollier and Pain (1996) indicated that in the Yilgarn Craton, which has been a land area since the Permian with a humid tropical climate for at least 200 million years, this might give a surface lowering of 4 km on granite, and 8–12 km on the greenstones. According to these authors, two main objections may be raised to total landscape lowering. First, details of weathering profiles and catenas may produce evidence of lateral movement of solution, which would be an effective alternative to vertical movement. Second, many landscapes have very old features and deposits that are incompatible with surface lowering of more than a few metres. Examples include Permian glacial pavements, Tertiary lava flows, sediments deposited during marine incursions, and even ferruginous duricrusts dated (by palaeomagnetism) to Early Tertiary or Mesozoic times.

Data on ferruginous duricrusts from the Yilgarn Craton suggest that both vertical and lateral accumulation of Fe have contributed to their formation depending on the landscape position. Some of these situations (Figure 75) illustrate this point. Lowering of the landsurface in the formation of lateritic residuum is suggested through collapse, accompanied by some removal of Fe oxides and clays by physical erosion and chemical dissolution (Anand 1998). Here, the relationship between the Fe in residuum and the underlying bedrock suggests that Fe is largely derived from weathering of underlying rocks by upward and downward movement with minor lateral input (Table 9). For example, felsic andesite has 6% Fe_2O_3 and the overlying ferruginous duricrust approximately 25%. The concentration factor of 4 is the same for TiO_2 and Zr, from which it can be concluded that the Fe, Ti and Zr represent the relatively insoluble elements from the weathering of the underlying rock that formerly occupied a greater thickness. Similarly, examination of Davy's (1979) data by Eggleton and Taylor (1998)

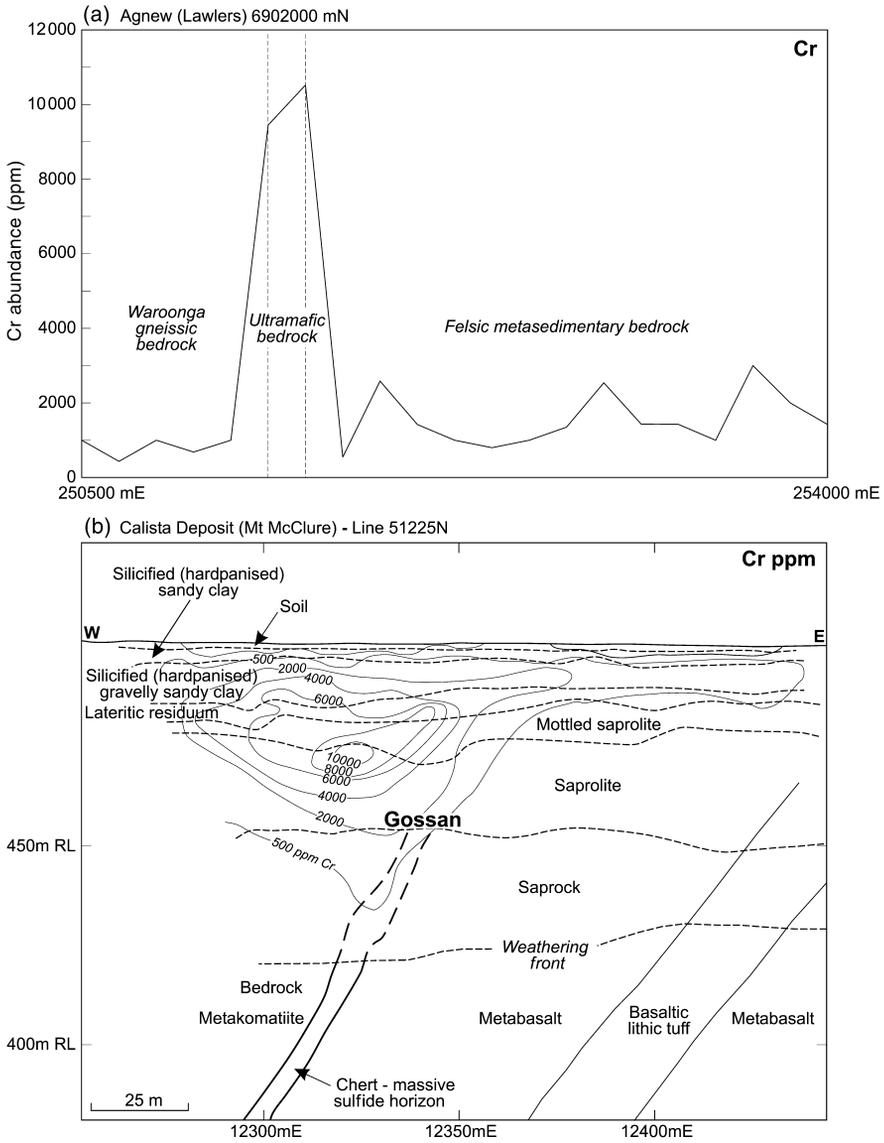

Figure 73 (a) Chromium abundance variation in lateritic residuum related to bedrock type at Lawlers (after Twomey 1992). (b) Cross-section showing contoured Cr abundances for buried lateritic residuum at the Calista deposit. The concentrations of Cr in lateritic residuum reflect the underlying lithologies (after Williamson 1992).

indicated that, assuming Ti, Zr and Nb are relatively insoluble, the Fe in the profile is largely locally derived. However, it is not believed that the duricrust is a condensed sequence of the order of magnitude suggested by Tardy and Roquin (1992). Lowering of a few metres is probable and consistent with preservation of Permian and Eocene sediments in old valleys in the eastern Yilgarn.

There has been significant lateral accumulation of Fe in materials developed in sediments (Figure 75). It is envisaged that Fe is concentrated by both lateral and vertical accumulations in 'type (b)' ferricretes where pisoliths have formed *in situ* (Figure 75d). This contrasts with 'type (a)' ferricretes that have developed in a variety of materials in lowlands and palaeodrainages, largely by lateral accumulation of Fe. Some of these now form low hills due to relief inversion (Figure 75).

ENVIRONMENTS OF FORMATION OF NODULES AND PISOLITHS

Pisoliths and nodules can form in a variety of weathering and sedimentary environments. Their morphology and characteristics suggest three environments of formation, in soil, saprolite and subaqueous environments (Figure 76) (Anand *et al.* 1989a; Anand 1995; Clarke & Chenworth 1995). Pisoliths formed in soil are homogeneous, compound and concentric, whereas those formed in saprolite are commonly lithic (lithorelict and pseudomorphic). Those formed in subaqueous environments (lakes and rivers) are typically concentric. Nodules formed in saprolite are dominated by goethite and hematite. Maghemite is typically absent. Those formed in soil are hematite- and maghemite-rich. Concentric pisoliths from subaqueous environments are dominated by goethite with varying proportions of hematite; these are described above (under the heading: Sediments). Possible pathways of formation of nodules and pisoliths in soils and saprolite are shown in Figure 77.

Formation of ferruginous nodules and pisoliths in surficial environments

Pisoliths in surficial environments (soil, colluvium, alluvium) are formed by replacement or cementation of

soil or sedimentary materials by Fe oxides. They result from pedogenic activity in the upper part of the profile and are formed by leaching, migration and accumulation of Fe oxides in the clay matrix or in voids. This is not a single event, but involves multiple leaching and precipitation of Fe oxides. The process begins with the weathering of bedrock, leaching of more mobile elements and kaolinisation. Much of the ferrous iron released during weathering of the primary minerals is oxidised and precipitated near the surface. A red soil horizon develops in the upper part of the profile (Figure 77a). Alternatively, colluvium or alluvium are deposited on saprolite. As the weathering front is lowered, upward transport of Fe becomes an important process. The Fe^{2+} ion released at the weathering front is subjected to combined upward diffusion and lateral migration by groundwater flow (Mann & Ollier 1985). Iron is subsequently precipitated by oxidation (as Fe^{3+} oxides) and accumulates near the water table. In the early stages, hematite or goethite mottles are formed, largely by local migration and accumulation of Fe. The Fe moves as Fe^{2+} in solution gradually depleting the surrounding soil, which becomes bleached and kaolinitic. The Fe oxide mineralogy of the soil is controlled by the microenvironment (Tardy & Nahon 1985). In small pores in kaolinite crystals, water activity is low, so that hematite precipitates; whereas between the crystals goethite precipitates. Organic material has undoubtedly played an important part in mobilising and segregating Fe. Humid tropical regions support abundant vegetation and there are strong relationships between mottling and tree roots. For example, in Kerala, India, roots penetrate to 25 m. A similar relationship can also be seen in the higher rainfall areas of the Darling Range. In these situations, microbial decay of organic matter has produced conditions that reduce, redistribute and segregate Fe within the saprolite, where it oxidises to form ferric iron-rich mottles.

Accumulation of hematite and replacement of kaolinite continues until hard hematite-rich nodules form. The surrounding kaolinite–quartz domains are bleached yellow-white or white due to Fe loss. With longer weathering, this clay-rich mass becomes modified by solution and redeposition, destroying original fabrics. Voids develop in the clay surrounding the nodules that allow water to come in close proximity to the hematite, resulting in progressive inward hydration of the hematite-rich nodules to form thin (0.2–0.5 mm) goethite-rich cutans (Tardy & Nahon 1985). The process may eventually lead to the formation of multiple goethite cutans around hematitic cores. Formation of concentric pisoliths by this mechanism is shown by irregular dissolution of edges and scattered remnants of the original nucleus within a pisolith (Figure 68d). Further water percolation leads to dissolution of kaolinite, forming macrovoids and cracks. The nodular–pisolitic horizon then collapses to closely packed nodules and pisoliths. Alternatively, tubular macrovoids may become infilled with authigenic kaolinite, secondary silica and/or occupied with clay spherites to form a vermiform duricrust. In places, these pisoliths and nodules either coalesce to a massive duricrust as Fe is redissolved and precipitated between them (McFarlane 1976) or are recemented by the introduced matrix to form nodular–pisolitic duricrust. The range of duricrust types are variations on a theme.

Formation of ferruginous nodules and pisoliths in saprolite

A characteristic of ferruginous materials developed in saprolite is the preservation of rock fabrics within nodules (Anand *et al.* 1989a; Tardy 1992). These nodules are developed by ferruginisation of saprolite. Initially, the saprolite was impregnated by Fe depositing as tiny particles of goethite and hematite (Figure 77b). In places, ferruginisation is controlled by subvertical foliation of the bedrock. Further weathering results in a marked porosity at the mesoscopic scale, similar to that described above, causing coarse voids. Where such voids are intensively developed, the mass is generally referred to as vesicular duricrust. Amalgamation of these coarse voids leads to collapse of the duricrust. However, much of the void space may be occupied by eluvium from upper parts of the regolith. Cutans are deposited on the surface of the fragments (large nodules) and the whole mass may be recemented, forming a complex, fragmentary brecciform duricrust.

Ferruginous mottles

A lag of Fe-rich irregularly shaped yellowish-brown to dark-red fragments, commonly in the pebble size range (4–64 mm), may occur on low rises. They largely consist of hematite, goethite and kaolinite and show numerous dissolution cavities. Maghemite is typically absent. The lag is considered to be composed of hardened mottles that have been eroded from a mottled regolith. Ferruginous mottles are formed by the accumulation of Fe-rich material in saprolite, residual clays or sediments.

Figure 74 Examples of ferricretes. (a) Conglomeratic ferricrete, deposited over a profile formed from ultramafic bedrock, contains a variety of clasts from hematite–maghemite-rich ferruginised lithic clasts (1) to nodules (2) and pisoliths (3) set in a goethite-rich matrix (4). Dissolution of goethite shows dissolution cavities (5): Ora Banda (sample 07-1524). (b) Photomicrograph of a polished thin-section taken in nrl showing hematitic–maghemite-rich pisoliths (1) cemented by goethite (2). Note the presence of quartz (3): Ora Banda (thin-section 07-1524). (c) Pisolitic ferricrete showing concentric pisoliths with a variety of cores: Madoonga (sample 02-5062). (d) Photomicrograph of a polished thin-section taken in xpl showing pisoliths with fragmented and truncated inner cutans (1) that have been subject to transportation and encased by goethite-rich concentric cutan accretion (2). Goethitic wood fragments (3) also occur: Madoonga (thin-section 02-5062). (e) Massive/vesicular ferricrete (goethite-rich) in sandy sediments: Cobiac pit, Darling Range (sample 07-4619). (f) Photomicrograph of a polished thin-section taken in xpl showing rounded quartz grains (1) embedded in goethite-rich matrix (2): Cobiac pit, Darling Range (thin-section 07-4619). (g) Pisolitic–nodular ferricrete formed in sandy sediments overlying weathering profiles formed from mafic rocks: Mt Gibson: (sample 07-0303). (h) Photomicrograph of a polished thin-section taken in ppl showing abundant angular to subrounded quartz in both nodules (1) and matrix (2). Note the presence of clay spherites (3), which are common features in some ferruginous duricrusts: Mt Gibson (thin-section 07-0303). Photographs by the authors; xpl, transmitted light with crossed polarisers; ppl, transmitted plane-polarised light; nrl, normally reflected light.

Ferruginous saprolite

Where the bedrock is rich in Fe, pseudomorphic replacement of the kaolinite by Fe oxides has led to strongly indurated goethite-rich ferruginous saprolite. This may form cappings over mafic and ultramafic rocks and occupy rises and low hills. Fragments of ferruginous saprolite may occur as a lag. They are yellowish-brown, irregular to platy, with a common size range of 30–100 mm. The matrix shows relict rock fabrics. They are typically non-magnetic and

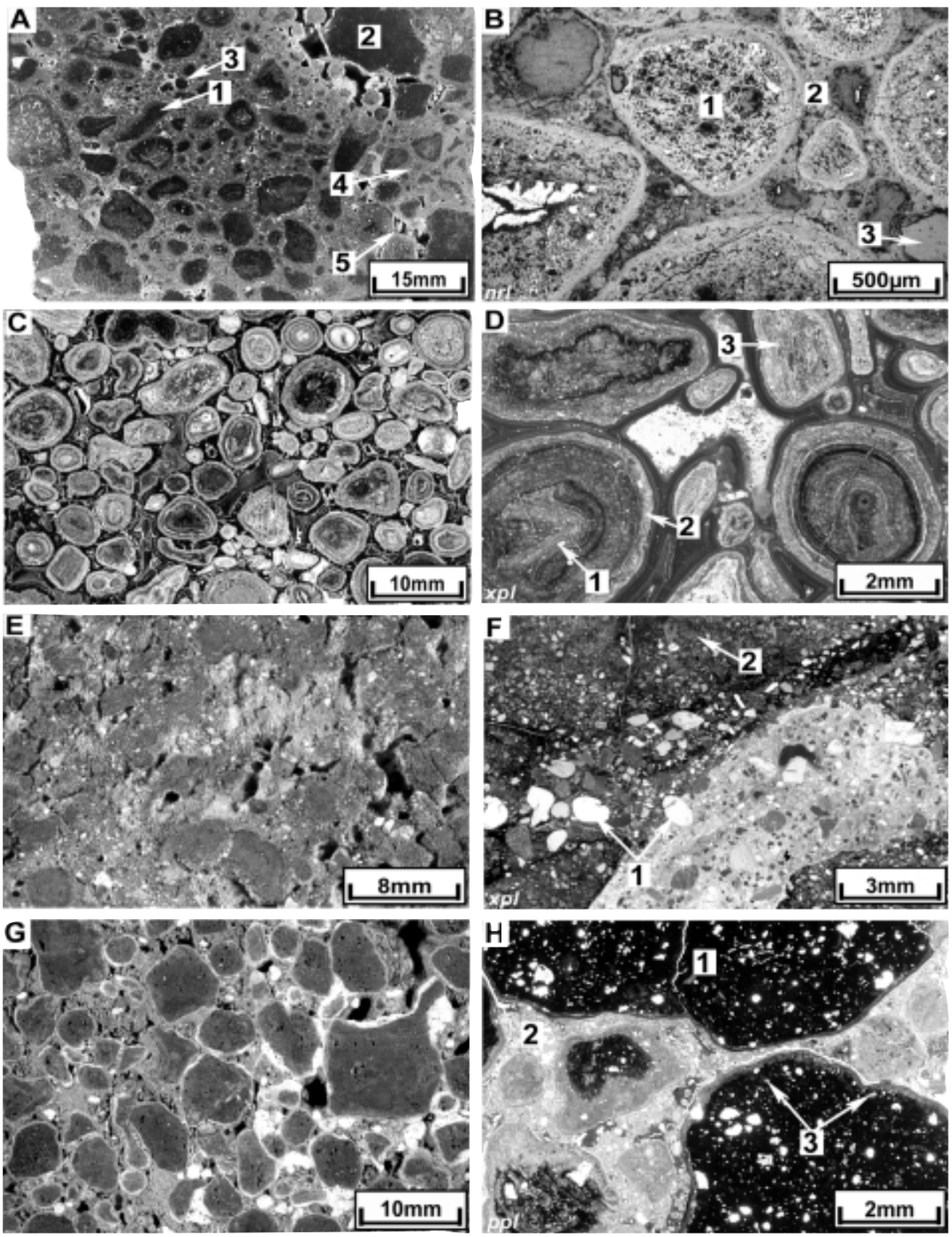

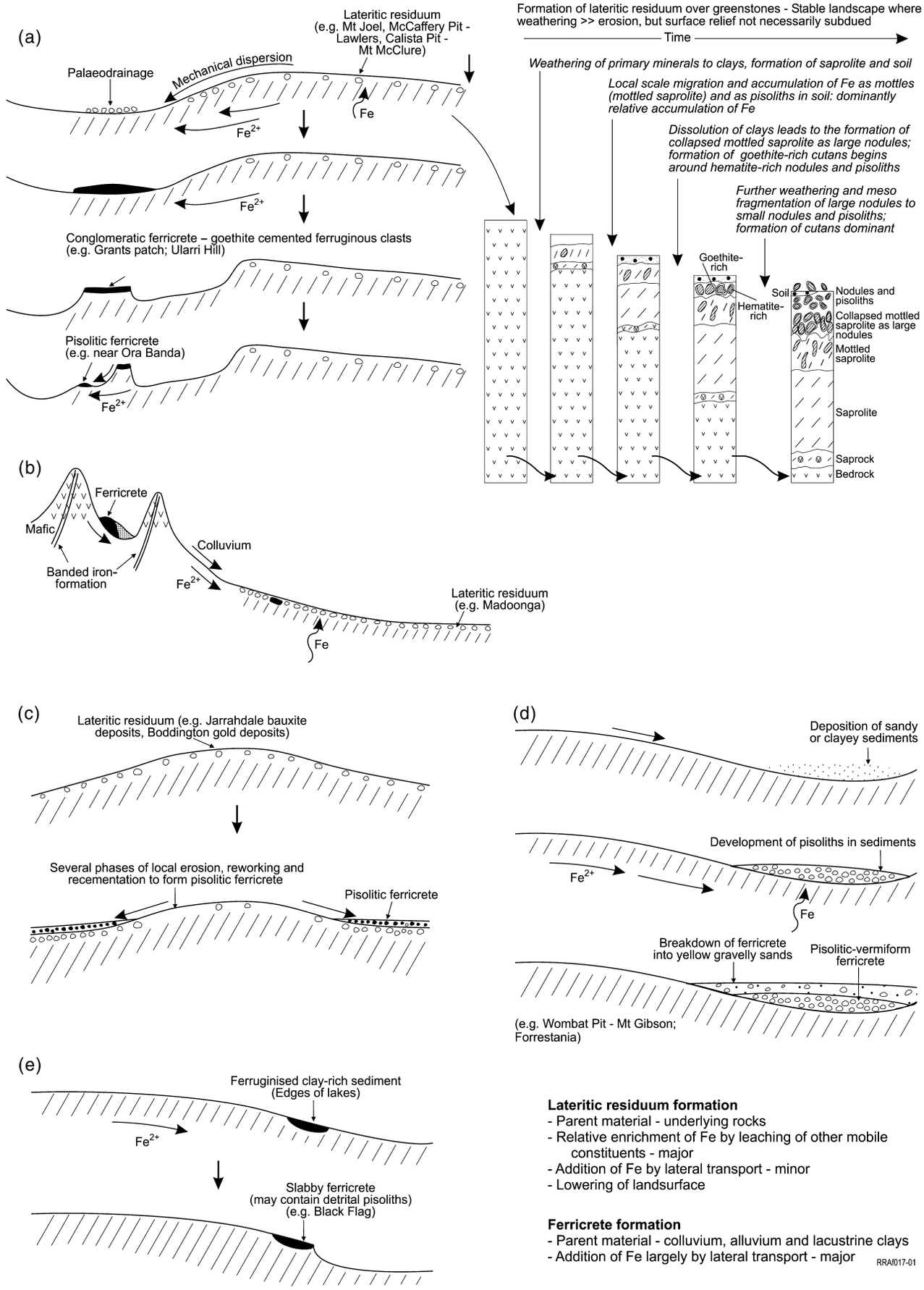

Figure 75 (a–e) Interpreted models of the formation of ferruginous materials in residuum and sediments.

largely composed of goethite and kaolinite, with small amounts of hematite.

Iron segregations after sulfide-rich rocks

Iron segregations forming low hills and gently undulating tracts up to several kilometres in length are common in the northern Yilgarn (e.g. Bronzewing, Mt McClure and Lawlers districts). As well as occurring in place along the strike of sulfide-rich rocks, they also occur loose as lag at the surface, having been detached from their original position by weathering and erosion. The McCaffery pit at Lawlers and its surroundings provide an excellent example of the development of these iron segregations (Figure 78) (Anand *et al.* 1991b). Mottled saprolite and the upper parts of the saprolite contain discrete Fe-enriched bodies ranging from a few centimetres to several metres in size. These are localised by breccias and structural surfaces (joints, schistosity, bedding). Their flinty appearance contrasts with the firm, but rather fragile, mottled saprolite that surrounds them. Erosion exposes these materials at the surface, where they disintegrate and contribute significantly to the lag particularly on low hills.

Iron segregations are dense, dark-brown to black and are non-magnetic. Where gossanous, they show boxwork textures and goethite pseudomorphs after pyrite, pyrrhotite and other sulfides. Such boxwork textures in gossans have already been described by numerous workers (Andrew 1980; Nickel 1984). The interiors of iron segregations are riddled with solution cavities filled with chalcedony or with brownish-yellow, highly crystalline goethite. Similar characteristics of iron segregations from the Mt McClure and Bronzewing districts have been described by Varga *et al.* (1997) and Anand and Williamson (2000).

The major and minor element compositions of iron segregations are different from that of lateritic residuum (iron segregations have more Fe, Mn, Zn, Co and less Al, Ti, Cr, V and Zr than lateritic residuum) (Table 9). Iron segregations are very similar to conglomeratic ferricretes in Fe (69.9% Fe_2O_3) and Al (3.8% Al_2O_3), but are much poorer in Cr (48 ppm), V (335 ppm) and Zr (26 ppm) and higher in Mn (2300 ppm), Zn (321 ppm) and Co (82 ppm). The latter group of elements (Mn, Zn, Co) is diagnostic of gossans (Nickel 1984). However, Mn and Zn contents are highly variable in iron segregations. Electron microprobe analysis of Fe oxides that pseudomorph sulfides showed that Mn and Zn range from 1720 ppm to 36 140 ppm and from 360 ppm to 2250 ppm, respectively (Anand *et al.* 1991b). Hydrous Mn oxides compete for Zn and Co with goethite and there are strong correlations between Mn, Zn and Co.

Maghemite distribution in ferruginous materials

The distribution of maghemite in ferruginous materials varies according to its position in the profile and the terrain type (Figure 79). In ferruginous gravel and duricrust-dominated terrain, maghemite-rich pisoliths are restricted to the surface or near-surface. For example, in the Darling Range, maghemite is common in pisolitic lag and pisolitic duricrust, but is generally absent from underlying fragmental duricrust and bauxite zone. A similar trend occurs inland where maghemite occurs in surface or near-surface pisoliths, but is absent in underlying nodular duricrust and mottled saprolite. In saprolite-dominated terrain, maghemite is absent in exposed mottled saprolite, ferruginous saprolite or iron segregations related to sulfide-rich rocks. In sediment-dominated terrain, magnetic pisoliths occur as lag, scattered granules or as lenses within colluvial–alluvial sequences or as lenses, and are interpreted to have been derived from the erosion of pisolitic duricrust.

CALCRETE

Introduction

Calcrete is extensively distributed in the semiarid regions of the Yilgarn Craton. In most semiarid and arid regions, the lack of leaching by rainfall leads to substantial accumulations of carbonate in the regolith. In many cases, carbonate accumulations (nodular, pisolitic, laminar or massive) are associated with calcareous soils; elsewhere they precipitate in specific parts of the landscape, such as drainages. They are commonly described as calcrete, but are also known by other names such as caliche, nari and kunkur (kankar). Cemented forms, such as nodules, boulders and massive sheets, are termed calcrete, which in some classifications (Netterberg 1969) also includes soft and powdery forms. Calcrete and other regolith carbonates are terrestrial materials that have accumulated in and/or replaced and/or cemented pre-existing regolith.* They are composed principally of calcite and/or dolomite, either of which may be dominant; in addition, silica, smectite, magnesite and gypsum may be present and even abundant.

Carbonates may accumulate and calcrete may form in either the vadose or phreatic zone and may vary in nature and abundance, including: thin encrustations on freshly weathering rocks; minor diffuse enrichments, friable powders, nodules and pisoliths in soils; sheets of indurated carbonate or carbonate-cemented regolith material. Two general types of calcrete are recognised, pedogenic (vadose) and groundwater (phreatic) (Sanders 1974; Butt *et al.* 1977; Arakel 1982). A genetic classification of calcrete is given in Figure 80. Groundwater and pedogenic calcretes are end members of a continuum that varies according to landscape setting and origin. Groundwater calcretes are linear, tabular limestone bodies, occurring at or close to the surface and forming gentle mounds. They are distinct from pedogenic calcrete and carbonate accumulations in residual and transported regolith, which may occur in many landform situations farther south. Pedogenic calcretes occur near-surface and are laterally extensive for tens of kilometres.

*Calcrete: terrestrial material composed predominantly, but not exclusively, of calcium carbonate and involves the cementation in, and/or replacement of, greater or lesser quantities of soil, rock and weathered material (Goudie 1973).

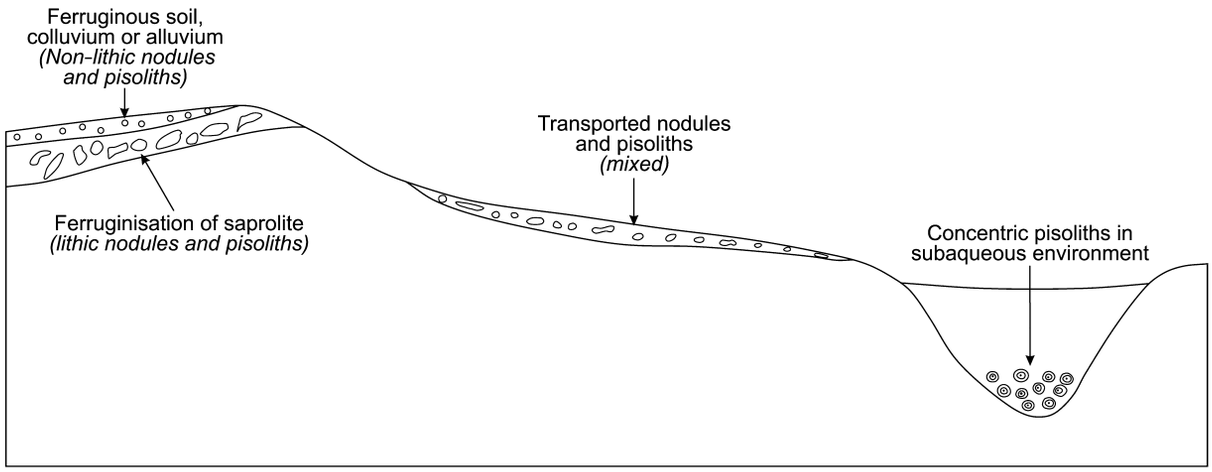

Figure 76 Interpreted environments of formation of ferruginous nodules and pisoliths. Pisoliths formed in soil are non-lithic (homogeneous and concentric), whereas those formed in saprolite are commonly lithic (lithorelict and pseudomorphic). Those formed in subaqueous environments (lakes and rivers) are typically concentric (after Anand *et al.* 1989a; Clarke & Chenworth 1995).

Groundwater calcretes

Most studies in Western Australia have concentrated on groundwater calcretes. Groundwater calcretes are associated with present or past drainages and are found over much of the Western Shield and the adjacent sedimentary basins (Sofoulis 1963; Sanders 1974; Butt *et al.* 1977; Carlisle 1978; Mann & Horwitz 1979). However, their development ceases in the south and southwest, the limit being the Menzies Line (Butt *et al.* 1977). Downstream (west) from the Meckering Line, the calcretes are being destroyed and generally form terraces above the present river level. Upstream from the Meckering Line, the calcretes are intact. Groundwater calcretes vary in width from a few hundred metres to 3–5 km or more and may be over 100 km in length; thickness is usually 5–10 m, but often exceeds 30 m along the axis. Longitudinal gradients are commonly less than 1 in 1000. Calcretes frequently lead to playa lakes where they broaden out to deltaic platforms. Calcrete forms major aquifers and has significance both as a source of potable and irrigation water, and as sites for secondary uranium deposition. Comprising both calcrete and dolocrete, groundwater calcretes cement and replace detritus which, in the uraniferous areas, is largely derived from the weathered granite (Butt *et al.* 1977; Mann & Horwitz 1979; Butt 1988). They are earthy to aphantic in fabric, but highly permeable as a result of shrinkage cracks and karstic features, especially with abundant 'mound' structures.

The calcrete at Yeelirrie, as studied in detail by Butt *et al.* (1977), is located in the upper section of a broad palaeodrainage (Figure 81b on Plate 12), which has a 1–1.5 km wide central channel covered with light calcareous soils, a few clay pans and outcrops of calcrete. Precipitation of calcite or dolomite at the water table has forced the overburden upwards, forming mounds (Butt *et al.* 1977; Butt 1988) and diapirs (Figure 81a on Plate 12). The groundwater calcretes form elongated lenses over a distance of 85 km in semicontinuous sheets at 0–7 m depth, with soil-filled depressions in their surfaces (Figure 81a on Plate 12). The largest calcrete sheet contains the Yeelirrie U orebody and is 20 km long and 0.5–2.5 km wide.

Carnotite occurs as coatings in cavities in calcrete and in the sepiolite clay or finely disseminated in kaolinite–quartz clay at the base of the calcrete. Some carnotite occurs in the veins of opaline silica. Uranium is precipitated from groundwater by evaporation. Vanadium concentrations increase where carnotite dissolves incongruently. The carnotite, generally yellow, is greenish at depth, probably due to V reduction. Groundwater calcrete has a high Mg content (19% MgO), but Ca can be dominant in the overburden (4% CaO). Pedogenic calcrete is similarly poor in Mg and rich in calcite.

Two types of groundwater calcretes were identified at Yeelirrie: earthy and hard (Butt *et al.* 1977). Earthy calcrete is buff and friable and forms lenses in the base of the soil horizon. It contains progressively less soil and alters to nodular, white, porous, hard calcrete with depth. The clay content is greater than 25% and there is less Fe–Mn dolomite and more calcite. Hard calcrete locally contains smectite. It has cracks and caves up to 1 m. Some is silicified.

The calcretes frequently form positive relief features in the valleys, being raised and mounded to 3 m or more above the flanking alluvial plains (Butt *et al.* 1977; Mann & Horwitz 1979). This is probably due to the precipitation of dolomite or calcite at the water table—as a 'groundwater evaporite'—with voids often infilled by sepiolite and other magnesian clays (Butt 1988), although some mounding may be due to pedogenic modification (Arakel & McConchie 1982). The relief may be emphasised by erosion due to creeks and washes flanking the calcrete body. However, particularly in upper sections of the valleys, the calcretes may be covered by red-brown hardpan or sediments such as alluvium, evaporites and aeolian sands. Discontinuous bands of hardpan and alluvium also occur within the calcrete, appearing to have been engulfed by the precipitating

Figure 77 Proposed pathways for the formation of pisoliths and nodules in soil, colluvium and alluvium (a) and nodules and pisoliths in saprolite (b). Pisoliths formed in soil are generally non-lithic, whereas those formed in saprolite are lithic.

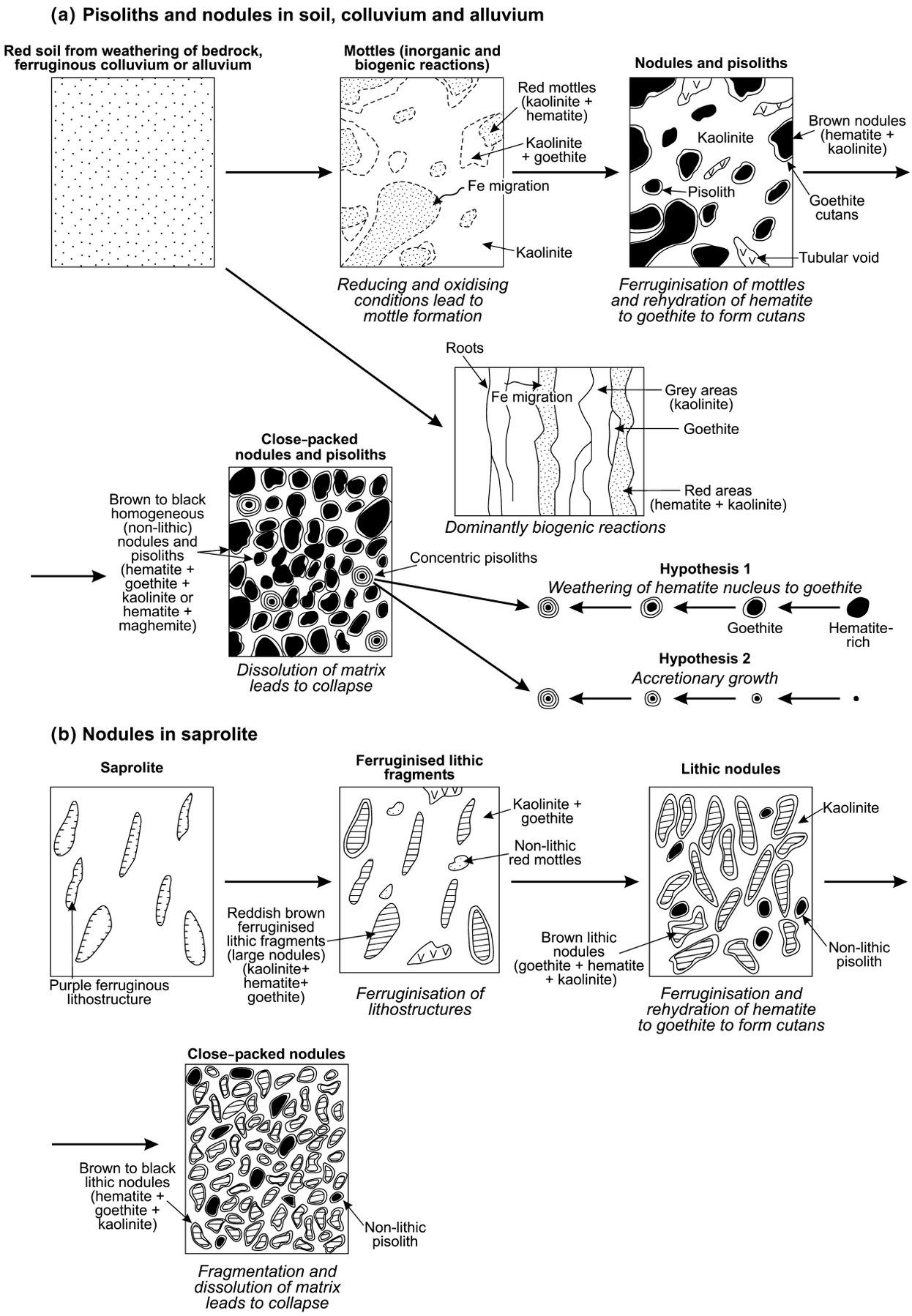
(a) Pisoliths and nodules in soil, colluvium and alluvium
Red soil from weathering of bedrock, ferruginous colluvium or alluvium
Mottles (inorganic and biogenic reactions)
Red mottles (kaolinite + hematite)
Kaolinite + goethite
Fe migration
Kaolinite
Nodules and pisoliths
Kaolinite
Brown nodules (hematite + kaolinite)
Pisolith
Goethite cutans
Tubular void
Reducing and oxidising conditions lead to mottle formation
Ferruginisation of mottles and rehydration of hematite to goethite to form cutans
Roots
Fe migration
Grey areas (kaolinite)
Goethite
Red areas (hematite + kaolinite)
Dominantly biogenic reactions
Close-packed nodules and pisoliths
Brown to black homogeneous (non-lithic) nodules and pisoliths (hematite + goethite + kaolinite or hematite + maghemite)
Concentric pisoliths
Hypothesis 1
Weathering of hematite nucleus to goethite
Goethite
Hematite-rich
Hypothesis 2
Accretionary growth
Dissolution of matrix leads to collapse
(b) Nodules in saprolite
Saprolite
Purple ferruginous lithostructure
Ferruginised lithic fragments
Reddish brown ferruginised lithic fragments (large nodules) (kaolinite+ hematite+ goethite)
Kaolinite + goethite
Non-lithic red mottles
Ferruginisation of lithostructures
Lithic nodules
Brown lithic nodules (goethite + hematite + kaolinite)
Kaolinite
Non-lithic pisolith
Ferruginisation and rehydration of hematite to goethite to form cutans
Close-packed nodules
Brown to black lithic nodules (hematite + goethite + kaolinite)
Non-lithic pisolith
Fragmentation and dissolution of matrix leads to collapse

carbonate. Calcrete precipitation is probably still active in areas of internal drainage, but where rivers are rejuvenated, such as in the west, the calcrete remains as isolated remnants up to 30 m above the present valley floor.

Calcrete occurrences appear to be related to areas of summer rainfall, where run-off, rapid infiltration and high evapotranspiration limit the period of soil dampness and plant respiration. Dissolved Ca and Mg and bicarbonate in deep groundwater precipitate in drainage axes and depressions after concentration by evaporation or CO_2-degassing due to upwelling or capillary rise. Mann and Horwitz (1979) envisaged four stages of development: (i) formation of a broad drainage line with an alluvial fill; (ii) precipitation of carbonate from laterally moving solutions beneath the water table; (iii) formation of pods and domes of carbonate as deposition proceeds, creating mounds that displace alluvium and colluvium upwards [although Carlisle (1983) did not find any evidence of calcrete migration upward with sedimentation]; and (iv) a phase of maturation in which older carbonate, lifted above the water table, is continually displaced upwards (where it may be dissolved) and is replaced by younger carbonate from beneath.

Pedogenic calcrete

PEDOGENIC CALCRETE PROFILES AND FORMS OF CALCRETE

Pedogenic calcretes are extensive in the southern Yilgarn. Carbonate enrichment occurs in the upper 10 m of the regolith, most commonly in the top metre, irrespective of whether material is *in situ* or transported (Anand *et al.* 1989b, 1991c, 1993a, 1997; Lintern 1989; Lintern *et al.* 1990; Butt *et al.* 1991, 1997b; Churchward *et al.* 1992; Dell 1992). Calcrete occurs on all lithologies, but is more common on greenstones. For example, at Mt Gibson calcrete is largely restricted to greenstones and particularly absent in sandplains formed on granite (Figure 82). In places calcrete is common on granitic terrain (e.g. the Federal pit area in the Kalgoorlie region). In greenstone terrain, profiles either overlie Ca-poor or Ca-rich substrate (Figure 83). Calcrete profiles commonly display three horizons, from top to bottom these are: (i) a less calcareous or even non-calcareous loose A horizon; (ii) a horizon characterised by calcareous accumulations and referred to as Bca; and (iii) a mildly calcareous to non-calcareous C horizon (parent bedrock, weathered products or sediments) (Read 1974; Dan 1977; Arakel 1982).

Netterberg (1969) classified calcrete into calcareous soils, calcified soils, powdery calcretes, nodular calcretes, honeycomb calcretes, hardpan calcretes and calcrete boulders and cobbles. Following this classification scheme, there are great variations in the forms of calcrete on greenstones. The calcrete types consist of coatings and stringers, and powdery, nodular, pisolitic, laminar and platy boulders and cobbles within the top 0.3–2 m of the regolith. Some of these forms are shown in Figures 83; 84 on Plate 13 and 85 on Plate 14. The calcrete forms vary both vertically within a profile and laterally across the landscape. Thus, it is difficult to recognise certain patterns with sufficient repetition. The horizons themselves may be repeated several times or be absent altogether. Many sites have profiles that are a composite and may include combinations of various calcrete types (Figure 84e on Plate 13).

The calcrete forms are largely controlled by the nature and porosity of the host material and the landscape position (Figure 83). In poorly developed fine-textured silty clayey soils on saprock on low hills and erosional plains, stringers and powdery calcrete are common with few or no calcrete nodules. Any nodules present are generally weak and friable. Stringers are generally elongated in a near-vertical orientation and are up to several centimetres long (Figure 84a, b on Plate 13). Powdery calcrete is generally structureless, fine grained and unconsolidated. Nodular and pisolitic calcretes (Figures 84c, d on Plate 13; 85a–c on Plate 14) are common in gravelly soils. They are gravel-sized, carbonate-cemented host particles in a matrix of powdery calcretes and occupy a variety of landscape situations including ferruginous duricrust-capped profiles on topographically higher areas as well as in colluvium and alluvium on slopes and plains. Nodules and pisoliths are strong and can have a variety of nuclei including indurated soil, colluvium, ferruginous nodules and rock or saprolite fragments. Nodules are generally calcitic, but may be dolomitic on ultramafic bedrock (e.g. at Matt Dam: Anand *et al.* 1993a). They vary in shape from nearly concentric (pisolitic) to irregular, while platy and elongated forms also occur. The colour differences between different layers of the concentric pisoliths (Figure 85c on Plate 14) may be produced by the presence of organic material and by staining with Fe and Mn oxides. Nodules and pisoliths with varying degrees of calcification of host material by calcite and/or dolomite can be observed within a single hand specimen (Anand *et al.* 1997). Complex calcrete nodules show the inclusion of many smaller nodules surrounded

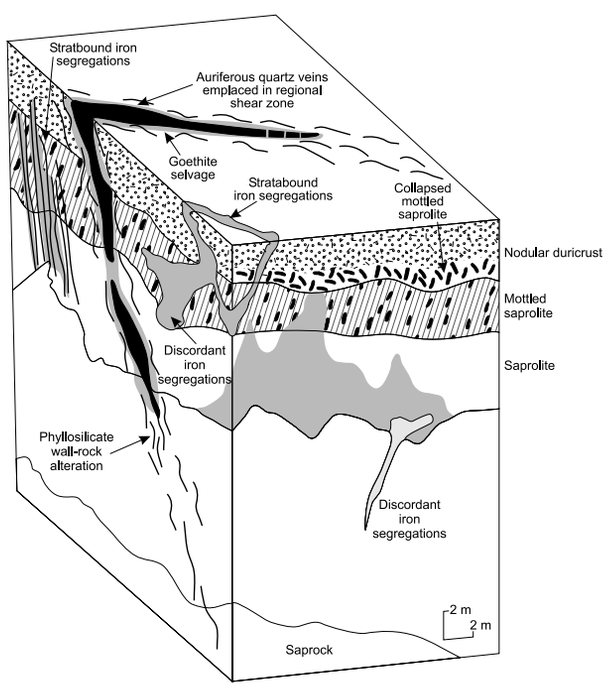

Figure 78 Detailed block diagram showing field relationships for iron segregations, McCaffery pit, Lawlers (after Anand *et al.* 1991b).

by laminar rinds, suggesting a complex history of formation. In places, nodules have weakly coalesced and feature large void spaces: they are referred to as having a honeycomb morphology (Netterberg 1969).

Laminar to platy calcretes are firm to hard, finely laminated (Figure 85d, e on Plate 14) undulose calcrete layers and are especially common in red-brown hardpan dominated low-lying colluvial–alluvial areas (Figure 83). In places, laminar calcrete may develop along the interface between the regolith and the fresh bedrock. Individual laminae are generally several millimetres in thickness and well defined with sharp contact boundaries between adjacent laminae. Laminar calcretes are dominated by calcite. They may be disrupted into boulder or cobbly calcrete, which is hard to very hard; the fragments vary from subrounded to subangular and blocky (Figure 84e on Plate 13).

Massive calcrete is a very hard, impermeable, sheet-like horizon and is the plugged horizon of Gile *et al.* (1966) and may show large void spaces (Figure 85f on Plate 14). It occupies slopes and plains. Netterberg (1969) grouped both laminar and massive calcretes under hardpan calcrete.

PEDOGENIC CALCRETE – LANDSCAPE RELATIONSHIP

Calcrete profiles show that there is a trend in the thickness of calcrete in the landscape. Generally, calcrete on hills, steep slopes and erosional plains is thin, but it may thicken on gentle slopes and depositional plains. However, calcrete may be absent in actively draining areas.

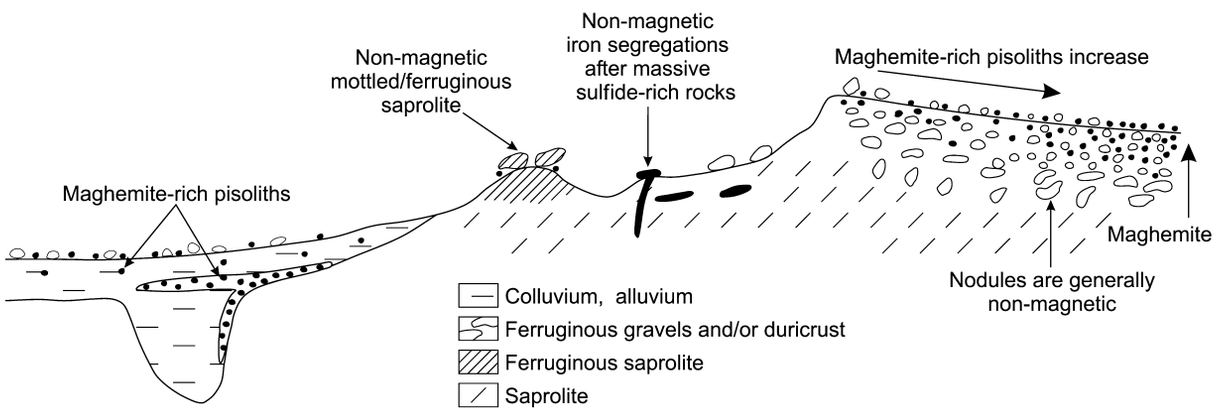

Figure 79 Schematic relationship between the distribution of maghemite and regolith units of a weathering profile and landscape.

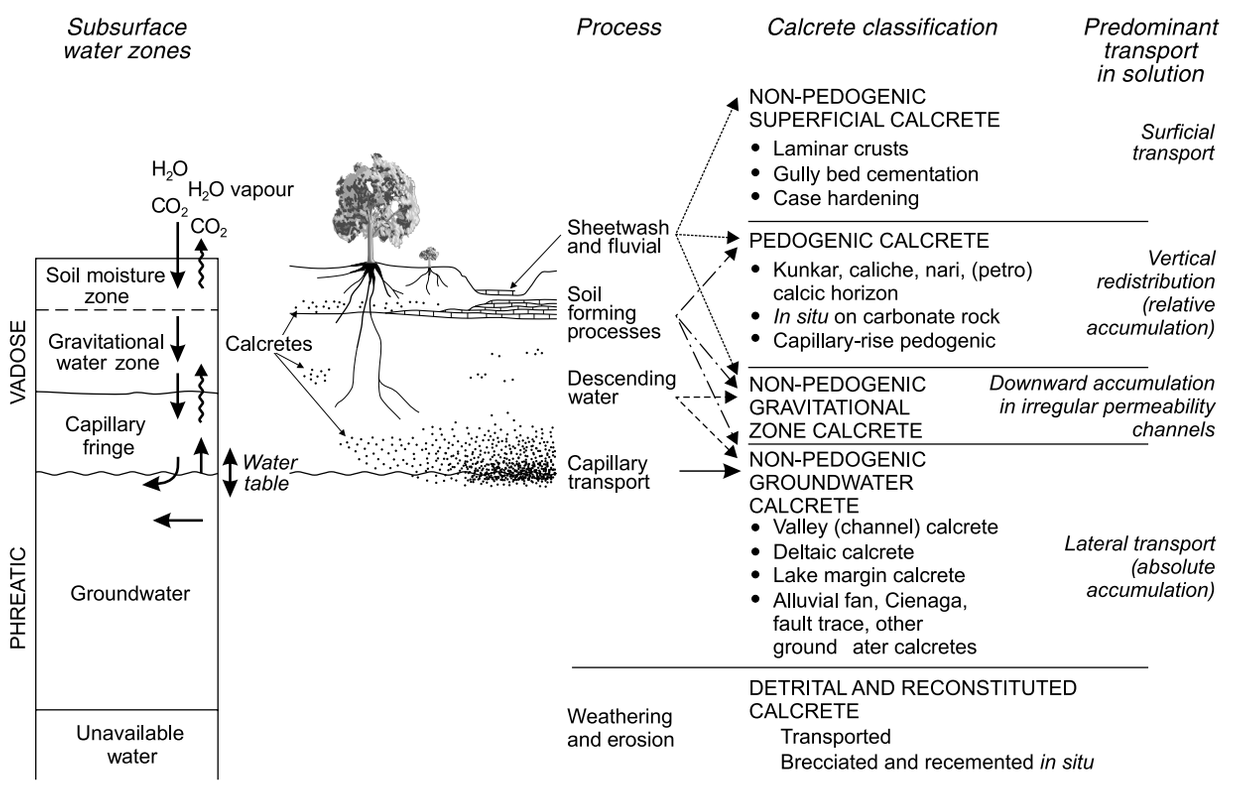

Figure 80 Calcrete classification (after Carlisle 1983). Reproduced from Residual Deposits: Surface Related Weathering Processes and Materials, Carlisle, Concentration of Uranium and vandium in calcretes and gypcretes, pp. 185–195, 1983, with permission from Blackwell Science Ltd.

For example, at Mt Gibson, a thin (20–30 cm) layer of calcrete overlies saprock on low hills, while it is 1–1.5 m thick on gentle slopes flanking low hills. At Ora Banda, the calcrete horizon on a high hill flanked by steep slopes on gabbro is approximately 30 cm thick, while on the colluvial–alluvial plain it varies from 70 cm to 2 m thick. Similarly, at Matt Dam, the calcrete over saprolite is shallow (10–30 cm) on low hills; by contrast, the calcrete horizon over the plain was relatively deep (0.5–2 m). Ruellan (1971) noticed similar variations in the thicknesses of calcrete in African profiles and these are regarded as indicating significant lateral migration of carbonate in the catena.

CHEMICAL COMPOSITION OF PEDOGENIC CALCRETE FORMS

The bulk chemical analyses presented in Table 10 for various types of calcrete show that, in addition to Ca, only Mg, Si, Al and Fe are generally present in significant amounts. Aluminium occurs in kaolinite, Si in kaolinite and quartz, and Fe in goethite and hematite. Pisolitic calcretes (Figure 85g on Plate 14) may contain significant amounts of Fe (mean 24.3% Fe_2O_3), reflecting the presence of ferruginous cores. Massive, laminated and pisolitic calcretes are richer in Ca compared with powdery calcretes, which may reflect the maturity of the calcrete development.

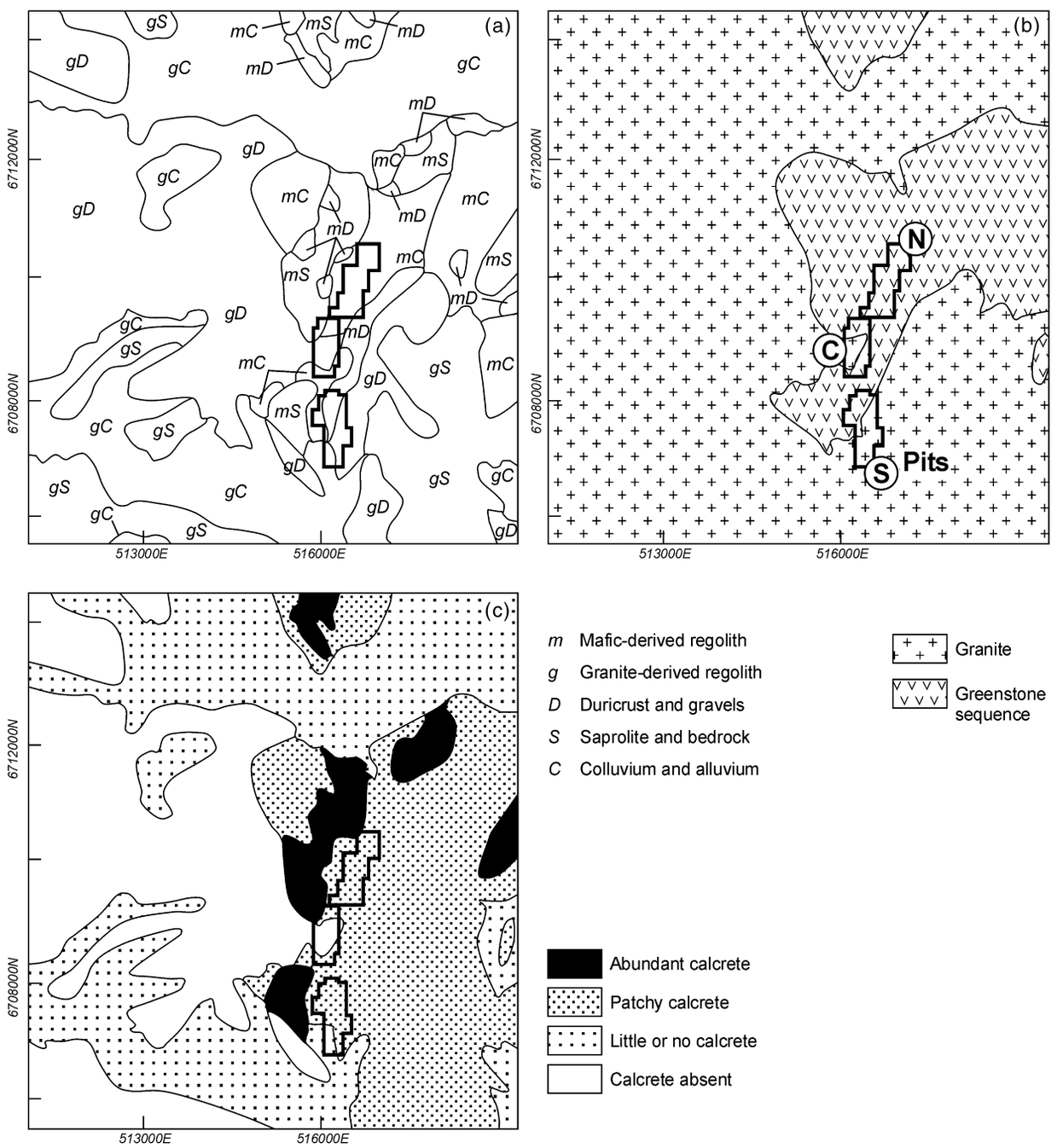

Figure 82 Distribution of (a) regolith, (b) basement lithologies and (c) calcrete in the Mt Gibson area (after Anand *et al.* 1997)

MINERALOGY AND CHEMISTRY OF PEDOGENIC CALCRETE PROFILES ON Ca-RICH SUBSTRATE

Calcrete profiles commonly occur on Ca-rich bedrocks and saprocks and the thickness of the calcrete profiles varies from 0.2 m to 2.0 m (Anand *et al.* 1991c, 1997; Churchward *et al.* 1992; Varga *et al.* 1997). There are great variations in the abundance of calcrete on greenstones. At Ora Banda, a comparison of the chemistry of soils developed on gabbro and talc–chlorite schist showed that soils developed over gabbro contain more Ca (CaO = 9.5–14.1%) and less Mg (MgO = 4.6–4.9%) than

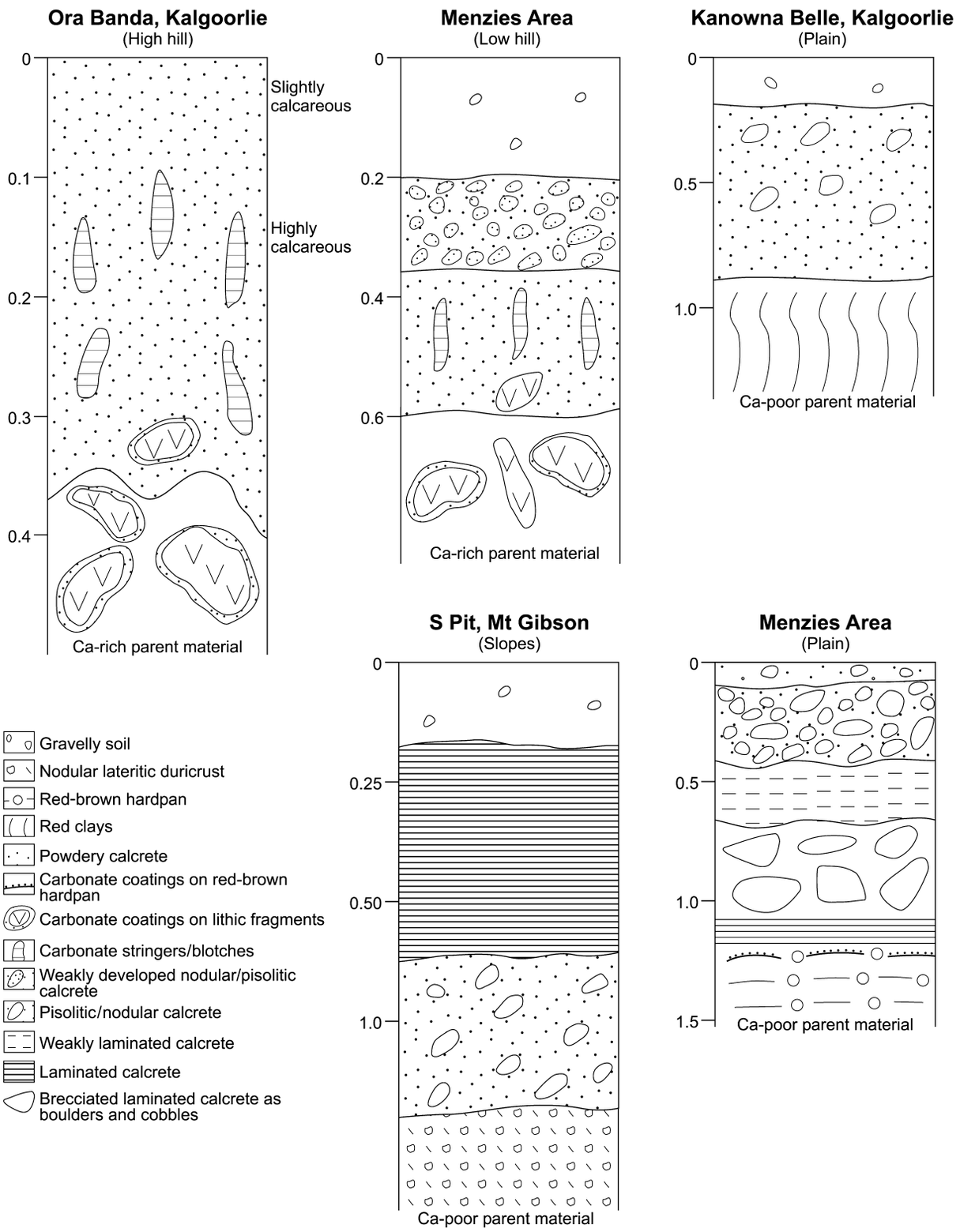

Figure 83 Calcrete profiles, landscapes and parent materials (R. R. Anand unpubl. data).

over talc–chlorite schist (CaO = 0.9%, MgO = 10.4%: see Table 6) (Anand *et al.* 1997). This is consistent with the original Ca contents of the bedrock. Gabbro contains 14.3% CaO, whereas talc–chlorite schist contains 0.4%. At the base (50–65 cm) of a soil profile over gabbro, the decrease in Ca and Mg content relative to the parent rock reflects decomposition of plagioclase and amphibole to smectite, mixed layer clays and kaolinite. At a depth of 35–50 cm, an increase in Ca concentration signifies selective loss of Mg and the formation of a carbonate-rich zone. Calcite and dolomite are present almost in equal amounts here, although significant amounts of gypsum also occur. Dolomite and gypsum are absent above 35 cm, but calcite increases towards the surface. This is consistent with the work of Milnes and Hutton (1983) who discovered in many cases in South Australia a progressive decrease in Ca/Mg ratio with depth. However, at Ora Banda and at other localities (e.g. Mt Gibson), Ca and Mg occur in both carbonate and non-carbonate forms. Calcium in soils over gabbro occurs as calcite, dolomite, gypsum and relict primary minerals (feldspars, amphiboles). Magnesium occurs as dolomite, amphibole and smectite. Over talc–chlorite schist, Mg largely occurs as talc because talc is resistant to weathering. Thus, Ca/Mg ratios do not directly reflect carbonate chemistry. Silicon, Al, Na, K and Fe comprise the non-carbonate fraction, which is mainly kaolinite, smectite, mixed-layer clays, quartz, Fe oxides and relict primary minerals together with Fe oxides. As discussed earlier (under the heading: Sediments), these profiles contain an aeolian component indicated by the presence of quartz, mica and K-feldspars.

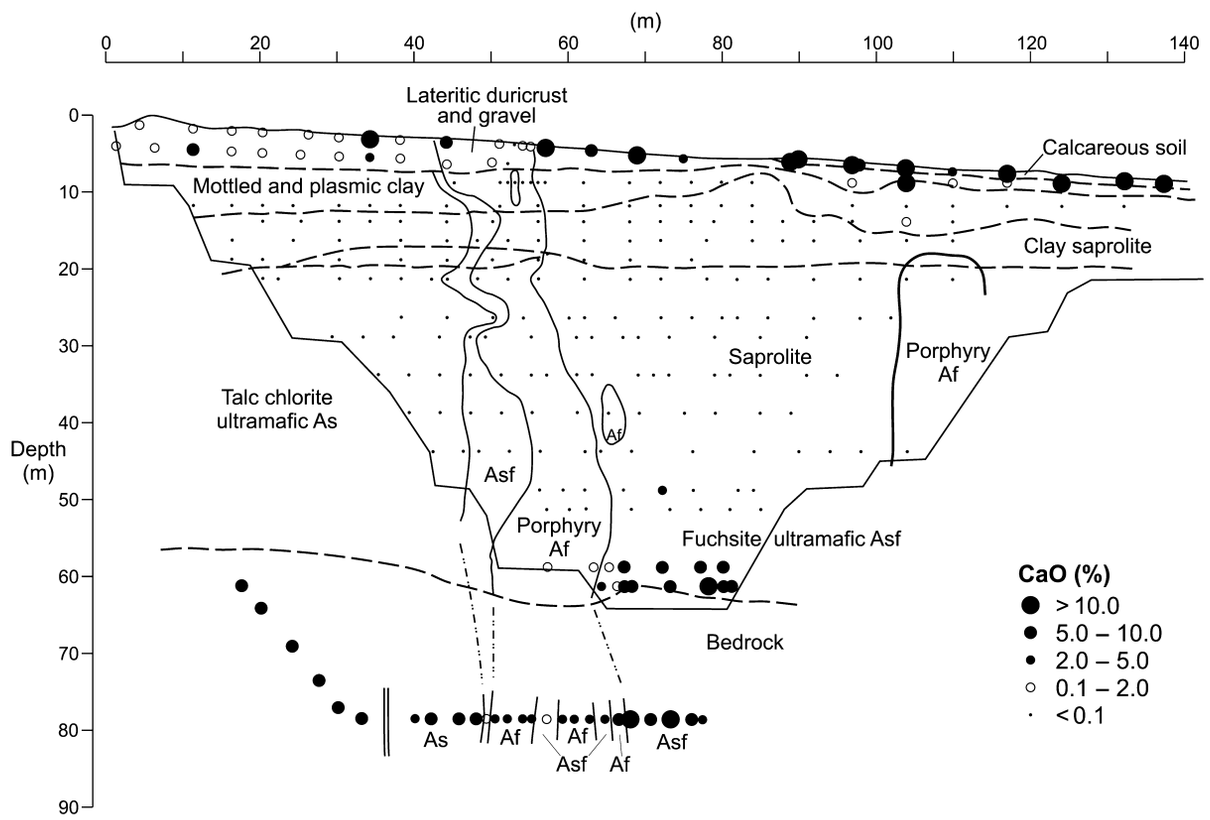

Figure 86 Distribution of Ca in weathering profiles, Mt Percy (after Butt 1991). Note the significant presence of Ca in calcareous soil and its absence in the underlying saprolite. Af, porphyry; As, talc–chlorite ultramafic; Asf, fuchsite ultramafic.

Table 10 Chemical composition (mean %) of various forms of calcrete.

	Powdery calcrete $n = 7$	Nodular–pisolitic calcrete $n = 6$	Boulder calcrete $n = 2$	Laminated calcrete $n = 3$	Massive calcrete $n = 4$
SiO_2	45.2	17.4	10.5	15.9	18.5
Al_2O_3	8.5	9.2	3.4	3.8	3.8
Fe_2O_3	4.6	24.3	3.7	1.5	1.6
MgO	4.97	6.25	1.22	2.79	1.98
CaO	14.10	15.32	42.19	38.61	37.76
Na_2O	0.47	0.13	0.04	0.05	0.06
K_2O	0.80	0.07	0.21	0.37	0.22
TiO_2	0.39	0.03	0.09	0.13	0.13
LOI	20.20	26.10	28.50	35.00	34.10

MINERALOGY AND CHEMISTRY OF PEDOGENIC CALCRETE PROFILES ON Ca-POOR SUBSTRATES

In the Kalgoorlie region, calcrete occurs on all topographic positions on greenstones (Ollier *et al.* 1988; Lintern 1989; Lintern *et al.* 1990; Butt *et al.* 1991; Anand *et al.* 1993a, 1997). Thus, it is not only abundant in areas of subcropping Ca-rich saprock–bedrock, but it is also common in the Ca-poor saprolite, where it can be separated from the bedrock by 10–50 m of carbonate-free, dominantly kaolinitic regolith (Figure 86). The occurrence of calcrete in these materials introduces a problem concerning the source of calcium. For example, at Kanowna Belle, pale-orange, powdery to nodular calcrete, 0.5–1.5 m thick, overlies 2–5 m thick non-calcareous, red clay, which in turn overlies bleached saprolite (Figure 83). Calcium and Mg contents are strongly concentrated in the top metre of the profile. Despite very low concentrations in underlying red clay (CaO 0.28%) and saprolite, Ca and Mg are abundant in the overlying calcrete (CaO 7.4%; MgO 1.3%) (Table 11) and occur as calcite and dolomite. Other minerals include kaolinite, quartz and hematite. Red clay is dominated by kaolinite, quartz and hematite. At Mt Percy, pedogenic calcrete overlies a 'complete' lateritic profile capped with ferruginous duricrust (Figure 86). Calcium is at concentrations below 0.1% throughout much of the regolith. However, at the surface Ca is precipitated in pedogenic calcretes as calcite and, less commonly, dolomite at concentrations up to 10–19% CaO (Butt 1991). The calcrete occurs as coatings on blocks of ferruginous duricrust, as rhizoconcretions, pendants, nodules and irregular masses, and as a friable matrix to lateritic gravels.

Particle-size analysis of calcareous soils (e.g. Matt Dam) showed that carbonates largely occur in fine fraction (<75 μm) (Table 12). The intermediate size fraction 75–710 μm (not shown in Table 12) consists dominantly of quartz whereas the 710– 2000 μm fraction consists largely of goethite and hematite.

MICROMORPHOLOGY OF PEDOGENIC CALCRETES

Carbonate crystals in calcretes from several profiles show two distinct micromorphologies—(i) needle and microrods; and (ii) euhedral rhombohedral—the first being the more common (Anand *et al.* 1997). Needle and microrod calcite probably resulted from replacement of fungi and bacteria (Klappa 1979; Callot *et al.* 1985; Phillips *et al.* 1987). Calcified filaments on nodular calcrete are concentrated dense mats, resembling mycelia, which are conspicuous with a hand lens or binocular microscope. The needle-fibre calcite may be divided into two distinct morphological groups (Anand *et al.* 1997) similar to those described by Phillips *et al.* (1987).

(1) Single microrod. These rods are straight or curved, up to 20 μm long with round terminations. They are assumed to be the calcified remains of rod-shaped bacteria that developed in the organic matter of the hyphae, as proposed by Phillips *et al.* (1987).

(2) Needles. These crystals form straight or gently curved needles 20–160 μm long that vary in diameter from 0.5 μm to 2.0 μm (Figure 35a). Branching is common, with

Table 11 Some summary statistics on element concentrations in pedogenic calcrete and the underlying substrate.

	Pedogenic calcrete				Substrate (red clays)			
	Kanowna Belle[a] (n = 18) 0–1 m		Bounty[b] (n = 14) 0–1 m		Kanowna Belle (n = 18) 2–3 m		Bounty (n = 14) 2–3 m	
	Mean	Range	Mean	Range	Mean	Range	Mean	Range
%								
SiO_2	50.9	45.9–55.7	60.9	47.7–70.7	57.4	38.9–67.7	58.4	38.0–89.0
Al_2O_3	10.7	9.2–14.3	11.1	8.5–13.7	13.1	5.6–17.7	15.4	11.6–22.0
Fe_2O_3	12.3	9.9–17.4	6.5	3.9–11.9	17.8	11.1–34.4	19.3	6.9–32.8
MgO	1.34	1.11–1.58	3.24	0.92–5.29	0.85	0.32–1.23	0.38	0.13–0.69
CaO	7.41	4.62–10.80	5.49	2.23–8.82	0.28	0.07–2.32	0.11	0.03–0.79
Na_2O	0.50	0.21–0.96	0.47	0.30–0.80	0.77	0.31–1.16	0.77	0.07–3.07
K_2O	0.87	0.64–1.07	0.67	0.36–1.33	0.66	0.31–1.05	0.23	0.10–0.72
TiO_2	0.59	0.51–0.72	0.48	0.40–0.58	0.79	0.55–1.04	0.66	0.49–0.99
LOI	13.60	9.70–15.40	NA	NA	7.4	4.00–10.10	NA	NA

[a]Dell (1992); [b]Lintern (1989)

Table 12 Some summary statistics on element concentrations (%) in various fractions of pedogenic calcrete from the Matt Dam prospect (after Anand *et al.* 1993a).

	<75 μm fraction (n = 26)		710–2000 μm fraction (n = 26)	
	Mean	Range	Mean	Range
SiO_2	39.7	26.3–51.1	24.5	9.6–45.2
Al_2O_3	15.0	7.1–21.0	9.2	4.8–14.8
Fe_2O_3	7.3	3.5–10.9	46.3	12.6–74.4
MgO	2.90	1.23–6.45	1.46	0.24–7.75
CaO	11.24	0.49–23.80	3.99	0.27–13.70
Na_2O	0.48	0.14–1.27	0.09	0.03–0.18
K_2O	0.88	0.47–1.48	0.17	0.02–0.50
TiO_2	1.25	0.65–2.13	1.24	0.64–1.96
LOI	21.10	12.90–30.20	10.80	3.70–24.50

short subsidiary filaments or extensive, ramifying networks. Elongated flat laths, 5–25 μm, wide with serrated edges are also common. The gaps between the serrations vary along the length. The most common spatial arrangement of the needles is a self-supporting, random, open mesh of curved and straight rods, up to 160 μm long, infilling the centres of voids and root channels in weakly to moderately indurated nodular calcrete.

Calcified microfilaments, needle calcite and microrods in the calcite appear to have developed from fungal hyphae at a depth where the soil solutions were saturated with respect to Ca^{2+} and HCO^{3-}. Fungi concentrate $CaCO_3$ around and within their individual hyphae and their mycelial strands (Mohamed & Braund 1994). Bacteria in the organic matter of the fungal hyphae release needle calcite from mycelial strands, thereby infilling pores with microrods and needle calcite, ultimately resulting in cementation of this horizon.

Euhedral rhombohedral crystals of calcite and dolomite range in diameter from 5 μm to 40 μm (Figure 35e). They probably resulted from slow crystallisation of these minerals in a solution supersaturated with respect to Ca^{2+}, Mg^{2+} and HCO^{3-} (Durand 1979).

SOURCES OF Ca IN PEDOGENIC CALCRETE

Calcretes from other parts of the world have been reported to form by several mechanisms, both *in situ* and external (Gile 1961; Gile *et al.* 1965, 1966; Ruellan 1971; Klappa 1979; Milnes & Hutton 1983; Wang *et al.* 1994; Quade *et al.* 1995; Chiquet *et al.* 1999; Zachary *et al.* 2000). Six major sources of calcium (in carbonate-free substrate) are discussed: (i) aeolian carbonate particles; (ii) soluble Ca and bicarbonate in rainwater (cyclic Ca^{2+}); (iii) weathering of parent material to release Ca; (iv) upward capillary movement of Ca-charged groundwater; (v) lateral migration; and (vi) accumulation of Ca by plants. Carbon dioxide is produced by root and microbial respiration and dissolves readily in water, forming HCO^{3-}, which in turn reacts with free Ca^{2+} to precipitate as calcite as saturation is reached, probably because of water being removed by evaporation. Milnes (1992) indicated that the results of investigations on the macroscopic features of calcretes in the desert regions of New Mexico (Gile 1961; Gile *et al.* 1965, 1966) appear to have had the most impact on our concepts of calcrete formation. Gile and his coworkers argued that the secondary calcite originated largely from aeolian dust that accumulated at the soil surface, dissolved on wetting, and infiltrated the soil profile as calcium bicarbonate in solution via pore spaces as a result of evaporation. Recently, many studies have demonstrated that dust is an important source of Ca in soils (Rehies *et al.* 1995; Whipkey *et al.* 1999).

In the Yilgarn Craton, calcretes range from Ca-rich accumulations dominated by calcite through to dolomite. The accession of alkalis and alkaline earth elements as aerosols with rainfall has been well established (Hingston & Gailitis 1976) and is largely responsible for the salinisation of groundwaters. However, aerosols and dust cannot readily account for the observed lithodependence of the carbonate distribution, namely being more abundant over mafic rocks and less abundant over granite and ultramafic rock. Airborne accession, as aerosols or dust, would give a relatively even distribution. Thus, weathering of bedrock, lateral transport by soil creep and soil solutions, upward flow through tree roots and redistribution by biological processes are equally important sources (Figure 87). Mapping of regolith in the Kalgoorlie region over an area of 10 000 km^2 revealed that: (i) areas comprising saprolite formed from mafic and ultramafic bedrock, and fresh bedrock constitute approximately 40% of the landscape; and (ii) there are basement highs with an irregular weathering front, which protrude through the more weathered parts of the regolith (Anand *et al.* 1997). Thus, on weathering, the surrounding landforms could provide the Ca for calcrete formation (Figure 87), either in dissolved form, related to short- or long-distance transfer by soil solutions (Ruellan 1971; Nahon 1991; Anand *et al.* 1997), or the calcretes may have been derived by lateral transportation and redeposition of weathered fragments of calcite, derived from these upland areas, which are then dissolved and precipitated at the top of the profile. For example, these relationships occur in the Cawse area near Ora Banda where the upper backslopes that trend down from the duricrust-capped are mantled with a shallow (10–15 cm) highly calcareous soil directly underlain by Ca-rich slightly altered mafic bedrock. The calcrete thickens to 1 m downslope, suggesting its derivation from lateral migration of carbonate in the catena. The depth and extent of

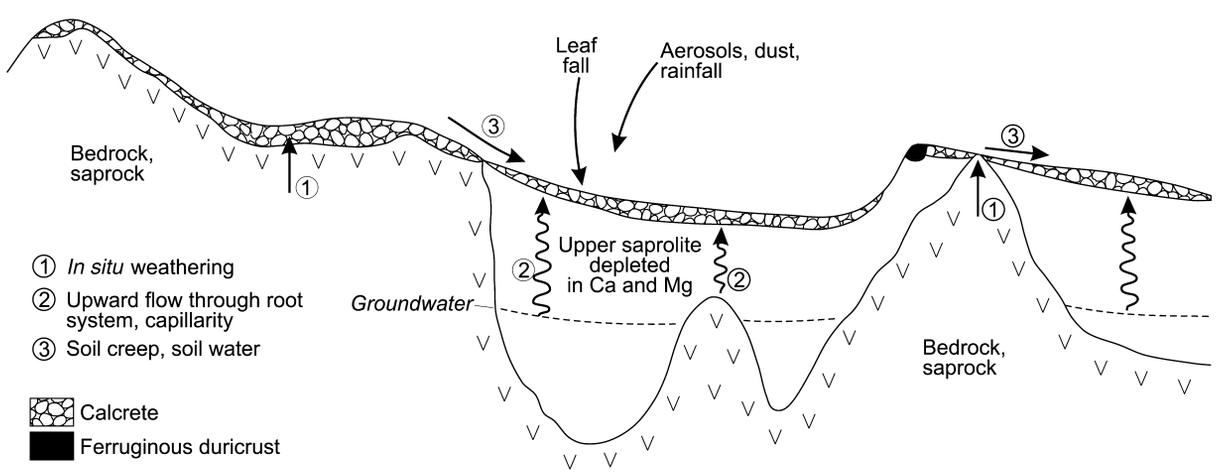

Figure 87 Interpreted model of calcrete formation particularly highlighting the sources of Ca.

lateral distribution of carbonate is probably due to a combination of many factors including proximity to carbonate source rocks, topography, drainage, infiltration rates and soil type.

The intimate association of calcified microorganisms with carbonate minerals in calcrete records a significant biological influence. In Ca-rich soils, microbes excrete excess Ca, which concentrates on their external surfaces and reacts with HCO^{3-} in the soil solution (Chadwick & Graham 1999). Evidence of root penetration to at least 2 m was clearly observed in pits. The role of plants in the formation of the carbonates is also supported by the presence of up to 20% Ca and Mg in the ash of vegetation and litter (Lintern 1989).

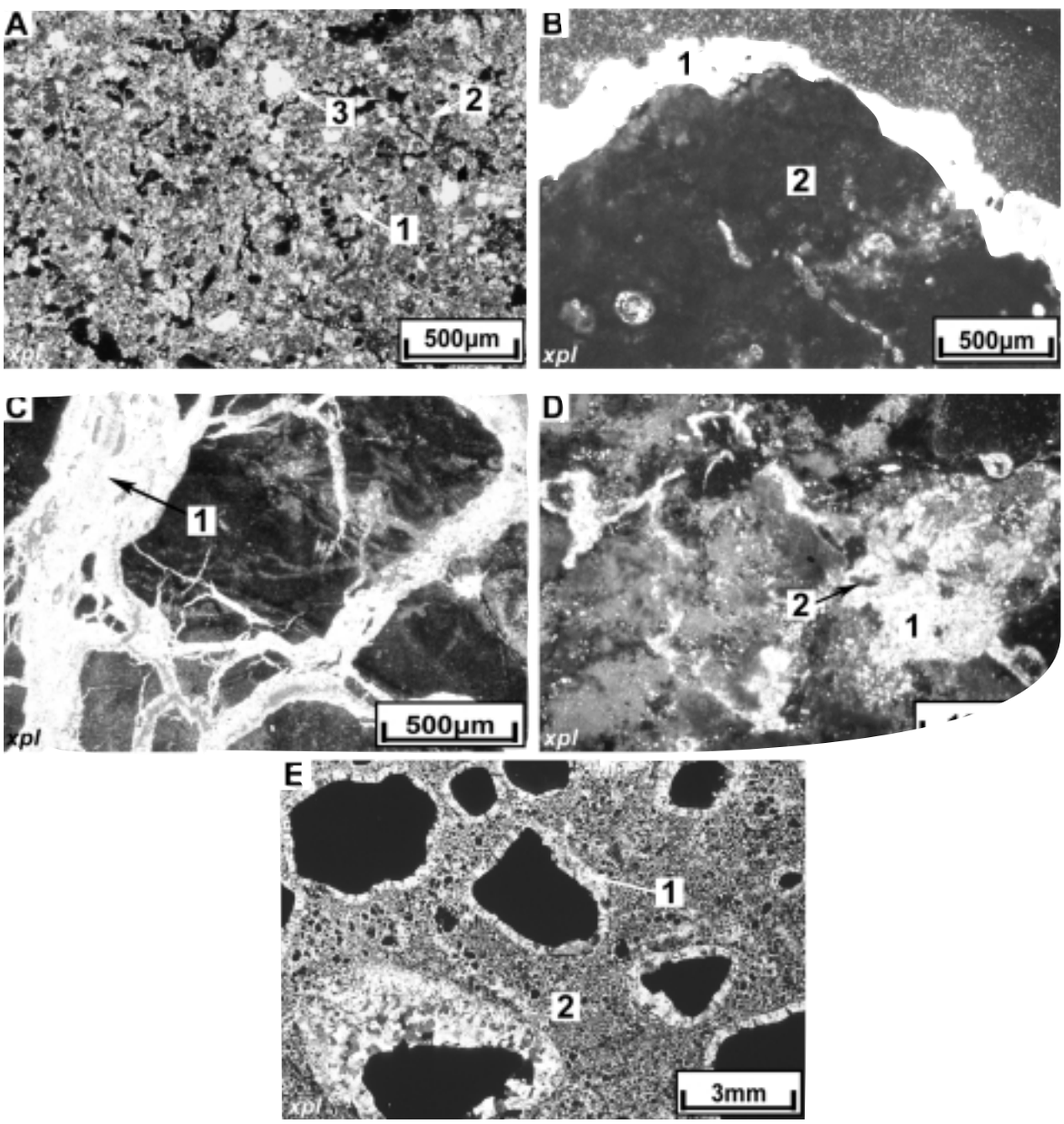

Figure 88 Photomicrographs of calcrete. (a) Polished thin-section taken in xpl showing calcrete developed over gabbro with areas of calcite (1) and kaolinite–calcite (2) and quartz (3): Ora Banda (thin-section 07-2216). (b) Polished thin-section taken in xpl showing a cutan of calcite (1) rimming a hematitic-rich nodule (2): Ora Banda (thin-section 07-2347B). (c) Polished thin-section taken in xpl showing complete infilling of cracks and voids (1): Ora Banda (thin-section 07-1525). (D) Polished thin-section taken in xpl showing partial replacement of hematite by calcite (1) leaving islands of hematite (2): Ora Banda (thin-section 07-1525). (e) Polished thin-section taken in xpl showing calcite needles developed tangentially to detrital ferruginous nodules (1) set in a micritic calcite matrix (2) in a calcrete from Bronzewing (thin-section 07-0304b). Photographs by C. Phang; xpl, transmitted light with crossed polarisers; ppl, transmitted plane-polarised light.

REGIONAL VARIATIONS

In the southwest, in the high rainfall (700–1400 mm) areas of the Darling Range, pedogenic calcretes are absent due to greater rainfall and leaching. In more arid regions inland, pedogenic calcretes are extensive in the south of the Menzies Line and groundwater calcretes are abundant in the north of the Menzies Line. According to Butt *et al*. (1977) and Carlisle (1983) the differences in the distribution of pedogenic and groundwater calcretes between the south and north is related mostly to differences in rainfall seasonality. They suggested that the preferential occurrence of pedogenic calcretes in winter rainfall regions (south) is probably due to the longer growing regime that in consequence results in greater root microbial respiration and evolution of CO_2 and, hence, higher carbonate in soil moisture. Recently, Hill *et al*. (1999) reported that a similar distribution pattern of 'regolith carbonates' extends across South Australia and western and central New South Wales, although they suggested that rainfall chemistry rather than seasonality or quantity is a major control on the distribution of such 'regolith carbonates'. Their conclusions

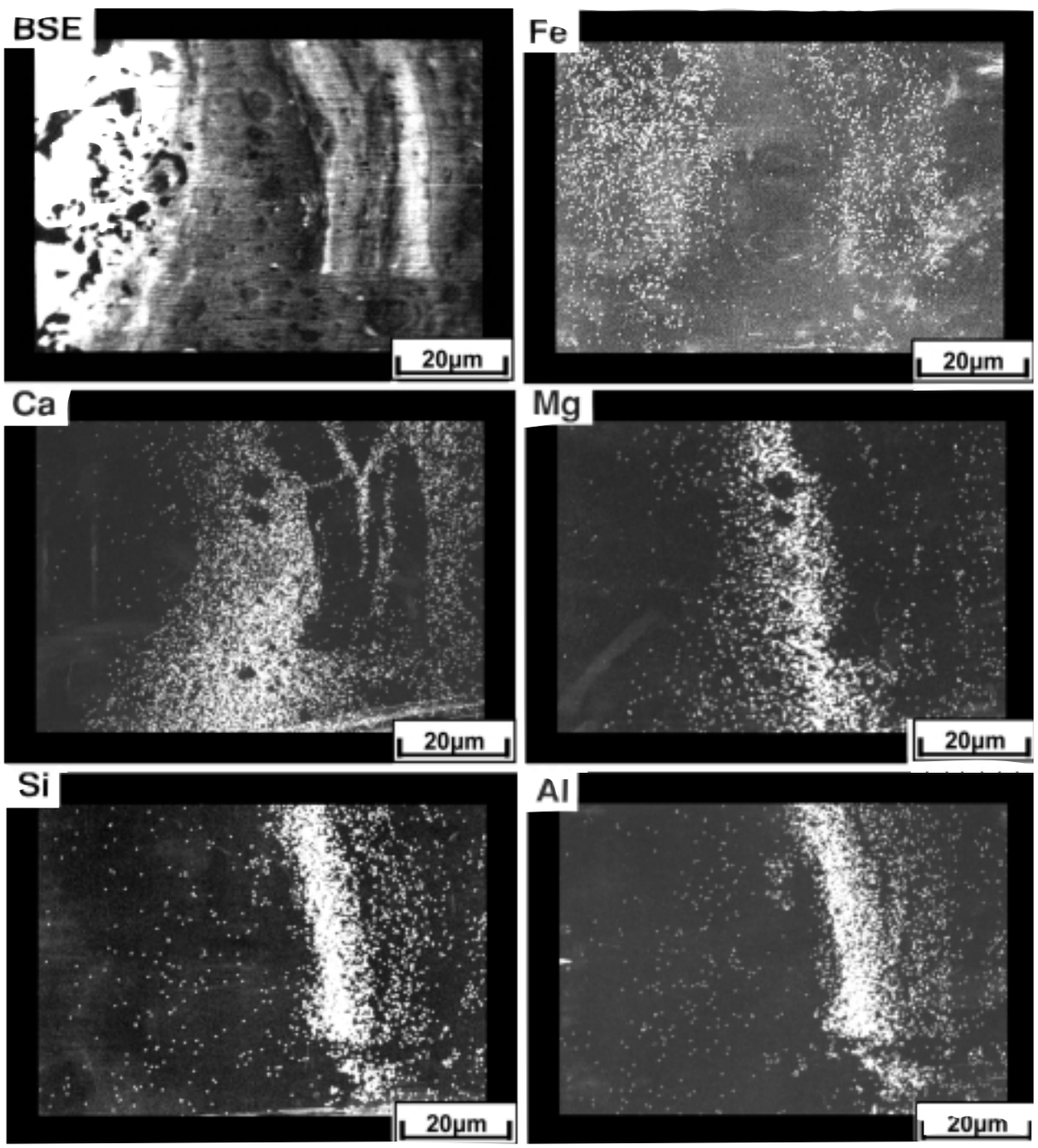

Figure 89 Backscattered electron (BSE) image and X-ray images showing the distribution of Fe, Ca, Mg, Si and Al in a calcified ferruginous nodule (after Anand *et al*. 1989b). Calcite and dolomite have formed coatings around an Fe-rich core.

appear to be based on a recent study of rainfall along a north–south transect through central Australia, which revealed major chemical differences between two rainfall regimes (Keywood *et al.* 1997). Keywood *et al.* (1997) suggested that winter-dominated rainfall is largely derived from the Southern Ocean and, therefore, has a strong marine chemical signature and, thus, an abundance of calcium and magnesium. Areas to the north are beyond the extent of regular winter-dominated rainfall and feature summer-dominated rainfall largely derived from the north of Australia. As the summer-rain-bearing system passes over northern Australia its marine chemical signature is dramatically diminished within approximately 200 km of the north coast. At the southern extent of this rainfall regime (immediately north of the Menzies Line and in northwestern New South Wales) the rainfall has a very low marine chemical signature and, therefore, provides very little Ca and Mg in the regolith (Hill *et al.* 1999). However, the rainfall data obtained by Hingston and Gailitis (1976) for Western Australia is less conclusive. These authors found that accession of salt from the atmosphere is an order of magnitude greater in the southwest than in the north of Western Australia. They also noted that it is difficult to determine the extent of movement of salts inland from the coast because no clear distinction can be made between terrestrial and oceanic contributions to ions in precipitation. For example, high values of Ca were found near coastal centres (e.g. Eucla, Esperance), but high values for Ca were also found in the north near salt lakes. Isotopic studies are needed to trace the sources of Ca (Zachary *et al.* 2000).

MECHANISMS OF PEDOGENIC CALCRETE DEVELOPMENT

In fine-textured soils developed on saprock and bedrock, micrite calcite generally occurs as an invading phase precipitated in voids and matrix (Figure 88a) (Anand *et al.* 1997), whereas in places dolomite appears to have replaced smectite pseudomorphs and matrix. The profile is composed of weatherable minerals with high porosities and permeabilities. Accumulations of calcite form elongate glaebules and vertically orientated rhizoliths (stringers) as a result of vertical water movements and the presence of taproots, respectively (Klappa 1983). Precipitation of calcite, without significant cementation, forms the powdery horizon of the calcrete profile. As the accumulation of calcite increases, porosity and permeability of the profile decrease. Original constituents of the host material are progressively replaced and/or displaced with increasing amounts of calcite.

In gravelly soils, calcrete nodules are common. Formation of calcrete nodules and pisoliths generally involves progressive addition of carbonate to any substrate, be it a ped, a ferruginous nodule or a pisolith. The substrate forms the core of the calcrete nodule or pisolith, although it is possible that a calcrete nodule or pisolith could be formed independently. Depending on the porosity and permeability of the substrate, carbonate addition generally occurs both by deposition of layered coatings as well as invasion of the cracks and porous matrix with micrite calcite (Figure 88b–d). Sparry calcite may also occur sometimes as needles (Figure 88e). The distribution of Ca and Mg in X-ray images shows that calcite and dolomite have formed coatings around the nucleus and have also infiltrated the Fe oxide species (Figure 89). It appears that if this process is taken to completion it would eventually result in the formation of the calcrete nodules.

In the Yilgarn Craton, the relationships observed between various morphological forms and the texture of soils and the mechanism of calcrete development appear to be very similar to those observed by Birkeland (1984) and Milnes (1992). Birkeland (1984) suggested that pedogenic calcite commonly progresses through distinct evolutionary stages. He observed that the morphologic expression of calcrete is different for gravelly soils compared to fine-textured soils. Because gravelly soils have less total pore space than fine-textured soils, segregated calcite accumulates more rapidly, precipitating readily on pebbles bounded

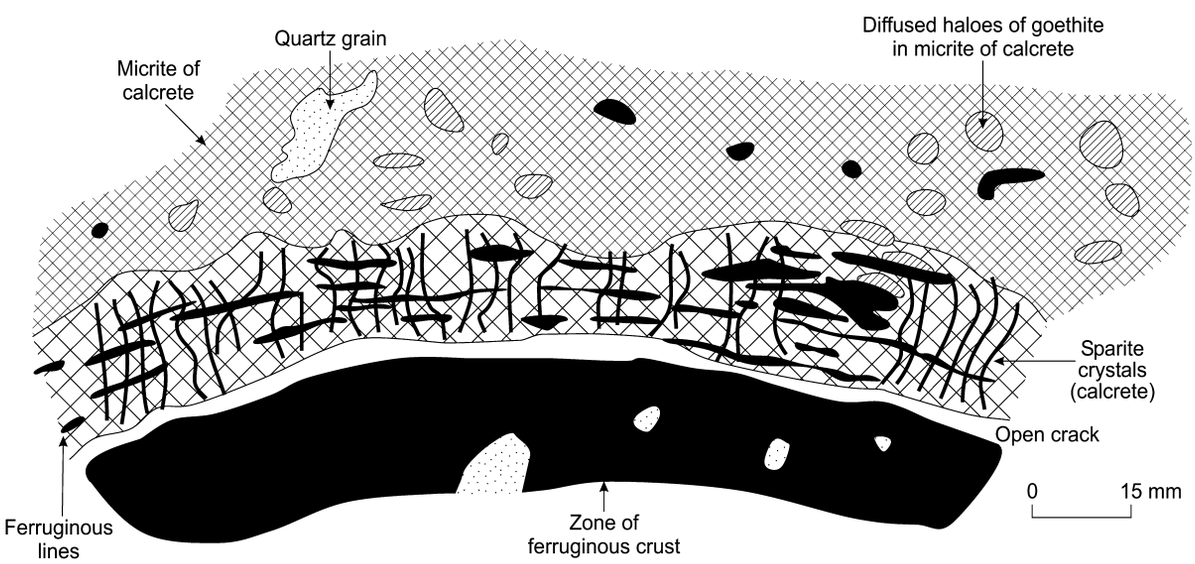

Figure 90 Petrography of the margin of a ferruginous crust within calcrete (after Nahon 1991). Reprinted by permission of John Wiley & Sons Inc.

by relatively large pores. In fine-textured soils, calcite precipitates first as filaments in root pores and then as soft masses. Eventually a calcite-cemented horizon forms in which carbonate plugs nearly all the pores (Milnes 1992) and laminar plates of carbonate build up at the interface between the overlying horizons and the plugged ones. Calcite is considered to be at once illuviated from overlying horizons and precipitated from soil solutions. The evolution of calcrete nodules by the replacement of Fe oxides by calcite can be explained using Nahon's (1991) model (Figure 90). Nahon (1991) observed that alkaline solutions first enter open cracks of the blocks of iron crust and precipitate calcite inside them. During each dry season, contraction of the calcitic cement pulls away a ferruginous film, creating a new open crack. The process is repeated several times, as demonstrated by the numerous ferruginous lines, which show that individual crystals of sparite do not result from a single episode of crystallisation, but rather from a series of successive crystallisations. Finally, the ferruginous lines are incorporated into the micritic cement to the calcrete through reprecipitation of calcite. Iron diffuses in haloes and oxides are, thus, pulverised into minute particles or partially dissolved and integrated into the calcite as Fe^{2+}. The rising of calcrete within the old sequences with ferruginous crusts gradually leads, through the above process, to their replacement.

The laminar and massive calcretes form by plugging of the profile through the accretion and eventual coalescence of carbonates (Gile *et al.* 1966; Arakel 1982). Ponding on the surface of plugged hardpan horizon then results in the deposition of the laminated subfacies. Laminar calcrete has been commonly ascribed to inorganic processes of carbonate precipitation. Calcrete boulders and cobbles are the result of fragmentation and weathering of laminated or massive calcrete.

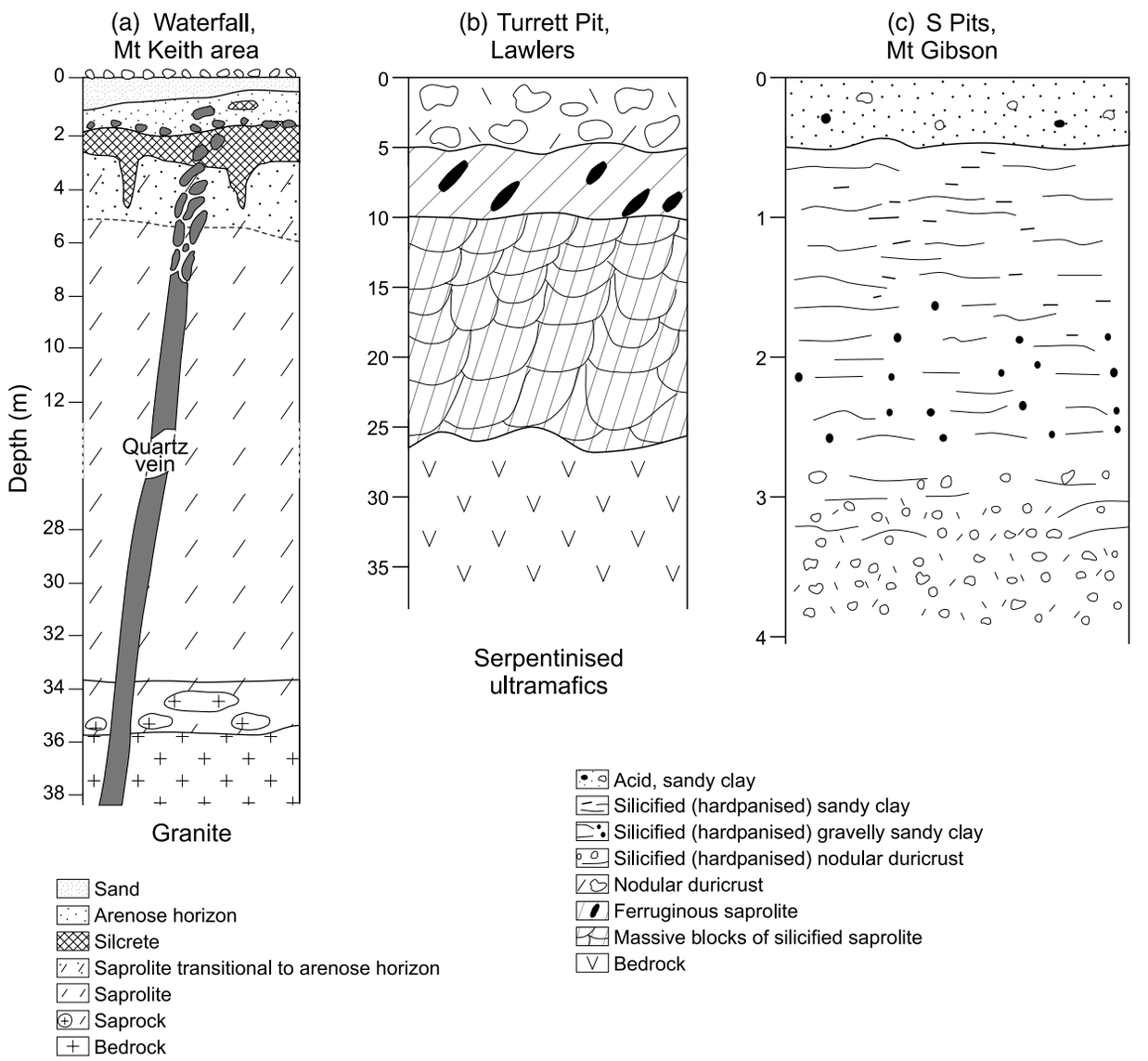

Figure 91 Examples of types of silicification. (a) Silcrete on granite (after Butt 1985). (b) Silicified saprolite on serpentinised ultramafics and (c) on silicified colluvium, alluvium and duricrust (red-brown hardpan) (after Anand *et al.* 1991b, 1989b).

SILCRETE AND SILICIFICATION

Introduction

Silica-indurated material is a feature of the regolith across Australia, both in the semiarid to arid regions (Hutton *et al*. 1978) and in humid areas, from Cape York (Pain *et al*. 1994) to Tasmania (Yim 1985). Silicification has affected a variety of materials on the Yilgarn Craton. Silica-indurated materials include silcrete, silicified saprolite, silica veins and segregation, silica-cemented colluvium and alluvium, and siliceous red-brown hardpans. The red-brown hardpans are particularly abundant in the Yilgarn Craton (Teakle 1936; Bettenay & Churchward 1974). Siliceous materials are characterised as very hard, white, buff to red-brown, with a morphology and field appearance largely determined by that of the material being cemented.

Silcrete generally contains at least 90% SiO_2 and is almost depleted of Al, Mg, K, Ca, Fe and P. Arguments about silcrete formation are similar to those concerning ferruginous duricrust and depend on the provenance of the silica and the conditions under which it has been mobilised. Extreme positions have been taken on both issues. Long-distance transport of silica from the humid environments of the eastern Highlands of Australia into the interior basins was advocated by Stephens (1971), but Wofner (1978) and Butt (1985) have proposed that silica is drawn mainly from the kaolinised profiles and toposequences within which it is found. Some authors assumed that silcrete indicates arid or semiarid conditions. Although some silcrete may form in this way, there is increasing evidence that it can also form in humid climates (Wopfner 1978; Taylor & Ruxton 1987).

Silcrete and silicified saprolite

In the Yilgarn Craton, silcretes form over any lithology, but they are common on granitic rocks and in transported materials, although they are not as common as ferruginous duricrusts. Pedogenic silcrete (Thiry & Milnes 1991) is most commonly seen as a prominent duricrust protecting mesas and cuesta-like landforms, but its lateral, subsurface extent is largely unknown. Pedogenic calcretes typically form high in the regolith profile. Massive, sheet-like or columnar structures up to 1.5 m long are common. The upper part of many silcretes shows signs of physical breakdown and chemical dissolution, resulting in a pebbly, siliceous layer. Silcretes have formed both in residual and transported materials. Pedogenic silcrete on weathered granite has been described from the Barr-Smith Range in the northeast (Figures 91a; 92a on Plate 15) (Butt 1985). Weathering profiles developed on granitic rocks exposed in the breakaways consist of kaolinitic saprolites merging upwards into silcrete, sandstone and grit. The sandstone and grit may also form columns or dykes, penetrating downwards into the saprolite. Silcretes are characterised by floating quartz grains in a matrix of cryptocrystalline silica (terrazzo fabric: Smale 1973) and have significant concentrations of relict zircon and secondarily mobilised Ti, as anatase and aluminosilicates, in the cement (Figure 92b on Plate 15). The cement not only separates individual crystals in the quartz grains, but also penetrates fine cracks in optically continuous crystals, apparently fracturing them into highly angular fragments. Silcretes are almost entirely depleted of Al, Ca, Mg, Na, Fe and K (Table 13). The sandstones are cemented by aluminosilicates, either apparently amorphous (as siliceous allophane) or partly crystalline, as kaolinite and opaline silica.

Groundwater silcretes (Thiry & Milnes 1991) are mostly massive, quartz-rich silcretes, which may preserve the original fabric of the host material. They generally form at the subsurface due to the introduction of silica in groundwater solutions. At Federal pit near Broad Arrow, silicification has affected palaeochannel sandy deposits and weathered granite. Here, massive silcrete approximately 1 m thick, developed in palaeochannel sediments, overlies silicified saprolite formed on granite. There is a sharp contact between the overlying silcrete and the underlying saprolite. The horizontal alignment of silcrete suggests some water-table control over silicification. Ollier *et al*.

Table 13 Chemical composition (mean) of silcrete and red-brown hardpan.

	Silcrete over granite (n = 8) (after Butt 1985)		Red-brown hardpan in colluvium and alluvium over greenstones (n = 34) (after Ward 1993)		Red-brown hardpan in colluvium and alluvium over granitic rocks (n = 16) (A. Mahizhnan unpubl. data)	
	Mean	Range	Mean	Range	Mean	Range
%						
SiO_2	88.9	87.7–90.3	57.2	47.5–64.4	59.4	50.8–67.4
Al_2O_3	5.3	3.2–6.4	15.4	12.0–18.9	14.0	9.5–17.4
Fe_2O_3	0.2	0.2–0.4	13.1	5.9–22.6	9.5	6.8–13.2
MgO	0.10	0.03–0.24	0.47	0.27–1.90	0.90	0.70–1.70
CaO	0.09	0.06–0.14	0.32	0.19–0.73	1.80	0.30–5.90
Na_2O	<0.01	<0.01–0.01	0.13	0.06–0.19	0.30	0.20–0.50
K_2O	0.04	0.03–0.08	0.49	0.26–0.64	0.60	0.40–0.70
TiO_2	1.26	0.22–4.26	0.67	0.38–1.00	0.50	0.40–0.50
LOI	NA	NA	11.2	9.5–13.6	NA	NA
ppm						
Mn	NA	NA	1013	239–3430	232	155–465
Ba	NA	NA	1294	219–7020	376	171–848
Zr	373	143–894	196	120–290	106	90–121

(1988) also described silicified transported material near Seven Mile Hill, southwest of Kalgoorlie. The silicified, slightly ferruginised and mottled transported gravels and sands pinch out against the underlying, truncated, 'pallid zone', which is only slightly silicified and consists of weathered, Archaean, fine sedimentary rock. The silcrete is approximately 2 m thick.

Over serpentinised ultramafics, the upper part of saprolite may be strongly overprinted by silica (Figure 91b) (Butt & Nickel 1981; Anand *et al.* 1991b; Lawrance 1996). This grades from the fine quartz veinlets and local friable networks of interconnecting siliceous veins in ferruginous saprolite to pervasive indurated silica flooding in which primary texture is preserved, such as blades of talc and magnetite grains. The massive form of silica resists further weathering and erosion, and in erosional landscapes may be exposed as topographic highs or subcrop under cover.

Mechanism of silcrete formation

The origin of silcretes has been discussed in numerous papers, mostly with respect to their development over sedimentary rocks and in association with basalts (see Langford-Smith 1978). Silcretes on granitic rocks have been described only rarely (Smale 1973; Watts 1975, 1977; Wopfner 1978; Butt 1985). The detailed mechanisms for the dissolution and precipitation of siliceous cements in silcrete remain poorly understood.

Butt (1985) and Singh *et al.* (1992) suggested that at Barr-Smith Range the pedogenic silcrete developed on granite represents a once-unconsolidated, near-surface horizon originally composed of quartz sand and, presumably, organic matter that has since decomposed. At the top of the profile kaolinite appears to have been dissolved leaving a residual sand that essentially consists of quartz. The absence of hydrous Al oxides in any horizon indicates that kaolinite dissolved congruently under conditions in which these oxides are unstable. Congruent dissolution of kaolinite occurs below pH 5.0 (Norton 1973). Such low pH values are consistent with weathering of poorly buffered kaolinitic saprolite under the humid conditions in the past. The close association of quartz and anatase in quartz–anatase–zircon cement implies that solution, migration and precipitation of Si and Ti took place together (Butt 1985). Titanium mobilisation occurs below pH 4.0 (Baes & Mesmer 1976). Similar conditions could also release silica by dissolution of quartz, kaolinite and zircon, as evident from the presence of skeleton relicts in the cement. Introduction and precipitation of aluminosilicates occurred during a late stage in the evolution of the profile, associated with reduced leaching due to aridity. Aluminosilicate cement consists of very small kaolinite crystals uniformly distributed in opaline silica (Singh *et al.* 1992).

The relationship between silcrete formation and the kaolinitic profile is frequently debated. Many authors (Wopfner 1978) consider that, like lateritisation, silcrete formation is associated with deep kaolinisation. Stephens (1971) considered that lateritisation and silcrete formation were contemporaneous, occurring under different conditions, but both causing deep kaolinisation. Butt (1985) showed that the silcretes post-date the main period of kaolinisation, a conclusion in agreement with that of Senior (1978), Watts (1975; 1977) and Mabbutt (1980). In the northeast Yilgarn Craton, kaolinisation was probably contemporaneous with and equivalent to lateritisation, but while basic rocks and, near the coast, Fe-poor acid rocks developed ferruginous upper horizons, such acid rocks in the interior merely gave rise to unconsolidated sand, which is now cemented as silcrete and sandstone (Butt 1981). Jessup (1960) considered the absence of ferruginous horizons to be due to erosion; however, in view of their preservation on more basic lithologies it is probable that they never formed. Van de Graaff 1983) suggested a relationship between landscape position, silcrete and 'laterite' in the Carnarvon and Officer Basins.

The timing of the silcrete formation is unclear. Dating suggests that the main period of silicification was Eocene–Miocene, generally post-dating deep kaolinisation (Idnurm & Senior 1978; Wopfner 1978). As silcrete pre-dates ferruginous duricrust in places it is not possible to invoke Late Tertiary aridity to account for silcrete formation. As silicification requires the contemporary release of silica by chemical weathering an adequate rainfall is indicated. Thus, a humid tropical or subtropical environment of low relief was suggested by Summerfield (1983). However, precipitation, whether at the surface or at depth, requires concentration presumably by excess evaporation. Accordingly, it seems that silicification is possibly a feature of transitional periods between humid and arid phases (Mabbutt 1980; Butt 1985), with Si accumulating in groundwater as drainage becomes less competent, and precipitating at seepages, water tables and porosity barriers (Taylor & Butt 1998). Silicification is either absolute or, less commonly, relative enrichment. The source of Si may be kaolinised profile and local toposequence within which it is found.

Red-brown hardpan

INTRODUCTION

Silicification is also a feature of younger sediments (Taylor 1978) and regolith units. The red-brown hardpan is a regional feature (Northcote *et al.* 1975) and comprises alluvial and/or colluvial sediments (Bettenay & Churchward 1974) and, in places, saprolite weakly cemented by opaline Si. The first published description of red-brown hardpan was by Teakle (1936) who recognised it over many thousands of square kilometres in semiarid and arid Western Australia. Brewer *et al.* (1972) were the first to study the micromorphology of red-brown hardpan from Bulloo Downs, central Western Australia. Bettenay and Churchward (1974) described hardpan from the Wiluna region and referred to it as Wiluna Hardpan.

FIELD RELATIONSHIP AND MORPHOLOGY

Red-brown hardpan occurs near the surface and may vary from less than 1 m thick to over 10 m. It may affect both sedimentary and residual units (Figures 91c; 92c, d on Plate 15) and occurs on subdued landscapes (gently inclined

slopes and plains), but not on hills and steeper, active pediments. Red-brown hardpans are typically red to red-brown indurated material and are very hard when both wet or dry. The degree of cementation decreases with depth. Structure is generally platy or may be blocky. Subhorizontal to horizontal laminations are developed within the upper few metres of the profile, commonly marked by thin coatings of precipitated MnO_2 (Figure 92c–e on Plate 15). Fracture and cleavage faces generally have a dull, porous appearance.

In the XRD patterns, a broad diffraction band in a region centred around 3.9 Å and 4.10 Å indicates amorphous Si (Ward 1993). Micromorphological observations show that isotropic and anisotropic coatings occur in both voids and within the matrix itself. The matrix consists of kaolinite and amorphous silica, with varying amounts of goethite, hematite, barite, calcite and smectite. It displays typical soil structures related to infiltration and downward percolation of water (clay illuviation). The photomicrograph in Figure 92f on Plate 15 shows several alternating clay coatings on a quartz grain and amorphous Si filling the voids. Most of the clay is well-oriented (Figure 93a) and ferruginous. The coarse fraction varies considerably in size, amount, shape and composition. More commonly the coarser fraction in silicified sediments consists of detrital ferruginous nodules and pisoliths (Figure 92e on Plate 15), lithic fragments and quartz. The surfaces of quartz and feldspar fragments show some pitting and etching. Manganese oxides have a distinctive botryoidal morphology and in a few places they occur as disseminated lenses. Where the silicification has affected the saprolite, clays and amorphous Si penetrate the cracks, veins and solution channels of saprolite and separate the component lithic fragments of saprolite (Figure 92g, h on Plate 15). Lithic

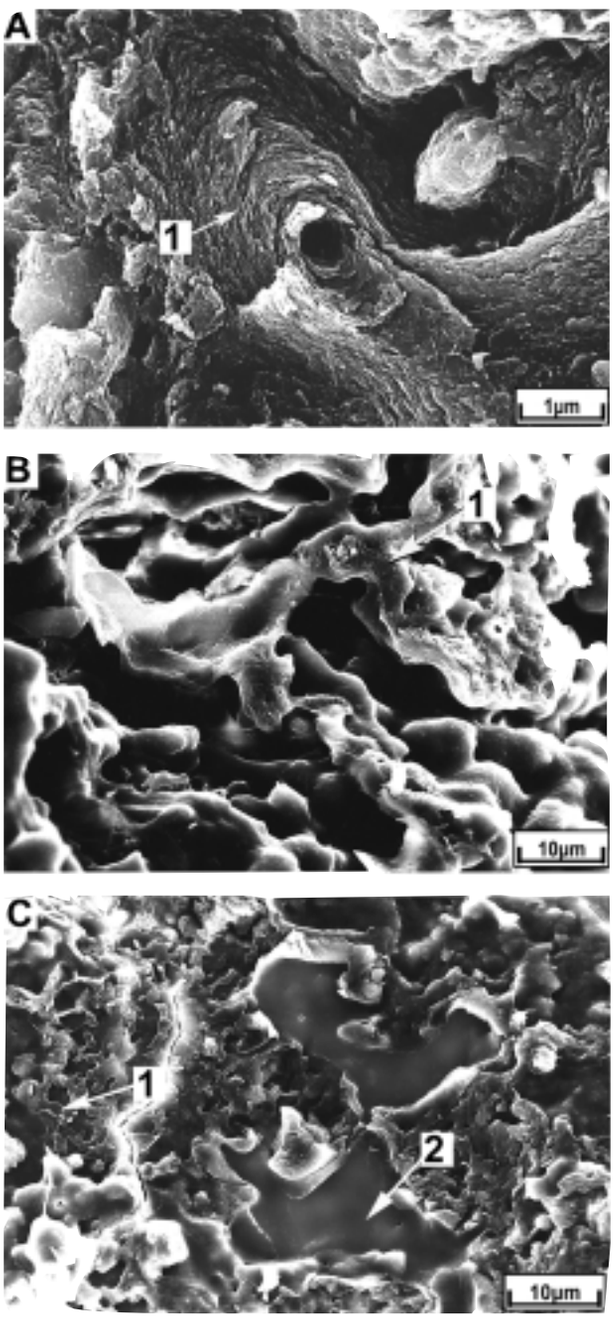

Figure 93 Scanning electron micrographs of broken surfaces of silicified colluvium (red-brown hardpan) from Lawlers showing illuviation features and morphologies of amorphous material. (a) Clay cutans (1) are characteristic of hardpanised colluvium. (b) Grain surfaces apparently coated with smooth, massive Si-rich amorphous material (1). (c) Finger-shaped (1) and cradle-shaped hollow (2) of Si-rich amorphous material. (R. R. Anand unpubl. data).

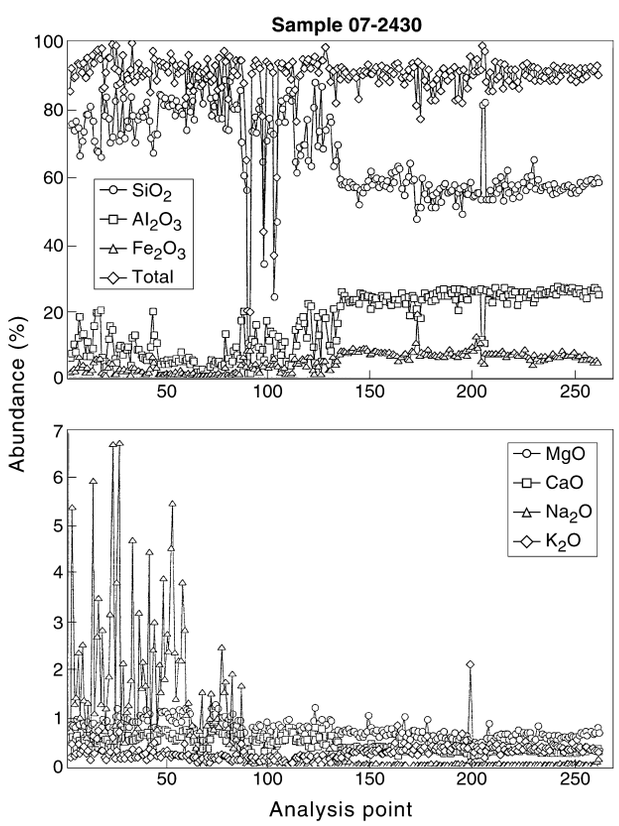

Figure 94 Electron microprobe analysis of a polished section of hardpanised colluvium from Lawlers showing the variation in the abundance of major elements. On the left hand side of the traverse, Si largely occurs as amorphous Si with small amounts in kaolinite, whereas on the right hand side of the traverse Si occurs as amorphous Si and kaolinite. Some Si and Al also occur as poorly crystalline aluminosilicates (R. R. Anand unpubl. data).

fragments may lose their original orientation and this may ultimately lead to their collapse. In many places (e.g. Mt Gibson, Bottle Creek), some carbonate has precipitated subsequent to hardpanisation. Duripans of the arid areas of the United States are similar (Flach *et al.* 1974; Chadwick *et al.* 1987).

Scanning electron microscope images from fracture surfaces of the hardpans show considerable variation in micromorphology of the matrix and cementing materials (Figure 93). In all cases, an amorphous material, rich in silica, coats both the larger quartz grains and the finer grains of the matrix, giving a visual impression of melted candle wax. The silica coatings are very smooth, vitreous and massive with only a few voids (Figure 93b, c). These voids may contain spheroids of silica up to 3 μm in size. Cradle-shaped hollows of amorphous materials occur between the quartz grains. Silica also forms finger-shaped protuberances, up to 5 μm long and 2 μm wide (Figure 93c), and silicified root remnants (Figure 35d). The latter are similar to the vegetative hyphae of actinomycetes, which are known to colonise root cells extensively subsequent to cell lysis (Mayfield *et al.* 1972).

CHEMICAL COMPOSITION

The chemical composition of hardpans developed in colluvium and alluvium over greenstone and granitic sequences is shown in Table 13. With the exception of Fe and K, there are no significant differences in the composition between the hardpans in granitic and greenstone-derived sediments. Silica occurs as amorphous Si and kaolinite, Al as kaolinite and Fe as largely detrital ferruginous clasts. The Mg, Ca, Na and K contents are very low. Calcium and Mg occur as calcite and dolomite and K as mica. Due to the low abundance of Mn oxides, their disordered structures and extremely small crystal size, XRD analysis is insensitive to them, making their positive identification difficult. A diagnostic peak at 3.14 Å on the XRD traces for Mn oxide-rich fragments from Genesis pit (Lawlers) indicated several Mn oxides (Ward 1993). However, of these, only birnsite is stable and capable of forming easily in the soil environments (McKenzie 1980). Barium occurs as barite.

Electron microprobe analyses of silica accumulations show large variable concentrations of silica, with small amounts of alumina (Figure 94). These data are consistent with the bulk analyses. Pure silica coatings are rare, but silica concentrations were always much greater than those of aluminium. The silica to aluminium ratio varies from 8:1 to 3:1, which suggests that silica and aluminium are largely present as amorphous silica, with small amounts as clay. However, recent investigations have revealed that Si and Al occur as poorly crystalline aluminosilicates (A. Mahizhnan pers. comm. 2000). Areas rich in Si also have high concentrations of Na, which is consistent with the observations of Charters and Norton (1994) who found a strong relationship between high Si concentrations and exchangeable sodium concentrations. They ascribed this to leaching of Si, Al and Na from A horizons or other overlying materials. Calcium and Mg occur in very small amounts, although there are some local concentrations of calcite. The Fe occurs as coatings of goethite. It is concluded that the red-brown hardpans are formed by partial replacement and cementation of the matrix and clasts by secondary silica, and possibly by poorly crystalline or amorphous aluminosilicates with lesser goethite and hematite, accompanied by clay illuviation.

SOURCES OF SILICA IN RED-BROWN HARDPAN

Litchfield and Mabbutt (1962) observed that episodic flooding and saturation of the soil on smooth slopes and plains caused leaching and acidification of the upper soil horizons, the leached Si being deposited as a hardpan during subsequent drying. However, quartz and feldspar weathering also appear to be important sources of Si. Pitting of sand-sized, quartz and feldspar grains indicates dissolution of silica *in situ*. Another source of amorphous Si is likely to be biogenic opal, which is actually opal A produced as part of the plant structures known as phytoliths. In soils

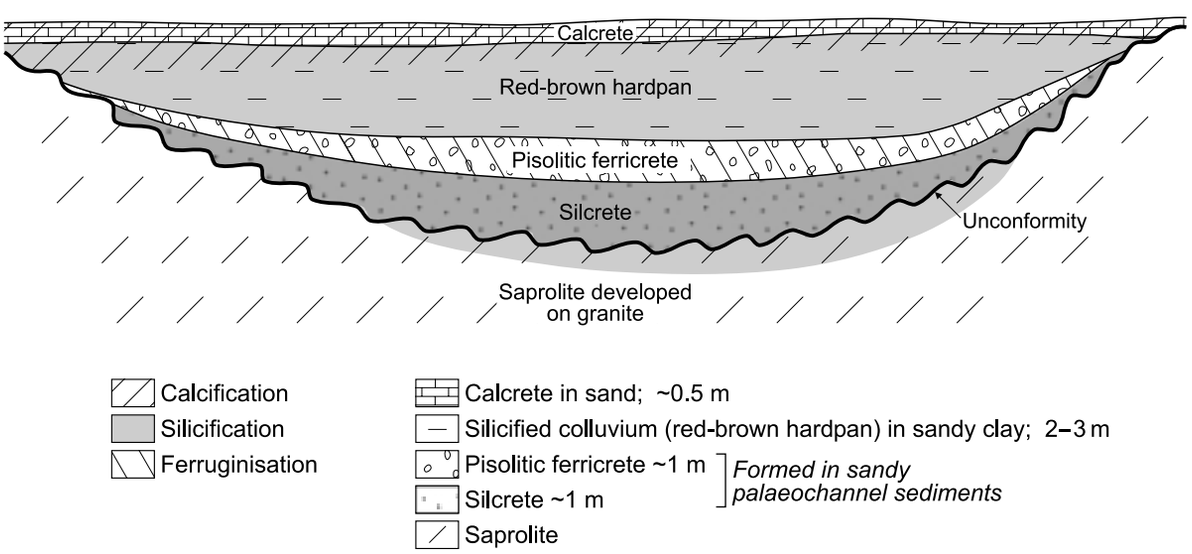

Figure 95 Example of calcification, silicification and ferruginisation in a single weathering sequence from Federal pit, Kalgoorlie region (A. Mahizhnan unpubl. data).

that are depleted of primary mineral silica, weathering of phytoliths provides a significant portion of the $Si(OH)_4$ in solution (Alexander *et al.* 1997).

Many landsurfaces on which hardpan occurs are subject to flooding. However, there is no clear relationship between the catchment size and incidence of hardpan. Absence of hardpan from steeper slopes, more active pediments and its occurrence on more gently inclined slopes, indicate that landsurface stability is necessary for hardpan development. Furthermore, hardpan may form in transported and residual ferruginous duricrust, in colluvium, alluvium and in saprolite, and must be regarded as a modification of a pre-existing regolith rather than as a specific horizon. The formation of hardpan appears to be still active.

MULTIPLE DURICRUSTS

Duricrusts have been reported in many different associations. Stephens (1971) suggested that 'laterite' and silcrete have antithetic distributions. Van de Graaff (1983) described silcrete in Western Australia as having a very complex relationship to 'laterite' and topography. Laterite occurs topographically lower, whereas silcrete is best developed on topographic highs. Ollier and Pain (1996) observed that Tertiary deposits generally have scattered nodules of both laterite and silcrete in the New England area of Australia. They suggested that their original relationship is difficult to determine, but they apparently formed in the same material at about the same time.

An example of multiple duricrust is provided by the Federal pit near Broad Arrow in the Kalgoorlie region. Here, duricrust of Fe, Si and Ca occurs in a single profile (Figure 95). Pisolitic ferricrete overlies silcrete which, in turn, overlies silicified saprolite developed on granite. The pisolitic ferricrete is characterised by a silicified matrix. Above the ferricrete is silicified colluvium and alluvium (red-brown hardpan), which is overlain by calcrete. Ferricrete and silcrete appear to have developed in older, sandy palaeochannel sediments, whereas the overlying red-brown hardpan and calcrete are formed in younger massive, sandy clays. Thus, at this site, there seem to be two phases of silicification and phases of ferruginisation and calcification. The timing of events is difficult to determine. However, field relationships suggest that one phase of silicification (silcrete) preceded ferricrete formation, whereas the other phase of silicification (red-brown hardpan) post-dated ferruginisation. Calcification is the youngest event and post-dates silicification.

The relationship between red-brown hardpan and silcrete is not understood. None of the red-brown hardpans could be regarded as classical silcrete ('grey billy') because of their greater porosity, lower hardness and very different fracture. The main difference between the red-brown hardpan and silcrete is perhaps the degree of silicification, i.e. infilling of pores. Ollier *et al.* (1988) suggested that there is a relationship between silcrete and red-brown hardpan, but the reasons were not given. Most silcretes contain >95% SiO_2, much too high to be considered red-brown hardpan, although similar silica-cementation processes could form silcretes and red-brown hardpans.

Carbonates have precipitated subsequent to red-brown hardpan formation and, in places, this has led to the destruction of red-brown hardpans.

REGIONAL DISTRIBUTION AND PATTERNS OF REGOLITH ON THE YILGARN CRATON

INTRODUCTION

As an introduction to the regolith distribution in this region, Churchward (1983) presented a somewhat conceptual map at a scale of 1:12 000 000 developed mainly from data provided by CSIRO soil and land system surveys and by the Atlas of Australian Soils (Northcote *et al.* 1967). This earlier study focused on the distribution of sandplains, saprolites, calcrete and the Wiluna Hardpan. Chan *et al.* (1992), as a part of an overview regolith terrain map of Australia, mapped the Kalgoorlie region at 1:500 000 scale. Recently, regolith mapping at regional and district scales by AGSO, CSIRO, GSWA and CRC LEME enabled Churchward and Anand (2000) to compile a regional map at 1:500 000 scale of an area of 290 000 km^2, covering approximately 75% of the Yilgarn. The scales of the maps that provided the basic information generally ranged from 1:100 000 to 1:250 000 and were developed by interpretation of aerial photographs and stereoscopic photographs and Landsat imagery, accompanied by field checks. A simplified version of the map is shown in Figure 96 on Plate 16 and salient features of regolith for the four regions (southwest, south, northeast and northwest) are given in Table 14.

THREE BROAD GROUPS OF MAPPING UNITS

Seven regolith–landform mapping units were identified that relate, directly or indirectly, to the preservation or partial or total erosion of the deeply weathered mantle (Figure 96 on Plate 16). The regolith materials that make up these units were either horizons of a deep profile developed by *in situ* weathering of bedrock or consist of unconsolidated, transported debris, parts of which are secondarily cemented. Regolith–landform mapping units can be placed in three major groups (Figure 97).

The first group is dominated, in the upper parts of the regolith, by deep (up to 10 m) sand, ferruginous gravel and ferruginous duricrust (GS in Figure 97); these commonly overlie mottled zones and saprolites. The ferruginous gravels and duricrust may be developed in weathered Archaean bedrock, or younger sediments that have themselves been weathered and/or indurated by Fe oxides.

The regolith of the second group is mainly saprolite (SP in Figure 97) with, in some areas, extensive fresh rock. These may have been exposed by erosion of a pre-existing weathered material, or may represent the most weathered form of the parent rock, which had never been capped with a ferruginous duricrust.

The third group represents sediment-dominated areas (SD in Figure 97) whose upper regolith units comprise fluvial, lacustrine or aeolian deposits, commonly several metres thick and may be underlain by ferruginous gravels, ferruginous duricrust, saprolite or bedrock. They may be highly variable in genesis, provenance, composition and thickness. The sediments were either derived from erosion of fresh and weathered Archaean bedrocks or the reworking of younger sediments, either locally or from many kilometres away. The sediments themselves may have been subjected to extreme post-depositional weathering.

These three groups are associated with all lithologies. However, in some areas, the sediments of the third group, particularly those in major drainage axes, cannot be ascribed to any specific lithology or geological province.

NATURE AND ORIGIN OF THE THREE BROAD GROUPS

Sand, ferruginous gravel and ferruginous duricrust-dominated terrain

The sand, ferruginous gravel and ferruginous duricrust-dominated terrain is characterised by thick, deeply weathered regolith that commonly occupies broad hill crests, gently inclined surfaces forming backslopes to breakaways and elevated undulating tracts (Figure 97a–d). The topography of these uplands on granitic rocks appears to be more broadly undulating and less complex than that of greenstones. The terrain comprises deep-weathering profiles comparable to those described by earlier workers (Walther 1915; Stephens 1946; Prescott & Pendleton 1952) in having an upper ferruginous zone that gives way, at depth, to mottled and saprolitic horizons and then to fresh rock. The ferruginous zone may be indurated (as ferruginous duricrust) or consist of loose, nodular and pisolitic gravels, a zone having uniform ferruginisation or one with significant mottling. As discussed earlier, ferruginous duricrusts are developed in a variety of residual and transported materials.

In granitic terrain, outcrop and subcrop of ferruginous duricrust and gravel is common on hill crests with deep sands and loose ferruginous gravels, commonly extending down adjacent smooth, gentle slopes. These undulating, sandy tracts are extensive in granitic areas and have been referred to as sandplains or lateritic sandplains (Figure 98a on Plate 17). There has been considerable debate on the origin of sandplains. In several early studies, the sands were considered to be remnants of ancient soils developed on deep lateritic profiles (Prescott 1931, 1954; Prider 1966). However, this cannot account for the great extent of deep sand over a variety of substrates. Carroll (1939) concluded that there were essentially two different sandplains in the Yilgarn, both essentially *in situ*: one related to metamorphic bedrock and the other to granitic bedrock. This interpreted difference was based on the analysis of heavy mineral suites. Mulcahy (1960) and Mulcahy and Hingston (1961) presented evidence, largely of a sedimentological nature, in support of colluviation of thick sands, while Brewer and Bettenay (1973), observing sand-sized spherites in both nodular duricrust and adjacent sand sheets, concluded that the sand had been derived from the nodular

Table 14 Salient environmental, regolith and landform patterns on the Yilgarn Craton (after Butt *et al.* 1977; Anand & Smith 1993).

	Southwestern region	Southern region (South of 'Menzies Line')	Transition zone[a]	Northeastern region (North of 'Menzies Line')	Northwestern region (North of 'Menzies Line')
Average rainfall	1000 mm	200–400 mm		200 mm	200 mm
Vegetation	Eucalyptus (Jarrah)	Eucalyptus (Salmon gum dominated)		Acacia (Mulga dominated)	Acacia (Mulga dominated)
Annual potential evaporation	1400–2000 mm	<3300 mm		>3300 mm	>3300 mm
Rainfall seasonality	Winter maximum	Winter maximum		Summer maximum	Summer maximum
Groundwater	Moderate to low salinity	Saline hypersaline		Moderate to low salinity	Moderate to low salinity
Soils	Acid to neutral	Neutral to alkaline		Neutral to acid	Neutral to acid
Landform	Undulating plateau, high relief	Gently undulating terrain, low relief		Gently undulating terrain, low relief	Gently undulating terrain, low relief
Pedogenic calcrete	Minor to absent	Abundant		Minor	Minor
Groundwater calcrete	Absent	Minor		Common	Common
Red-brown hardpan	Absent	Minor		Common	Common
Sand and ferruginous gravel plains	Common	Common		Moderate	Minor
Ferruginous duricrust	Extensive on hills and slopes, bauxitic	Patchy as mesas, kaolinitic		Common, discontinuous as mesas, kaolinitic[b]	Patchy as mesas, kaolinitic
Iron segregations after sulfide-rich rocks	Absent	Minor		Abundant	Common
Modification of ferruginous duricrusts	Bauxitic, degradation by dissolution	Calcified in places to form calcrete		Commonly hardpanised (silicified)	Commonly hardpanised (silicified)
Massive, structureless, red clays	Absent	Abundant		Common	Common

[a]Transition zone of 70 km; [b]buried ferruginous duricrusts are common

duricrust by colluviation. However, Killigrew and Glassford (1976) and Glassford and Semeniuk (1995) presented an alternative view on the origin of spherites. They invoked aeolian processes to account for the widespread occurrence of the clay spherites in the region and appear to favour this process to account for the sandy materials. Other workers (Butt 1985; Ollier *et al.* 1988; Anand *et al.* 1989b; Newsome & Ladd 1999) suggested that despite some possible reworking of the upper parts of the sandplains, an *in situ* origin is probable for the bulk of the regolith including the sands. From field evidence in the more arid parts of the region Mabbutt (1961, 1963) and Churchward (1977) suggested a balance between these processes to explain some of the regolith patterns. While it cannot be denied that aeolian activity could have played some part in moulding these areas, the dominant pattern of a complex of gravelly convex hills in juxtaposition with valley forms with deep sand strongly suggests that mild localised stripping followed by colluviation is a suitable working hypothesis to explain broad trends.

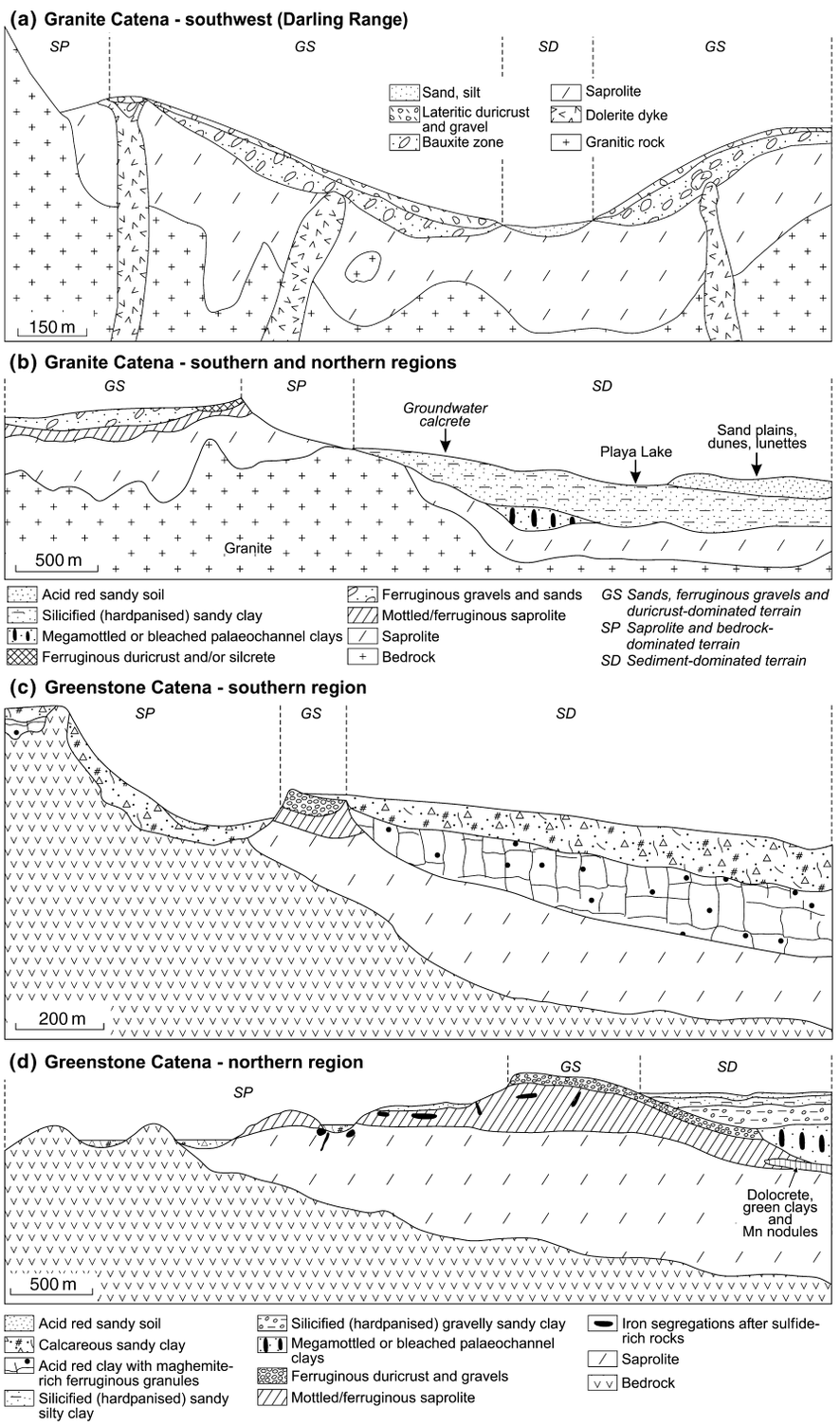

Figure 97 Schematic cross-sections showing the general relationships between landforms and regolith developed on granitic (a, b) and greenstone sequences (c, d). Ferruginous gravels and duricrust-capped areas are exposed, eroded or buried.

Mulcahy (1960) observed that ferruginous duricrusts and gravel horizons were not a continuous feature in the deep sands of the sandplains and commonly the best expression of ferruginous duricrust was in the face of breakaways. This is consistent with the observations of later workers (Bettenay 1984; Anand *et al.* 1989b; Von Perger 1992) who found that ferruginous duricrust and gravels may occur as extensive sheets beneath sand on a local scale [e.g. the Darling Range (Figure 98b on Plate 17); Mt Gibson; Madoonga], but in a regional sense, the duricrust is a discontinuous feature of many areas and does not always represent the upper part of an *in situ* weathering profile.

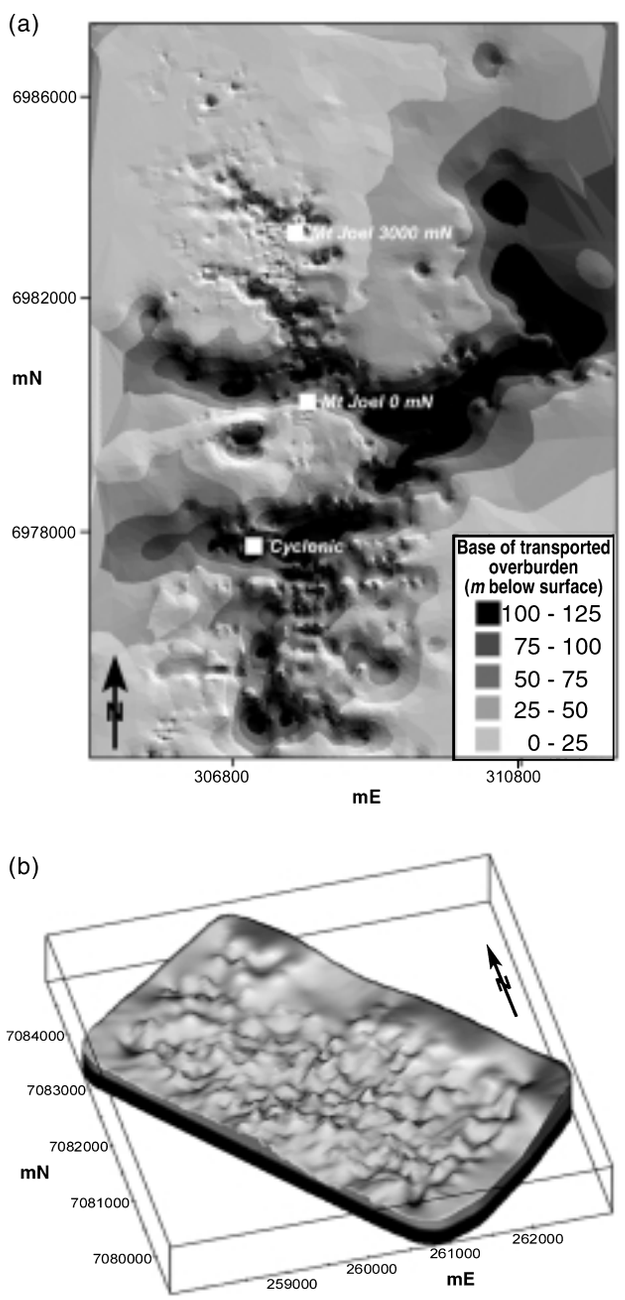

Figure 99 (a) Contoured 3-D surface representing the base of transported overburden about the Mt Joel area (modified after Anand *et al.* 1999a). (b) Contoured 3-D surface representing the top of fresh rock about the Jundee gold deposits (modified after Anand *et al.* 1999a).

This conclusion presents a complex picture, one which contrasts with the earlier model put forward by Woolnough (1927), which proposed that the ferruginous duricrust is continuous on these deeply weathered landsurfaces and is a diagnostic feature of them.

On greenstone terrain, brown to red soils, with a fine sand fraction and a high proportion of hard, Fe-rich brown to black ferruginous duricrust (Figure 98c on Plate 17) and ferruginous gravels occur on broad hill crests and backslopes (Figure 97c, d). Reworked aeolian sands occur particularly in the upper metre (Anand *et al.* 1993a; Robertson 1999). Iron-rich duricrusts are important features in the southern and northern parts of the Yilgarn. However, in detail, there are differences in their abundance, particularly on backslopes and plains between the southern and northern regions. Black ferruginous duricrusts on mafic and ultramafic bedrocks are common on hill crests in the Kalgoorlie region but, despite an abundant lag of black, Fe-rich pisoliths on backslopes (e.g. Ora Banda, Kanowna Belle and Matt Dam), there is little ferruginous duricrust on backslopes and plains. Instead, these are characterised by transported red clays (Figure 97c) that may contain lenses of abundant ferruginous debris (Anand *et al.* 1993a). The same is not true for the north (e.g. Lawlers, Mt McClure, Bronzewing, Madoonga and Bottle Creek districts), where ferruginous gravels and duricrust are especially common on valley margins beneath variable thicknesses of transported overburden (Figure 97d) (Anand *et al.* 1991b; Churchward *et al.* 1992; Von Perger 1992; Williamson 1992; Varga *et al.* 1997). It is suggested, therefore, that extensive duricrust may not have developed in the Kalgoorlie region. Alternatively, ferruginous duricrust and red soils may have developed at specific sites, reflecting bedrock geology and local drainage environments (Anand *et al.* 1993a).

Saprolite and bedrock-dominated terrain

The regolith comprising most of the saprolite and bedrock-dominated terrain is dominated by saprolite and saprock, usually as subcrop, locally with fresh rock outcrop. Thick sheets of ferruginous duricrust, gravel and sand are not a feature of this terrain. Inland, low erosional scarps (breakaways) flank the sand, ferruginous gravel and duricrust and silcrete terrain giving way to gently inclined, slightly undulating tracts (Figures 97; 98c, d on Plate 17). These extend away from the breakaways and are commonly traversed by shallow, connected drainages. Thus, they are considered to be an erosional environment, in contrast to the relatively smooth aspect of the sand, gravel and duricrust terrain (Stephens 1946; Mulcahy 1960; Mabbutt *et al.* 1963). In places, undulating erosional tracts occur in isolation, without adjacent gravel units.

Breakaways are most extensive and best-developed on granitic (Figure 98d on Plate 17) rather than on greenstone terrain (Figure 98c on Plate 17). Ideally, breakaways comprise two principal slope facets. An upper, generally vertical, free face, is protected by the hard capping of the breakaway. Below this is a linear, steep, debris slope maintained by the overlying hard-cap. The capping on granitic rocks is generally case-hardened, greyish white, kaolinitic clay. The case-hardening is by mild ferruginisation (Figure 98d on Plate 17), silicification and/or

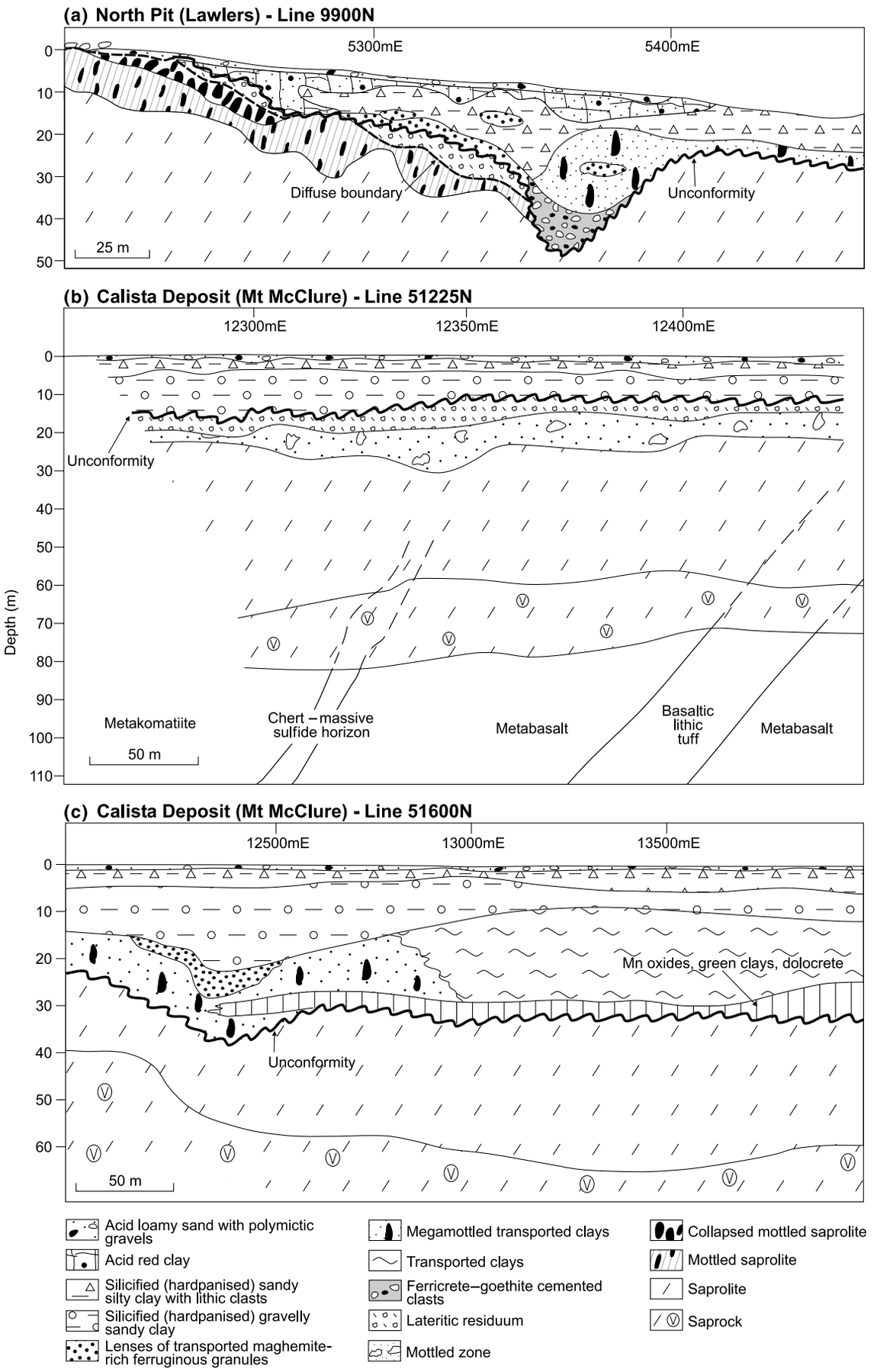
(a) North Pit (Lawlers) - Line 9900N
5300mE
5400mE
Diffuse boundary
Unconformity
25 m
(b) Calista Deposit (Mt McClure) - Line 51225N
12300mE
12350mE
12400mE
Depth (m)
Unconformity
Metakomatiite
Chert – massive sulfide horizon
Metabasalt
Basaltic lithic tuff
Metabasalt
50 m
(c) Calista Deposit (Mt McClure) - Line 51600N
12500mE
13000mE
13500mE
Mn oxides, green clays, dolocrete
Unconformity
50 m
Acid loamy sand with polymictic gravels
Acid red clay
Silicified (hardpanised) sandy silty clay with lithic clasts
Silicified (hardpanised) gravelly sandy clay
Lenses of transported maghemite-rich ferruginous granules
Megamottled transported clays
Transported clays
Ferricrete–goethite cemented clasts
Lateritic residuum
Mottled zone
Collapsed mottled saprolite
Mottled saprolite
Saprolite
Saprock

aluminosilicates cementation provides much of the bold appearance of breakaway scarps on the granitic rocks. In contrast, many breakaway scarps on weathered greenstones are developed on more Fe-rich duricrust (Figure 98c on Plate 17) or uniformly ferruginous saprolite (Figure 98e on Plate 17).

Generally, the scarps and pediments are commonly mantled with a scree of gravels, silcrete cobbles and small boulders derived from the erosion of the ferruginous or siliceous duricrusts that cap the breakaway. The saprolite down slope may be buried by a metre or more of sediments. In many places, the scarps are still active and scored with gullies that extend on to the pediments (Figure 98d on Plate 17). Here, saprolite is exposed extensively on the upper parts of the breakaway. In erosional areas below the breakaways, a complex pattern of duplex soils and red and yellow earths occur, controlled largely by the nature of underlying colluvium and the exposed residuum.

Iron segregations related to Fe-rich and/or sulfide-rich rocks forming low hills and gently undulating tracts up to several kilometres in length are common in the northern portion of the Yilgarn Craton (Figure 98f on Plate 17) (e.g. Bronzewing, Mt McClure, Lawlers and Madoonga districts). As well as occurring in place along the strike of sulfide-rich rocks, they also occur as loose lag at the surface, having been detached from their original position by weathering and erosion.

Sediment-dominated terrain

Glaciofluvial, glacial, lacustrine, colluvial, alluvial, evaporative and aeolian sediments occur extensively on lower slopes, gently inclined to flat plains, drainage floors and salt lakes. Colluvial deposits are very extensive on very gently inclined plains, commonly as fan-shaped lobes that are many metres thick. Broad alluvial plains occur adjacent to salt lakes and are horizontal to gently inclined. Some fluvial deposits display well-defined sedimentary structures. Sets of Wanderrie banks (Mabbutt 1963) can occur on fluvial deposits. These are the result of differential deposition by unchanneled sheet floods that have moulded the coarse fractions into low, sandy rises roughly parallel to the contours. Included in this terrain are areas dominated by thick, valley calcrete deposits. Calcrete-cemented valley fills are common along drainages.

Salt lakes are extensive and indicate a palaeodrainage system with broad valleys. The major lakes are generally separated by areas of sand dunes, smaller lakes and fringing depositional flats. The regolith consists of evaporites and lacustrine sediments in lakes, aeolian sediments in dunes and lunettes, and alluvial sediments on fringing flats.

Although the surface distribution indicates a general relationship between the surface regolith types and landforms, evidence from drilling and mines in sediment-dominated areas, mainly on greenstone sequences, shows features not evident on the surface. The regolith at any particular location commonly comprises several horizontal zones. The 3-D distribution of regolith in depositional areas has indicated an undulating palaeotopography and highly variable substrate below the cover, more than the present surface would otherwise suggest. This was observed in a number of districts. For example, at Bronzewing the present surface is essentially flat, whereas the base of transported overburden (Figure 99a) indicates that the palaeolandscape had a relief of approximately 100 m compared to the present 15 m. Similarly, the topography of the weathering front is also much more irregular (Figure 99b). The present relief rarely reflects that of the palaeosurface(s). Saprolite and saprock are common, but there are places, particularly in the north, where extensive sheets of ferruginous duricrust and ferruginous gravels are preserved beneath sediments of various ages. In addition, palaeochannels and associated deposits can reach 100 m in thickness. For example, in the Lawlers district (900 km^2) outcrop, shallow subcrop of ferruginous duricrust comprises only approximately 10% of the landscape, yet it is the substrate to more than 60% of the colluvial–alluvial plains (Anand *et al.* 1991b). Here, lateritic residuum and ferricrete are overlain by varying depths of a variety of transported cover (Figure 100a). At Mt McClure, mapping over 200 km^2 has suggested that the ferruginous duricrust is present beneath 15–30 m of colluvial–alluvial sediments over approximately half of the study area (Figure 100b) (Williamson 1992; Anand & Williamson 2000), whereas the other half is underlain by saprolite or saprock (Figure 100c). Similarly, thick sheets of lateritic residuum and ferricrete beneath variable thicknesses of sediments occur at Mt Magnet, Bronzewing (Figure 101a, b), Madoonga (Von Perger 1992) and Bottle Creek (Churchward *et al.* 1992). However, in the Kalgoorlie region [Gindalbi (King 1991); Kanowna Belle (Dell 1992); Matt Dam (Anand *et al.* 1993a)], colluvial–alluvial units more commonly overlie saprolite (Figure 102a).

It is common to have 10–20 m of upper fluvial and aeolian deposits over thick palaeochannel sediments with saprolitic materials or fresh bedrock appearing at a depth of 40–50 m (Figures 100–102). Palaeochannels have been partly filled with clay-rich sediments. Mostly these consist of grey or light-brown clay, which may be mottled and have a tendency to crack on drying. At Calista (Mt McClure), there is also prominent development of smectite-rich dolocrete at approximately 30 m depth that overprints both the transported and residual regolith (Figure 100c). This unit also contains high concentrations of Mn nodules (5–15 mm in diameter) that are dominated by pyrolusite and lithiophorite. The formation of Mn nodules is possibly related to the redox front associated with the water table. On the western side of Discovery pit at Bronzewing (Figure 101b), a layer of green smectite with siliceous nodules occurs above the residual–transported interface.

After deposition of the palaeochannel clays, there has been deposition of massive, red clays that may contain black, hematite–maghemite-rich detrital ferruginous granules (Figures 101b, 102a). These fine-grained red clays were presumably derived from erosion of an old soil profile. The red clayey unit may grade upwards into overlying extensive colluvial gravelly or sandy silty units. The colluvium is derived from the erosion of weathering profiles and the gravels consist predominantly of sub-

Figure 100 Regolith distribution in depositional regimes at (a) North pit, Lawlers (after Anand *et al.* 1991b) and (b, c) Calista deposit, Mt McClure (after Williamson 1992).

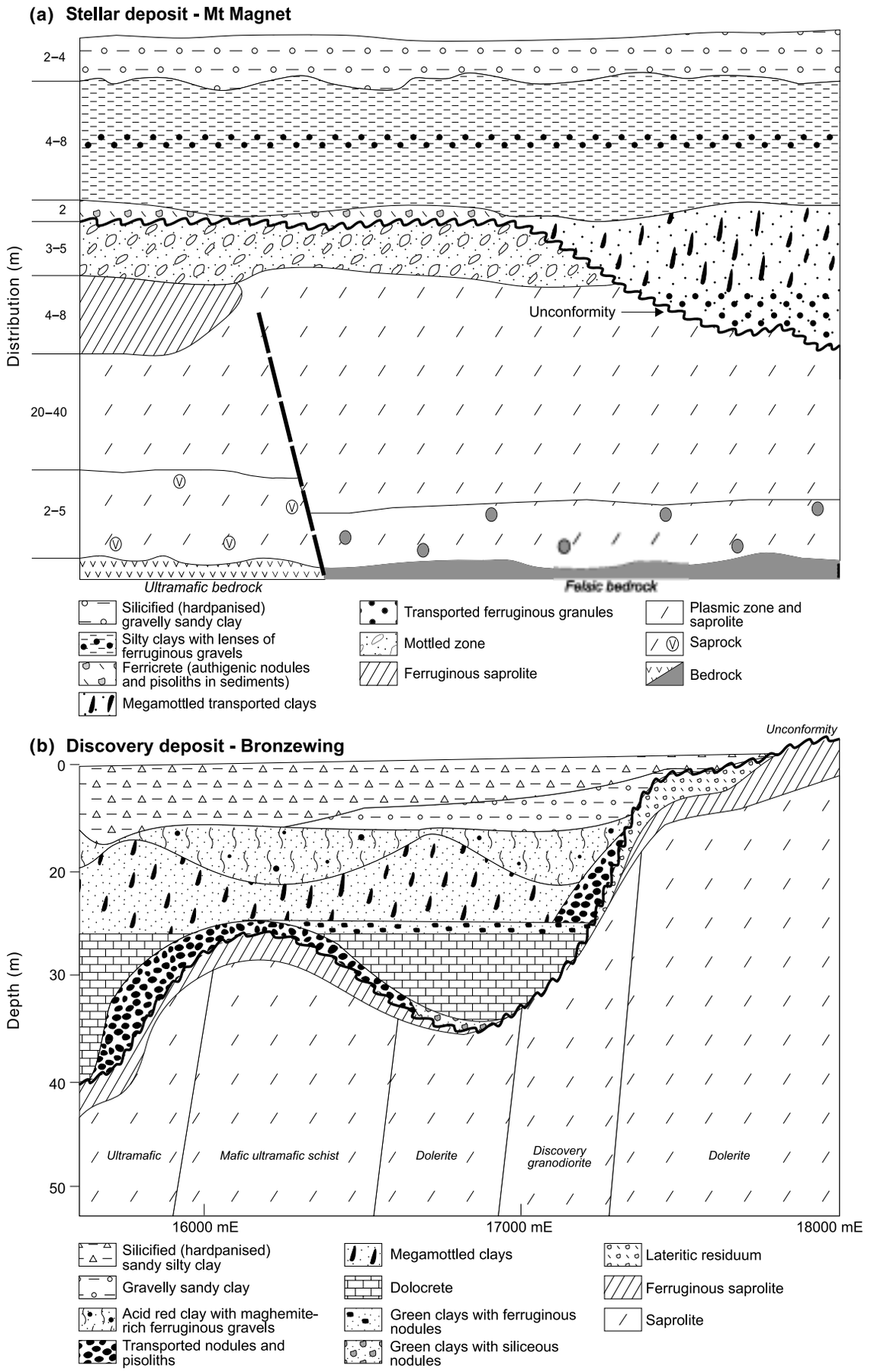
(a) Stellar deposit - Mt Magnet
Distribution (m)
2–4
4–8
2
3–5
4–8
20–40
2–5
Unconformity
Ultramafic bedrock
Felsic bedrock
Silicified (hardpanised) gravelly sandy clay
Silty clays with lenses of ferruginous gravels
Ferricrete (authigenic nodules and pisoliths in sediments)
Megamottled transported clays
Transported ferruginous granules
Mottled zone
Ferruginous saprolite
Plasmic zone and saprolite
Saprock
Bedrock
(b) Discovery deposit - Bronzewing
Unconformity
Depth (m)
0
20
30
40
50
Ultramafic
Mafic ultramafic schist
Dolerite
Discovery granodiorite
Dolerite
16000 mE
17000 mE
18000 mE
Silicified (hardpanised) sandy silty clay
Gravelly sandy clay
Acid red clay with maghemite-rich ferruginous gravels
Transported nodules and pisoliths
Megamottled clays
Dolocrete
Green clays with ferruginous nodules
Green clays with siliceous nodules
Lateritic residuum
Ferruginous saprolite
Saprolite

rounded to rounded ferruginous clasts, detrital quartz and ferruginous lithic fragments. The matrix generally comprises silty kaolinite, but where the source rocks are mainly granitic, it tends to be richer in sand. These upper fluvial and aeolian deposits are generally silicified (red-brown hardpan) or calcified (calcrete) near the surface. In places, sands derived from granitic profiles, up to 10 m thick, cover mafic-derived regolith. Such is the case at Mt Gibson (Figure 102b) and Forrestania (Figure 102c), where these sediments are ferruginised. The sediments themselves have been weathered to form megamottles and pisoliths.

REGOLITH PATTERNS

The principal regolith pattern is a patchwork of GS (sand, ferruginous duricrust and gravel-dominated terrain) set in a matrix of SP (saprolite and bedrock-dominated terrain) and SD (sediment-dominated terrain) (Figure 97). This pattern will be considered by focusing on trends in the regolith associated with granitic rocks, the dominant lithology of the region.

Regional changes in this pattern are, to a large degree, associated with changes in valley morphology down from drainage divides, in particular, the major divide between the west- and east-trending valley systems. On the regional divide between the western and eastern drainages, sandplains cover a great part of the landsurface. In moving down-drainage either to the east or to the west the extent of these sandplains decreases notably, with saprolite and sediment-dominated areas occupying an increasing proportion of the landscape. Thus, there is little sandplain by approximately 200 km west (Murchison and the Greenough catchments) of the major divide to the east of Sandstone. A trend such as this would suggest that there would be little or no GS terrain along the western limits of the Yilgarn. Thus, for the Swan–Avon drainage in the southwest, a gradual decrease in sandplain takes place, and the regolith is dominated by SP terrain, particularly those with extensive rock outcrop. This trend is expected to continue to the western edge of the Yilgarn given that this is the focus of the most active stream erosion. Thus, the relativel extensive terrain of GS at the western edge of the Darling Plateau could be seen as being anomalous. Here, the ferruginous duricrust occupies horizontal upland areas with an average elevation of approximately 280–320 m and high annual rainfall. The duricrusts are thicker (up to 3 m) and physically more competent than duricrusts on other granitoid terrains in the region and could restrict the effects of the erosional environment provided by the adjacent steep-sided, deep valleys. The great thickness of duricrust might be accounted for by a climatic gradient (past and present) and more effective stream incision close to the scarp. The swarms of dolerite dykes, a feature of this zone, would have contributed towards the genesis of a more physically competent ferruginous duricrust than is the case for the more characteristic granitoid terrains with sparse dolerite dykes.

Inland, the gravels and duricrust take the form of mesas or breakaways with Fe-oxide-cemented resistant horizontal upper surfaces, with the softer parts of the profile below comprising the steeper slopes of breakaways. The very gravelly unit gives way to more sandy types interspersed with less ferruginous gravels. The sand and gravel units appear to form a close association and can be seen as variations of the same theme, one merging into the other (i.e. gravelly to sandy sandplains). Mulcahy (1960) suggested a sharp decrease in sandplains downstream of the point at which the major valley floors of the Avon drainage are incised by channels. He proposed a point at which these changes took place, largely on the adjacent slopes and hill crests, which corresponded to the Meckering Line. This marked the position where the channelled drainage of the valley floors, downstream, gave way to salt lakes, upstream.

The change from playas to channelled valley floors reflected in the Meckering Line is sharp, but on adjacent slopes these are not clearly apparent. While not denying that there could be a multiphase drainage rejuvenation, the thalwegs presented by Mulcahy (1960) show increasing declivity downstream, although it has not been clearly established that the inflections are indicators of stages of drainage rejuvenation rather than being due to structural features. In contrast, it could be suggested that the change of drainage status from playa to channel could represent a response to increasing rainfall towards the west, possibly complemented by increasing catchment size and complexity. These factors, along with increasing valley depth (a feature that is very likely the consequence of uplift) and concomitant greater valley-side declivity downstream, could result in the increased stripping of the weathered mantle. Thus, the essential process in the development of this pattern is seen as the erosional modification leading to partial or complete removal of a deeply weathered mantle and there are a number of factors that might be controlling this process.

The sands are yellow in the south and southwest and change to red towards the north, perhaps as a consequence of climatic trends. The yellow mineral in the sand is goethite; redness implies hematite. High temperature and low moisture content favour formation of hematite in the northern half of the Yilgarn Craton. Aeolian modification of the surface sands is more apparent towards the northeast and northwest. This includes sporadic longitudinal dunes. The upper metre of the regolith can reflect aeolian winnowing of fines whether it is part of a gravel and sand unit or a sheetflow deposit. This process could contribute significantly to a sandy upper regolith and, thus, to the extent of the sandplains. Dunes are very rare on the yellow sandplains to the south, but are not uncommon, and are not extensive on the red sandplains to the northwest and northeast.

OTHER REGIONAL FEATURES

Pedogenic calcretes, groundwater calcretes, red-brown hardpans, red clays and bauxites have distinctive distributions (Table 14).

Figure 101 Regolith distribution in depositional regimes at (a) Stellar deposit, Mt Magnet (after Robertson *et al.* 1994) and (b) Discovery deposit, Bronzewing (after Varga *et al.* 1997).

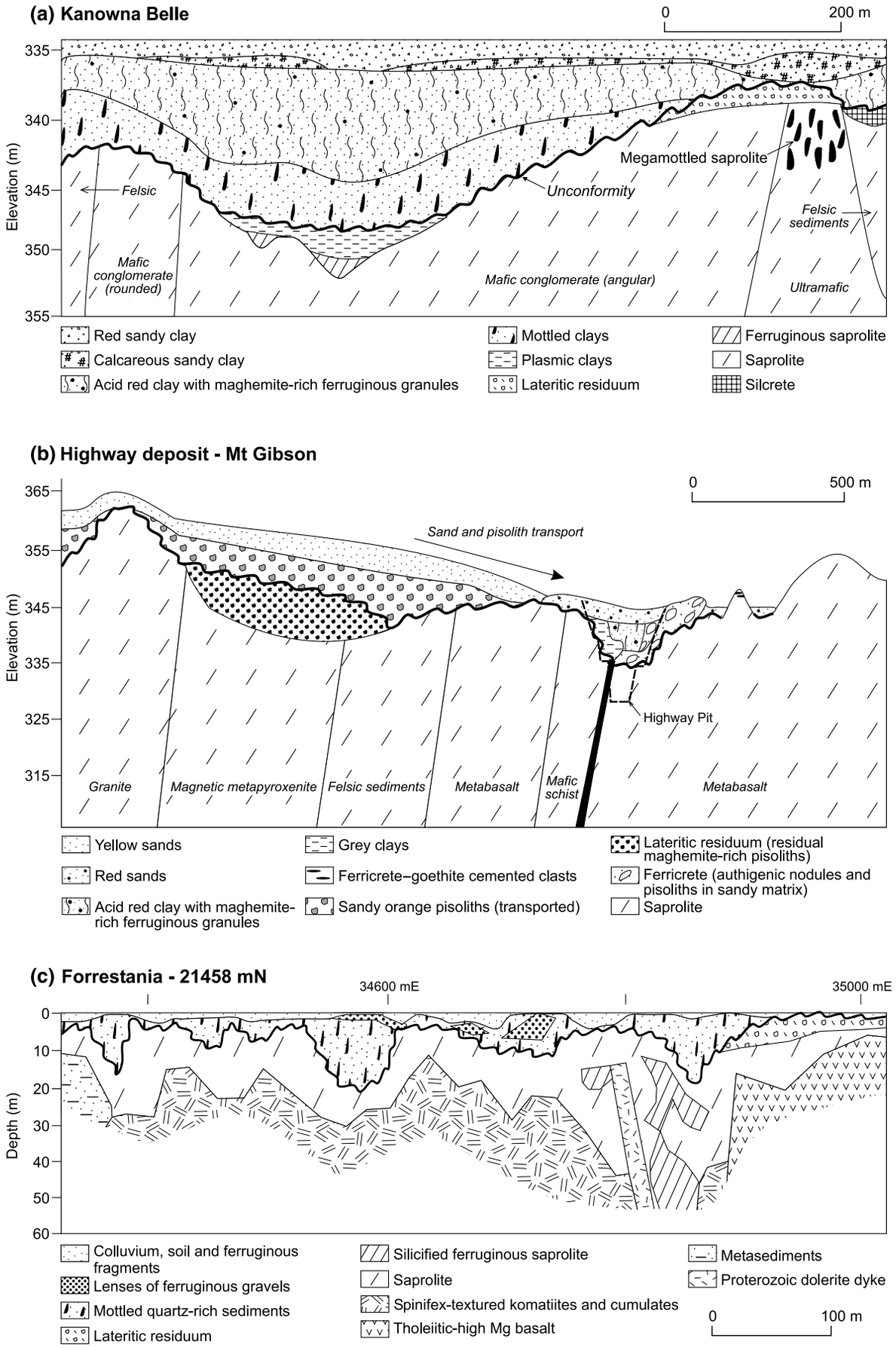
(a) Kanowna Belle
0
200 m
335
340
345
350
355
Elevation (m)
Megamottled saprolite
Unconformity
Felsic
Felsic sediments
Mafic conglomerate (rounded)
Mafic conglomerate (angular)
Ultramafic
Red sandy clay
Calcareous sandy clay
Acid red clay with maghemite-rich ferruginous granules
Mottled clays
Plasmic clays
Lateritic residuum
Ferruginous saprolite
Saprolite
Silcrete
(b) Highway deposit - Mt Gibson
0
500 m
365
355
345
335
325
315
Elevation (m)
Sand and pisolith transport
Highway Pit
Granite
Magnetic metapyroxenite
Felsic sediments
Metabasalt
Mafic schist
Metabasalt
Yellow sands
Red sands
Acid red clay with maghemite-rich ferruginous granules
Grey clays
Ferricrete–goethite cemented clasts
Sandy orange pisoliths (transported)
Lateritic residuum (residual maghemite-rich pisoliths)
Ferricrete (authigenic nodules and pisoliths in sandy matrix)
Saprolite
(c) Forrestania - 21458 mN
34600 mE
35000 mE
0
10
20
30
40
50
60
Depth (m)
Colluvium, soil and ferruginous fragments
Lenses of ferruginous gravels
Mottled quartz-rich sediments
Lateritic residuum
Silicified ferruginous saprolite
Saprolite
Spinifex-textured komatiites and cumulates
Tholeiitic-high Mg basalt
Metasediments
Proterozoic dolerite dyke
0
100 m

Pedogenic calcrete

Three general situations reflect trends in the distribution of pedogenic calcretes on the Yilgarn.

(1) In the northeast and northwest, pedogenic calcretes are limited to saprolitic terrain on greenstone with shallow soils and occasional rock outcrop. Very little pedogenic calcrete appears in the sandplain soils developed on granitic rocks.

(2) In the south, between Kalgoorlie and Southern Cross, pedogenic calcretes occur in deposits derived from greenstones. These deposits are typically separated from the underlying bedrock by 10–50 m of carbonate-free, predominantly kaolinitic regolith. They are also very extensive in shallow stony soils on the greenstones. Calcretes are less common in soils derived from granitic rocks. However, they occur on all lithologies in the wheatbelt and are widespread and thick in the far southeast.

(3) In the southwest, in the high rainfall areas of the Darling Range, pedogenic calcretes are insignificant.

Groundwater calcretes

Groundwater calcretes are found over much of the craton and adjacent sedimentary basins. However, their development ceases in the south where pedogenic calcretes are found instead.

Red-brown hardpan

Red-brown hardpan is an extensive feature in the northern Yilgarn, but it is very rare in the south and southwest (Bettenay & Churchward 1974) and this pattern of distribution of red-brown hardpan became the basis of the so called Menzies Line (Butt *et al.* 1977). However, red-brown hardpans and calcrete have been found 70 km south of Menzies (A. Mahazanin pers. comm. 2000). This distribution may suggest that red-brown hardpans were once more extensive and have been subsequently replaced and/or displaced by carbonates to form calcretes. This new understanding on the distribution of red-brown hardpans may lead to redefining the Menzies Line. In the south, some ferruginous duricrusts are replaced and/or displaced by carbonates (Anand *et al.* 1997). In the north, silicification (hardpanisation) of duricrusts is common.

Figure 102 Regolith distribution in depositional regimes at (a) Kanowna Bell, (b) Highway deposit, Mt Gibson (J. E. Wildman, C. Phang and R. R. Anand unpubl. data) and (c) Forrestania (after Kelly 1994).

Red clays

One of the characteristic features of the southern region is an extensive blanket of massive, structureless red clays that are generally overlain by calcareous red earths. They are less common in the north and are absent in the southwest of the Yilgarn Craton.

Bauxites

Bauxites are extensive in the southwest (Darling Range), but are absent inland. However, there is a clearly defined area in which economic bauxite mineralisation is concentrated in the Darling Range. The area extends approximately 30 km east from the Darling Scarp and 150 km south from Perth's eastern suburbs to the Harris River area north of Collie (Hickman *et al.* 1992). Field relationships reveal a northwest linearity to zones of bauxite concentration. This orientation corresponds to both the structural grain of the underlying bedrock and, commonly, to lithological boundaries. The latter have influenced topography so that ridges and valleys tend to be orientated in a northwest direction.

GEOMORPHIC HISTORY OF THE YILGARN CRATON

RATES OF EROSION AND LANDFORM DEVELOPMENT

Palaeogeographical reconstructions indicated that some of Western Australia has been exposed to subaerial conditions since the Neoproterozoic (Figure 103). It has been suggested that the present landsurface of the Yilgarn Craton is only a few metres below the essentially flat-lying, sub-Proterozoic unconformity, and the overall flatness of the landscape suggests that the plateau may represent a Proterozoic erosion surface (Daniels 1975; Fairbridge & Finkl 1979; Finkl & Fairbridge 1979). Similarly, earlier features, such as broad valleys and deeper channels, may have survived locally (Finkl & Fairbridge 1979).

Glaciation occurred during the Late Carboniferous and Early Permian (BMR Palaeogeographical Group 1990), as evidenced by the wide scatter of glaciogene sediments near Laverton, Lawlers and north and south of the Wiluna–Meekatharra area (Hobson & Miles 1950; Gower 1976; Van de Graaf *et al.* 1977; Mabbutt 1980) and in the Collie Basin. Recently, Eyles and de Broekert (2001) discovered Permian sediments in the Eastern Goldfields near Kalgoorlie (Sand King). There have been various estimates of the amount of material eroded from the Yilgarn Craton (Finkl & Fairbridge 1979; Van de Graaff 1981; Le Blanc Smith 1993; Clarke 1994a; Killick 1998; Kohn *et al.* 1998). Finkl and Fairbridge (1979) assumed that there has been little erosion of the Yilgarn Craton since the Proterozoic, whereas Van de Graaff (1981) and Clarke (1994a) estimated that up to 400 m of erosion has been necessary to generate sediments infilling the surrounding basins. Van de Graaff (1981) argued that the shield was peneplanated in the post-Permian as a result of substantial uplift resulting from rifting and continental breakup of India and Australia in the Early Triassic to Early Cretaceous. He calculated rates of denudation of 4.5–5 m/10^6 y. More recently, Killick (1998) suggested that approximately 4 km of material has been removed from the western margin of the craton over the past 490 million years, a rate of approximately 8 m/10^6 y. There is strong support for the Van de Graaff and Killick models along the western margin of the shield adjacent to the Perth Basin where the geomorphic or sedimentary record of Late Palaeozoic glaciation appears to have been completely removed with the exception of small outliers of Permian glacial strata and coals preserved in depositional rifts (Mishra 1996). It should be noted, however, that the extensive denudation model of Van de Graaff (1981) has been questioned by Sircombe and Freeman (1999) and Cawood and Nemchin (2000) who identified low numbers of shield-derived zircon grains in deposits of the Perth Basin. They suggested that this is evidence that the westernmost part of the shield was not a significant source of sediment during the Phanerozoic and, thus, unlikely to have experienced deep stripping.

Le Blanc Smith (1993) has suggested that up to 6.5 km of sediment may have been removed from an originally 8 km-thick deposit of Permian and younger rocks in the Collie Basin. Kohn *et al.* (1998) suggested that up to 2 km of these sediments were removal prior to the Mesozoic in conjunction with a significant period of uplift.

The recent discovery of Permian sediments in the Kalgoorlie region led Eyles and de Broekert (2001) to believe that any deep dissection and planation of the eastern craton occurred prior to Late Palaeozoic glaciation, not after as suggested by Van de Graaf. These authors suggested that the geographical contrast in the depth of post-Permian dissection from west to east is probably the result of differential uplift associated with Gondwana breakup commencing in the Early Cretaceous. Thus, minimal uplift to the east allowed preservation of a relict Permian landscape near Kalgoorlie along the margins of the Officer Basin (Eyles & de Broekert 2001).

CLIMATES AND GEOCHRONOLOGY OF DEEP WEATHERING

Long periods of tectonic stability since the Permian glaciation have provided the setting for a variety of climatic conditions (Table 15) and landscape settings to interact and develop the various types of regolith and landscape (Ollier 1978; Ollier *et al.* 1988). After the glacial episode, conditions suitable for abundant plant growth persisted until the Jurassic. Conditions during the Jurassic were moderately warm (17–24°C) in summer, but as low as –20°C in winter (Frakes & Barron 2001). The climate is thought to have began to dry at approximately 160 Ma, and at approximately 140 Ma it became humid again. The humidity persisted and with it the landscape became forested (Truswell & Harris 1982; Frakes *et al.* 1987). The temperatures may have ranged from cool temperate (Bird & Chivas 1989; Taylor *et al.* 1992) to mediterranean to subtropical, depending on the palaeolatitude of various regions before and during continental breakup. Landscapes were well-vegetated, predominantly with rainforest (Truswell & Harris 1982; Frakes *et al.* 1987).

Major changes in vegetation from widespread rainforest to more arid conditions began in the Late Miocene (Frakes & Barron 2001). During the Late Tertiary, aridity began to become a factor (Bowler 1976) and the nature and distribution of the vegetation became similar to that currently prevailing. The Quaternary is generally regarded as a period of alternating aridity and humidity, brought about largely by a series of glacial maxima and minima (Cockbain & Hocking 1990).

Many previous studies of deeply weathered Australian regolith have assumed that it formed under seasonally humid conditions. However, the origins of landforms and regolith in tropical climates is not universally accepted (Stephens 1971; Taylor *et al.* 1992; Bird & Chivas 1993; Clarke 1994a). Deep weathering may occur in cooler climates, but over longer periods. A rule of thumb of thermodynamics is that reaction rates double with every 10°C increase in temperature. More recently, Brady and Carrol (1994) have shown from experimental studies that weathering rates of silicates may increase by a factor of 2–5 for an increase in

temperature from 15°C to 25°C. Over million of years, these reaction rates would have significant implications on the relative masses of regolith generated under warm-humid versus cold-humid conditions.

The ages of the deeply weathered profiles are difficult to determine. Dating by radiocarbon, luminescence and U-series disequilibrium generally yield ages confined to the past few hundred thousand years (Pillans 1998). Techniques such as K/Ar and $^{40}Ar/^{39}Ar$ can be used from approximately 250 ka back to the age of the solar system (Vasconcelos 1995), but appropriate and datable mineral phases are uncommon in the regolith. The profiles are also open systems and it is difficult to relate the ages of particular materials (determined isotopically, palaeontologically or palaeomagnetically) to that of the profile as a whole. Several estimates of the timing of weathering for Western Australia regoliths have been put forward by several workers.

(1) Interpretation of palaeomagnetic results from sediments of the Perth Basin indicating a Late Oligocene to Early Miocene age for 'lateritisation' by comparison with the Australian apparent polar wander path (Schmidt & Embleton 1976). Palaeomagnetic age estimates in weathered regolith materials are based on the assumption that weathering processes have produced secondary iron oxides, which preserve a record of the magnetic field at the time they formed. However, more recent revisions of the Australian apparent polar wander path (Idnurm 1985, 1994) indicate that the Schmidt and Embleton (1976) data correspond to Late Miocene or Pliocene age (10 ± 5 Ma).

(2) A summary of palaeomagnetic results including new data provided by B. Pillans (pers. comm. 2000) from the eastern and northeastern Yilgarn is given in Table 16. Of particular interest is the fact that only one site (Site 3, Bronzewing Central pit) gives a statistically similar pole (and hence age) to the Perth Basin pole reported by Schmidt and Embleton (1976). However, at four sites the resultant poles are statistically identical to the pole determined for the Morney weathering profile in the Eromanga Basin, southern Queensland (Idnurm & Senior 1978). Comparison with the Australian apparent polar wander path (Idnurm 1985, 1994), indicates an age estimate of 60 ± 10 Ma (latest Cretaceous to Early Paleocene) for the Morney Profile and the four Yilgarn sites (Table 16).

(3) Three sites in the eastern Yilgarn yield palaeomagnetic poles that gave Pre-Tertiary ages by comparison with the Australian apparent polar wander path. Site 13 at Mt Percy intersects the Mesozoic segment of the Australian apparent polar wander path (Embleton 1981) in two places—mid-Cretaceous and Jurassic. A mid-Cretaceous age is ruled out because the samples contain both normal and reverse polarities, whereas the mid-Cretaceous is characterised by normal polarity field directions only. Thus, a Jurassic age is indicated. The other two sites, at 35 m depth in pits at both Mt Percy and Lawlers (Table 16), yield poles that are consistent with Carboniferous ages by comparison with the Palaeozoic Australian apparent polar wander path (Li *et al.* 1990).

(4) Oxygen isotope analysis of kaolinites in weathering profiles developed on granites at Coolgardie and Collie are interpreted to indicate a mid- to Late Tertiary (Bird & Chivas 1989).

(5) K/Ar ages of alunites from Kanowna (Kalgoorlie) and Wonyulgunna Hill (central Western Australia) indicate ages of weathering of 4.9 Ma and 60.9 Ma, respectively (Bird *et al.* 1990).

(6) Stratigraphic evidence for the ages of regolith in the Kambalda area of the eastern Yilgarn was summarised by Clarke (1994a). Middle and Upper Eocene marine sediments occur in palaeovalleys cut into older weathered regolith, which must, therefore, be pre-Middle Eocene in age. Weathering profiles that subsequently developed in

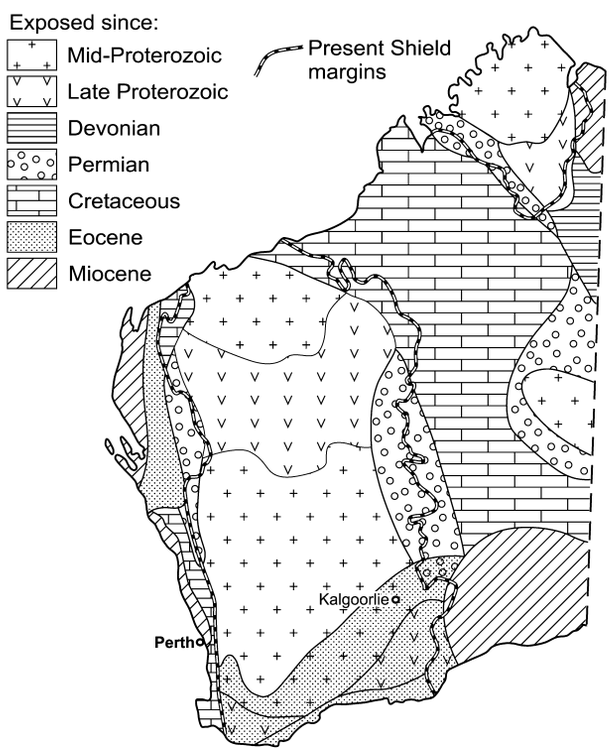

Figure 103 Periods of exposure to subaerial weathering, Western Australia [after Butt 1989 figure 2 (slightly modified)]. Compiled from Daniels (1975) and Playford *et al.* (1975). Reprinted with permission from Economic Geology.

Table 15 Principal climatic episodes in the Southern Yilgarn Craton (after Ollier 1978).

	Age (Ma)	Climate
Early Permian	280–270	Glaciation
Mesozoic	230–65	Temperate to warm; humid
Paleocene to Middle Miocene	65–15	Subtropical to tropical; humid; probably seasonal (savanna)
Middle Miocene to Pliocene	15–1.8	Subtropical; aridity increasing; cooler after 2.5 Ma
Quaternary	1.8–0	Temperate to warm; semiarid to arid (25–13 ka peak aridity, glacial maximum)

Table 16 Summary of palaeomagnetic results from weathered saprolite, Yilgarn Craton (B. Pillans written comm. 2000).

Site	Location	Component[a]	$n(+)$[b]	Remanence		Directions		South Pole				Age (Ma)
				Decl.	Incl.	k	α_{95}	Long	Lat	K	A_{95}	
Bronzewing (121.0°E, 27.4°S)												
3	Central Pit, 58 m depth	IT, HT	15(7)	003.0	–56.3	117.8	3.54	108.3E	80.0S	67.9	4.67	10
14,17	Central Pit, 45–54 m depth	HT	19(11)	000.3	–71.4	908.3	1.11	120.6E	61.3S	354.5	1.78	60
Lawlers (120.4°E, 28.0°S)												
5,18	North Pit, 35 m depth	IT	21(0)	030.1	–59.5	822.3	1.11	064.8E	62.4S	421.4	1.55	Pz
21	Turret Pit, 20 m depth	IT	13(13)	359.3	–73.3	268.6	2.53	121.1E	58.8S	91.8	4.35	60
Mt Percy (121.5°E, 30.7°S)												
11	Main Pit, 12 m depth	IT, HT	15(5)	319.4	–68.4	40.5	6.08	164.5E	53.3S	19.3	8.93	Mz
13	Main Pit, 35 m depth	IT, HT	13(13)	201.3	63.9	281.0	2.48	079.4E	67.7S	120.6	3.79	Pz
29,31	Union Club Pit, 15–20 m depth	HT	12(5)	004.7	–73.6	503.0	1.94	116.6E	60.8S	177.0	3.27	60
Kanowna Belle (121.6°E, 30.6°S)												
28	Consols Pit, 20 m depth	HT	10(8)	005.2	–74.5	486.9	2.19	116.7E	59.2S	176.1	3.65	60
Perth Basin (Schmidt & Embleton 1976)												
PB	Permian to Cret. sediments	HT	128(?)	–	–	–	–	109.9E	82.7S	–	2.4	Cz
Morney profile, **Qld** (Idnurm & Senior 1978)												
MP		–	37(17)	017.8	–68.3	–	2.4	118.5	59.8	–	3.8	Cz

[a]IT, intermediate temperature component (<580°C); HT, high temperature component (>580°C)
[b]n = number of specimens; (+), number of specimens with positive inclination.
k, K, precision parameters; α_{95}, A95, are semi-angles of the 95% cone of confidence.
Pz, Palaeozoic; Mz, Mesozoic; Cret, Cretaceous; Cz, Cenozoic.

the palaeovalley sediments must, therefore, be post-Late Eocene in age. The headwaters of the north-flowing palaeovalley drainage networks extend south to, and are truncated by, the present coast. If the headwater regions lay to the south, they must have been in Antarctica prior to the start of continental rifting in the Jurassic. The regolith into which the palaeovalleys were incised must, therefore, be at least as old as Jurassic.

(7) K/Ar and $^{40}Ar/^{39}Ar$ ages for K-bearing Mn oxides (cryptomelane–hollandite minerals) in weathering profiles across the Yilgarn Craton were reported by Dammer *et al.* (1999) and are listed in Table 17: the ages range from 36 Ma to 0 Ma. Dammer *et al.* (1999) argued that Mn oxides formed through mobilisation of Mn into solution near the surface and reprecipitation as tetravalent oxides lower in the weathering profile under conditions of intense weathering in relatively humid climatic conditions. Furthermore, the essentially zero age for the sample from Mundijong near Perth (Table 17) and the general lack of such young ages in drier areas led them to suggest that intense weathering may still be active today in coastal areas with abundant precipitation and inactive elsewhere. Thus, Dammer *et al.* (1999) inferred that the dominance of older ages in the central and eastern Yilgarn might reflect the time when the regional climate became too arid for K–Mn oxide formation. Finally, they speculated that the lack of pre-Tertiary ages in the Yilgarn (and elsewhere across the Australian continent) indicated that pre-Tertiary Mn oxides were scarce in the Australian regolith, perhaps because older Mn oxides had been dissolved during younger weathering events or removed by erosion.

CONTINUOUS VERSUS EPISODIC WEATHERING

A current controversy is whether weathering continued through time or was subject to a more episodic evolution. The continuous weathering model implies that weathering profiles underwent weathering reactions at a continuous rate and rates of reaction are independent of climate. The episodic weathering model implies that reactions in weathering profiles are mostly driven by water–rock interaction. During times when abundant water is available, weathering reactions are favoured and the mass of newly formed minerals is significant. Many authors (Frakes *et al.* 1987; McGowran 1994; Vasconcelos 1995; Dammer *et al.* 1999) suggested that weathering was episodic, but others (Mabbutt 1980; Taylor *et al.* 1992; Bourman 1993) preferred a continuous weathering model and argued that observed deep weathering profiles are more a function of preservation than episodic weathering. However, it is inevitable that the processes of weathering were continuous, but their relative intensity would have changed over time in response to climate.

The dating of the Yilgarn weathering profiles shows a polyphase evolution. Because weathering is an ongoing process that has affected the Yilgarn Craton throughout the Phanerozoic, the weathered regolith at any one site could preserve imprints of more than one age. For example, from the palaeomagnetic results discussed above, there are indications of Tertiary, Mesozoic and Palaeozoic weathering imprints at Mt Percy. Furthermore, it appears that processes akin to 'lateritisation' are proceeding today on the Swan coastal plain (Lowry 1965) and in some trunk valleys in southwestern Australia (Bettenay *et al.* 1976). Leaching is taking place within nearby bauxitic duricrust at Boddington (Davy & El-Ansary 1986). At Del Park, approximately 60 km northwest of the Boddington deposit, groundwater contains not only Na, K, Mg and Ca ions, but also those of Al, Fe, Mn, Cu and Zn. Alternate wetting and drying, caused by winter rainfall and summer drought, provides conditions in which the products of summer oxidation may be flushed by winter rains. The measured soil pH is close to that necessary for lateritisation, calculated by Norton (1973), and lateritisation (kaolinisation, gibbsitisation) in the Darling Range is probably still active (Anand 1998; Eggleton & Taylor 1998). This is consistent with the work of Dammer *et al.* (1999) who found the zero age for cryptomelane from Mundijong near Perth and suggested that, at present, intense weathering might be still active in the coastal areas with abundant precipitation (1000 mm/y and more). The dominance of older ages of K–Mn oxides (between 36 Ma and 20 Ma) obtained in the central part of the Yilgarn Craton, relative to those obtained from southern and southwestern coastal areas, may reflect the time when climate in the Eastern Goldfields became too arid to enable the formation of K–Mn oxides in the regolith. This may indicate that differences in climate similar to present conditions between the central and coastal regions have existed since the Late Miocene (Dammer *et al.* 1999).

FERRUGINISATION, SILICIFICATION, CALCIFICATION AND BAUXITISATION: CLIMATES AND GEOCHRONOLOGY

Ferruginisation, silicification and calcification have affected a variety of residual and transported materials over long periods, and ferruginisation and silicification have clearly occurred more than once. Evidence of ferruginisation from the pre-Eocene through to at least the Pliocene can be seen in the arid parts of the Yilgarn Craton. Eocene sediments contain detrital pisoliths apparently eroded from ferruginous duricrust, indicating that ferruginous duricrust formed before the end of the Eocene. Clarke (1994a) suggested that the Triassic may have seen the earliest formation of ferruginous duricrusts. Evidence of continued ferruginisation lies in weathering profiles

Table 17 K/Ar and $^{40}Ar/^{39}Ar$ ages for K–Mn oxides, Western Australia (after Dammer *et al.* 1999).

Sample no.	Location	Age (Ma)
S4068	Wallangie	36.4 ± 0.5
S4104	Sudden Jerk	29.6 ± 7.6
S4110	Broad Arrow	19.9 ± 0.3
MDC3938	Kalgoorlie	24.5 ± 2.0
S4067	Hamersley River	5.5 ± 0.3
S4092	Hamersley River	23.9 ± 1.1
S4069	Phillips River	8.1 ± 1.4
S4073	Mt Desmond	12.7 ± 0.1
S4076	Mundijong	1.4 ± 1.4
MDC3947	Mt Gordon	5.6 ± 0.4

in underlying bedrocks and in sediments, including palaeochannel sediments, which have strongly mottled and pisolitic upper horizons and cemented duricrusts. It appears that transport of Fe, which formed a variety of ferruginous duricrusts in inland areas, is related to ancient wet epochs and not to recent times in the eastern Yilgarn, which are now too dry to permit significant transport from the upland to the slope bottom. Therefore, most duricrusts are old and have little to do with the present climate. However, ferruginisation is still operating in humid regions of the Darling Range, where ferricrete (bog iron) is forming on the edges of valley floors.

The duration of ferruginous duricrust formation is unknown. Mann and Ollier (1985) demonstrated that a 1 m-thick Fe oxide-rich duricrust could be formed in 10 000 years by ionic diffusion, but they did not suggest that this actually happened for most real duricrusts. Field evidence indicated much greater ages for some, probably a million years (Ollier & Pain 1996). It has also been suggested by Nahon (1986) that ferruginous duricrust a few metres thick, overlying saprolite of tens of metres, needs several million years to form. Recently, Theveniaut and Freyssinet (1999) used palaeomagnetic data to interpret the succession of horizons, from the weathering front to the top of the duricrust surface, of a thick bauxitic profile in French Guiana. The duricrust is divided into two levels within the massive facies; the base of the duricrust shows palaeomagnetic directions that fit with the present-day situation, whereas the upper part records directions of the South American pole wander path older than 10 Ma. These authors concluded that hematite precipitation was not uniform within the duricrust during 'lateritisation', and seems to preserve traces of successive and distinct lateritisation phases. Thus, the lower duricrust is formed during a recent lateritisation period, whereas upper massive duricrust has preserved a palaeomagnetic signal of an older (>10 Ma) phase.

There are at least two widespread episodes of silicification that have affected materials of various types. One episode is related to silcrete formation and the other to red-brown hardpan formation. The timing of the silcrete formation is unclear. Dating suggests that the main period of silicification was the Eocene–Miocene, generally post-dating deep kaolinisation (Idnurm & Senior 1978; Wopfner 1978). As silcrete pre-dates ferruginous duricrust in places it is not possible to invoke Late Tertiary aridity to account for silcrete formation. As silicification requires the contemporary release of silica by chemical weathering an adequate rainfall is indicated. Thus, a humid tropical or subtropical environment of low relief was suggested by Summerfield (1983). However, precipitation whether at the surface or at depth requires concentration, presumably by excess evaporation. Accordingly, it appears that silicification probably occurred during transitional periods between humid and arid phases (Mabbutt 1980; Butt 1985) between the Late Eocene to Oligocene, with silica accumulating in the groundwaters as drainages became less competent, and precipitation at seepages, water tables and porosity barriers (Taylor & Butt 1998). Soil processes became dominated by calcification and silicification rather than ferruginous duricrust formation with the change to aridity in the Late Miocene or Pliocene. Extensive hardpanisation of the younger sediments and residual regolith indicates widespread mobilisation of silica. The cementation still appears to be active particularly in the north. Calcification is the youngest event and post-dates the onset of silicification. Precipitating carbonates, amorphous silica and aluminosilicates may displace and replace the host matrix, including saprolite and ferruginous duricrust, whether *in situ* or transported.

The characteristics of weathering profiles in inland and southwestern Australia indicate that they were formed under similar weathering conditions. However, there is an important difference in the abundance of gibbsite between the Darling Range and inland of the Yilgarn Craton. The timing of bauxitisation in the Darling Range is not clear. High rainfall and good drainage promote deep chemical weathering and removal of Si, Ca, Na, K and Mg and alteration of clays to gibbsite. Where leaching is particularly intense, the parent material is transformed directly into gibbsite (Anand *et al*. 1985). The influence of climate on the Darling Range bauxites has been discussed by several authors. Tomich (1964), Geidens (1973) and Sadleir and Gilkes (1976) observed that an increase in gibbsite content corresponds with areas of high rainfall (>1000 mm/y), which indicates that either recent rainfall was a factor or that the present rainfall distribution patterns were similar to those when the gibbsite was formed. However, Geidens (1973) noted that rainfall patterns could not explain the progressive thinning of the bauxitic duricrust southwards from the Willowdale–Collie area; rainfall in this southern area is similar to, or greater than, that in the Jarrahdale–Willowdale district, but temperatures are considerably lower in the south. Butt (1976) suggested that at the time of bauxite formation the present pattern of decreasing rainfall inland from the Darling Scarp may have been enhanced by an increase in orographic rainfall associated with greater uplift of the scarp nearer the coast. Therefore, the marginal areas of the southwest have been wetter and more strongly leached than those in the interior. It appears that the bauxite formation in the Darling Range is related to the present mediterranean climate. The seasonal climate provides a favourable environment for the strong leaching and active formation of gibbsite under the winter rainfall of the mediterranean climate (Anand *et al*. 1985) compared to lesser leaching and the formation of kaolinite in uplifted plateaux in savannas having a similar, but summer, rainfall (Butt & Zeegers 1992).

Recent overprinting of ferruginisation has continued both inland and in the Darling Range. Inland, biogenic-related processes, calcification or silicification appear to have triggered deferruginisation of duricrusts and mottled zones. The processes of calcification and silicification have clearly resulted in removal of Fe, possibly by replacement, although the mechanisms are not well understood. In the Darling Range, degradation of bauxitic duricrust continues by dissolution of goethite and gibbsite at or near the surface.

EXISTING LANDSCAPE-EVOLUTION MODELS

The recognition and interpretation of ancient landsurfaces have been a major theme of Australian landscape studies.

The relatively low relief of much of the continent has helped to promote interpretations of large parts of the Australian landsurface as palaeoplains within the context of various genetic models, including peneplains and pediplains. Many early geomorphological studies favoured the Davisian idea (Davis 1899) that a vast area of the Australian landscape has evolved through cycles of landscape lowering and relief reduction, punctuated by episodes of landscape rejuvenation. A notable example is the concept of the 'Great Peneplain', thought to be a single, regionally extensive landsurface found across much of the continent (Andrews 1903; Woolnough 1927).

In the Yilgarn Craton, the interpretations of regional peneplains have been suggested by Jutson (1914, 1934), who referred to gently undulating uplands as portions of an 'Old Plateau' that are capped by deeply weathered profiles, sand and 'laterite'. Jutson perceived a 'New Plateau' developing as a consequence of the erosion of the 'Old Plateau' (Figure 1). In this case, the New Plateau would be free of 'laterite'. In reconstructing former lateritised landscapes,

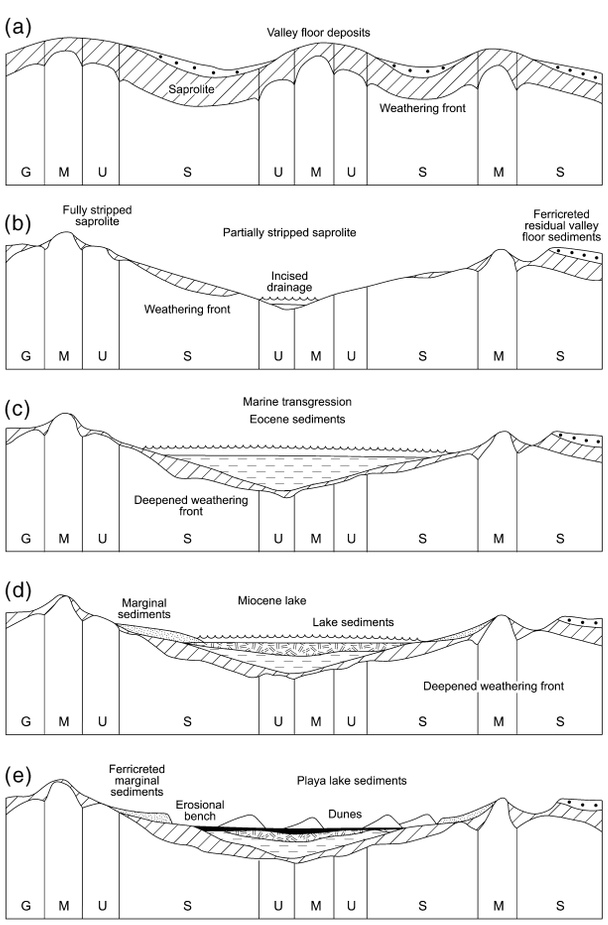

Figure 105 Schematic evolution of the Kambalda regolith (vertical scale hundreds of metres and horizontal scale tens of metres). (a) Pre-Jurassic topography and saprolitic mantle (G, granite; M, mafic; U, ultramafic; S, sediment). (b) Jurassic–Eocene drainage incision and deepening of weathering front. (c) Eocene drainage infill and deepening of weathering front. (d) Miocene fluviolacustrine sedimentation. (e) Pliocene–Holocene incision and deposition of playa lake and dune systems (Clarke 1994a figure 3).

Jutson and others (Woolnough 1918; Stephens 1946; Prescott & Pendleton 1952) assumed former continuity of isolated, present-day ferruginous duricrust. Jutson also noted that cavernous weathering is commonly developed at the base of breakaways. He addressed the question of landscape evolution by means of retreating escarpments and realised that scarps capped by resistant material tended to retreat parallel to themselves until late in the elimination of the upland. Slope form was connected to structure so that the New and Old Plateaux were in places connected to gentle slopes and the absence of a hard cap on portions of the Old Plateau facilitates this form.

Mulcahy (1960) and Bettenay and Hingston (1961), while mapping soils on deeply weathered tracts in southwest Australia, recognised relatively stable and relict tracts characterised by sand, ferruginous gravel and duricrust that contrasted with adjacent tracts that had extensive saprolite or fresh rock exposure. Nevertheless they also proposed that the former were a complex of erosional and depositional areas dominated by ferruginous gravels and/or duricrust and adjacent sandy depositional areas. Mabbutt *et al.* (1963) relied extensively on a 'New Plateau – Old Plateau' model to interpret landform evolution in the Wiluna–Meekatharra area.

Finkl and Churchward (1973) applied the etchplain concept (Wayland 1933) to the southwestern region of Western Australia. At the heart of this concept is the presumption that a continuous sheet of duricrust-capped profiles covered the entire area now classed as etchplain (Figure 2). Where the duricrust-capped lateritic profile is nearly complete and continuous the landform is said to be incipient etchplain; where the ferruginous duricrust is intermittent, but the mottled zone or saprolite is continuous, is called partial etchplain; and where the duricrusts are widely spaced with saprolite or bedrock between, is called semi-stripped etchplain. Ollier (1984) presented an etchplain map of the Yilgarn simplified from Finkl (1979).

More recently, Ollier *et al.* (1988) suggested a very different interpretation of the evolution of the Yilgarn landscape. According to these authors, the landscape displays a recurring sequence in which the Old and New Plateaux are topographically higher than each other. The breakaways do not correlate into a single planation surface or peneplain. They concluded that weathered material has been repeatedly deposited in valleys, after which the relief became inverted so that relics of alluvium occur as a duricrust capping (Figure 3). Thus, they do not accept the concept of a former extensive lateritised landsurface, and rather suggest that these deposits are relict valley-flanking sediments. A similar model of landscape evolution for the Darlot region was suggested by Krcmarov *et al.* (2000) (Figure 104 on Plate 18). According to these authors, differential erosion and chemical modification of the landsurface in the Darlot region has produced a variety of regolith materials and intricate regolith–landform relationships. Stripped erosional-regime regolith is largely restricted to the margins of the granite and greenstone succession. 'Relict'-regime regolith comprises a range of ferruginous duricrusts, saprolite and lag. A small proportion of the duricrusts are genuine *in situ* 'laterites', but the majority are unconformity-related ferricretes, formed during an earlier depositional phase

and subsequently cemented prior to inversion to topographic highs by further erosion. Another view is expressed by Glassford and Semeniuk (1995) who suggested that the eastern Yilgarn lateritic profiles are a composite of *in situ* weathering and sedimentary deposits. They contend that the profile consists of *in situ* saprolite overlain by dominantly aeolian facies that now form the mottled and pallid zones of the lateritic profile. They argue that the laterite and bauxite are formed from altered sandy duststones. Brimhall *et al.* (1991) also advocated significant aeolian accession to the bauxitic profiles of the Darling Range.

Clarke (1994a) presented a landscape model for the Kambalda region. His study has revealed a complex of superimposed landforms, whose history extends back into the Palaeozoic. Four stages in the geomorphic evolution of the Kambalda area are postulated (Figure 105). These comprise Permian–Jurassic weathering, Jurassic–Eocene erosion and weathering, post-Eocene sedimentation and weathering, and the current arid regime. Formation of the regolith largely pre-dates the incision of the palaeodrainage which, in its deepest parts, has cut through to fresh rock. The relict saprolite dates back to the Late Permian – Middle Jurassic. Stripping of this regolith occurred in the Middle Jurassic – Early Eocene during the formation of the palaeodrainage system. Further deep weathering occurred concurrently with erosion. Increasing aridity led to disorganisation of the drainage to form a chain of lakes. Pliocene times saw increased aridity in the Kambalda area with the establishment of the current semiarid geomorphic regime. Arid conditions have persisted for only 2% of the history of the Kambalda landscape. Thus, arid geomorphic models are inappropriate for understanding all but the most recent evolution of the regolith.

PROPOSED LANDSCAPE-EVOLUTION MODELS

Introduction

On the basis of the present topography, the degree of differential erosion and the distribution of ferruginous duricrusts, two broad regional situations, with many local variations, are envisaged in the Yilgarn Craton.

First, in the southwest, the Darling Range is a broadly undulating topographic surface mantled by extensive sheets of bauxitic ferruginous duricrust. Some duricrusts occur on slopes of 5–20° and completely mantle valleys wider than 1 km with a relief amplitude of 100 m (Mulcahy 1960). Bauxitic ferruginous duricrusts are thickest on mid-slopes and thinnest on the crests. In parts of the Darling Range, there is clear evidence of physical transport and recementation of pisoliths on slopes. Breakaways are generally minor or absent.

Second, inland in the southern and northern regions, the landscape is characterised by low relief and an array of erosional features that occur notably as scattered breakaways generally capped by either ferruginous duricrust, ferruginous saprolite or silicified saprolite. Backslopes behind the breakaways are mantled with ferruginous gravels, ferruginous duricrust and ferruginous saprolite. Immediately below the breakaways, the regolith is dominated by a thinner mantle of saprolite and saprock as subcrop and fresh bedrock may outcrop. The colluvial–alluvial plains extend from pediments, burying either ferruginous duricrust-capped or saprolite profiles. Buried palaeochannels generally occupy the lower parts of the landscape and may be 1–3 km wide and many kilometres long. They are incised into pre-existing weathered regolith. Thus, despite the low relief of the present landscape, palaeotopography depicts a broadly undulating terrain similar to that of the Darling Range.

In detail, there are differences in regolith and landforms between the southern and northern regions. In the southern (Kalgoorlie) region, higher hills generally flanked by steep slopes rise above the regolith-dominated terrain and expose fresh rock. Ferruginous duricrusts on mafic and ultramafic rocks are common on rises and the edges of breakaways but, despite an abundant lag of black, Fe-rich pisoliths, ferruginous duricrust is minor on backslopes and plains. Instead, these are covered by red clays, which form an extensive blanket on all landscape positions except hills and rises. In comparison, further north, ferruginous gravels and duricrust are common on backslopes and plains beneath colluvium and alluvium, which also commonly contain detrital hematite–maghemite-rich ferruginous gravels.

Can the Jutson model be applied?

The contrast between the sand, ferruginous gravel and duricrust-dominated and saprolite–bedrock-dominated terrains is reflected in the 'Old & the New Plateau' of Jutson (1934). In parts of the Yilgarn, there are areas that could, within the context of this hypothesis, be classified as 'Old Plateau'. However, they are not clearly separated from

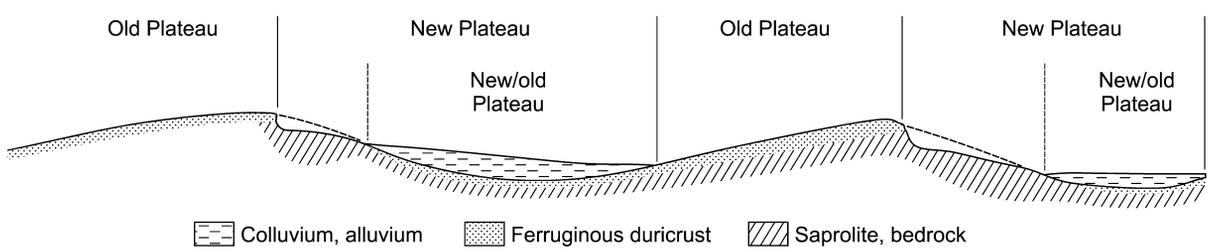

Figure 106 Jutson (1934) model suggests that the Old Plateau is separated from the New Plateau. This diagram shows that Old and New Plateaux are not clearly separated, but merge under long, gentle slopes and by burial under extensive sheets of transported detritus. Transported detritus forming the New Plateau may overlie the Old Plateau.

the younger surface and merge with it by way of long, gentle slopes and by burial under extensive sheets of transported detritus, mainly derived from discontinuous erosional tracts (Figure 106). In reconstructing former lateritised landscapes, Jutson and others (Woolnough 1918; Stephens 1946; Prescott & Pendleton 1952) assumed former continuity of isolated, present-day ferruginous duricrust. These authors implied that the formation of duricrust was restricted to peneplains.

The overall original extent of ferruginous duricrust in the Yilgarn Craton cannot be determined, but it appears that a continuous blanket may never have existed. However, there is evidence for its widespread occurrence.

(1) In the Darling Range, ferruginous duricrust forms an extensive, but not continuous, blanket over granitic and greenstone terrains on an undulating landsurface. Inland, it is extensive in some districts (e.g. Lawlers, Mt McClure, Bronzewing, Mt Magnet, Madoonga, Mt Gibson, Bottle Creek), whereas in others it is patchy (e.g. Ora Banda, Kanowna Belle, Wombola). Ferruginous duricrusts are developed on all lithologies, but are best developed on mafic and ultramafic bedrocks. The greater thickness of duricrust in the Darling Range might be accounted for by a climatic gradient (past and present) and more effective drainage (stream incision close to the Darling Scarp). The swarms of dolerite dykes, so much a feature of this zone, could have also contributed towards the genesis of a physically more competent ferruginous duricrust than is the case for more characteristic granitoid terrain with sparse dolerite dykes.

(2) Inland in the southern and northern regions, ferruginous duricrust not only occurs at or close to the surface, but is intermittently present in many depositional areas, buried beneath alluvial and colluvial sediments particularly in the northeast and northwest. The abundance of ferruginous detritus in depositional areas implies that the duricrust was once more widespread and has since been eroded. In many instances, in depositional regimes, the stratigraphy is inverted in relation to a residual profile. Ferruginous nodules and pisoliths occur at the base of the colluvial–alluvial sediments and are overlain by fine, sandy clay sediments. This stratigraphy would seem to indicate progressive stripping of a lateritic profile, with the ferruginous clasts derived from the erosion of duricrust and the clays from the erosion of saprolite.

(3) Nodules and pisoliths, which occur as a lag on saprolite-dominated areas, could be remnants of a previous, at least partly, ferruginous surface.

(4) It is generally considered that maghemite has largely formed at the surface by the heating of goethite or hematite during bush fires (Schwertmann & Fechter 1984; Milnes *et al*. 1985; Anand & Gilkes 1987b). Subsequently, large proportions of these surficial magnetic gravels have been eroded and redeposited elsewhere in the landscape especially in palaeochannels. Transportation has occurred at both proximal and distal scales.

The stratigraphy and composition of sediments in the Kalgoorlie region suggest that the landscape not only included profiles with ferruginous duricrust, but also profiles of uniformly Fe-oxide-stained, red earths (Anand & Smith 1993; Anand *et al*. 1993a). Both red earths and duricrust appear to have developed in the upper parts of the profile in different sites, possibly in response to differences in geology and topography. Similar red earths, referred to as latosols, ferrallitic soils or ferrasols, have been reported from other parts of the world, for example, in humid equatorial rainforest environments and, in particular, on well-drained upper slopes (Chauvel 1975). Because of their susceptibility to erosion, red earths would have been eroded and have contributed much to sediments in depositional regimes.

It is concluded that despite the extensive sheets of duricrust and gravels in places, ferruginous duricrusts have never been continuous across the landscape. They can occur at different levels in the landscape and are formed in a variety of residual and transported materials of diverse ages. Thus, it is unwise to assign a single age to all ferruginous duricrusts or imply a single extensive duricrust-capped surface of planation of continental extent. Thus, Jutson's model of landscape evolution cannot be applied on a regional scale. However, breakaways and mesas capped with duricrusts of similar origin may be correlated on local to district scales.

Can the Ollier *et al.* model be applied?

According to Ollier *et al*. (1988), duricrusts were formed in transported material in ancient dendritic alluvial channel systems and now occupy high ground by virtue of relief inversion. Several lines of evidence indicate that the relief inversion is not a major mechanism of ferruginous duricrust preservation on a regional scale.

(1) Extensive sheets of bauxitic duricrust on all landscape positions in the Darling Range cannot be explained by relief inversion. They could not have formed at seepage sites on lower slopes. There is no doubt that the ferruginous duricrusts have developed in a variety of materials and there has been local transportation and recementation of ferruginous gravels, particularly on lower slopes. Nevertheless, the general relationship between the chemical composition of bedrock and that of ferruginous duricrust in the Darling Range is well established (Baker 1971; Sadleir & Gilkes 1976; Davy 1979; Murray 1979; Ball & Gilkes 1987; Hickman *et al*. 1992; Anand 1994). Dolerite dykes have been located by chemical analysis of the overlying duricrust, suggesting minimal transport during its formation (Sadleir & Gilkes 1976; Hickman *et al*. 1992).

(2) Although much less abundant than in the Darling Range, ferruginous duricrust and gravel have formed on all landscape positions, particularly on mafic and ultramafic rocks on greenstone belts inland. They have formed in residuum, colluvium and alluvium and may be regarded as representing a continuum that has lateritic residuum and ferricrete as end-members. This varies according to landscape position. Where duricrust is residual (lateritic residuum), the control of lithology on its thickness, chemical composition and fabrics is evident (Butt & Sheppy 1975; Churchward 1977; Smith 1977; Davy *et al*. 1988; Pringle 1994; Anand 1995, 1998; Robertson *et al*. 1998). In contrast, ferricretes develop by impregnation and cementation of sediments of distal origin by Fe oxide, itself precipitated following lateral mobilisation in groundwater, so that they have little direct relationship with the underlying rocks (Anand 1995, 1998). In places, the ferricretes now form low

hills because of local relief inversion. Other members of the continuum have developed in a variety of locally derived materials. However, it is commonly difficult to identify the nature of parent material because of extreme weathering and ferruginisation.

No evidence for large-scale relief inversion is evident. It is relevant to note that major palaeodrainages, some filled with Permian sediments, still predominantly occupy lower parts of the present landscape. However, relief inversion on a local scale is well established (Anand *et al.* 1991b; Butt *et al.* 1992; Davy & Gozzard 1995; Anand 1998) in the Yilgarn Craton. Ferricretes that now occupy topographically higher areas may have formed in seepage sites or palaeodrainages. Regional-scale relief inversion as suggested by Ollier *et al.* (1988) is doubtful. Other authors (Conacher 1991; Dusci 1994; Davy & Gozzard 1995) have also questioned regional-scale landscape relief inversion. Conacher (1991) pointed out that duricrust that now caps low hills and ridges could not have been located at low-lying positions in a prior landscape of low erosion in the mid- or even Early Tertiary. According to Conacher, denudation rates reported from a number of locations across Australia are far too slow to permit this interpretation. To quote Davy and Gozzard (1995 p. 13): 'Ollier (1991; Figure 3) shows the distribution of ferricrete on the Leonora 1:250 000 topographic map. He believes this ferricrete to be material formed in an ancient dendritic alluvial channel system that has since undergone relief inversion, and uses this evidence to suggest that many ferricretes were formed in transported material on low sites, but now occupy high ground by virtue of relief inversion. Ground inspection shows that the ferricrete of Ollier is "in fact" partly kaolinised and/or silicified granitoid, outcropping on ridges separating the main drainages (cf. the map of Thom & Barnes 1977)'.

It can be concluded that there is no single model that can describe the formation of all ferruginous duricrusts. The residual and transported nature of duricrusts may vary within short distances. Some duricrusts are residual, whereas others are Fe-cemented sediments.

SUMMARY OF REGOLITH–LANDFORM HISTORY

Introduction

The present, relatively flat, surface of the Yilgarn Craton indicates little of the complex regolith beneath. Recent mapping and the establishment of regolith relationships and distributions from drilling and mine exposures has revealed details of the subsurface regolith and palaeolandscape from which the landscape history can be deduced. Palaeomagnetic dating results have been used to constrain the Late Palaeozoic to Cenozoic landscape evolution. When combined, the field relationships and palaeomagnetic results indicate that since the Late Palaeozoic, the landscape of the Yilgarn Craton has evolved through several episodes of erosion and deposition as well as periods of relative stability during which the thick regolith formed. Four broad stages in the regolith–landform evolution of the Yilgarn Craton are postulated and are illustrated in Figure 107 on Plate 19.

Pre-Tertiary weathering

It has been generally proposed that the protolith from which the landscape evolved was the ice-scoured terrain that emerged from the Permo-Carboniferous glaciation. During the glaciation, much of the region was covered by a thick sedimentary sequence, which has subsequently been largely removed due to later denudation (Figure 107a on Plate 19). Palaeomagnetic results indicate that significant weathering occurred during the Palaeozoic and despite substantial erosion (Van de Graaff 1981; Clarke 1994a; Killick 1998) remnants of the regolith formed during the Palaeozoic have survived in places (e.g. Mt Percy, North pit Lawlers). The contribution from reworked Permian is unknown, although undoubtedly important (Clarke 1994a). Alley and Clarke (1992) reported the presence of reworked Late Permian palynomorphs in Cretaceous sediments from the Great Australian Bight, indicating the presence of sediments of this age in the hinterland at the time of deposition even though none are now preserved.

Sediments younger than Late Permian and older than Middle Jurassic are rare along the margins of the Yilgarn Craton, indicating that this was a period of weathering with only limited erosion and sediment deposition (Clarke 1994a). Triassic sediments are known only from the Perth Basin (BMR Palaeogeographical Group 1990). These observations appear to be consistent with the palaeomagnetic data that suggest that weathering occurred during the Mesozoic (Jurassic). The Mesozoic landscape comprised hills and broad, shallow valleys. Broadly contemporaneous weathering of topographically higher parts and palaeovalleys formed saprolite, lateritic residuum and ferricrete, with the valleys being more prone to ferruginisation (Figure 107a on Plate 18). Lateritic residuum and ferricrete were subsequently mechanically dispersed into younger palaeochannels within the palaeovalleys to form accumulations of detrital ferruginous gravels. The palaeodrainage systems may have been active since the Triassic (Finkl & Fairbridge 1979), pre-Jurassic (Clarke 1994b), Early Cretaceous (Jones 1990) or Early Eocene (Morgan 1993). The characteristically narrow, linear distribution of some ferricretes coincides with dendritic palaeodrainage patterns revealed by shallow, high-frequency maghemite signals in aeromagnetic data (Anand 2000; Wildman & Compston 2000). Therefore, these elevated ferricretes are mostly relics of a former, now inverted, depositional surface. Chan *et al.* (1992) described dendritic ferricretes as possibly being of Cretaceous age. Differential erosion of ferricretes led to local relief inversion and now ferricretes occupy a topographically higher position.

Partial stripping of the regolith occurred during the Middle Jurassic and Early Eocene with uplift and incision of the palaeodrainage system (Clarke 1994a). Erosion followed uplift of the Yilgarn along the Jarrahwood Axis during the Triassic (Johnstone *et al.* 1973; Cope 1975). Lateritic residuum and ferricrete relicts of the earlier palaeodrainage were preserved as isolated remnants.

Early to mid-Tertiary erosion and sedimentation

By the Eocene, drainage incision along palaeovalleys on the weathered landsurface had resulted in the development of 'younger' channels that are 1–3 km wide and many

kilometres long (Figure 107b on Plate 19). Palaeochannels are younger than the 'palaeodrainage' system of broad, shallow valleys in which they occur and were probably incised during the final stages of the breakup of Gondwana in the Early – mid-Tertiary (P. de Broekert pers. comm. 2000). Fluvial, estuarine, marine and lacustrine sediments were deposited in the palaeochannels and other low elevation areas during the Eocene (Clarke 1993). This essentially marked the end of significant fluvial erosion. Lignites were deposited in the lower river channels south of latitude 31°S. Carbonaceous material was also common in sediments much further north of this latitude, but has been largely destroyed by weathering in later dry climates (Morgan 1993). Two main depositional episodes have been recognised, a sand facies sequence (Wollubar Sandstone) and a clay facies sequence (Perkolilli Shale) (Kern & Commander 1993), the composition of which is highly dependent on the composition of the surrounding Archaean basement. The sand facies sequence represents the fluvial basal units. Thereafter, a major change in either climate or sea-level led to the deposition of a thick clay probably in lacustrine and shallow swampy environments. The palaeodrainage system was choked with clay and lacks evidence of a period of reactivation with erosional cycles, or an influx of sediments (Dusci 1994). Such a massive thick clay sequence may be partly attributed to the regional tilting interpreted by Cope (1975) to have occurred in the Late Eocene, although Clarke (1994b) suggests a Jurassic age for this event.

The sand and clay facies sequences were deposited as far inland as the Yandal belt, suggesting that the elevation of the northern craton at that time was much lower than present. Palaeovalleys around Darlot are filled with clays to topographically higher levels than the present lake surface, implying that flooding was originally much more extensive than the present area of the lake, and the hydraulic gradient consequently somewhat lower (Anand 2000; Krcmarov *et al*. 2000). The landscape following deposition of sediments probably comprised slightly elevated (but dissected) areas of pre-Tertiary terrain, surrounded by lower elevation sediment-covered terrain (Figure 107b on Plate 19). The similarities in the nature and characteristics of palaeochannel sediments between the Kalgoorlie (Roe palaeochannel) and northern regions suggest that similar regional conditions prevailed not only during the deposition of sediments, but also during their subsequent weathering. Several authors (Clarke 1994b; Dusci 1994; Ladhams 1994) suggested that the change from an active channel erosion to low-energy deposition may be explained by a rise in base level related to the Tortachilla Transgression during the Middle Eocene as observed in the sediments of the Lefroy and Cowan palaeodrainage systems. This may be true in the Kalgoorlie region, but the effect of this transgressive event for areas such as Bronzewing and Lawlers, which are topographically higher than the Kalgoorlie region, remains unclear. It is possible that the northern portion of the craton has undergone post-depositional uplift.

Mid- to Late Tertiary weathering

Based on the palaeomagnetic results from the saprolite, weathering occurred during the Miocene (Figure 107c on Plate 19). Eocene sediments and the underlying bedrock were subjected to widespread weathering including ferruginisation and silicification to form ferruginous duricrusts and silcretes, thus indicating a shift towards a climate with more seasonally variable rainfall. Mixing occurred between the accumulating sediments and the underlying saprolite, possibly as the result of the formation of palaeosols. The pendant-like features and associated nodular–pisolitic materials are interpreted to have formed during this period. Palaeochannel sediments have strongly leached lower horizons, strongly mottled upper horizons and are locally cemented to form mottled duricrusts, which contain pisoliths formed *in situ*.

Dolocretes at the base of palaeochannel sediments in several localities in the northeast (e.g. Bronzewing) are likely to be relict forms equivalent to those in deep sediments in the Roe palaeochannel (Kern & Commander 1993). They may have formed by evaporation of Mg-rich lakewaters during a period of high evaporation. Dolocretes survived post-depositional weathering possibly because they remained submerged beneath alkaline, Mg-rich groundwaters. Alternatively, they are features of later arid phases. The dolocretes differ from the valley calcretes, which are surficial deposits in major, active drainages.

Late Tertiary to Quaternary sedimentation and weathering

During the Late Tertiary to Quaternary another stage of instability and erosion, caused by tectonic uplift and a change in the climate to semiarid to arid conditions (Bowler 1976), led to the dissection of parts of the landsurface. A variety of sediments were deposited, mostly as the result of fluvial, colluvial and aeolian processes (Figure 107d on Plate 19). Although certain regolith units have been indurated by irreversible dehydration (e.g. lateritic duricrust) or by introduced cements such as silica and Fe oxides (e.g. silcrete and ferricrete), much of the regolith was soft and unconsolidated and, hence, susceptible to erosion by water (and wind), even in areas of low relief. Inland, in the absence of an effective drainage system the resulting superficial deposits have been retained in the landscape. Near the coast, in the south, but extending far upstream in the west, rivers had a more competent drainage, erosion was to the oceanic base-level and there was some loss of sediment. This influence extends to a nick point at the Meckering Line (Mulcahy 1967). However, in the high rainfall areas of the Darling Range, abundant duricrust has produced a barrier to further erosion.

The timing of deposition of patchy, shallow, sandy clay to sandy sediments that may overlie palaeochannel sediments, ferruginous duricrust or saprolite is not clear. In places, these sediments form a uniform cover approximately 5 m thick (e.g. Forrestania). Glassford and Semeniuk (1995) suggested that these are mainly aeolian deposits derived, via fluvial units, locally from basement saprolite and are referred to as the Mulline Formation. These sediments consist of well-rounded, sand-sized, flint clay grains termed kaolin spherites and are commonly overprinted by Fe to form mottled, pisolitic or vermiform ferricretes (e.g. Mt Gibson). Increased erosion resulted in deposition of gravelly and silty clay sediments in low-lying areas, the composition of which broadly reflects that of the

catchment. Clasts are dominated by ferruginous gravels derived from erosion of duricrust, whereas silty clay is derived from saprolite and mottled zone. In places, there is a stratigraphy in the sediments that is inverted in relation to the nearby residual profile. Ferruginous nodules and pisoliths occur at the base of the colluvial–alluvial cover and are overlain by fine, clay-rich sediments.

Inland, these sediments are extensively overprinted by products of current soil-forming and groundwater-related processes. During relatively wet periods, Fe and other elements leached from the higher parts of the landscape would have been flushed from the regolith by significant groundwater recharge and throughflow. The onset of more arid conditions resulted in reduced recharge and the precipitation of elements leached from the upper parts of the regolith profile in topographic lows. Consequently, the topographically lower areas became enriched in Fe, Si and Ca to form ferricrete, ferruginous saprolite, silcrete, red-brown hardpan and calcrete (Figure 107d on Plate 19). In places, this process armoured the upper regolith against further erosion and it subsequently became topographically inverted.

With increased aridity, drainage became limited and the groundwaters became saline, and geochemical effects, such as chloride, began to dominate chemical reactions. The major valleys became the sites of chains of salt lakes. Aeolian processes became dominant, including the formation of gypsum dunes, lunettes and lake parnas, the genesis of which has been discussed by Bettenay (1962). There is a significant aeolian component in many soils. In contrast, aeolian deflation has left vast areas covered by polished, ferruginous, siliceous, lithic, or polymictic lag, which, in some places, forms gibber plains. Lithosols are associated with fresh rock or saprock and areas of steeper slopes. Soils contain abundant calcrete and smectite from the recent weathering of mafic rocks.

IMPLICATIONS FOR EXPLORATION

ECONOMIC SIGNIFICANCE OF REGOLITH

The presence of thick regolith over much of Australia has two main implications for the mineral industry. First, the presence of regolith presents numerous exploration problems, affecting geological, geophysical and geochemical mapping and exploration techniques, and constraining their use (Table 18). However, dispersion during regolith formation and evolution potentially yields much larger exploration targets than the mineralisation itself. Second, the regolith materials may themselves represent economically significant mineral deposits.

Several important types of mineral deposit formed during the development and evolution of the regolith.

(1) Weathering products of otherwise 'unmineralised' rocks: bauxites, some Fe and Mn ores, Ni–Co laterites, and various industrial minerals, including clays such as kaolinite. These are some of Australia's major mineral resources, including bauxites at Darling Range, Weipa, Gove and Mitchell Plateau, and Mn at Groote Eylandt. Demonstrated resources of bauxite in Australia are estimated at more than 8300 Mt, of which at least 3000 Mt are economically demonstrated resources, the highest in the world (Lambert & Perkin 1998). Darling Range is the world's leading alumina-producing region. In Western Australia, Ni laterite resources amount to approximately 600 Mt of Ni metal and represent the sixth largest laterite resource in WA. The Ni is hosted primarily by silicate minerals (silicate–smectite type deposits), including Bulong and Murrin Murrin, whereas in the remainder the Ni is hosted by Fe and Mn oxides (oxide type deposits) (Brand *et al*. 1996).

(2) Weathering resistates and placer deposits: mineral sands, diamonds and alluvial gold. Terrestrial deposits are mostly minor, although mineral sands in old marine terraces and shorelines are, ultimately, weathering resistates. Rare-earth elements and apatite sands, accumulated over carbonatites (e.g. Mt Weld Range, Yilgarn Craton), may be a mixture of primary and secondary minerals.

(3) Secondary enrichment of primary mineralised systems: supergene Au, Cu and U deposits. Most important of these are the numerous Au deposits found in Western Australia, the Northern Territory and, increasingly in eastern Australia (e.g. Mt Gibson, Boddington, Paddington, Tanami and Northparkes). Some of these developed on significant primary mineralisation and others, mostly smaller operations, where the primary source is uneconomic.

(4) Epigenetic enrichment in sediments: Fe, U and, possibly, some Au deposits in palaeochannel sediments and shallow basins. Iron ores, such as the Robe River deposits, and both oxidised (e.g. Yeelirrie) and reduced (e.g. Lake Frome Basin) styles of U deposit have formed by precipitation in redox-controlled trap sites in sediments, distant from a dispersed source.

REGOLITH–LANDFORM MAPPING FOR GEOCHEMICAL EXPLORATION

Introduction

Geochemical procedures may be applied at all stages of exploration from regional appraisal to prospect evaluation. However, the development and evolution of the landscape give rise to several problems (Table 18) in the effective application of geochemical procedures that use soil and other regolith materials as sample media. Effective geochemical exploration can only be achieved by recognition of the problems caused by the evolution of the landscape and regolith, and by the selection of sampling media and data interpretation techniques appropriate to the target being sought. Thus, it is important to assess the nature and origin of the regolith, geomorphological processes, styles of weathering and regolith–landform relationships to

Table 18 Some exploration problems caused by deep weathering and sediment cover (from Butt *et al*. 1997b).

Problem	Cause
Geology and geochemistry	
Difficulty in recognising parent lithology	Mineralogical, chemical and morphological change
Variable regolith thickness and surface horizon	Differential weathering and partial erosion
Subtle surface expression	Strong leaching of most ore-related elements
Spurious secondary enrichment of target elements in weathered, unmineralised rocks	Mobility and re-concentration during weathering, erosion and deposition
Complex geochemical signatures	Superimposition of multiple weathering events
Masking by transported overburden and basin sediments, themselves weathered	Ineffective chemical dispersion during post- depositional weathering and diagenesis
Geophysics	
Attenuation or masking of responses	Increased distance between sensor and target
Development of false anomalies:	
Magnetics	Concentration of magnetite, maghemite.
Electromagnetics, induced polarisation	Low resistivity and marked resistivity contrasts.
Radiometrics	Presence of transported anomalies; disequilibrium due to chemical mobility
Seismic and gravity	Zonation, transitional contacts, density contrast
Remote sensing	Surface response—transported anomalies

devise effective sampling strategies and to interpret the geochemical data sensibly. This can be best achieved by regolith–landform mapping. An outline of the procedure for regolith–landform mapping for exploration is shown in Figure 108.

Regolith–landform mapping has gained greater importance and wider acceptance and usage in the mineral industry over the past decade. However, it is still not a routine procedure despite the many benefits to an exploration program in regolith-dominated terrain. Ideally, regolith and landform maps should be produced at the start of an exploration program. These can include factual maps, which show the units present with little or no genetic bias, and interpretative maps, which summarise the most appropriate geochemical sampling strategies for each terrain unit.

'Factual' maps

The first step is always to make an objective or 'factual' map (Anand & Smith 1993; Anand *et al.* 1993b; Craig & Anand 1993). A regolith–landform map shows regolith–landform units. A regolith–landform mapping unit is an area delineated on a map that occurs as a specific association of regolith materials, landform and possibly bedrock geology. It may consist of multiples or subdivisions of tones, textures, patterns and/or multispectral images visible in aerial photographs, satellite imagery, radiometric or

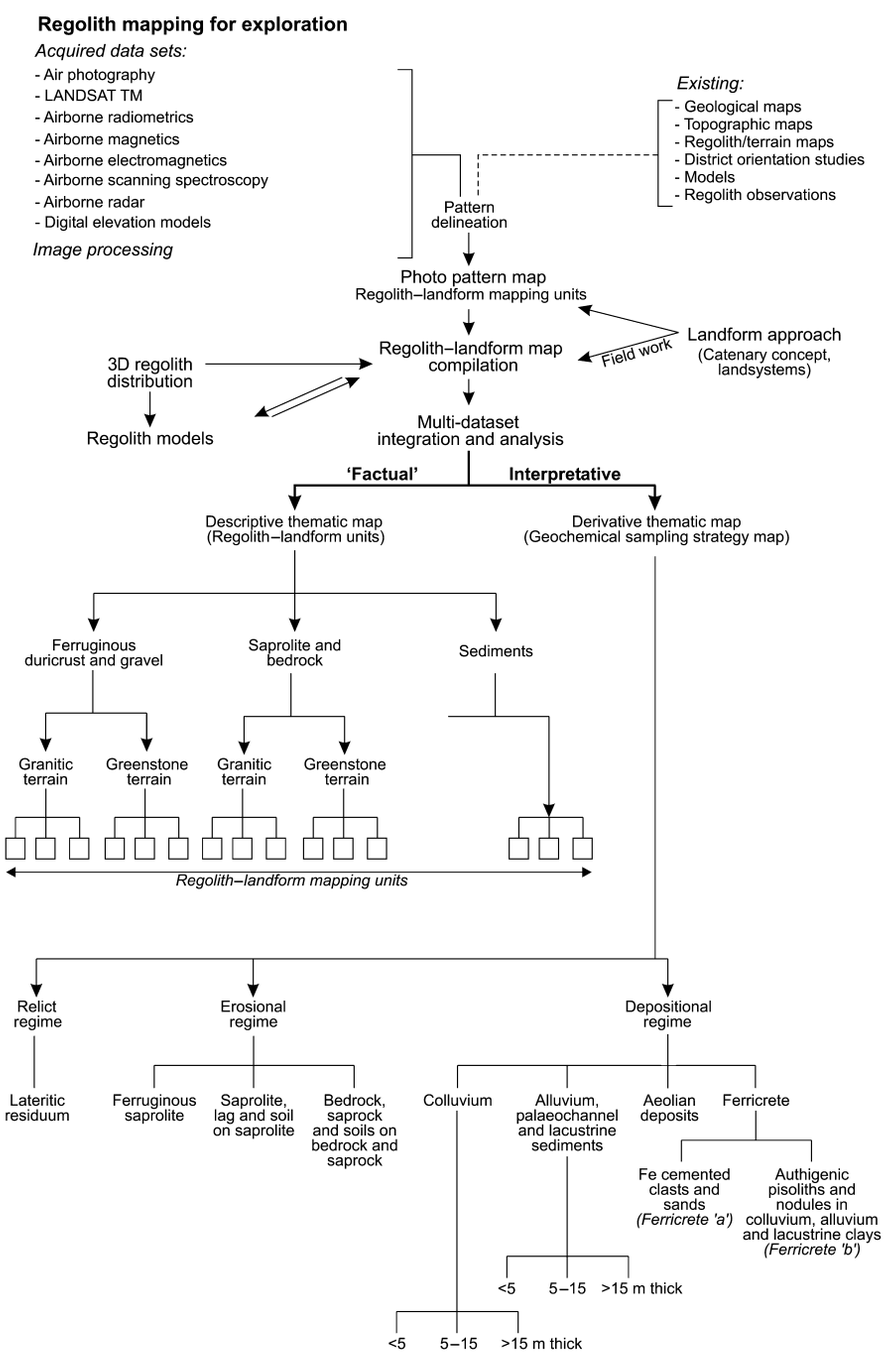

Figure 108 Simplified flow chart of regolith mapping for exploration.

other remotely sensed data. Due to the variability of regolith materials both spatially and compositionally it is commonly difficult to map regolith directly or, more importantly, consistently across an area. Landforms and regolith are formed largely by the same group of processes and once the interrelationships between regolith and landforms are understood, landforms can be used to predict regolith patterns in mapping areas. The landform approach owes much to Christian and Stewart's (1953) early work with CSIRO in the Northern Territory of Australia. There are now enough regolith maps available for various parts of the Yilgarn Craton. This ranges from the detailed work done by the CSIRO Division of Exploration and Mining (Anand & Smith 1993) to the regional mapping of AGSO, CRC LEME and GSWA (Chan *et al.* 1992; Craig & Anand 1993; Kojan & Faulkner 1994; Craig & Churchward 1995; Craig 1995a, b, c; Kojan *et al.* 1996; Lintern *et al.* 1996, 1997). A crucial component to the work is reconciliation of observed regolith–landform relationships with carefully selected field traverses in each mapping unit. Field work should seek information on the distribution of surface and subsurface regolith materials in relation to landscape position. Subsurface information should be established at strategically chosen sites using drilling, escarpments, road cuttings, costeans, mine workings and mine pits. Because most exploration drilling is done by rotary air blast or air core, only chips and powder are available for examination. Skill is required to use the data to interpret regolith correctly. The recognition of lag types, natural vegetation associations, soil and even termitaria types can be useful in the classification and identification of regolith units. Reconnaissance drilling, specifically to establish regolith distribution in areas of sedimentary cover, provides valuable data that should benefit planning where exploration is focused on a district (e.g. 100–500 km^2) rather than on a region.

An essential feature of regolith–landform mapping is the concurrent development of a model(s) of regolith and landform evolution. Regolith–landform models are developed from analysis of the broad regolith–landform framework of an area including elevation distribution, location of major landform features, regolith studies at a detailed scale and drainage-pattern analysis. Such models reflect an understanding of the distribution of regolith materials, in relation to landform and regolith geology. Their predictive qualities can lead to a more efficient and effective mapping program.

A choice of mapping scales is also important. The scale of aerial photographs will influence the choice and definitions of regolith–landform units because of the practicalities of representing heterogeneous assemblages at these scales. The more detailed the scale, the closer the mapping units relate to regolith variations. Regolith–landform mapping in the Yilgarn by CRC LEME uses the RTMAP database and field-mapping system (Pain *et al.* 1991). Regolith and landform types for each regolith–landform mapping unit are indicated by a series of three- or four-letter codes, which describe the unit's major regolith and landform types.

Regolith–landform units can be divided into three principal groups (see above under the heading: Regional Distribution): they include ferruginous duricrust and gravel, saprolite and bedrock and sediments. Distinction between these groups is based mainly on descriptive properties rather than on genesis. Each of these groups, with the exception of the sediments, can be divided into granitic and greenstone terrains.

Mapping methods

REMOTE-SENSING TECHNIQUES FOR REGOLITH DISCRIMINATION

In the Yilgarn Craton, Landsat TM imagery proved to be a highly effective regolith mapping tool particularly in the areas of relative sparse vegetation cover (Gozzard & Tapley 1992). Landsat TM data, when spectrally enhanced, exhibit considerable variation that can be related to the nature of regolith materials. Appropriate processing methods are those that are scene-independent. A very effective enhancement technique that meets this requirement is Band Rationing (the division of one spectral band by another). The particular ratio combination that provided a good range of hues (colours) for the several districts in the Yilgarn Craton was TM bands 5/7, 4/7 and 4/2 and is referred to as CSIROREG. These ratios aid in discrimination of Fe oxides, phyllosilicates and other hydroxyl-bearing minerals and quartz-rich material. The use of these TM bands (Figure 109a on Plate 20) is exemplified by the Lawlers district (Gozzard & Tapley 1992). Correlating the image colours with information collated from the interpretation of aerial photographs and selected ground traverses indicated that this particular image enhancement was a very valuable aid for mapping regolith–landform associations in the Lawlers area. In particular, specific colours in image linked to particular landform settings, proved to be a reliable means for predicting the nature and distribution of regolith materials.

The processed imagery may be used to extend or further subdivide regolith units, particularly in areas of poor landform expression. For regolith mapping, specific techniques have also been devised to model and subtract the influence of vegetation, including principal component analysis (Glikson 1996) and least-squares fit band 7 (LSFIT 7) (Gozzard & Tapley 1994).

Interpretation of the image is enhanced when combined with digital elevation models. Three-dimensional perspective views, which integrate Landsat TM imagery and digital elevation models, allow the TM response to be interpreted within a geomorphological framework.

Further refinements to regolith boundaries can be made with the integration of geophysical data. Airborne gamma-ray spectrometry is used to quantify the radioelement content of the upper 25 mm of the landsurface (Darnley *et al.* 1995). Due to the general association of the radioelements K, Th and U with certain rock types and the varying mobility of these elements under weathering conditions they are useful discriminators of the regolith lithology and its ongoing mechanical and chemical transportation. Crawford *et al.* (1996) and Sanders *et al.* (1997) have made comparisons between the K_2O, Th and U values obtained from the analyses of regolith materials and airborne radiometric data. There is generally good agreement between K_2O and radiometric K, which provides

support for the validity of both the sampling procedure and airborne spectrometry. Some variation is noted between radiometric U values and those obtained from regolith sampling (Sanders & Coker 1997).

Recently the interpretation of airborne synthetic aperture radar (AIRSAR) data has shown that it is capable of providing significant mapping capability not obtainable from other remote sensing tools (such as surface roughness, limited depth penetration and surface inclination) and that it contributes to our understanding of soil and landscape-forming processes (Figure 109b on Plate 20) (Tapley 1998). A recently developed multispectral tool, Hy-map, which measures 128 bands in the reflectance spectra from 400 nm to 2500 nm with a resolution of 15 nm, is proving to be very useful in mineralogical mapping of the landscape.

Aeromagnetic data are primarily collected and used for geological use, but they do provide information to regolith mapping. Not many magnetic minerals occur in the regolith, but maghemite commonly occurs in near-surface materials and materials redistributed by erosion. These maghemite-rich deposits are easy to map on aeromagnetic images. For example, in the Yandal greenstone belt, maghemite-rich gravels are common and have been reworked by drainage systems that are also different from the region at present. The advent of regional aeromagnetic coverage has the potential to provide detail on the distribution of palaeodrainage systems, particularly where the channels contain maghemite.

INTERPRETATIVE OR DERIVATIVE (GEOCHEMICAL SAMPLING-STRATEGY) MAPS

The factual map forms the basis of derivative or interpretative maps based on genetic groupings of the regolith and associated geomorphological features. A geochemical sampling-strategy map is a derivative map that may assist in identifying probable dispersion models. It is based on a genetic interpretation and indicates the most appropriate methods, including sample selection and procedures, sample interval, and data interpretation. It delineates areas or units within which data may be treated uniformly. If the variation in the sample media characteristics is too great, true geochemical anomalies will be lost. For example, bleached saprolite is separated from ferruginous saprolite; thick (>5 m) colluvial cover, which is likely to have a weak or no geochemical response, is separated from thin colluvium over saprolite or duricrust (Figure 108). Each unit within these groups describes regolith properties in a geochemical context. Similarly, lateritic residuum is separated from ferricrete.

Regolith–landform units can be broadly grouped into three major regimes, i.e. relict, erosional and depositional regimes (Churchward *et al.* 1992; Anand *et al.* 1993b; Butt *et al.* 1997a). This scheme is a means of interpreting factual regolith maps of deeply weathered terrain initially developed for application to geochemical exploration on the Yilgarn Craton. It is based on the concept of a landscape that was characterised by an extensive blanket of ferruginous duricrust and which has been modified by erosion and deposition. An interpretation was established based on several districts and for brevity has been referred to as the RED (Relict, Erosional, Depositional) scheme. The relict regime represents a grouping of regolith mapping units in regolith-dominated terrain that are characterised by lateritic residuum at or close to the surface. An erosional regime represents a grouping of regolith mapping units in partly eroded regolith-dominated terrain characterised by saprolite and/or bedrock. A depositional regime is characterised by widespread sediments that may be many metres thick and may overlie lateritic residuum, saprolite or bedrock. This concept is a simplification, because the lateritic residuum (relict regime) did not form a widespread, continuous unit on a peneplaned surface, but rather a discontinuous cover on a broadly undulating plateau, and there have been several cycles of weathering and erosion. Furthermore, the regolith distribution and composition of sediments suggest that the landscape not only included ferruginous duricrust, but also uniformly Fe oxide-stained, red clay soils (Anand *et al.* 1993a). Because of their susceptibility to erosion, red clays have probably contributed much to the sediments in the depositional regimes. For this reason, residual red soil profiles no longer occur in the present landscape and are not included in the definition of the relict regime purely for practical purposes, although theoretically they would. Despite these conceptual limitations, the scheme provides a practical guide for geochemical sampling and interpretation and has application in equivalent terrains elsewhere.

There are several types of ferruginous duricrusts on the Yilgarn Craton. These have formed in a variety of residual and transported materials at different times and cannot all be grouped together. Lateritic residuum is grouped under relict regime, whereas ferricrete is included in the depositional regime.

Appropriate sampling media and geochemical dispersion models can, thus, be deduced for the relict and erosional regimes, whereas in depositional areas, further information is required by drilling in order to establish the model from the degree of preservation of the concealed residual regolith. Geophysical methods have the potential to map subsurface regolith distribution in areas of sedimentary cover. Broadly similar regimes and models apply across many deeply weathered terrains, although depositional units are much more extensive in arid regions. Having established the model type, some broad characteristics of the geochemical expression of mineralisation can be predicted and can be used to design sampling strategies (Figure 110).

DISTINCTION OF RESIDUAL AND TRANSPORTED REGOLITH

Introduction

Discrimination between transported overburden and the underlying residual regolith is highly important in mineral exploration. In view of the wide variety of initial compositions and subsequent changes, finding a universal set of criteria is very difficult. Thus, in assessing the origin of a particular regolith type, it is necessary to combine all types of evidence, including field relationships, fabric, mineralogy and geochemistry. In logging drill spoil, where transported cover is present, it is recommended to work upwards

from recognisable residual materials. This is to avoid mistaking shallow weathering profiles developed in cover sequences for a deeper weathering profile developed from basement. The following criteria may be used to identify transported overburden or to alert geologists to its likelihood.

Geomorphological setting

A general understanding of the geomorphological framework of the area is advantageous. Valuable information on erosional and depositional processes can be obtained from radiometric surveys, Landsat, digital terrain models and aeromagnetic surveys. The topography closely reflects the nature and thickness of the transported cover, except in places of relief inversion. Transported overburden is shallower or absent in upland areas and is thicker in the low-lying areas. Airborne gamma-ray spectrometry can quantify the radioelement content of the upper 25 mm of the land surface. Due to the general association of the radioelements K, Th and U with certain lithologies and the varying mobility of these elements under weathering conditions, they are useful discriminators of the regolith geology and its ongoing mechanical and chemical transportation. Similarly, where aeromagnetic responses clearly indicate the dendritic pattern associated with palaeochannels, the upper 20–30 m of regolith in the lower reaches of the palaeochannels is likely to be transported clays or mottled clays rather than mottled saprolite. Ferruginised sediments (ferricrete) coinciding with the heads of these patterns in topographically high areas may suggest relief inversion.

Fabric and mineralogy

Preservation of primary or metamorphic bedrock fabrics or quartz veins is a key indicator of residual regolith. However, recognition of primary fabric is difficult in deeply weathered environments, as their colour, fabric, mineralogy and compositions have been altered significantly. However, pseudomorphed primary fabrics in the saprolite considerably assist bedrock identification. Care needs to be taken in identifying the extent of rock fabric as gravel- to boulder-sized alluvial, colluvial and glacial pebbles may weather over a long time to produce local patches of saprolite.

Minerals that do not weather or weather only slightly, such as chromite, talc, zircon, muscovite, rutile and tourmaline, may be wholly or partly preserved throughout the profile and give some suggestions of bedrock composition.

The presence of bedding and other sedimentary features in the regolith profile indicate a transported origin, unless these features are preserved in saprolite developed on a sequence of metasedimentary rocks. An unconformity may be recognised by a stone line formed as a lag on the erosional surface.

Polymictic gravels and fractured ferruginous fragments suggest that sediments were derived from a distal rather than a proximal source. Lenses of maghemite-rich gravels at depth indicate material once at the land surface. Nodules

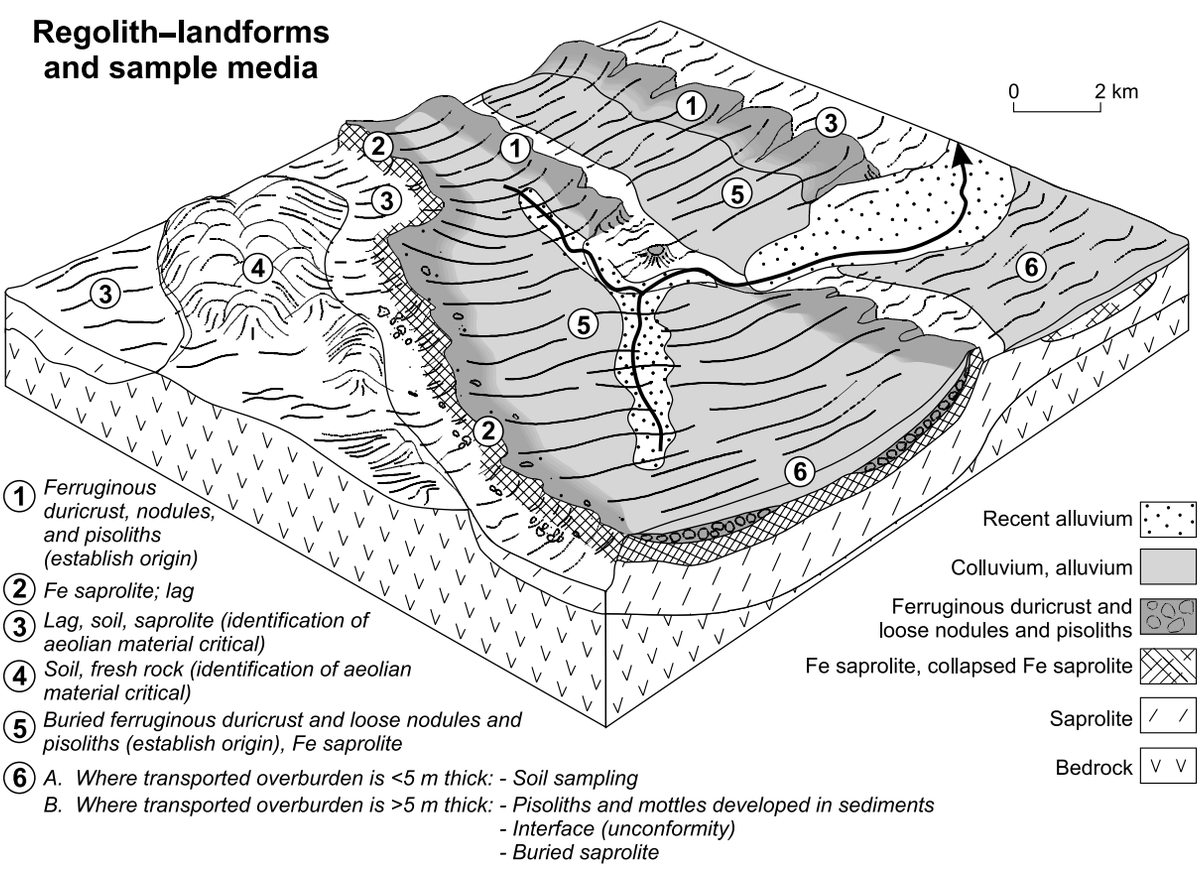

Figure 110 Block diagram illustrating effective sample media available in different regolith–landform units.

and pisoliths with angular shapes and diffuse external borders may have formed *in situ*. Thin yellowish-brown to olive-green cutans are believed to be confined to nodules and pisoliths that have formed *in situ* or have undergone minimal transport. However, cutans may be misleading in palaeochannels where pisoliths with finely laminated cutans have developed *in situ* within transported materials.

Palaeochannels filled with massive, structureless clays may have some rounded, fine-grained (1–10 mm) quartz. The clays are commonly megamottled in the central part of the palaeochannel rather than the edge. Concentric pisoliths, with a variety of nuclei, in grey clays are typical of palaeochannel environments. In reducing environments, carbonaceous material may be present; marine sediments occur in the southeast Yilgarn.

Hardpan (red-brown cementation, Mn oxide precipitates on partings) is not an indication of transportation because it can be developed in most regolith materials (residual or transported). There is generally a significant proportion of aeolian material in near-surface regolith. Silty quartz may be difficult to recognise in the field particularly where sandy soils overlie granitic rocks. Grainsize distributions show a high proportion of fine material. The silt-sized material may be accompanied by clay spherites derived from wind-blown sediments and the Ti/Zr ratio of these materials are low.

Large amounts of colloform, low-Al-substituted goethite is an indicator of ferricrete. Fossil wood on its own cannot be used to indicate transport because roots may penetrate both duricrust and saprolite (Davy & Gozzard 1995). However, relatively large amounts of fossil plant clasts may suggest transport and accumulation in a lake or swamp environment.

Typical of transported overburden is poorly crystalline kaolin, which can be determined by the Portable Infrared Mineral Analyser (PIMA).

Geochemistry

Where the composition of the transported regolith is very similar to that of the residual regolith (e.g. one derived from the other), i.e. where transport has been of limited extent, geochemical discrimination is likely to be difficult or impossible. In some places, even with the best exposure, it is not possible to define the contact between residual and transported regolith precisely due to the complex relationships between the two (e.g. development of a palaeosol, collapse and minor lateral movement of the top of the residual regolith or downward eluviation of clays from the transported regolith into cavities in the residual regolith). These possibilities should be considered in any interpretation of geochemistry. However, sudden changes in chemistry (e.g. K, Zr, T, Si) can indicate an unconformity.

SAMPLE MEDIA

Introduction

Over the past two decades, substantial research has focused on establishing the patterns of geochemical dispersion from concealed mineral deposits through orientation studies. Sampling procedures for different regolith–landform settings have been developed, using a variety of sample media including surficial or buried lateritic residuum, ferruginous saprolite, soil, saprolite and groundwater. Summaries related to the Yilgarn Craton are provided by Butt and Smith (1980), Butt *et al.* (1991, 1997a), Smith *et al.* (1992, 1997), Anand *et al.* (1993a) and Anand (2001).

Ferruginous materials

Ferruginous materials have potential in mineral exploration in many deeply weathered terrains around the world. Costa *et al.* (1999) noted that in the Brazilian Amazon, the 'laterites' offer practically the only geochemical sampling medium available. Ferruginous materials may concentrate ore-related elements, including Au by residual accumulation, local vertical solution transport and precipitation and lateral solution transport and precipitation of elements. All these mechanisms operate to some extent in a particular setting, but the degree to which a particular mechanism dominates is governed by the nature of the ferruginous substrate, the topography and climate. Thus, understanding of the evolution of the landscape is essential to interpreting anomalous element distributions.

Several weathering and landscape processes are involved in forming the geochemical dispersion patterns in lateritic residuum. As a consequence of landscape lowering during weathering, a variety of relatively resistant minerals are incorporated in lateritic residuum. These include partly weathered ferruginised lithorelics, resistant minerals, Fe oxide segregations and gossan fragments derived from oxidised sulfides. Gold in lateritic residuum is concentrated in part by chemical mobility in solution during lateritic weathering, as complexes formed with humic acids produced by rapid degradation of organic matter in the soil. Reduction of the complexes results in the incorporation of fine-grained Au with low Ag contents in Fe oxides (Mann 1984). Because lateritic residuum is developed on undulating landscape, dispersion may occur in sites ranging from upland plateaux and slopes to lowlands. Where lateritic residuum forms in lower parts of the landscape, it is likely that at least part of the Fe accumulated in it has been transported for some distance. Some trace elements (As, Cu) may have behaved similarly, resulting in large dispersion haloes. It is expected that the timing of formation of lateritic residuum may contribute to the strength and size of geochemical anomaly, but there are no data available to support this. Mechanical dispersion affects elements (such as Sn, Au, Cr, W and Zr) held in resistate minerals. However, where mechanical dispersion of gravels has occurred over long distances (>100 m), it has enlarged the halo, although simultaneously causing dilution of element concentrations due to addition of exotic material. Elements, such as As, Cu, W and Sb, which can be anomalous in surface gravels, seem merely to indicate the general area of (or even potential for) mineralisation rather than the position of specific veins or mineralised horizons. In places, physical transport of anomalous nodules and pisoliths can result in local concentrations and thus secondary geochemical anomalies

composed of detrital gravels overlying barren lithologies. The anomaly may be distant from the source. The distance the pisoliths and nodules are moved laterally will depend on several factors such as slope angle, the amount of water that flows over the surface as sheetwash and the proximity to a major drainage channel. Here the understanding of the palaeotopography is essential to the interpretation of anomaly of this type. Conversely, geochemically barren detrital gravels may overlie mineralised lateritic residuum and primary mineralisation.

In the Darling Range (e.g. Boddington), high rainfall and soil waters rich in organic ligands have resulted in leaching of Au from surface pisoliths and reprecipitated it at the base of the bauxite zone (Anand 1994). An implication for exploration is that Au does not necessarily dominate the surface expression anomaly of a Au deposit in lateritic terrain, in this case in a seasonally humid climate.

Lateritic residuum has undergone several cycles of transformation, Fe oxide precipitation and continued dissolution of clay. The same processes have also resulted in Au mobilisation and reprecipitation in various facies of the lateritic residuum. This is evidenced, for example, by the presence of Au in cutans that have developed at various times during the history of the pisolith formation (Anand in press). Similar conclusions have been reported from southern Mali by Freyssinet (1993).

There are generally significant differences in the abundance of Au and trace elements between the magnetic and non-magnetic fractions. The mineralogy of the magnetic and non-magnetic fraction plays a role in element concentrations. The magnetic fraction contains maghemite, which has been demonstrated to form from heating of goethite and hematite during bushfires (Anand & Gilkes 1987b). The non-magnetic fraction contains mainly goethite and hematite. Observations made in synthesis experiments (Sidhu *et al.* 1980) suggest that some elements are ejected during the transformation of goethite to maghemite. Selective dissolution experiments using 6M HCL by Xie (1994) demonstrated that metals incorporated in goethite and hematite, which are subsequently transformed to maghemite and hematite, are more readily extracted during the initial stages of dissolution than in the original mineral phases. This was considered to be due to metal migration to crystal boundaries and defect sites, where the metals are then released during the initial stages of dissolution.

Lateritic residuum geochemistry has been applied successfully in the Yilgarn Craton in exploration for base metals (Smith & Perdrix 1983), Au (Smith *et al.* 1992; Anand *et al.* 1993a; Anand 2001) and for detecting metallogenic provinces (Smith *et al.* 1989). Lateritic residuum (lateritic nodules, pisoliths or duricrust) may be collected from the surface or from the near-surface in duricrust-capped areas or by drilling in depositional regimes. However, in mediterranean environments (as at Boddington), where leaching may have caused depletion of Au from the surface horizons, sampling of lower units (e.g. fragmental duricrust) is recommended (Anand 1994; 2001). Sample intervals may vary from 1 km for regional surveys to as close as 50 m for delineation of drill targets and, ideally analysed for a range of pathfinder elements (such as As, Bi, Sb) in addition to Au. Where exposed, samples should be collected over a 5–10 m radius. Where buried, samples may represent individual 1 m drill intervals or composites over two or more metres. However, where composites are used, they should be from the same unit and should not be a mixture of adjacent units. In drilling to sample buried lateritic residuum, it is important to recognise it and distinguish it from transported gravels and ferricrete. There appears to be no advantage in sampling magnetic nodules and pisoliths instead of the whole sample (Anand 1995; Robertson 1996).

The dispersion halo formed in ferricrete and mottled sediments may result from chemical dispersion by lateral and vertical movements of groundwater. In these situations, deep weathering has continued after deposition of the sedimentary sequence. Such weathering involves vertical and lateral movements of groundwater, which can flow through the weathered *in situ* rocks as well as through the sedimentary cover. This leads to the possibilities of geochemical dispersion into the cover sequence (Anand 2001).

Critical assessment of ferricretes is needed. Where pisoliths have developed *in situ* in sediments there may be enrichment of Au from the underlying mineralisation during their formation. Detrital ferricretes are generally unsuitable as sample media on a local scale, but may contain indications of distal mineralisation, either within their detrital component or in the hydromorphically derived goethite cement. The use of mottles developed in sediments may be appropriate in some locations, but not in others. This should be tested by orientation surveys.

Where lateritic residuum is absent, ferruginous saprolite, mottled saprolite and iron segregations are suitable sampling media, although much closer sampling intervals are necessary (Anand *et al.* 1993a). Drilling is necessary in depositional regimes. Different thresholds must be applied to each sample type.

In mottled saprolite, lateritic residuum or ferricrete, there may be a depleted Au signal in the ferruginous component and enriched Au content in the clayey or silicified matrix. Thus, sampling procedures should be adapted to this strong difference of Au content between the components of the ferruginous zone.

Soils

Soil sampling is very widely used in exploration in deeply weathered terrains. However, soils are developed in a variety of substrates. The geochemical response and the success of the technique depend on the composition of the substrate which, in turn, is determined by the regolith–landform setting. In the duricrust and gravel-capped areas, the soil composition reflects that of duricrust, and dispersion patterns will be similar. However, geochemical contrasts may be strongly reduced due to dilution from transported material. Accordingly, it is probably better to sample lateritic residuum. Alternatively, the coarse fraction of the soil may be a suitable compromise because it commonly consists of lateritic nodules and pisoliths.

In erosional regimes, soils are derived from saprolite and bedrock. Dispersion haloes are generally small (a few metres or tens of metres). Dispersion in soil is greater than

in saprolite and, depending on the truncation of the profile and the extent of past and present leaching, contrasts tend to be greater than in lateritic residuum. Thus, soil sampling is very effective in erosional regimes, particularly for prospect evaluation. Optimum sampling horizons, size fractions and intervals should be determined by orientation surveys. Many soils in erosional areas are hybrid in nature—partly residual and partly aeolian. The use of more than one technique is essential for confident identification. Where these occur over basic or ultramafic rocks, the Ti/Zr ratio and quartz contents readily identify any aeolian contribution.

Soil sampling is of limited value in a depositional regime. As the soils have developed in transported overburden and in the absence of effective hydromorphic or mechanical dispersion, there is little surface expression of buried mineralisation. Where the cover is thin (<5 m), there may be some expression of concealed mineralisation. A range of partial extraction analyses have been used to detect subtle hydromorphic anomalies in soils in depositional areas, but these generally show similar patterns to total analysis and/or give false positive anomalies. Tests of several techniques applied to Au exploration in some well-characterised soils in the Yilgarn Craton showed that they were no more successful in detecting buried mineralisation than total analysis (Butt *et al.* 1997a; Gray *et al.* 1999; Anand 2000). Geochemical responses in soil and shallow transported overburden attributable to buried mineralisation were only found when the sedimentary cover was <5 m thick (with a possible maximum, locally, of 10 m), and in such circumstances were always evident from total analysis.

Pedogenic calcrete

Pedogenic calcrete in the regolith has both advantages and disadvantages for mineral exploration (Butt 1992). It represents a consistent, easily identified sampling medium (generally corresponding to a B or illuvial horizon) for exploration purposes. One of the first records of calcrete as a geochemical sampling medium appears to have been in the Yilgarn Craton when it was investigated as a means to explore for Ni deposits. Calcrete was considered as a geochemical diluent (Mazzucchelli 1972) and many pedogenic forms represent absolute accumulation to soils, and their precipitation causes dilution of the already low abundance of many elements. In addition, their high pH reduces the chemical mobility and dispersion of many elements. Conversely, gold can be enriched in calcareous horizons of soils and may give rise to, or enhance, a near-surface expression of concealed primary or secondary mineralisation (Lintern 1989; Anand *et al.* 1993a; Lintern & Butt 1993). The distributions of Au and Ca (and Ca–Mg) carbonates are very closely correlated, commonly in the top 1–2 m of the soil profile, thereby possibly giving surface expression to mineralisation concealed by up to 10 m of transported overburden. The calcrete horizon is the preferred surface sample medium for Au prospecting, except where residual ferruginous materials are present. No other ore-related elements show this association—indeed most are diluted by the carbonate. Calcrete sampling can be used for regional and prospect evaluation and is commonly done using truck-mounted power augers, collecting the whole calcareous horizon where possible. Alternatively, shallow pits are dug by hand and the indurated calcrete horizon is sampled using a crowbar or similar device (Lintern in press).

Despite their widespread occurrence, the calcretes do not provide equivalent samples across the landscape because, as with conventional soil samples, background and threshold values of Au in calcrete vary according to the substrate as determined by the regolith–landform regimes. Calcrete may occur in different forms and/or positions in the soil profile, representing different ages, stages of development or climatic episodes that may have different levels of metal concentration or dilution. The effectiveness of carbonate sampling in depositional regimes is open to question, particularly where the sediments exceed 5–10 m (Butt *et al.* 1997a; Lintern in press). Furthermore, false or coincidental anomalies can be present over mineralisation where they are derived from detrital, Au-bearing ferruginous granules or saprolite sourced from upslope outcropping mineralisation. Thus, an appreciation of regolith–landform settings in which a variety of calcrete types have developed is essential if these materials are to be used successfully in exploration.

Calcrete sampling reached maturity as an exploration technique when it found the Challenger Gold Deposit (Gawler Craton, South Australia) in 1995. Since then, calcrete has been acclaimed for finding many other Au deposits, especially in Australia.

Sediments

Sediments present formidable problems and challenges to exploration. On the one hand, because of their exotic origin, they have commonly been considered unsuitable as a sample medium; on the other hand, because many of the sediments are ancient and have been subjected to diagenesis and post-depositional weathering, it has been thought that there is potential for their composition to be influenced by hydromorphic dispersion from underlying mineralisation. Hydromorphic dispersion would be expected to enrich the fine fraction. Where the sediments are thin, bioturbation can physically mix sediments and relocate particles to the near-surface. Partial erosion of previously mineralised weathered residuum and deposition in the overburden may lead to a clastic dispersion halo in the colluvial and alluvial sediments. It appears that dispersion into the sediments, whether clastic or hydromorphic, is generally restricted to within approximately 3 m of the unconformity and sampling above this is ineffective (Butt *et al.* 1997b; Anand 2000). The composition of the sediments may broadly reflect those of the catchment but, in general, the catchments are too large and the sediments too difficult to characterise for the provenance to be determined.

Transported and residual materials, above and below the unconformity ('interface' samples) respectively, are sites for secondary enrichment of elements. Dispersion may occur during erosion, during the formation of a residual or partly transported palaeosol, and after sedimentation when the unconformity itself may be a zone for preferential seepage or flow of groundwater. Accurate logging is

essential in order to locate the unconformity and if composite samples are used they should, as far as possible, not mix the sedimentary and residual components.

The saline groundwaters of the Yilgarn can chemically disperse Au, depleting the upper horizons of the regolith and enriching the lower horizons. In residual regolith, this is commonly observed in the saprolite. However, where weathered mineralised systems abut palaeochannels, significant Au dispersion (clastic or chemical) may occur in the palaeochannel sediments. Controls on the location, formation mechanisms and timing of mineralisation are uncertain, but are probably related to specific redox conditions during the continuing arid periods (Butt *et al.* 1997b). The location of the channels is, in part, structurally controlled and follows major faults and shears, many of which are intermittently mineralised.

Lag

Lag is most useful as a sample medium when the fragments are lateritic in origin, and consist of pisoliths, nodules, mottles or fragments of ferruginous saprolite. Lag sampling is most appropriately employed in erosional areas where there is an abundant lag of ferruginous fragments. Here, lag may give broader anomalies than the soils due to mechanical dispersion at the surface. Lag (1 kg) may be swept from the surface and is best sieved to reject both fine transported material and coarse fragments (Robertson 1996). Except for ease of sampling, lag sampling offers little or no advantage over lateritic residuum or (coarse fraction) soil sampling in relict regimes and, indeed, may be much less satisfactory if the lag is derived from a veneer of transported material. As with soil, lag is generally an inappropriate sample medium in depositional areas, except where the transported cover is thin (<2 m) and bioturbation has brought fragments of lateritic residuum to the surface. The compositions of lag, soil and transported overburden reflect that of their provenance, not the underlying bedrock. Where the provenance can be established, lag may be useful for regional sampling, equivalent to drainage sediments.

Saprolite

Geochemical anomalies in saprolite are mostly residual and hydromorphic dispersion haloes rarely extend for more than a few tens of metres from the oxidised mineralisation, although they may exceed 100 m in some semiarid environments (Butt & Zeegers 1992). Thus, drill spacing and depth are critical. Where samples are collected deep in the saprolite, dispersion may be so restricted that the anomaly is much the same width as the primary mineralisation itself. In semiarid environments there may be strong Au depletion (to 100 ppb or lower) from the upper saprolite to depths of 40–50 m, commonly with an underlying, subhorizontal zone of supergene enrichment (Butt 1989), a consequence of Au mobilisation in acid oxidising saline groundwaters. However, the common pathfinder elements, such as As, Sb, Bi and W, are retained through the depletion zone even in highly saline environments; hence, multi-element analysis can assist in the recognition of leached mineralisation. Some of the most technically challenging situations for exploration are posed in depositional areas, where transported overburden lies directly on saprolite. If present, ferruginous saprolite close to the unconformity may provide the most suitable sample medium but, otherwise, carefully targeted, deep drilling, coupled with multi-element analysis, is the best option.

ACKNOWLEDGEMENTS

Many of the studies summarised in this paper were originally part of a series of large multi-disciplinary research projects conducted by CSIRO and CRC LEME through the Australiam Minerals Industry Research Association. Acknowledgement is made to the numerous mining and exploration companies that have supported the research. This paper benefited from constructive reviews by Charles Butt, Colin Pain, Graham Taylor and Ian Robertson. The authors also thank the journal reviewers Bob Bourman and Jonathan Nott for their comments, which helped to improve the final manuscript. Drafting of the figures was done by the Visual Resources Unit of the CRC LEME, Perth and we thank Travis Naughton, Angelo Vartesi and Colin Steel. Pearl Phillips assisted in editing the document. The work was supported by the Australian Government's Cooperative Research Centres Program. We thank Ray Smith for his support during the preparation of this manuscript.

REFERENCES

ALEVA G. J. J. 1986. Classification of laterites and their textures. *In*: Banerjee P. K. ed. *Lateritisation Processes*, pp 8–28. Geological Survey of India Memoir **120**.

ALEVA G. J. J. (Compiler) 1994. *Laterites—Concepts, Geology, Morphology and Chemistry.* International Soil Reference and Information Centre (ISRIC), Wageningen.

ALEXANDER A., MEUNIER J. D., COLIN F. & MATHIAS KOUD J. M. 1997. Plant impact on the biogeochemical cycle of silicon and related weathering processes. *Geochimica et Cosmochimica Acta* **61**, 677–682.

ALEXANDER L. T. & CADY J. G. 1962. Genesis and hardening of laterite in soils. *US Department of Agriculture Technical Bulletin* **1282**.

ALLEN A. D. 1994. Hydrogeology. *In*: Howes K. M. W. ed. *An Inventory and Condition Survey of Rangelands in the North-Eastern Goldfields, Western Australia*, pp. 36–51. Western Australia Department of Agriculture Technical Bulletin **87**.

ALLEN A. D. 1996. Hydrogeology of the Northeastern Goldfields Western Australia. *Geological Survey of Western Australia Record* **1996/4**.

ALLEN B. L. & HAJEK B. F. 1989. Mineral occurrence in soil environments. *In*: Dixon J. B. & Weed S. B. eds. *Minerals in Soil Environments* (2nd edition), pp. 199–278. Soil Science Society of America, Madison.

ALLEY N. F. & CLARKE J. D. A. 1992. Stratigraphy and palynology of Mesozoic sediments from the Great Australian Bight area, southern Australia. *BMR Journal of Australian Geology & Geophysics* **13**, 113–130.

ANAND R. R. 1994. Regolith-landform evolution and geochemical dispersion from the Boddington gold deposit, Western Australia. *CSIRO Division of Exploration and Mining Restricted Report* **24R** (re-issued as Open File Report 3, CRC LEME, Perth, 1998).

ANAND R. R. 1995. Genesis and classification of ferruginous regolith materials in the Yilgarn Craton: implications for mineral exploration. *CSIRO Australia Division of Exploration and Mining Research News* **3**, 3–5.

ANAND R. R. 1997. Some aspects of regolith-landform evolution of the Yilgarn Craton—implications for exploration. *In*: Cassidy K. F., Whitaker A. J. & Liu S. F. eds. *Kalgoorlie '97: An International Conference on Crustal Evolution, Metallogeny and Exploration of the Yilgarn Craton – an Update. Extended Abstracts*, pp. 213–218. Australian Geological Survey Organisation Record **1997/41**.

ANAND R. R. 1998. Distribution, classification and evolution of ferruginous materials over greenstones on the Yilgarn Craton—implications for mineral exploration. *In*: Eggleton R. A. ed. *The State of the Regolith. Proceedings of the 2nd Australian Conference on Landscape Evolution and Mineral Exploration*, pp. 175–193. Geological Society of Australia Special Publication **20**.

ANAND R. R. 2000. Regolith and geochemical synthesis of the Yandal greenstone belt. *In*: Phillips G. N. & Anand R. R. eds. *Yandal Greenstone Belt—Regolith, Geology and Mineralisation*, pp. 79–112. Australian Institute of Geoscientists Bulletin **31**.

ANAND R. R. 2001. Evolution, classification and use of ferruginous regolith materials in gold exploration, Yilgarn Craton, Western Australia. *Geochemistry: Exploration, Environment, Analysis* **1**, 221–236.

ANAND R. R. & BUTT C. R. M. 1988. The terminology and classification of the deeply weathered regolith. *CSIRO Division of Exploration Geoscience Discussion Paper*.

ANAND R. R., CHURCHWARD H. M. & SMITH R. E. 1991c. Regolith-landform development and siting and bonding of elements in regolith units, Mt Gibson district, Western Australia. *CSIRO Division of Exploration Geoscience Restricted Report* **165R** (re-issued as Open File Report 63, CRC LEME, Perth, 1998).

ANAND R. R., CHURCHWARD H. M., SMITH R. E. & GRUNSKY E. C. 1991b. Regolith-landform development and consequences on the characteristics of regolith units, Lawlers District, Western Australia. *CSIRO Division of Exploration Geoscience Restricted Report* **166R** (re-issued as Open File Report 62, CRC LEME, Perth, 1998).

ANAND R. R., CHURCHWARD H. M., SMITH R. E., SMITH K., GOZZARD J. R., CRAIG M. A. & MUNDAY T. J. 1993b. Classification and atlas of regolith-landform mapping units—exploration perspectives for the Yilgarn Craton. *CSIRO Division of Exploration and Mining Restricted Report* **440R** (re-issued as Open File Report 2, CRC LEME, Perth, 1998).

ANAND R. R. & GILKES R. J. 1984a. Weathering of ilmenite in a lateritic pallid zone. *Clays and Clay Minerals* **32**, 363–374.

ANAND R. R. & GILKES R. J. 1984b. Weathering of hornblende, plagioclase and chlorite in meta-dolerite, Australia. *Geoderma* **34**, 261–280.

ANAND R. R. & GILKES R. J. 1984c. Mineralogical and chemical properties of weathered magnetite grains from lateritic saprolite. *Journal of Soil Science* **35**, 559–567.

ANAND R. R. & GILKES R. J. 1987a. Iron oxides in lateritic soils from Western Australia. *Journal of Soil Science* **35**, 607–622.

ANAND R. R. & GILKES R. J. 1987b. The association of maghemite and corundum in Darling Range laterites, Western Australia. *Australian Journal of Soil Research* **35**, 303–311.

ANAND R. R. & GILKES R. J. 1987c. Muscovite in Darling Range laterites. *Australian Journal of Soil Research* **25**, 445–450.

ANAND R. R., GILKES R. J., ARMITAGE T. M. & HILLYER J. W. 1985. Feldspar weathering in lateritic saprolite. *Clays and Clay Minerals* **33**, 31–43.

ANAND R. R., GILKES R. J. & ROACH G. I. D. 1991a. Geochemical and mineralogical characteristics of bauxites, Darling Range, Western Australia. *Applied Geochemistry* **6**, 233–248.

ANAND R. R., PHANG C., WILDMAN J. E. & LINTERN M. J. 1997. Genesis of some calcretes in the southern Yilgarn Craton, Western Australia: implications for mineral exploration. *Australian Journal of Earth Sciences* **44**, 87–103.

ANAND R. R., PHILLIPS G. N., COMPSTON D., COX A., GALLOWAY N., ELY K., PAINE M., PHANG C., ROTHERAM J. & WILDMAN J. E. 1999a. Regolith and geochemistry of the Yandal greenstone belt, Yilgarn Craton, Western Australia. *Australian Institute of Geoscientists Bulletin* **30**, 13–33.

ANAND R. R. & SMITH R. E. 1993. Regolith distribution, stratigraphy and evolution in the Yilgarn Craton—implications for exploration. *In*: Williams P. R. & Haldane J. A. eds. *An International Conference on Crustal Evolution, Metallogeny and Exploration of the Eastern Goldfields: Kalgoorlie '93 Abstracts*, pp. 187–193. Australian Geological Survey Organisation, Canberra.

ANAND R. R., SMITH R. E., INNES J. & CHURCHWARD H. M. 1989b. Exploration geochemistry about the Mt Gibson gold deposits, Western Australia. *CSIRO Division of Exploration Geoscience Restricted Report* **20R** (re-issued as Open File Report 35, CRC LEME, Perth, 1998).

ANAND R. R., SMITH R. E., INNES J., CHURCHWARD H. M., PERDRIX J. L. & GRUNSKY E. C. 1989a. Laterite types and associated ferruginous materials, Yilgarn Block, WA: terminology, classification and atlas. *CSIRO Division of Exploration Geoscience Report* **60R**.

ANAND R. R., SMITH R. E., PHANG C., WILDMAN J. E., ROBERTSON I. D. M. & MUNDAY T. J. 1993a. Geochemical exploration in complex lateritic environments of the Yilgarn Craton, Western Australia. Volumes 1–3. *CSIRO Division of Exploration and Mining Restricted Report* **442R** (re-issued as Open File Report 58, CRC LEME, Perth, 1998).

ANAND R. R., WILDMAN J. E., VARGA Z. S. & PHANG C. 2000. Regolith evolution and geochemical dispersion in transported and residual regolith—Bronzewing gold deposit. *In*: Phillips G. N. & Anand R. R. eds. *Yandal Greenstone Belt—Regolith, Geology and Mineralisation*, pp. 313–332. Australian Institute of Geoscientists Bulletin **31**.

ANAND R. R. & WILLIAMSON A. 2000. Regolith evolution and geochemical dispersion in residual and transported regolith—Calista deposit, Mt McClure district. *In*: Phillips G. N. & Anand, R. R. eds. *Yandal Greenstone Belt—Regolith, Geology and Mineralisation*, pp. 333–349. Australian Institute of Geoscientists Bulletin **31**.

ANDREW R. L. 1980. Supergene alteration and gossan textures of base metal ores in southern Africa. *Mineral Science Engineering* **12**, 193–215.

ANDREWS E. C. 1903. An outline of the Tertiary history of New England. *Geological Survey of New South Wales Record* **7**, 140–216.

APLIN T. E. H. 1975. The vegetation of Western Australia. *In*: *Western Australian Yearbook 14,* pp. 66–81. Western Australian Government Printer, Perth.

Arakel A. V. 1982. Genesis of calcrete in Quaternary soil profiles, Hutt and Leeman Lagoons, Western Australia. *Journal of Sedimentary Petrology* **52**, 109–125.

Arakel A. V. 1986. Evolution of calcrete in palaeodrainages of the Lake Napperby area, Central Australia. *Palaeogeography, Palaeoclimatology, Palaeoecology* **54**, 283–303.

Arakel A. V. & McConchie D. 1982. Classification and genesis of calcrete and gypsite lithofacies in palaeodrainage systems of inland Australia and their relationship to carnotite mineralisation. *Journal of Sedimentary Petrology* **52**, 1149–1170.

Aspandiar M. F. 1992. Weathering of basalt microsystems and mineralogy. MSc thesis, Australian National University, Canberra (unpubl.).

Backhouse J. 1989. Palynology of samples from the Kalgoorlie regional groundwater assessment boreholes KRM-1, KRN-1 and KRN-3. *Geological Survey of Western Australia Palaeontology Report* **1989/1** (unpubl.).

Baes C. F. & Mesmer R. E. 1976. *The Hydrolysis of Cations*. John Wiley and Sons, New York.

Baker G. F. U. 1971. Bauxite deposits of the Darling Range, Western Australia. 12th Pacific Science Congress, Canberra, 1971 (unpubl.).

Baker G. F. U. 1972. Origin of Darling Range bauxites, Western Australia. *Economic Geology* **60**, 215–225.

Ball P. J. & Gilkes R. J. 1987. The Mt Saddleback bauxite deposit, South Western Australia. *Chemical Geology* **60**, 215–225.

Balme B. E. & Churchill D. M. 1959. Tertiary sediments at Coolgardie, Western Australia. *Journal of the Royal Society of Western Australia* **42**, 37–43.

Banfield J. F. & Eggleton R. A. 1990. Analytical transmission electron microscope studies of plagioclase, muscovite and K-feldspar weathering. *Clays and Clay Minerals* **38**, 77–89.

Bardossy G. & Aleva G. J. J. 1990. *Lateritic Bauxites*. Elsevier, Amsterdam.

Beard J. S. 1973. *The elucidation of palaeodrainage patterns in Western Australia through vegetation mapping*. Vegmap Publications, Applecross WA. Occasional Paper **1**.

Bettenay E. 1962. The salt lake system and their associated aeolian features in the semiarid regions of Western Australia. *Journal of Soil Science* **13**, 10–17.

Bettenay E. 1984. Origin and nature of the sandplains. *In*: Pate J. S. & Beard J. S. eds. *Kwongan—Plant Life of the Sandplain*, pp. 51–68. University of Western Australia Press, Perth.

Bettenay E. & Churchward H. M. 1974. Morphology and stratigraphic relationships of the Wiluna hardpan in arid Western Australia. *Journal of the Geological Society of Australia* **21**, 73–80.

Bettenay E. & Hingston F. J. 1961. The soils and land use of the Merredin area, Western Australia. *CSIRO Australia, Division of Soils Soils and Land Use Series* **41**.

Bettenay E. & Hingston F. J. 1964. Development and distribution of soils in the Merredin area, Western Australia. *Australian Journal of Soil Research* **2**, 173–186.

Bettenay E. & Mulcahy M. J. 1972. Soil and landscape studies in Western Australia. Valley forms and surface features of the south-west drainage division. *Journal of the Geological Society of Australia* **18**, 349–357.

Bettenay E. & Smith R. E & Butt C. R. M. 1976. Physical features of the Yilgarn Block. *In*: Smith R. E., Butt C. R. M. & Bettenay E. eds. *Superficial Mineral Deposits and Exploration Geochemistry*, pp. 5–10. 25th International Geological Congress, Sydney, Excursion Guide **41C**.

Bird M. I. & Chivas A. R. 1989. Stable-isotope geochronology of the Australian regolith. *Geochimica et Cosmochimica Acta* **61**, 677–682.

Bird M. I. & Chivas A. R. 1993. Geomorphic and palaeoclimatic implications of an oxygen-isotope geochronology for Australian deeply weathered profiles. *Australian Journal of Earth Sciences* **40**, 345–358.

Bird M. I., Chivas A. R. & McDougall I. 1990. An isotopic study of alunite in Australia. 2. Potassium–argon geochronology. *Chemical Geology* **80**, 133–145.

Birkeland P. W. 1984. *Soils and Geomorphology*. Oxford University Press, New York.

Blatchford T. 1899. So called deep leads at Kanowna: Western Australia. *Geological Survey of Western Australia Annual Report for 1897*, 51–52.

BMR Palaeogeographic Group 1990. *Australia: Evolution of a Continent*. Bureau of Mineral Resources, Canberra.

Borchardt G. 1989. Smectites. *In*: Dixon J. B. & Weed S. B. eds. *Minerals in Soil Environments* (2nd edition), pp. 625–727. Soil Science Society of America, Madison, WI.

Bourman R. P. 1993. Perennial problems in the study of laterite: a review. *Australian Journal of Earth Sciences* **40**, 387–401.

Bourman R. P., Milnes A. R. & Oades J. M. 1987. Investigations of ferricretes and related surficial ferruginous materials in parts of southern and eastern Australia. *Zeitschrift für Geomorphologie* **64**, 1–24.

Bowler J. M. 1976. Aridity in Australia: age, origins and expression in aeolian landforms and sediments. *Earth Science Reviews* **12**, 279–310.

Brady P. & Carrol S. 1994. Direct effects of CO_2 and temperature on silicate weathering: possible implications for climate control. *Geochimica et Cosmochimica Acta* **58**, 1853–1856.

Brand N. W. 1997. Chemical and mineralogical characteristics of weathered komatiitic rocks, Yilgarn Craton, Western Australia: discrimination of nickel sulphide bearing and barren komatiites, PhD thesis, University of Western Australia, Perth (unpubl.).

Brand N. W., Butt C. R. M. & Hellsten K. J. 1996. Structural and lithological controls in the formation of the Cawse nickel laterite deposits Western Australia-implications for supergene ore formation and exploration in deeply weathered terrains. *In*: Grimsey E. J. & Neuss I. eds. *Nickel '96, mineral to market*, pp. 185–191. Australasian Institute of Mining and Metallurgy Special Publication **6/96**.

Braun J. J., Pagel M., Herbillon A. & Rosin C. 1993. Mobilisation and redistribution of REEs and thorium in a syenitic lateritic profile: a mass balance study. *Geochimica et Cosmochimica Acta* **57**, 4419–4434.

Brewer R. & Bettenay E. 1973. Further evidence concerning the origin of the Western Australian sandplains. *Journal of the Geological Society of Australia* **19**, 533–541.

Brewer R., Bettenay E. & Churchward H. M. 1972. Some aspects of the origin and development of the red and brown hardpan soils of Bulloo Downs, Western Australia. *CSIRO Australia Division of Soils Technical Paper* **13**.

Brimhall G. H., Lewis C. J., Ague J. J., Dietrich W. E., Hampel J., Teague T. & Rix P. 1988. Metal enrichment in bauxites by deposition of chemically mature aeolian dust. *Nature* **333**, 819–824.

Brimhall G. H., Lewis C., Ford C., Bratt J., Taylor G. & Warin O. 1991. Quantitative geochemical approach to pedogenesis: Importance of parent material reduction, volume tric expansion, and eolian influx in laterization. *Geoderma* **51**, 51–91.

Brindley G. W. & Robinson K. 1946. Randomness in the structures of kaolinite clay minerals. *Transactions of the Faraday Society* **42B**, 198–205.

Brown H. Y. L. 1873. General report on a geological expedition of that portion of the colony of Western Australia lying southward of the Murchison River and westward of Esperance Bay. Paper No. 1, Votes and Proceedings, Legislative Council, WA, pp 1–20.

Buchanan F. 1807. *A Journey from Madras through the countries of Mysore, Canara and Malabar*. East India Company, London, pp. 436–461.

Bunting J. A., Van de Graaff W. J. E. & Jackson M. L. 1974. Palaeogeography of the Eastern Goldfields, Gibson Desert and Great Victoria Desert. *Geological Survey of Western Australia Annual Report for 1973*, 45–50.

Bureau of Meteorology 1990. *Climate data, Western Australia*. National Climate Centre, Melbourne.

Butler B. E. & Churchward H. M. 1983. Aeolian Processes. *In*: *Soils: an Australian Viewpoint,* pp. 91–101. CSIRO, Melbourne and Academic Press, London.

Butt C. R. M. 1976. Bauxite deposits of the Darling Range. *In*: Smith R. E., Butt C. R. M. & Bettenay E. eds. *Superficial Mineral Deposits and Exploration Geochemistry*, pp. 11–14. 25th International Geological Congress, Sydney, Excursion Guide **41C**.

Butt C. R. M. 1981. The nature and origin of the lateritic weathering mantle, with particular reference to Western Australia. *In*: Doyle H. A., Glover J. E. & Groves D. I. eds. *Geophysical Prospecting in Deeply Weathered Terrains*, pp. 11–29. Geology Department and Extension Service, University of Western Australia Special Publication **6**.

Butt C. R. M. 1983. Aluminosilicate cementation of saprolites, grits and silcretes in Western Australia. *Journal of the Geological Society of Australia* **30**, 179–186.

Butt C. R. M. 1985. Granite weathering and silcrete formation on the Yilgarn Block, Western Australia. *Australian Journal of Earth Sciences* **32**, 415–432.

Butt C. R. M. 1988. Genesis of supergene gold deposits in the lateritic regolith of the Yilgarn Block, Western Australia. *In*: Keays R. R., Ramsay W. R. H. & Groves D. I. eds. *The Geology of Gold Deposits: The perspective in 1989*, pp. 460–470. Economic Geology Monograph **6**.

Butt C. R. M. 1989. Major uranium provinces: Yilgarn Block and Gascoyne Province. *In*: *Recognition of Uranium Provinces,* pp. 273–304. International Atomic Energy Commission, Vienna.

Butt C. R. M. 1991. Dispersion of gold and associated elements in the lateritic regolith, Mystery Zone, Mt Percy, Kalgoorlie, Western Australia. *CSIRO Division of Exploration Geoscience Restricted Report* **156R** (re-issued as Open File Report 45, CRC LEME, Perth. 1998).

Butt C. R. M. 1992. Semi-arid and arid terrains. *In*: Butt C. R. M. & Zeegers H. eds. *Regolith Exploration Geochemistry in Tropical and Subtropical Terrains*, pp. 295–301. Handbook of Exploration Geochemistry **4**. Elsevier, Amsterdam.

Butt C. R. M., Gray D. J., Lintern M. J., Robertson I. D. M., Taylor G. F. & Scott K. M. 1991. Gold and associated elements in the regolith-dispersion processes and implications for exploration. *CSIRO Division of Exploration Geoscience Restricted Report* **167R** (re-issued as Open File Report 29, CRC LEME, Perth, 1998).

Butt C. R. M., Gray D. J., Robertson I. D. M., Lintern M. J., Anand R. R., Britt A. F., Bristow A. P., Munday T. J., Phang C., Smith R. E. & Wildman J. 1997b. Geochemical exploration in areas of transported overburden, Yilgarn Craton and environs, WA. *CSIRO Division of Exploration and Mining Restricted Report* **36R** (re-issued as Open File Report 86, CRC LEME, Perth, 2001).

Butt C. R. M., Horwitz R. C. & Mann A. W. 1977. Uranium occurrences in calcretes and associated sediments in Western Australia. *CSIRO Division of Mineralogy, Perth, Report* **FP16**.

Butt C. R. M., Lintern M. J. & Anand R. R. 1997a. Evolution of regoliths and landscapes in deeply weathered terrain—implications for geochemical exploration. *In*: Gubins A. G., ed. *Proceedings of Exploration '97: Fourth Decennial International Conference on Mineral Exploration*, pp. 323–334. CSIRO Division of Mineralogy, Floreat Park.

Butt C. R. M. & Nickel E. H. 1981. Mineralogy and geochemistry of the weathering of the disseminated nickel sulfide deposit at Mt Keith, Western Australia. *Economic Geology* **76**, 1736–1751.

Butt C. R. M. & Sheppy N. R. 1975. Mineralogy and geochemistry of the weathering of the disseminated nickel sulphide deposit at Mt Keith, Western Australia. *Economic Geology* **76**, 1736–1751.

Butt C. R. M. & Smith R. E. 1980. Conceptual models in exploration geochemistry—Australia. *Journal of Geochemical Exploration* **12**, 89–365.

Butt C. R. M., Williams P. A., Gray D. J., Robertson I. D. M., Schorin H., Churchward H. M., McAndrew J., Barnes S. J. & Tenhaff M. F. 1992. Geochemical exploration for platinum group elements in weathered terrain. *CSIRO Division of Exploration Geoscience Restricted Report* **332R** (re-issued as Open File Report 85, CRC LEME, Perth, 2001).

Butt C. R. M. & Zeegers H. (Editors) 1992. *Regolith exploration geochemistry in tropical and subtropical terrains*. Handbook of Exploration Geochemistry **4**. Elsevier, Amsterdam.

Callot G., Guyon A. & Mousain D. 1985. Inter-relations entre aiguilles de calcite et hyphes myceliens. *Agronomie* **5**, 209–216.

Calvert C. S. 1981. Chemistry and mineralogy of iron substituted kaolinite in natural and synthetic systems. PhD thesis, Texas A and M University, College Station (unpubl.).

Calvert C. S., Buol S. W. & Weed S. B. 1980. Mineralogical transformations of a vertical rock-saprolite-soil sequence in the North Caroline Piedmont. *Soil Science Society of America Journal* **44**, 1096–1112.

Carlisle D. 1978. The distribution of calcretes and gypcretes in south-western United States and their uranium favourability based on the study of deposits in Western Australia and South West Africa (Namibia). *US Department of Energy Open File Report* **GBX-29** (78).

Carlisle D. 1983. Concentration of uranium and vanadium in calcretes and gypcretes. *In*: Wilson E. C. L. ed. *Residual Deposits: Surface Related Weathering Processes and Materials*, pp. 185–195. Blackwell, Oxford.

Carroll D. 1939. Sandplain soils from the Yilgarn Goldfield. *Geological Survey of Western Australia Bulletin* **97**, 161–179.

Cawood P. A. & Nemchin A. A. 2000. Provenance record of a rift basin: U/Pb ages of detrital zircons from the Perth Basin, Western Australia. *Sedimentary Geology* **134**, 209–234.

Chadwick O. A. & Graham R. A. 1999. Pedogenic processes. *In*: Summer M. E. ed. *Handbook of Soil Science*, pp. F1–F20. CRC Press, Boca Raton.

Chadwick O. A., Hendricks D. M. & Nettleton W. D. 1987. Silica in duric soils. 1. A depositional model. *Soil Science Society of America Journal* **51**, 975–982.

Chan R. A., Craig M. A., Hazzel M. S. & Ollier C. D. 1992. Kalgoorlie Regolith Terrain Map and Commentary, Sheet SH51, Western Australia, 1:1 000 000 Regolith Series. *Australian Geological Survey Organisation Record* **1992/8**.

Charters C. J. & Norton L. D. 1994. Micromorphological and chemical properties of Australian soils with hardsetting and duric horizons. *In*: Ringrose-Voase A. J. & Humphreys G. S. eds. *Soil Micromorphology: Studies in Management and Genesis*, pp. 825–834. Developments in Soil Science **22**. Elsevier, Amsterdam.

Chauvel A. 1975. *Recherches Sur la Transformation Des Sols Ferrallitiques Dans la Zone Tropicale a Saisons Contrastees*. ORSTOM, Paris.

Chiquet A., Michard A., Nahon D. & Hamlin B. 1999. Atmospheric input vs in situ weathering in the genesis of calcretes: a Sr isotope study at Galvez (Central Spain). *Geochimica et Cosmochimica Acta* **63**, 311–323.

Christian C. S. & Stewart G. A. 1953. General report on survey of Katherine–Darwin region, 1946. *CSIRO Land Research Series* **1**.

Churchman G. 1990. J: Relevance of different intercalation tests for distinguishing halloysite from kaolinite in soils. *Clays and Clay Minerals* **38**, 591–599.

Churchman G. J. 1999. The alteration and formation of soil minerals by weathering. *In*: Summer M. E. ed. *Handbook of Soil Science*, pp. F3–F76. CRC Press, Boca Raton.

Churchman G. J. & Gilkes R. J. 1989. Recognition of intermediates in the possible transformation of halloysite to kaolinite. *Clay Minerals* **24**, 579–590.

Churchward H. M. 1977. *Landforms, regolith and soils of the Sandstone – Mt Keith Area, WA.* CSIRO Melbourne.

Churchward H. M. 1983. Landforms and regoliths of the Great Plateau, Western Australia. *In*: Wilford G. E. ed. *Regolith in Australia: Genesis and Economic Significance*, pp. 48–56. Bureau of Mineral Resources, Canberra.

Churchward H. M. & Anand R. R. 2000. *Regolith map of the Yilgarn Craton. 1:500 000 Special Edition Map*. CRC LEME/CSIRO Division of Exploration and Mining, Perth (unpubl.).

Churchward H. M., Butler I. K. & Smith R. E. 1992. Regolith–landform relationships in the Bottle Creek orientation study, Western Australia. *CSIRO Division of Exploration Geoscience Restricted Report* **247R** (re-issued as Open File Report 51, CRC LEME, Perth, 1998).

Churchward H. M. & Dimmock G. M. 1989. The soils and landforms of the northern jarrah forrest. *In*: Dell B. ed. *The Jarrah Forrest*, pp. 13–21. Kluwer Academic Publishers, Dordrecht.

Churchward H. M. & Gunn R. H. 1983. Stripping of deep weathered mantles and its significance to soil patterns. *In*: *Soils: an Australian Viewpoint,* pp. 72–81. CSIRO, Melbourne and Academic Press, London.

Clarke E. de C. 1920. Note on the occurrences of boulders, possibly glaciated, near Leonora and Laverton, about latitude 28 degrees 30 minutes South. *Journal of the Royal Society of Western Australia* **6**, 27–32.

Clarke J. D. A. 1993. Stratigraphy of the Lefroy and Cowan palaeo-drainages, Western Australia. *Journal of the Royal Society of Western Australia* **76**, 13–23.

Clarke J. D. A. 1994a. Geomorphology of the Kambalda region, Western Australia. *Australian Journal of Earth Sciences* **41**, 229–239.

Clarke J. D. A. 1994b. Evolution of the Lefroy and Cowan palaeodrainages, Western Australia. *Australian Journal of Earth Sciences* **41**, 55–68.

Clarke J. D. A. & Chenworth L. 1995. Classification, genesis and evolution of ferruginous surface grains. *AGSO Journal of Australian Geology & Geophysics* **16**, 213–221.

Cockbain A. E. & Hocking R. M. 1989. Revised stratigraphic nomenclature in Western Australia Phanerozoic Basins. *Geological Survey of Western Australia Record* **1989/15**.

Commander D. P., Kern A. M. & Smith R. A. 1991. Hydrogeology of the Tertiary palaeochannels of the Kalgoorlie region (Roe Palaeodrainage). *Geological Survey of Western Australia Record* **1991/10**.

Conacher A. J. 1991. Lateritic duricrust and relief inversion in Australia. The laterite profile, ferricrete and unconformity—a discussion. *Catena* **18**, 585–586.

Cope R. N. 1975. Tertiary epeirogeny in the southern part of Western Australia. *Geological Survey of Western Australia Annual Report for 1974*, 40–46.

Cornell R. M. & Schwertmann U. 1996. *The Iron Oxides*. VCH, Weinheim.

Costa M. L., Romulo S. & Costa A. N. 1999. The geochemical association of Au–As–B–(Cu)–Sn–W in latosols, colluvium, lateritic iron crust and gossans in Carajas, Brazil: importance for primary ore identification. *Journal of Geochemical Exploration* **67**, 33–49.

Coventry R. J., Taylor R. M. & Fitzpatrick R. W. 1983. Pedological significance of the gravels in some red and grey earths of central north Queensland. *Australian Journal of Soil Research* **21**, 219–240.

Craig M. A. 1995a. *Sir Samuel regolith–landforms. 1:250 000 Regolith Landforms Map*. Australian Geological Survey Organisation, Canberra.

Craig M. A. 1995b. *Leonora regolith–landforms. 1:250 000 Regolith Landforms Map*. Australian Geological Survey Organisation, Canberra.

Craig M. A. 1995c. *Menzies regolith–landforms. 1:250 000 Regolith Landforms Map*. Australian Geological Survey Organisation, Canberra.

Craig M. A. & Anand R. R. 1993. *Kalgoorlie–Kurnalpi regolith–landforms. 1:250 000 Special Edition Map*. CRCAMET/Australian Geological Survey Organisation, Canberra.

Craig M. A. & Churchward H. M. 1995. *Wiluna regolith–landforms. 1:250 000 Regolith Landforms Map*. Australian Geological Survey Organisation, Canberra.

Crawford R. A., Faulkner J. A., Sanders A. J., Lewis J. D. & Gozzard J. R. 1996. *Geochemical mapping of the Glengarry 1:250 000 sheet. Regolith Geochemistry Series Explanatory Notes*. Geological Survey of Western Australia, Perth.

D'Hoore J. 1954. Proposed classification of the accumulation zones of free sesquioxides on a genetic basis. *Sols Africains* **3**, 66–81.

Dammer D., McDougall I. & Chivas A. R. 1999. Timing of weathering-induced alteration of manganese deposits in Western Australia: evidence from K/Ar and $^{40}Ar/^{39}Ar$ dating. *Economic Geology* **94**, 87–108.

Dan J. 1977. The distribution and origin of nari and other lime crusts in Israel. *Israel Journal of Earth Sciences* **26**, 68–83.

Daniels J. L. 1975. Palaeogeographic development of Western Australia—Precambrian. *Geological Survey of Western Australia Memoir* **2**, 437–450.

Darnley A. G., Björklund A., Bølviken B., Gustavsson N., Koval. P. V., Plant J. A., Steenfelt A., Tauchid M. & Xie X. 1995. *A Global Geochemical Database for Environmental and Resource Management*. Report IGCP 259, UNESCO Publishing.

David T. W. E. 1911. Notes on some of the chief tectonic lines of Australia. Presidential Address. *Journal and Proceedings of the Royal Society of New South Wales* **65**, 1–60.

Davis W. M. 1899. The geographical cycle. *Geographical Journal* **14**, 481–504.

Davy R. 1979. A study of laterite profiles in relation to bedrock in the Darling Range, near Perth, WA. *Geological Survey of Western Australia Report* **8**.

Davy R., Clarke R., Sale M. & Parker M. 1988. The nature and origin of the gold-bearing laterite at Mount Gibson, Western Australia. *In*: *Proceedings 2nd International Conference on Prospecting in Arid Terrain, Perth, Western Australia,* pp. 45–47.

Davy R. & El-Ansary M. 1986. Geochemical patterns in the laterite profile at the Boddington gold deposit, Western Australia. *Journal of Geochemical Exploration* **26**, 119–144.

Davy R. & Gozzard J. R. 1995. Lateritic duricrusts of the Leonora area, Eastern Goldfields, Western Australia: a contribution to the study of transported laterites. *Geological Survey of Western Australia Record* **1994/8**.

Dell M. 1992. Regolith–landform relationships and geochemical dispersion about the Kanowna Belle gold deposit, WA. BSc (Hons) thesis, University of Tasmania, Hobart (unpubl.).

Dell M. R. & Anand R. R. 1995. Kanowna District. *In*: Butt C. R. M., Anand R. R. & Smith R. E. eds. *17th International Geochemical Exploration Symposium, Excursion 3: Regolith Geology and Exploration Geochemistry in the Yilgarn Craton, Western Australia*, pp. 95–110. CSIRO Division of Exploration and Mining, Floreat Park.

Della Marta J. & Anand R. R. 1998. Characteristics of the regolith at the Jundee deposit, Wiluna region, W.A. *In*: Britt A. F. & Bettenay L. eds. *New Approaches to an Old Continent, 3rd Australian Regolith Conference Abstracts, Regolith '98*, pp. 38–39. Cooperative Research Centre for Landscape Evolution and Mineral Exploration, Perth.

Durand R. 1979. La pedogenese en pays calcaire dans le nord-est de la France. *Sciences Geologiques Memoire* **55**, 198.

Dury G. H. 1969. Rational descriptive classification of duricrusts. *Earth Science Journal* **3**, 77–86.

Dusci M. E. 1994. Regolith–landform evolution of the Black Flag area with emphasis on the upper reaches of the Roe Palaeochannel System, Western Australia. BSc (Hons) thesis, Curtin University of Technology, Perth (unpubl.).

Eggleton R. A. 1998. Weathering. In: Eggleton R. A. ed. *The State of the Regolith. Proceedings of the 2nd Australian Conference on Landscape Evolution and Mineral Exploration*, pp. 126–140. Geological Society of Australia Special Publication **20**.

Eggleton R. A. (Editor) 2001. *Glossary of Regolith—Surficial Geology, Soils and Landscapes*. CRC LEME Publication, Perth.

Eggleton R. A. & Taylor G. 1998. Selected thoughts on 'laterite'. *In*: Taylor G. & Pain C. eds. *New Approaches to an Old Continent, 3rd Australian Regolith Conference Proceedings, Regolith '98*, pp. 209–226. Cooperative Research Centre for Landscape Evolution and Mineral Exploration, Perth.

Elias M., Donaldson M. J. & Giorgetta N. 1981. Geology, mineralogy and chemistry of lateritic nickel–cobalt deposits near Kalgoorlie, Western Australia. *Economic Geology* **76**, 1775–1783.

Ely K. 2000. Bedrock lithologies, mineralisation and deformation, and their relationship to weathering in the Yandal belt. *In*: Phillips G. N. & Anand R. R. eds. *Yandal Greenstone Belt—Regolith, Geology and Mineralisation*, pp. 115–123. Australian Institute of Geoscientists Bulletin **31**.

Embleton B. J. 1981. A review of the paleomagnetism of Australia and Antarctica. *In*: McElhinney M. W. & Valencio D. A. eds. *Paleoreconstruction of the Continents*, pp. 77–92. American Geophysical Union Geodynamics Series **2**.

Eswaran H. & Wong C. B. 1978. A study of a deep weathering profile on granite in Peninsular Malaysia. Parts I, II and III. *Soil Science Society of America Journal* **42**, 144–158.

Eyles N. & De Broekert P. 2001. Permian tillites and glacial 'tunnel' valleys in the Eastern Goldfields, Western Australia: evidence of a wet-based Pilbara Ice Sheet. *Palaeogeography, Palaeoclimatology, Palaeoecology* **171**, 29–40.

Fairbridge R. W. & Finkl C. W. 1979. Cratonic erosional unconformities and peneplains. *Journal of Geology* **88**, 69–86.

Finkl C. W. 1979. Stripped (etched) landsurfaces in southern Western Australia. *Australian Geographical Studies* **17**, 33–52.

Finkl C. W. & Churchward H. M. 1973. The etched landsurfaces of southwestern Australia. *Journal of the Geological Society of Australia* **20**, 295–307.

Finkl C. W. & Fairbridge R. W. 1979. Paleogeographic evolution of a rifted cratonic margin: SW Australia. *Palaeogeography, Palaeoclimatology, Palaeoecology* **26**, 221–252.

Fitzpatrick R. W. 1988. Iron compounds as indicators of pedogenic processes: examples from the southern hemisphere. *In*: Stucki J. W., Goodman G. A. & Schwertmann U. eds. *Iron in Soils and Clay Minerals*, pp. 351–396. Reidel, Dordrecht.

Fitzpatrick R. W. & Schwertmann U. 1982. Al-substituted goethite—an

indicator of pedogenic and other weathering environments in South Africa. *Geoderma* **27**, 335–347.

Flach K. W., Nettleton W. D. & Nelson R. E. 1974. The micromorphology of silica cemented soil horizons in western North America. *In*: Rutherford G. K. ed. *Soil Microscopy*, pp. 715–729. Limestone Press, Kingston, ON.

Fontes M. P. F. & Weed S. B. 1991. Iron oxides in selected Brazilian Oxisols. I. Mineralogy. *Soil Science Society of America Journal* **55**, 1143–1149.

Foo M. F. P. 1999. Host of gold and ore related elements in ferruginous materials in mineralised environments—implications for exploration. BSc (Hons) thesis, Curtin University of Technology, Perth (unpubl.).

Ford A. J. H. 1996. Re-interpreting the north eastern margin of the Cobar region, using drainage channel morphology. *In*: Cook W. G., Ford A. J. H., McDermott J. J., Standish P. N., Stegman C. L. & Stegman T. M. eds. *The Cobar Mineral Field*, pp. 113–223. Australasian Institute of Mining and Metallurgy, Melbourne, Spectrum Series **3/96**.

Frakes L. A. & Barron E. J. 2001. Phanerozoic general circulation model results and quantitative climate data for Australia. *Australian Journal of Earth Sciences* **48**, 643–655.

Frakes L. A., McGowran B. & Bowler J. M. 1987. Evolution of Australian environments. *In*: Dyne G. R. & Walton D. W. eds. *Fauna of Australia*, pp. 1–16. Australian Government Publishing Service, Canberra.

Freyssinet P. 1993. Gold dispersion related to ferricrete pedogenesis in South Mali: application to geochemical exploration. *Recherche Minere* **510**, 25–41.

Gardiner N. 1993. Regolith geology and geochemistry of the Steinway gold prospect, Kalgoorlie, Western Australia. BSc (Hons) thesis, University of Western Australia, Perth (unpubl.).

Gee R. E., Baxter J. L., Wilde S. A. & Williams I. R. 1981. Crustal Development in the Archaean Yilgarn Block, Western Australia. *In*: Glover J. E. & Groves D. I. eds. *Archaean Geology*, pp. 43–57. Geological Society of Australia Special Publication **7**.

Geidens L. 1973. Bauxitic laterites of the south-western part of Western Australia. *In*: *Australasian Institute of Mining and Metallurgy Conference Proceedings,* pp. 173–182.

Gile L. H. 1961. A classification of Ca horizons in soils of a desert region, Dona Ana County, New Mexico. *Soil Science Society of America Proceedings* **25**, 52–61.

Gile L. H., Peterson F. F. & Grossman R. B. 1965. The K horizon: a master soil horizon of carbonate accumulation. *Soil Science* **99**, 74–82.

Gile L. H., Peterson F. F. & Grossman R. B. 1966. Morphological and genetic sequences of carbonate accumulation in desert soils. *Soil Science* **101**, 347–360.

Gilkes R. J. 1998. Biology and the regolith: an overview. *In*: Eggleton R. A. ed. *The State of the Regolith. Proceedings of the 2nd Australian Conference on Landscape Evolution and Mineral Exploration*, pp. 110–125. Geological Society of Australia Special Publication **20**.

Gilkes R. J., Anand R. R. & Suddhiprakarn A. 1986. How the microfabric of soils may be influenced by the structure and chemical composition of parent materials. *In*: *Transaction International Congress Soil Science Proceedings, Hamburg,* pp. 1093–1105.

Gilkes R. J., Scholz G. & Dimmock G. M. 1973. Lateritic deep weathering of granite. *Journal of Soil Science* **24**, 523–536.

Gilkes R. J. & Suddhiprakarn A. 1979. Biotite alteration in deeply weathered granite. 11. The oriented growth of secondary minerals. *Clays and Clay Minerals* **27**, 361–367.

Glassford D. K. & Semeniuk V. 1995. Desert-aeolian origin of Late Cainozoic regolith in arid and semiarid South-western Australia. *Palaeogeography, Palaeoclimatology, Palaeoecology* **114**, 131–166.

Glikson A. Y. 1996. *Landsat Thematic Mapper-directed principal components, Pinderi Hills 1:100 000 sheet*. Australian Geological Survey Organisation, Canberra.

Goudie A. S. 1973. Duricrusts in tropical and subtropical landscapes. Clarendon Press, Oxford.

Goudie A. S. 1983. Calcrete. *In*: Goudie A. S. & Pye K. eds. *Chemical Sediments and Geomorphology: Precipitates and Residua in the Near-Surface Environment*, pp. 93–101. Academic Press, London.

Gower C. F. 1976. *Laverton, Western Australia 1:250 000 Geological Series Explanatory Notes*. Geological Survey of Western Australia, Perth.

Gozzard J. R. & Tapley I. J. 1992. Regolith–Landform Mapping in the Lawlers District—Terrain Classification Mapping. *CSIRO Division of Exploration Geoscience Perth Restricted Report* **240R**.

Gozzard J. R. & Tapley I. J. 1994. Landsat thematic processing techniques for regolith landform mapping in the NE Goldfields Region of Western Australia. *In*: *7th Australasian Remote Sensing Conference Proceedings, Canberra,* pp. 951–958.

Gray D. J. 1993. Investigation of the hydrogeochemical dispersion of gold and other elements in the Wollubar palaeodrainage, Western Australia. *CSIRO Division of Exploration Geoscience Restricted Report* **387R** (re-issued as Open File Report 33, CRC LEME, Perth, 1998).

Gray D. J. & Cudahy T. J. 1996. Pilot spectral study of the Mount Percy gold deposit, Western Australia. *CSIRO Australia Exploration and Mining Report* **175R**.

Gray D. J. & Lintern M. J. 1994. The solubility of gold in soils from semiarid areas of Western Australia. *CSIRO Australia, Exploration and Mining Research News* **1**, 8–9.

Gray D. J., Wildman J. E. & Longman G. D. 1999. Selective and partial extraction analyses of transported overburden for gold exploration in the Yilgarn Craton, Western Australia. *Journal of Geochemical Exploration* **67**, 51–66.

Gregory F. T. 1861. On the geology of a part of Western Australia. *Quarterly Journal of the Geological Society* **17**, 475–483.

Gregory J. W. 1914. The lake system of Westralia. *Geographical Journal* **80**, 656–664.

Grey I. E. & Reid A. F. 1975. The structure of pseudorutile and its role in the natural alteration of ilmenite. *American Mineralogist* **60**, 898–906.

Grimley M. J. 1995. Mechanisms of supergene gold deposition and dispersion in the weathered zone at Norseman, southern Western Australia. BSc (Hons) thesis, University of Queensland, Brisbane (unpubl.).

Grubb P. L. C. 1966. Some aspects of lateritisation in Western Australia. *Journal of the Royal Society of Western Australia* **49**, 117–125.

Grubb P. L. C. 1971. Mineralogical anomalies in the Darling Range bauxites at Jarrahdale, Western Australia. *Economic Geology* **66**, 1005–1016.

Hallberg J. A. 1984. A geochemical aid to igneous rock identification in deeply weathered terrain. *Journal of Geochemical Exploration* **20**, 1–8.

Hickman A. H., Smurthwaite A. J., Brown I. M. & Davy R. 1992. Bauxite mineralisation in the Darling Range, Western Australia. *Geological Survey of Western Australia Report* **33**.

Hill S. M., McQueen K. G. & Foster K. A. 1999. Regolith carbonate accumulations in Western and Central NSW: characteristics and potential as an exploration sampling medium. *In*: Taylor G. & Pain C. eds. *New Approaches to an Old Continent, 3rd Australian Regolith Conference Proceedings, Regolith '98*, pp. 191–208. Cooperative Research Centre for Landscape Evolution and Mineral Exploration, Perth.

Hills E. S. 1975. *The Physiography of Victoria*. Whitcombe and Tombs, Melbourne.

Hingston F. & Gailitis V. 1976. The geographic variation of salt precipitated over Western Australia. *Australian Journal of Soil Research* **14**, 319–335.

Hobson R. A. & Miles K. R. 1950. Geology of portion of the Mt Margaret Goldfield. *Geological Survey of Western Australia Bulletin* **103** (Part 1).

Hutton J. T., Twidale C. R. & Milnes A. R. 1978. Characteristics and origin of some Australian silcretes. *In*: Langford-Smith T. ed. *Silcretes in Australia*, pp. 19–39. Department of Geography, University of New England, Armidale.

Idnurm M. 1985. Late Mesozoic and Cenozoic palaeomagnetism of Australia—1. A redetermined polar wander path. *Geophysical Journal of the Royal Astronomical Society* **83**, 399–418.

Idnurm M. 1994. New Late Eocene pole for Australia, time-averaging of remanence directions, and palaegeographic reference systems. *Geophysical Journal International* **117**, 827–833.

Idnurm M. & Senior B. R. 1978. Palaeomagnetic ages of the Late Cretaceous and Tertiary weathered profiles in the Eromanga

Basin, Queensland. *Palaeogeography, Palaeoclimatology, Palaeoecology* **24**, 263–277.

Jennings J. N. & Mabbutt J. A. 1977. Physiographic outlines and regions. *In*: Jeans D. M. ed. *Australia: a Geography*, pp. 38–53. University Press, Sydney.

Jessup R. W. 1960. The lateritic soils of the south-eastern portion of the Australian arid zone. *Journal of Soil Science* **11**, 106–113.

Johnston S. L., Commander D. P. & O'Boy C. A. 1999. Groundwater resources of the Northern Goldfields, Western Australia. *Western Australia Waters and Rivers Hydrogeological Record Series Report* **HG 2**.

Johnston S. L., Mohsenzadeh H., Yesterener C. & Koomberi H. A. 1998. Northern Goldfields regional groundwater assessment bore completion reports. *Western Australia Water and Rivers Commission, Hydrogeology Report* **117** (unpubl.).

Johnstone M. H., Lowry D. C. & Quilty P. G. 1973. The geology of south-western Australia—a review. *Journal of the Royal Society of Western Australia* **56**, 5–15.

Jones B. G. 1990. Cretaceous and Tertiary sedimentation on the western margin of the Eucla Basin. *Australian Journal of Earth Sciences* **37**, 317–329.

Jones M. & Lidbury R. 1998. Unconformity-related weathered laterite profiles at Mt Gibson gold mine, Yilgarn Craton, Western Australia. *In*: Britt A. F. & Bettenay L. eds. *New Approaches to an Old Continent, 3rd Australian Regolith Conference Abstracts, Regolith '98,* p. 30. Cooperative Research Centre for Landscape Evolution and Mineral Exploration, Perth.

Jutson J. T. 1914. An Outline of the Physiographical Geology (Physiography) of Western Australia. *Geological Survey of Western Australia Bulletin* **61**.

Jutson J. T. 1934. The Physiography (Geomorphology) of Western Australia. *Geological Survey of Western Australia Bulletin* **95**.

Kelly A. J. 1994. Regolith–landform evolution and secondary nickel dispersion in the Takashi Ultramafic Belt, Forrestania, W.A. BSc (Hons) thesis, Curtin University of Technology, Perth (unpubl.).

Kelly A. & Anand R. R. 1995. Regolith–landform evolution and secondary nickel dispersion in the Takashi Ultramafic Belt, Forrestania, Western Australia. *In*: Camuti K. S. ed. *17th International Geochemical Exploration Symposium, Extended Abstracts*, pp. 132–134.

Kern A. M. & Commander P. 1993. Cainozoic stratigraphy in the Roe Palaeodrainage of the Kalgoorlie region, Western Australia. *Geological Survey of Western Australia Report* **34**, 85–95.

Keywood M. D., Chivas A. R., Field L. K., Cresswell R. G. & Ayers G. P. 1997. The accession of chloride to the western half of the Australian continent. *Australian Journal of Soil Research* **35**, 1177–1189.

Killick M. 1998. Phanerozoic denudation of the Western Shield of Western Australia. *Geological Society of Australia Abstracts* **49**, 248.

Killigrew L. P. & Glassford D. K. 1976. Origin and significance of kaolin spherites in sediments of south-western Australia. *Search* **7**, 393–394.

King L. 1950. C: The cyclic landsurfaces of Australia. *Proceedings of the Royal Society of Victoria* **62**, 79–95.

King J. 1991. Relation of bedrock geology to regolith–landform and geochemistry in the Gindalbi area, Western Australia. BSc (Hons) thesis, Curtin University of Technology, Perth (unpubl.).

Klappa C. F. 1979. Calcified filaments in Quaternary calcretes: organo–mineral interactions in the subaerial vadose environment. *Journal of Sedimentary Petrology* **49**, 955–968.

Klappa C. F. 1983. A process response model for the formation of pedogenic calcretes. *In*: Wilson R. C. L. ed. *Residual Deposits: Surface Related Weathering Processes and Materials*, pp. 211–220. Blackwell, Oxford.

Kohn B. L., O'Sullivan P. B., Gleadow A. J. W., Karner G. D. & Weissel J. K. 1998. Late Palaeozoic cooling of southwest Australian terranes inferred from apatite fission track thermochronology. *Geological Society of Australia Abstracts* **41**, 253.

Kojan C. J. & Faulkner J. A. 1994. *Geochemical mapping of the Menzies 1:250 000 Sheet. Regolith Geochemistry Explanatory Notes*. Geological Survey of Western Australia, Perth.

Kojan C. J., Faulkner J. A. & Sanders A. J. 1996. *Geological mapping of the Sir Samuel 1:250 000 Sheet. Regolith Geochemistry Explanatory Notes*. Geological Survey of Western Australia, Perth.

Krcmarov R., Beardsmore T. J., King J., Kellett R. & Hay R. 2000. Geology, regolith, mineralisation and mining of the Darlot–Centenary gold deposit Yandal belt. *In*: Phillips G. N. & Anand R. R. eds. *Yandal Greenstone Belt, Regolith, Geology and Mineralisation*, pp. 351–379. Australian Institute of Geoscientists Bulletin **31**.

Ladhams B. A. 1994. The sediments and regolith of the middle reaches of the Roe Palaeochannel near Kanowna, Eastern Goldfields, Western Australia. BSc (Hons) thesis, Curtin University of Technology, Perth (unpubl.).

Lambert I. B. & Perkin D. J. 1998. Australia's mineral resources and their global status. *AGSO Journal of Australian Geology & Geophysics* **17**, 1–14.

Lamplugh G. W. 1902. Calcrete. *Geological Magazine* **9**, 75.

Langford-Smith. T. 1978. *Silcrete in Australia*. Department of Geography, University of New England, Armidale.

Lawrance L. M. 1991. Distribution of gold and ore-associated elements within lateritic weathering profiles of the Yilgarn Block, Western Australia. PhD thesis, University of Western Australia, Perth (unpubl.).

Lawrance L. M. 1996. Geochemical responses within lateritic profiles over barren and mineralised ultramafic rocks.: implications for nickel exploration in the Yilgarn Block, Western Australia. *In*: Grimsey E. J. & Neuss I. eds. *Nickel '96, mineral to market*, pp. 173–178. Australasian Institute of Mining and Metallurgy Special Publication **6/96**.

Le Blanc Smith G. 1993. Geology and Permian coal resources of the Collie Basin, Western Australia. *Geological Survey of Western Australia Report* **38**.

Li Z. X., Powell C. McA. & Thruff G. A. 1990. Australian Palaeozoic palaeomagnetism and tectonics—II. A revised apparent polar wander path and palaeogeography. *Journal of Structural Geology* **12**, 567–575.

Lintern M. J. 1989. Study of the distribution of gold in soils at Mt Hope. *CSIRO Division of Exploration Geoscience Restricted Report* **24R** (re-issued as Open File Report 65, CRC LEME, Perth, 1998).

Lintern M. J. Exploration for gold using calcrete – lessons from the Yilgarn Craton, Western Australia. *Geochemistry: Exploration, Environment, Analysis* (in press).

Lintern M. J. & Butt C. R. M. 1993. Pedogenic carbonate: an important sampling medium for gold exploration in semiarid areas. *Exploration Research News* **7**, 7–11.

Lintern M. J., Churchward H. M. & Butt C. R. M. 1990. Multi-element soil survey of the Mount Hope area, Western Australia. *CSIRO Division of Exploration Geoscience Restricted Report* **109R** (re-issued as Open File Report 40, CRC LEME, Perth, 1998).

Lintern M. J., Craig M. A. & Carver R. N. 1997. Geochemical studies of the soil and vegetation at the Apollo Au deposit, Kambalda, Western Australia. *CSIRO Division of Exploration and Mining Restricted Report* **274R** (re-issued as Open File Report 103, CRC LEME, Perth, 2001).

Lintern M. J., Craig M. A., Walsh D. M. & Sheridan N. C. 1996. The distribution of gold and other elements in surficial materials from the Higginsville palaeochannel gold deposits, Norseman, Western Australia. *CSIRO Division of Exploration and Mining Restricted Report* **275R** (re-issued as Open File Report 102, CRC LEME, Perth, 2001).

Lintern M. J. & Gray D. J. 1995a. Progress statement for the Kalgoorlie Study Area—Kurnalpi Prospect, Western Australia. *CSIRO Division of Exploration and Mining Restricted Report* **97R** (re-issued as Open File Report 89, CRC LEME, Perth, 2001).

Lintern M. J. & Gray D. J. 1995b. Progress statement for the Kalgoorlie Study Area—Enigma Prospect (Wollubar), Western Australia. *CSIRO Division of Exploration and Mining Restricted Report* **98R** (re-issued as Open File Report 90, CRC LEME, Perth, 2001).

Litchfield W. H. & Mabbutt J. A. 1962. Hardpan soils of semiarid Western Australia. *Journal of Soil Science* **13**, 148–160.

Loughnan F. C. 1969. *Chemical Weathering of the Silicate Minerals*. American Elsevier Co., Inc, New York.

Lowry D. C. 1965. Geology of the southern Perth Basin. *Geological Survey of Western Australia Record* **65/17**.

Lowry D. C. 1968. Geology of the Western Australian parts of the Eucla Basin. *Geological Survey of Western Australia Bulletin* **122**.

Mabbutt J. A. 1961. A stripped land surface in Western Australia. *Transactions of the Institute of British Geographers* **29**, 101–114.

MABBUTT J. A. 1963. The Weathered Land Surface in Central Australia. *Zeitschrift für Geomorphologie* **9**, 82–114.

MABBUTT J. A. 1980. Weathering history and landform development. *Journal of Geochemical Exploration* **12**, 96–116.

MABBUTT J. A., LITCHFIELD W. H., SPECK N. H., SOFOULIS J., WILCOX D. G., ARNOLD J. M. & WRIGHT R. C. 1963. *General report on the lands of the Wiluna–Meekatharra area, Western Australia. 1958.* CSIRO, Melbourne.

MACLAREN M. 1906. On the origin of certain laterites. *Geological Magazine* **43**, 536–547.

MAIGNIEN R. 1966. *Review of research on laterites*. United Nations Educational Scientific and Cultural Organisation, Paris.

MAITLAND A. G. 1919. The Gold Deposits of Western Australia. *In*: *The Mining Handbook, Chapter 2.* Geological Survey of Western Australia Memoir **1** (republished 1984 by Hesperian Press, Perth).

MANN A. W. 1984. Mobility of gold and silver in laterite weathering profiles: some observations from Western Australia. *Economic Geology* **79**, 38–49.

MANN A. W. & HORWITZ R. C. 1979. Groundwater calcrete deposits in Australia: some observations from Western Australia. *Journal of the Geological Society of Australia* **26**, 293–303.

MANN A. W. & OLLIER C. D. 1985. Chemical diffusion and ferricrete formation. *Soils and Geomorphology, Catena Supplement* **62**, 151–157.

MARTIN F. J. & DOYNE H. C. 1932. *Soil Survey of Sierra Leone*. Department of Agriculture, Freetown, Sierra Leone.

MAYFIELD C. I., WILLIAMS S. T., RUDDICK S. M. & HATFIELD H. L. 1972. Studies on the ecology of actinomycetes in soil. IV. Observations on the form and growth of streptomycetes in soil. *Soil Biology Biochemistry* **4**, 79–91.

MAZZUCCHELLI R. H. 1972. Secondary geochemical dispersion patterns associated with nickel sulphide deposits at Kambalda, Western Australia. *Journal of Geochemical Exploration* **1**, 103–116.

MCCREA A. F., ANAND R. R. & GILKES R. J. 1990. Mineralogical and physical properties of lateritic pallid zone materials developed from granite and dolerite. *Geoderma* **47**, 37–57.

MCFARLANE M. J. 1976. *Laterite and Landscape*. Academic Press, London.

MCFARLANE M. J. 1991. Some sedimentary aspects of lateritic weathering profile development in the major bioclimatic zones of tropical Africa. *Journal of African Earth Sciences* **12**, 267–282.

MCGOWRAN B. 1994. Chronicling the Australian duricrusts: relevance of the marine succession. *Australian Geological Survey Organisation Record* **1994/56**.

MCKENZIE R. M. 1980. The manganese oxides in soils. *In*: Varentsov I. M. & Grasselly G. eds. *Geology and Geochemistry of Manganese*, Volume I: *Mineralogy, Geochemistry, Methods*, pp. 259–269. Schweizerbart'sche-Verlagsbuchhandlung, Stuttgart.

MELFI A. J., TRECASES J. J. & BARROS DE OLIVEIRA S. M. 1980. Les latérites nickélifères du Brésil. *Cahiers ORSTOM, Série Géologie* **11**, 15–42.

MILLOT G. 1964. *Geologie Des Argiles*. Masson, Paris.

MILNE L. A. 1998. Palynology report (ME 55) for 10 samples from Tertiary sediments. Waters and Rivers Commission, Western Australia (unpubl.).

MILNES A. R. 1992. Calcrete. *In*: Martini I. P. & Chesworth W. eds. *Weathering, Soils and Palaeosols*, pp. 309–347. Development in Earth Surface Processes Volume 2. Elsevier, Amsterdam.

MILNES A. R., BOURMAN R. P. & NORTHCOTE K. M. 1985. Field relationships of ferricretes and weathered zones in southern South Australia: a contribution to 'laterite' studies in Australia. *Australian Journal of Soil Research* **23**, 441–465.

MILNES A. R. & FITZPATRICK R. W. 1987. Titanium and zirconium minerals. *In*: Dixon J. B. & Weed S. B. eds. *Minerals in Soil Environments* (2nd edition), pp. 1131–1205. Soil Science Society of America, Madison, WI.

MILNES A. R. & HUTTON J. T. 1983. Calcretes in Australia. *In*: *Soils: an Australian Viewpoint,* pp. 119–62. CSIRO, Melbourne and Academic Press, London.

MISHRA H. K. 1996. Comparative petrological analysis between the Permian coals of India and Western Australia: palaeoenvironments and thermal history. *Palaeogeography, Palaeoclimatology, Palaeoecology* **125**, 199–216.

MOHAMED S. O. & BRAUND A. 1994. Morphology and genesis of secondary calcite in soils from Beauce, France. *In*: Ringrose-Voase A. J. & Humphreys G. S. eds. *Soil Micromorphology: Studies in Management and Genesis*, pp. 27–36. Developments in Soil Science **22**. Elsevier, Amsterdam.

MONTI R. & FAZAKERLEY V. W. 1996. The Murrin Murrin nickel cobalt project. *In*: Grimsey E. J. & Neuss I. eds. *Nickel '96, mineral to market*, pp. 191–195. Australasian Institute of Mining and Metallurgy Special Publication **6/96**.

MORGAN K. H. 1993. Development, sedimentation and economic potential of palaeoriver systems of the Yilgarn Craton of Western Australia. *Sedimentary Geology* **85**, 637–656.

MULCAHY M. J. 1960. Laterites and lateritic soils in south-western Australia. *Journal of Soil Science* **11**, 206–225.

MULCAHY M. J. 1961. Soil distribution in relation to landscape development. *Zeitschrift für Geomorphologie* **5**, 211–225.

MULCAHY M. J. 1967. Landscapes, laterites and soils in southwestern Australia. *In*: Jennings J. N. & Mabbutt J. A. eds. *Landform Studies from Australia and New Guinea*, pp. 211–230. Cambridge University Press, Cambridge.

MULCAHY M. J. 1973. Landforms and soils of southwestern Australia. *Journal of the Royal Society of Western Australia* **56**, 16–22.

MULCAHY M. J. & HINGSTON F. J. 1961. The development and distribution of soils of the York–Quairading area, Western Australia, in relation to landscape evolution. *CSIRO Soil Publication* **17**.

MURRAY A. M. 1979. Bauxite. *In*: Prider R. T. ed. *Mining in Western Australia*, pp. 101–110. University of Western Australia Press, Perth.

MYERS J. S. 1993. Precambrian history of the West Australian Craton and adjacent orogens. *Annual Review of Earth and Planetary Sciences* **21**, 453–481.

NAHON D. 1976. Cuirasses ferrugineuses et encroutements calcaires au Senegal Occidental et en Mauritanie, systemes evolutifs: geochimie, structures, relais et coexistence. *Sciences Geologiques Memoire* **44**.

NAHON D. 1986. Evolution of iron crusts in tropical landscapes. *In*: Colman M. & Dethiver X. eds. *Rates of Chemical Weathering of Rocks and Minerals*, pp. 169–191. Academic Press, London.

NAHON D. B. 1991. *Introduction to the Petrology of Soils and Chemical Weathering*. Wiley, New York.

NAHON D. & TARDY Y. 1992. The ferruginous laterites. *In*: Butt C. R. M. & Zeegers H. eds. *Regolith Exploration Geochemistry in Tropical and Subtropical Terrains*, pp. 41–55. Handbook of Exploration Geochemistry, Elsevier, Amsterdam.

NETTERBERG F. 1969. The interpretation of some basic calcrete types. *South African Archaeological Bulletin* **24**, 117–122.

NEWSOME D. & LADD P. 1999. The use of quartz grains microtextures in the study of the origin of sand terrains in Western Australia. *Catena* **35**, 1–17.

NICKEL R. E. 1984. The mineralogy and geochemistry of the weathering profile of the Teutonic Bore Cu–Pb–Zn–Ag sulphide deposit. *Journal of Geochemical Exploration* **22**, 239–264.

NORTHCOTE K. H., BETTENAY E., CHURCHWARD H. M. & MCARTHUR W. M. 1967. *Atlas of Australian Soils. Explanatory data for Sheet 5. Perth–Albany–Esperance Area*. CSIRO Division of Soils, Melbourne University Press, Melbourne.

NORTHCOTE K. H., HUBBLE G. D., ISBELL R. F., THOMPSON C. H. & BETTENAY E. 1975. *A Description of Australian Soils*. CSIRO, Melbourne.

NORTON S. 1973. A: Laterite and bauxite formation. *Economic Geology* **68**, 353–361.

OLIVERIA S. M. B., TRESCASES J. J. & MELFI A. J. 1992. Lateritic nickel deposits of Brazil. *Mineralium Deposita* **27**, 137–146.

OLLIER C. D. 1978. Early landform evolution. *In*: Jeans J. N. ed. *Australia, a Geography*, pp. 85–98. University Press, Sydney.

OLLIER C. D. 1984. D*: Weathering* (2nd edition). Longman, London.

OLLIER C. D. 1988. Deep weathering, groundwater and climate. *Geografiska Annaler* **70**, 285–289.

OLLIER C. D. 1991. Laterite profiles, ferricrete and landscape evolution. *Zeitschrift für Geomorphologie* **35**, 165–173.

OLLIER C. D. 1994. Exploration concepts in lateritic terrains. *Australasian Institute of Mining and Metallurgy Bulletin* **3**, 22–27.

OLLIER C. D., CHAN R. A., CRAIG M. A. & GIBSON D. L. 1988. Aspects of landscape history and regolith in the Kalgoorlie region, Western Australia. *BMR Journal of Australian Geology & Geophysics* **10**, 309–321.

OLLIER C. D. & GALLOWAY R. W. 1990. The laterite profile, ferricrete and unconformity. *Catena* **17**, 97–109.

Ollier C. D. & Pain C. F. 1996. *Regolith, Soils and Landforms*. John Wiley and Sons, Chichester.

Ollier C. D. & Rajaguru S. N. 1991. Laterite of Kerala (India). *Geografia Fisicia e Dinamica Quaternaria* **12**, 27–33.

Ostwald J. 1990. The biogeochemical origin of the Groote Eylandt manganese oxide pisoliths and ooliths, northern Australia. *Ore Geology Reviews* **5**, 469–490.

Pain C. F. 1998. Landforms and regolith. *In*: Eggleton R. A. ed. *The State of the Regolith, Proceedings of the 2nd Australian Conference on Landscape Evolution and Mineral Exploration*, pp. 54–62. Geological Society of Australia Special Publication **20**.

Pain C. F., Chan R., Craig M., Hazell M., Kamprad J. & Wilford J. 1991. RTMAP: BMR Regolith Database Field Handbook. *Bureau of Mineral Resources Record* **1991/29**.

Pain C. F., Wilford J. R. & Dohrenwend J. C. 1994. Regolith–landforms of the Ebagoola 1:250 000 sheet area (SD54-12), North Queensland. *Australian Geological Survey Organisation Record* **1994/7**.

Paquet H., Colin F., Duplay J., Nahon D. & Millot G. 1987. Ni, Mn, Zn, Cr-Smectites Early and Effective Traps for Transition Elements in Supergene Ore Deposits. *In*: Rodrigez-Clemente R. & Tardy Y. eds. *Geochemistry and Mineral Formation in the Earth Surface*, pp. 221–229. Consejo Superior de Investigaciones, Cientificas Centre National de la Récherche Scientifique.

Paton T. R. 1974. Origin and terminology for gilgai in Australia. *Geoderma* **11**, 221–242.

Pettijohn F. J. 1975. *Sedimentary Rocks*. Harper & Row, New York.

Phang C. & Anand R. R. 2000. Distinguishing transported and residual regolith material. *In*: Phillips G. N. & Anand R. R. eds. *Yandal Greenstone Belt, Regolith, Geology and Mineralisation*, pp. 125–133. Australian Institute of Geoscientists Bulletin **31**.

Phillips S. E., Milnes A. R. & Foster R. C. 1987. Calcified filaments: an example of biological influences in the formation of calcrete in South Australia. *Australian Journal of Earth Sciences* **35**, 463–481.

Pillans B. 1998. Regolith dating methods. A guide to numerical dating methods. Cooperative Research Centre for Landscape Evolution and Mineral Exploration, Perth (unpubl.).

Playford P. E., Cope R. N. & Cockbain A. E. 1975. Palaeogeographic development of Western Australia—Phanerozoic. *Geological Survey of Western Australia Memoir* **2**, 451–460.

Pontual S. & Merry N. 1996. An exploratory strategy to aid the differentiation of residual from transported kaolinites using field-based spectral analysis. Restricted Report, Auspec International, Melbourne.

Prescott J. A. 1931. *The Soils of Australia in Relation to Vegetation and Climate*. CSIRO Bulletin **52**.

Prescott J. A. 1954. Observations on laterite in Western Australia. *Australian Journal of Science* **17**, 11–14.

Prescott J. A. & Pendleton R. L. 1952. Laterite and lateritic soils. *Commonwealth Bureau of Soil Science, Farnham Royal, Bucks. Technical Communication Report* **47**.

Prider R. T. 1966. The lateritized surface of Western Australia. *Australian Journal of Science* **28**, 443–451.

Pringle H. J. R. 1994. Geomorphology. *In*: Howes K. M. W. ed. *An Inventory and Condition Survey of Rangelands in the North-Eastern Goldfields, Western Australi*a, pp. 83–97. Department of Agriculture, WA, Technical Bulletin **87**.

Pullan R. A. 1967. A morphological classification of lateritic ironstones and ferruginised rocks in Northern Nigeria. *Nigerian Journal of Science* **1**, 161–173.

Quade J., Chivas A. R. & McCulloch M. T. 1995. Strontium and carbon isotope tracers and the origins of soil carbonate in South Australia and Victoria. *Palaeogeography, Palaeoclimatology, Palaeoecology* **113**, 103–117.

Read J. F. 1974. Calcrete deposits and Quaternary sediments, Edel Province, Shark Bay, Western Australia. *American Association of Petroleum Geologists Memoir* **22**, 250–282.

Rehies M. C., Goodmacher J. C., Harden J. W., McFadden L. D., Rockwell T. K., Shroba R. R., Sowers J. M. & Taylor E. M. 1995. Quaternary soils and dust deposition in southern Nevada and California. *Geological Society of America Bulletin* **107**, 1003–1022.

Robertson I. D. M. 1996. Ferruginous lag geochemistry on the Yilgarn Craton of Western Australia: practical aspects and limitations. *Journal of Geochemical Exploration* **57**, 139–151.

Robertson I. D. M. 1999. Origins and applications of size fractions of soils overlying the Beasley Creek gold deposit, Western Australia. *Journal of Geochemical Exploration* **66**, 99–113.

Robertson I. D. M. & Butt C. R. M. 1993. Atlas of Weathered Rocks. *CSIRO Division of Exploration Geoscience Restricted Report* **390R** (re-issued as Open File Report 1, CRC LEME, Perth, 1998).

Robertson I. D. M., Butt C. R. M. & Chaffee M. A. 1998. Fabric and chemical composition: from parent lithology to regolith. *In*: Eggleton R. A. ed. *The State of the Regolith, Proceedings of the 2nd Australian Conference on Landscape Evolution and Mineral Exploration*, pp. 157–174. Geological Society of Australia Special Publication **20**.

Robertson I. D. M. & Eggleton R. A. 1991. Weathering of granitic muscovite to kaolinite and halloysite and of plagioclase-derived kaolinite to halloysite. *Clays and Clay Minerals* **39**, 113–126.

Robertson I. D. M., King J. D., Anand R. R. & Butt C. R. M. 1994. Regolith geology and geochemistry—Mt Magnet district. *CSIRO Division of Exploration and Mining Restricted Report* **48C** (re-issued as Open File Report 92, CRC LEME, Perth, 2001).

Rose A. W., Kato T. & MacHesky M. L. 1993. The significance of biogenic element cycling in ancient tropical soils. *Chemical Geology* **107**, 401–403.

Ruellan A. 1971. Les Sols a Profil Calcaire Differencie Des Plaines de la Basse Moulouya (Maroc Oriental). *Memoire ORSTOM* **54**.

Sadleir S. B. & Gilkes R. J. 1976. Development of bauxite in relation to parent material near Jarrahdale, Western Australia. *Journal of the Geological Society of Australia* **23**, 333–344.

Salama R. B. & Hawkes G. E. 1993. Surficial geology and stratigraphy of the Wallatin Creek area: a Western Australian model of Cainozoic sedimentary deposition on the Yilgarn Craton. *CSIRO Water Resources Research Division Report* **93/4**.

Sanders A. J. & Coker J. 1997. Delineation of regolith boundaries using remotely sensed data and correlation with regolith geochemistry. *In*: Cassidy K. F., Whitaker A. J. & Liu S. F. eds. *An International Conference on Crustal Evolution, Metallogeny and Exploration of the Yilgarn Craton – An Update, Kalgoorlie '97, Extended Abstracts*, pp. 187–191.

Sanders A. J., Morris P. A., Subramanya A. G. & Faulkner J. A. 1997. *Geochemical Mapping of the Mount Phillips 1:250 000 sheet. Regolith Geochemistry Series Explanatory Notes*. Geological Survey of Western Australia, Perth.

Sanders C. C. 1974. Calcrete in Western Australia. *Geological Survey of Western Australia Annual Report for 1993*, 12–14.

Schellmann W. 1981. Considerations on the definition and classification of laterites. *In*: *Proceedings of the International Seminar on Lateritisation Processes, Trivandrum, India,* pp. 1–10. A. A. Balkema, Rotterdam.

Schellmann W. A. 1983. A new definition of laterite. *Natural Resources and Development* **18**, 7–21.

Schmidt P. W. & Embleton B. J. J. 1976. Palaeomagnetic results from sediments of the Perth Basin, Western Australia, and their bearing on the timing of regional lateritisation. *Palaeogeography, Palaeoclimatology, Palaeoecology* **19**, 257–273.

Schulze D. G. 1984. The influence of aluminium on iron oxides. VIII. Unit cell dimension of Al substituted goethites. *Clays and Clay Minerals* **32**, 36–44.

Schwertmann U. 1985. The effect of pedogenic environments on iron oxide minerals. *Advances in Soil Science* **1**, 171–200. Springer-Verlag, New York.

Schwertmann U. 1988. Occurrence and formation of iron oxides in various pedoenvironments. *In*: Stucki J. W., Goodman B. A. & Schwertmann U. eds. *Iron in Soils and Clay Minerals*, pp. 267–308. D. Reidel Publishing Co., Dordrecht.

Schwertmann U. & Fechter H. 1984. The influence of aluminium on iron oxides. XI. Aluminium substituted maghemite in soils and its formation. *Soil Science Society of America Journal* **48**, 1462–1463.

Schwertmann U. & Kampf N. 1985. Properties of goethite and hematite in kaolinitic soils of southern and central Brazil. *Soil Science* **139**, 344–350.

Schwertmann U. & Taylor R. M. 1989. Iron Oxides. *In*: Dixon J. B. & Weed S. B. eds. *Minerals in Soil Environments*, pp. 379–438. Soil Science Society of America, Madison, WI.

Senior B. R. 1978. Silcrete and chemically weathered sediments in southwest Queensland. *In*: Langford-Smith T. ed. *Silcretes in Australia*, pp. 41–50. Department of Geography, University of New England, Armidale.

Sidhu P. S., Gilkes R. J. & Posner A. M. 1980. The behaviour of Co, Ni, Zn, Mn and Cr in magnetite during alteration to maghemite and hematite. *Soil Science Society of America Journal* **44**, 135–138.

Singh B. 1996. Why does halloysite roll?—A new model. *Clays and Clay Minerals* **44**, 191–196.

Singh B. & Gilkes R. J. 1991. Alteration of Cr-muscovite to kaolinite in a weathered quartzite. *Clays and Clay Minerals* **39**, 571–579.

Singh B. & Gilkes R. J. 1992a. Properties and distribution of Fe oxides and their association with minor elements in the soils of south-western Australia. *Journal of Soil Science* **43**, 77–98.

Singh B. & Gilkes R. J. 1992b. An electron-optical investigation of the alteration of kaolinite to halloysite. *Clays and Clay Minerals* **40**, 212–229.

Singh B. & Gilkes R. J. 1995. The natural occurrence of x-alumina in lateritic pisolites. *Clay Minerals* **30**, 39–44.

Singh B. & MacKinnon I. D. R. 1996. Experimental transformation of kaolinite to halloysite. *Clays and Clay Minerals* **46**, 101–106.

Singh B., Gilkes R. J. & Butt C. R. M. 1992. An electron optical investigation of aluminosilicate cements in silcretes. *Clays and Clay Minerals* **40**, 707–721.

Sircombe K. N. & Freeman M. J. 1999. Provenance of detrital zircons on the Western Australia coastline—implications for the geologic history of the Perth Basin and denudation of the Yilgarn Craton. *Geology* **27**, 879–882.

Sivarajasingham S., Alexander L. T., Cady J. G. & Cline M. J. 1962. Laterite. *Advances in Agronomy* **14**, 1–60.

Smale D. 1973. Silcretes and associated silica diagenesis in Southern Africa and Australia. *Journal of Sedimentary Petrology* **43**, 1077–1089.

Smith B. H. 1977. Some aspects of the use of geochemistry in the search for nickel sulphides in lateritic terrain in Western Australia. *Journal of Geochemical Exploration* **8**, 259–281.

Smith R. E. 1996. Regolith research in support of mineral exploration. *Journal of Geochemical Exploration* **57**, 159–173.

Smith R. E., Anand R. R. & Alley N. F. 1997. Use and implications of palaeoweathering surfaces in mineral exploration. *In*: Gubins A. G. ed. *Proceedings of Exploration '97: Fourth Decennial International Conference on Mineral Exploration*, pp. 335–346. Geo/Fx Division of AG Information Systems, Toronto.

Smith R. E., Anand R. R., Churchward H. M., Robertson I. D. M., Grunsky E. C., Gray D. J., Wildman J. E. & Perdrix J. L. 1992. Laterite geochemistry for detecting concealed mineral deposits, Yilgarn Craton, Western Australia. *CSIRO Division of Exploration Geoscience Restricted Report* **236R** (re-issued as Open File Report 50, CRC LEME, Perth, 1998).

Smith R. E., Birrell R. D. & Brigden J. F. 1989. The implications to exploration of chalcophile corridors in the Archaean Yilgarn Block, Western Australia, as revealed by laterite geochemistry. *In*: Jenness S. E. ed. *Geochemical Exploration, 1987*, pp. 169–184. Journal of Geochemical Exploration **32**.

Smith R. E. & Perdrix R. L. 1983. Pisolitic laterite geochemistry in the Golden Grove massive sulphide district, Western Australia. *Journal of Geochemical Exploration* **18**, 131–164.

Smyth E. L. & Button A. 1989. Gold exploration in Tertiary palaeodrainage systems of Western Australia. *In*: Bhappu R. B. & Harden R. J. eds. *Gold Forum on Technology and Practices, World Gold, '89. Proceedings of the First Joint International Meeting Between SME and AUSIMM, November 5–8, 1989, Reno, Nevada,* pp. 13–22. Society of Mining, Metallurgy and Exploration, Littleton.

Sofoulis J. 1963. The occurrence and hydrological significance of calcrete deposits in Western Australia. *Geological Survey of Western Australia Annual Report for 1962,* 38–42.

Stace H. C. T., Hubble G. D., Brewer R., Northcote K. H., Sleeman J. R., Mulcahy M. J. & Hallsworth E. G. 1968. *A Handbook of Australian Soils*. Rellim Technical Publication **206**. Rellim Technical Publications, Glenside.

Stephens C. G. 1946. Pedogenesis Following the Dissection of Lateritic Regions in Southern Australia. *CSIRO Bulletin* **206**.

Stephens G. C. 1971. Laterite and silcrete in Australia. *Geoderma* **5**, 5–52.

Suess E. 1906. *The Face of the Earth* (translated by H. B. C. Sollas), Vol. II., pp. 150–152. Oxford.

Summerfield A. M. 1983. Geochemistry of weathering profile silcretes, southern Cape Province, South Africa. *In*: Wilson R. C. L. ed. *Residual Deposits: Surface Related Weathering Processes and Materials*, pp. 167–178. Blackwell, Oxford.

Tapley I. J. 1998. Landform, regolith and geological mapping in Australia using polarimetric and interferometric radar datasets. *CSIRO Exploration and Mining Restricted Report* **529R**.

Tardy Y. 1992. Diversity and terminology of lateritic profiles. *In*: Martini I. P. & Chesworth W. eds. *Weathering, Soils and Paleosols*, pp. 379–406. Elsevier, Amsterdam.

Tardy Y. & Nahon D. 1985. Geochemistry of laterites, stability of Al-goethite, Al-hematite and Fe^{3+}-kaolinite in bauxites and ferricretes: an approach to the mechanism of concretion formation. *American Journal of Science* **285**, 865–903.

Tardy Y. & Roquin C. 1992. Geochemistry and evolution of lateritic landscapes. *In*: Martini I. P. & Chesworth W. eds. *Weathering, Soils and Paleosols*, pp. 407–443. Elsevier, Amsterdam.

Taylor G. 1978. Silcretes of the Walgett–Cumborah region of N.S.W. *In*: Langford-Smith T. eds. *Silcrete in Australia*, pp. 187–193. Department of Geography, University of New England, Armidale.

Taylor G. & Butt C. R. M. 1998. The Australian regolith and mineral exploration. *AGSO Journal of Australian Geology & Geophysics* **17**, 55–67.

Taylor G. & Eggleton R. A. 2001. *Regolith Geology and Geomorphology*. John Wiley & Sons Ltd., Chichester.

Taylor G., Eggleton R. A., Holzhaur C. C., MacOnachie L. A., Gordon M., Brown M. C. & McQueen K. G. 1992. Cool climate lateritic and bauxitic weathering. *Journal of Geology* **100**, 669–677.

Taylor G. & Ruxton B. P. 1987. A duricrust catena in southern Australia. *Zeitschrift für Geomorphologie* **31**, 385–410.

Taylor R. G. & Howard K. W. F. 1999. Lithological evidence for the evolution of weathered mantles in Uganda by tectonically controlled cycles of deep weathering and stripping. *Catena* **35**, 65–94.

Taylor R. M. 1987. Non-silicate oxides and hydroxides. *In*: Newman A. C. D. ed. *Chemistry of Clays and Clay Minerals*, pp. 129–201. Mineralogical Society, London.

Taylor R. M. & Schwertmann U. 1974. Maghemite in soils and its origin, Parts I and II. *Clays and Clay Minerals* **10**, 289–310.

Teakle L. J. H. 1936. The red and brown hardpan soils of the Acacia semi-desert scrub of Western Australia. *Journal of the Department of Agriculture, Western Australia* **13**, 480–499.

Teakle L. J. H. 1938. A regional classification of the soils of Western Australia. *Journal of the Royal Society of Western Australia* **24**, 123–197.

Theveniaut H. & Freyssinet P. 1999. Paleomagnetism applied to lateritic profiles to assess saprolite and duricrust formation processes: the example of Mont Badel profile (French Guiana). *Palaeogeography, Palaeoclimatology, Palaeoecology* **148**, 209–231.

Thiry M. & Milnes A. R. 1991. Pedogenic and groundwater calcretes at Stuart Creek opal field, South Australia. *Journal of Sedimentary Petrology* **61**, 111–127.

Thom R. & Barnes R. G. 1977. *Leonora, Western Australia, 1:250 000 Series Explanatory Notes*. Geological Survey of Western Australia, Perth.

Thomas M. F. 1965. An approach to some problems of landform analysis in tropical environments. *In*: Whittow J. D. & Wood A. D. eds. *Essays on Geography for Austin Miller*, pp. 118–144. University of Reading, Reading.

Thomas M. F. 1994. *Geomorphology in the Tropics*. Wiley, Chichester.

Thornber M. R. 1982. Weathering of sulphide bodies. *In*: Smith R. E. ed. *Geochemical Exploration in Deeply Weathered Terrain*, pp. 67–72. CSIRO Department of Mineralogy, Floreat Park.

Thornber M. R., Bettenay E. & Russell W. G. R. 1987. A mechanism of aluminosilicate cementation to form a hardpan. *Geochimica et Cosmochimica Acta* **51**, 2303–2310.

Thornbury W. D. 1954. *Principles of Geomorphology*. John Wiley and Sons, London.

Tilley D. B. & Eggleton R. A. 1996. Tohdite ($5Al_2O_3.H_2O$) in bauxites from Northern Australia. *Clays and Clay Minerals* **42**, 485–488.

Tomich S. A. 1964. Bauxite in the Darling Range, Western Australia. *Australasian Institute of Mining and Metallurgy Proceedings* **212**, 125–135.

TORRENT J., SCHWERTMANN U. & SCHULZE D. G. 1980. Iron oxide mineralogy of some soils of two river terrace sequences in Spain. *Geoderma* **23**, 191–208.

TRENDALL A. F. 1962. The formation of apparent peneplains by a process of combined lateritisation and surface wash. *Zeitschrift für Geomorphologie* **6**, 183–197.

TRESCASES J. J. 1992. Chemical weathering. *In*: Butt C. R. M. & Zeegers H. eds. *Regolith Exploration Geochemistry in Tropical and Subtropical Terrains*, pp. 25–39. Handbook of Exploration Geochemistry **4**. Elsevier, Amsterdam.

TRUSWELL E. M. & HARRIS W. K. 1982. The Cainozoic palaeobotanical record in arid Australia: fossil evidence for the origins of an arid-adapted flora. *In*: Barker W. R. & Greenslade P. J. M. eds. *Evolution of the Flora and Fauna of Arid Australia*, pp. 67–76. Peacock Publications, Frewville.

TWOMEY R. F. 1992. Regolith–landform relationships in the Agnew area and multi-element dispersion into the weathering profiles of the Genesis and Waroonga gold deposits, Lawlers. BSc (Hons) thesis, University of Western Australia, Perth (unpubl.).

VAN DE GRAAFF W. J. E. 1981. Palaeogeographic evolution of a rifted cratonic margin: S.W. Australia, a discussion. *Palaeogeography, Palaeoclimatology, Palaeoecology* **34**, 163–172.

VAN DE GRAAFF W. J. E. 1983. Silcrete in Western Australia: geomorphological settings, textures, structures, and their genetic implications. *In*: Wilson R. C. L. ed. *Residual Deposits: Surface Related Weathering Processes and Materials*, pp. 159–166. Blackwell, Oxford.

VAN DE GRAAFF W. J. E., CROWE R. W. A., BUNTING J. A. & JACKSON M. J. 1977. Relict early Cainozoic drainages in arid Western Australia. *Zeitschrift für Geomorphologie* **21**, 379–400.

VARGA Z. S., ANAND R. R. & WILDMAN J. E. 1997. Regolith–landform evolution and geochemical dispersion at the Bronzewing Deposit. *CSIRO Division of Exploration and Mining Restricted Report* **308R** (re-issued as Open File Report 108, CRC LEME, Perth, 2001).

VASCONCELOS C. & MCKENZIE J. 1997. Microbial mediation of modern dolomite precipitation and diagenesis under anoxic conditions (Lagoa Vermelha, Rio De Janeiro, Brazil). *Journal of Sedimentary Research* **67**, 378–390.

VASCONCELOS P. 1995. K–Ar and $^{40}Ar/^{39}Ar$ geochronology of weathering reactions. *In*: Camuti K. S. ed. *Exploring the Tropics, Extended Abstracts, 17th International Geochemical Exploration Symposium, Townsville*, pp. 45–56.

VEARNCOMBE J. R. 1997. Late Archaean deformation and gold mineralisation, the Archaean Yilgarn Craton: an overview. *Geological Society of Australia Abstracts* **44**, 69.

VON PERGER A. D. 1992. Regolith development and geochemistry of the Madoonga Area, W.A. BSc (Hons) thesis, Curtin University of Technology, Perth (unpubl.).

WADA K. 1989. Allophane and imogolite. *In*: Dixon J. B., Weed S. B. eds. *Minerals in Soil Environments*, pp. 1051–1088. Soil Science Society of America, Madison.

WALTHER J. 1915. Laterit in West Australien. *Zeitschrift de Deutschens Geologischen Gesellschaft* **67B**, 113–140.

WANG Q. 1988. Mineralogical aspects of monzonite alteration: an investigation by electron microscopy and chemistry. PhD thesis, Australian National University, Canberra (unpubl.).

WANG Y., NAHON D. & MERINO E. 1994. Dynamic model of the genesis of calcretes replacing silicate rocks in semiarid regions. *Geochimica et Cosmochimica Acta* **58**, 5131–5145.

WARD R. S. 1993. Regolith–landforms and geochemical dispersion in transported regolith in the Genesis gold deposit, Agnew region, Western Australia. BSc (Hons) thesis, Curtin University of Technology, Perth (unpubl).

WATTS S. H. 1975. An unusual occurrence of silcrete in adamellite—implications for duricrust genesis. *Search* **6**, 434–435.

WATTS S. H. 1977. Major element geochemistry of silcrete from a portion of inland Australia. *Geochimica et Cosmochimica Acta* **41**, 1164–1167.

WAYLAND E. J. 1933. Peneplains and some erosional platforms. *Uganda Geological Survey Department Notes* **1**, 77–79.

WELLS M. A., GILKES R. J. & ANAND R. R. 1989. The formation of corundum and aluminous hematite by the thermal dehydroxylation of aluminous goethite. *Clay Minerals* **24**, 513–530.

WESTAWAY J. M. & WYCHE S. 1988. *Geology of the Darlot 1:100 000 sheet: map and explanatory notes*. Geological Survey Western Australia, Perth.

WHIPKEY C. E., CAPO R. C., CHADWICK O. A. & STEWART B. W. 1999. The importance of sea spray to the cation budget of a coastal Hawaiian soil: a strontium isotope approach. *Chemical Geology* **168**, 37–48.

WHITE A. F. & BRANTLEY S. L. (Editors) 1995. *Chemical weathering rates of silicate minerals.* Reviews in Mineralogy **31**. Mineralogical Society of America, Washington.

WILDE S. A. 1976. The Saddleback Group—a newly discovered Archaean greenstone belt in the southwestern Yilgarn Block. *Geological Survey of Western Australia Annual Report for 1975*, 92–95.

WILDMAN J. E. & COMPSTON D. 2000. Magnetic expression of palaeodrainage systems in the Yandal greenstone belt: implications for exploration. *In*: Phillips G. N. & Anand R. R. eds. *Yandal Greenstone Belt, Regolith, Geology and Mineralisation*, pp. 157–164. Australian Institute of Geoscientists Bulletin **31**.

WILDMAN J. E., PHANG C. & ANAND R. R. 1998. The stratigraphy and evolution of regolith within palaeochannel environments at the Sundowner area, North Yilgarn Craton, Western Australia. *In*: Britt A. F. & Bettenay L. eds. *New Approaches to an Old Continent, 3rd Australian Regolith Conference Abstracts, Regolith '98,* p. 65. Cooperative Research Centre for Landscape Evolution and Mineral Exploration, Perth.

WILLIAMSON A. 1992. Regolith–landform evolution and geochemical dispersion from the Calista gold deposit, Mount McClure district. BSc (Hons) thesis, University of Western Australia, Perth (unpubl.).

WOODALL R. 1993. Exploration of blind orebodies. *Australian Geological Survey Organisation Record* **1993/54**, 207–209.

WOOLNOUGH W. G. 1918. The physiographic significance of laterite in Western Australia. *Geological Magazine* **5**, 385–393.

WOOLNOUGH W. G. 1927. Presidential address. Part I: The chemical criteria of peneplanation; Part II: The duricrust of Australia. *Journal and Proceedings of the Royal Society of New South Wales* **61**, 17–53.

WOOLRICH N. K. 1994. The stratigraphy and gold mineralisation of the Argo Tertiary Palaeochannel at Kambalda, Western Australia. BSc (Hons) thesis, Curtin University of Technology, Perth (unpubl.).

WOPFNER H. 1978. Silcretes of northern South Australia and adjacent regions. *In*: Langford-Smith T. eds. *Silcretes in Australia*, pp. 93–142. Department of Geography, University of New England, Armidale.

WYRWOLL K-H. & GLOVER J. E. 1988. Physical features and geology: the geological and geomorphological framework of Western Australia. *In*: Pink B. N. ed. *Western Australian Year Book*, pp. 8–33. Australian Bureau of Statistics, Western Australian Office.

XIE J. 1994. Characterisation of secondary iron oxides and the implications for surface geochemical sampling. PhD thesis, University of New South Wales, Sydney (unpubl.).

YIM W. W. S. 1985. Chrome-bearing spinels and silcrete formation in North West Bay, Southern Tasmania. *Search* **16**, 5–6.

ZACHARY N., QUADE J. & PATCHETT P. J. 2000. Isotopic evidence for eolian recycling of pedogenic carbonate and variations in carbonate dust sources throughout the southwest United States. *Geochimica et Cosmochimica Acta* **64**, 3099–3109.

Received 6 December 2000; accepted 16 November 2001

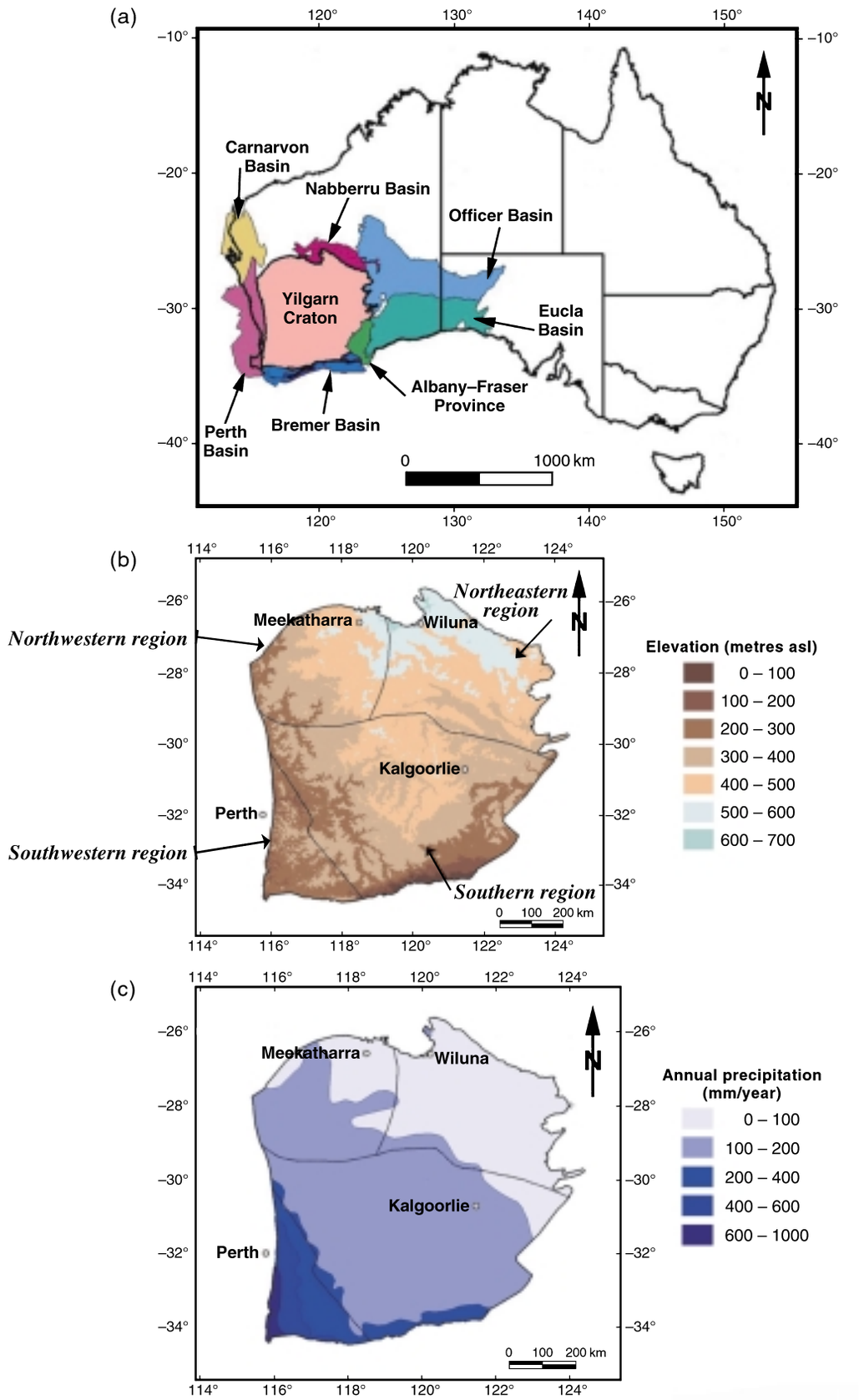

Figure 5 Location and physical attributes of the Yilgarn Craton. (a) Main geological units of southwestern Australia (modified from data provided by the Australian Geological Survey Organisation). (b) Digital elevation model for the Yilgarn Craton (data courtesy of the Australian Surveying and Land Information Group, Canberra, Australia. Crown Copyright ©. All rights reserved). (c) Annual precipitation (data provided by the Australian Bureau of Meteorology).

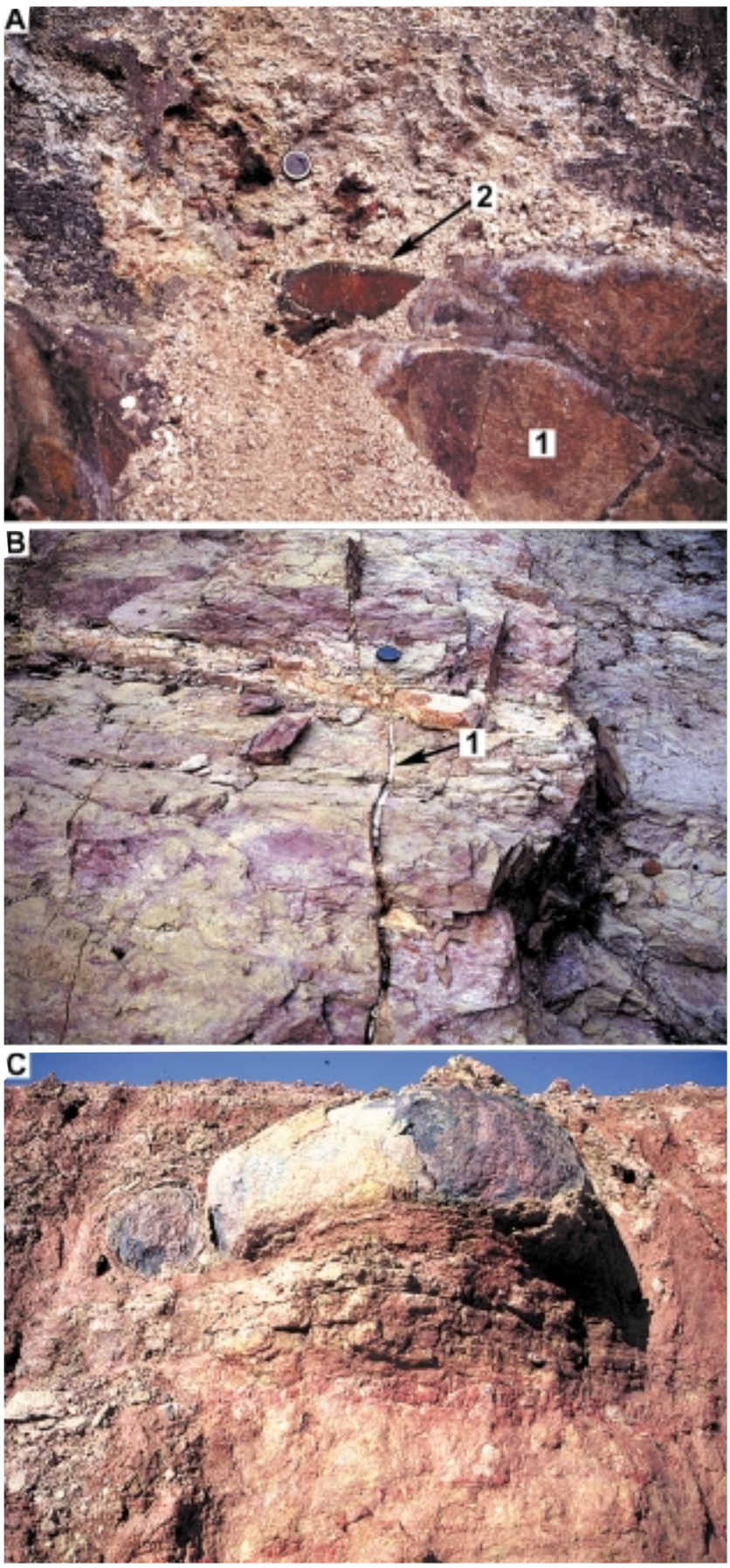

Figure 12 Field photographs of saprolite. (a) A sharp contact between dolerite (1) and the overlying saprolite (2). Here, the bedrock is fully weathered within 5 cm of the contact: Jarrahdale (411500mE, 64121000mN). Lens cap (6 cm diameter) for scale. (b) A thin quartz vein (1) passes through the saprolite, suggesting that saprolite is a product of a nearly isovolumetric weathering process: Gourdis pit, Jundee (approx. 281500mE, 7057000mN). Lens cap (6 cm diameter) for scale. (c) Corestone of dolerite set in a ferruginous saprolite: Boddington (approx. 441500mE, 6374500mN). Lens cap (6 cm diameter) for scale. Photographs by R. R. Anand.

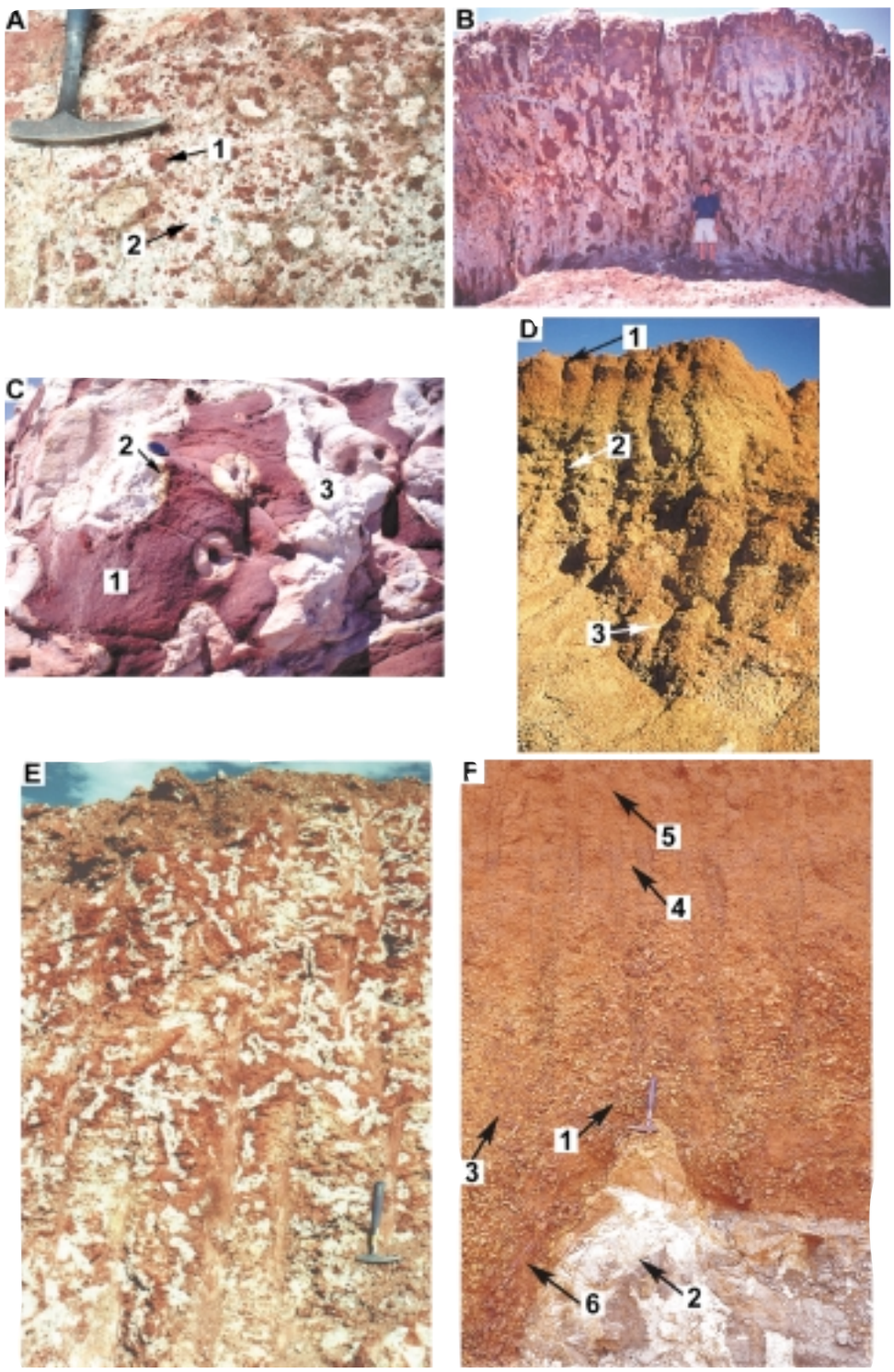

Figure 13 Field photographs of mottled zone and ferruginous duricrust. (a) Mottled zone showing hematite-rich minimottles (1) in a bleached structureless kaolinitic plasmic clay (2): Mt Gibson (517000mE, 6722000mN). Hammer for scale. (b) Megamottles in saprolite: Brown Lake (334000mE, 6576000mN). Figure for scale. (c) Close-up photograph of a megamottle showing transition of hematite mottle (1) to surrounding kaolinitic clay (3) through a few millimetres of goethite-rich cutan (2): Brown Lake (334000mE, 6576000mN). Lens cap (6 cm diameter) for scale. (d) Ferruginous zone of a weathering profile showing gravelly soil (1) on loose ferruginous gravel (2) and weakly indurated nodular duricrust (3): Mt Gibson (515950mE, 6708400mN). The intact profile is approximately 2 m high. (e) Bleaching along possible root channels, showing development of reticulate mottling: Bottle Creek (251500mE, 6772000mN). Hammer for scale. (f) Thin layer of collapsed mottled saprolite (1) developed on mottled saprolite formed from basalt (2). This grades upwards into lateritic residuum (3) and is overlain by gravelly (4) and silty (5) colluvium. Note the imbricate structure (6) of the tubular, mottled saprolite fragments that lie parallel to the lower contact: Bronzewing (302200mE, 6969800mN) (photo by I. D. M. Robertson). Hammer for scale. Photographs by R. R. Anand unless otherwise specified.

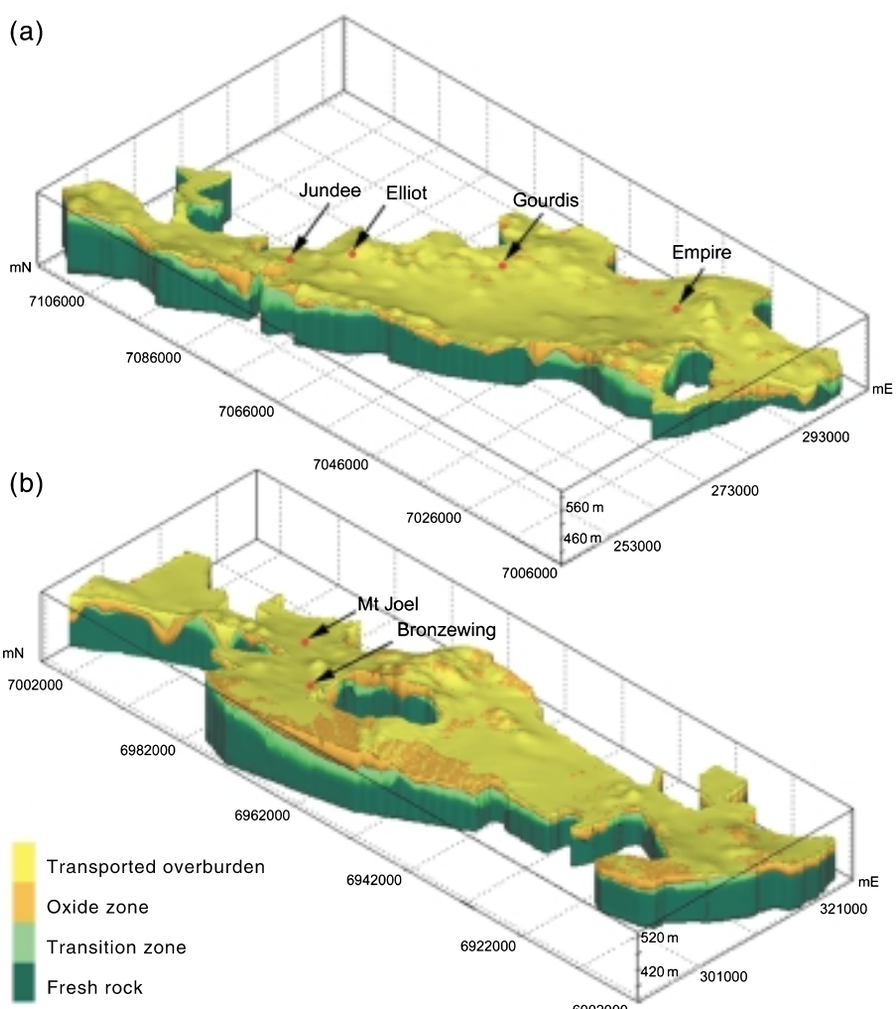

Figure 14 Thickness and elevation of various regolith boundaries for the (a) northern and (b) southern portions of the Yandal greenstone belt, northern Yilgarn Craton. Models were produced using Mining Visualisation Software (MVS) (after Anand 2000).

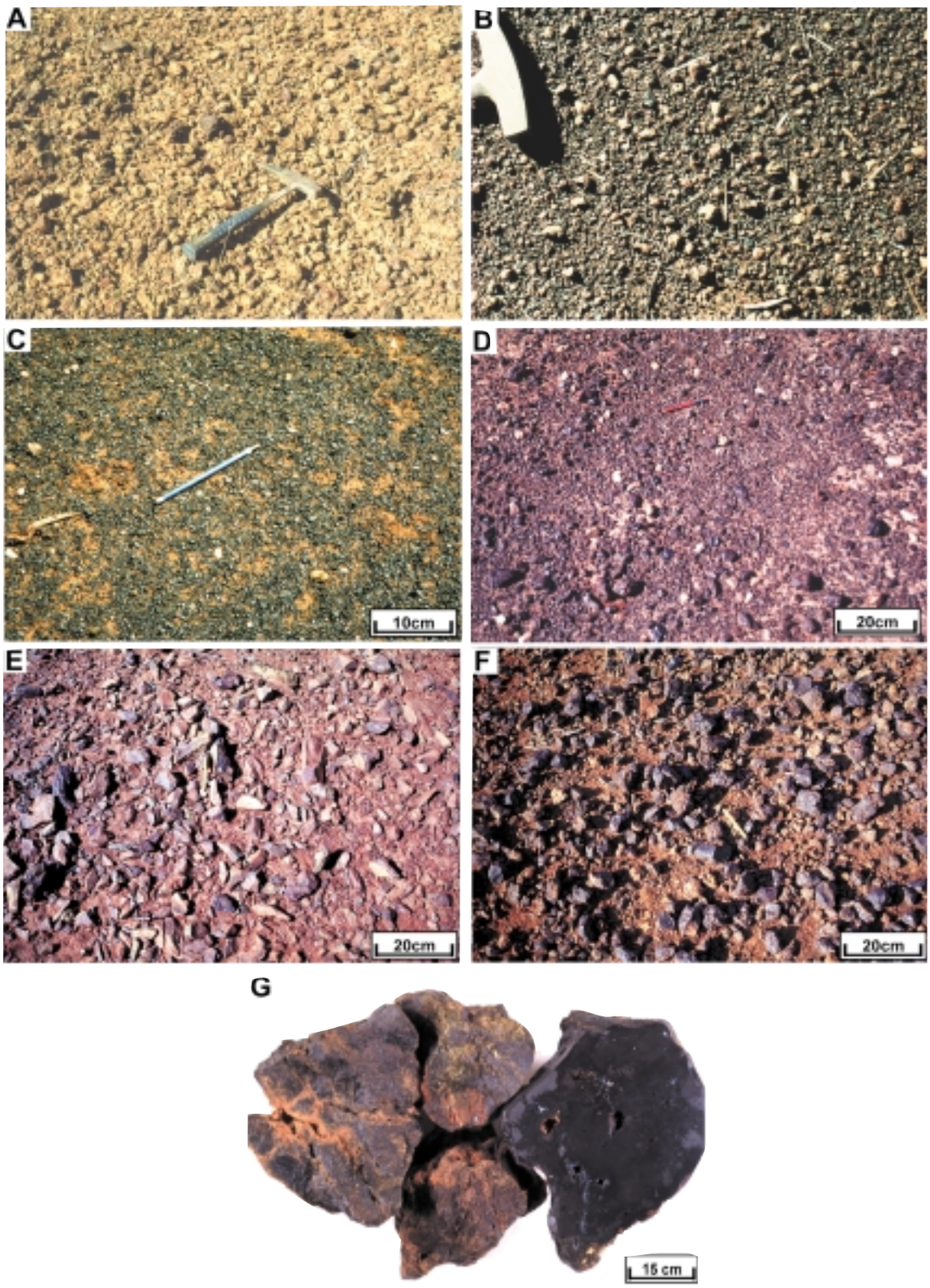

Figure 37 Field photographs of lag. (a) Coarse fragments of goethite–kaolinite-rich mottled saprolite with yellowish-brown cutans characteristic of broad ridge crests: Lawlers (260200mE, 6900970mN). Hammer for scale. (b) Hematite-rich ferruginous pisoliths and nodules with yellowish- to reddish-brown cutans on upper backslopes: Lawlers (260100mE, 6900950mN). Hammer for scale. (c) Fine, black hematite–maghemite-rich ferruginous pisoliths without cutans characteristic of lower slopes: Lawlers (258800mE, 6900000mN). (d) Polymictic lag on plains: Lawlers (270000mE, 6891600mN). The medium size fragments, though in minority, are a characteristic feature. They include Fe-saprolite, lithic fragments and quartz. (e) Coarse fragments of ferruginous saprolite on low hill: Lawlers (272560mE, 6891600mN). (f) Goethite-rich iron segregations after sulfide-rich rocks: Jundee. (g) Close-up photograph of an iron segregation. Photographs by R. R. Anand.

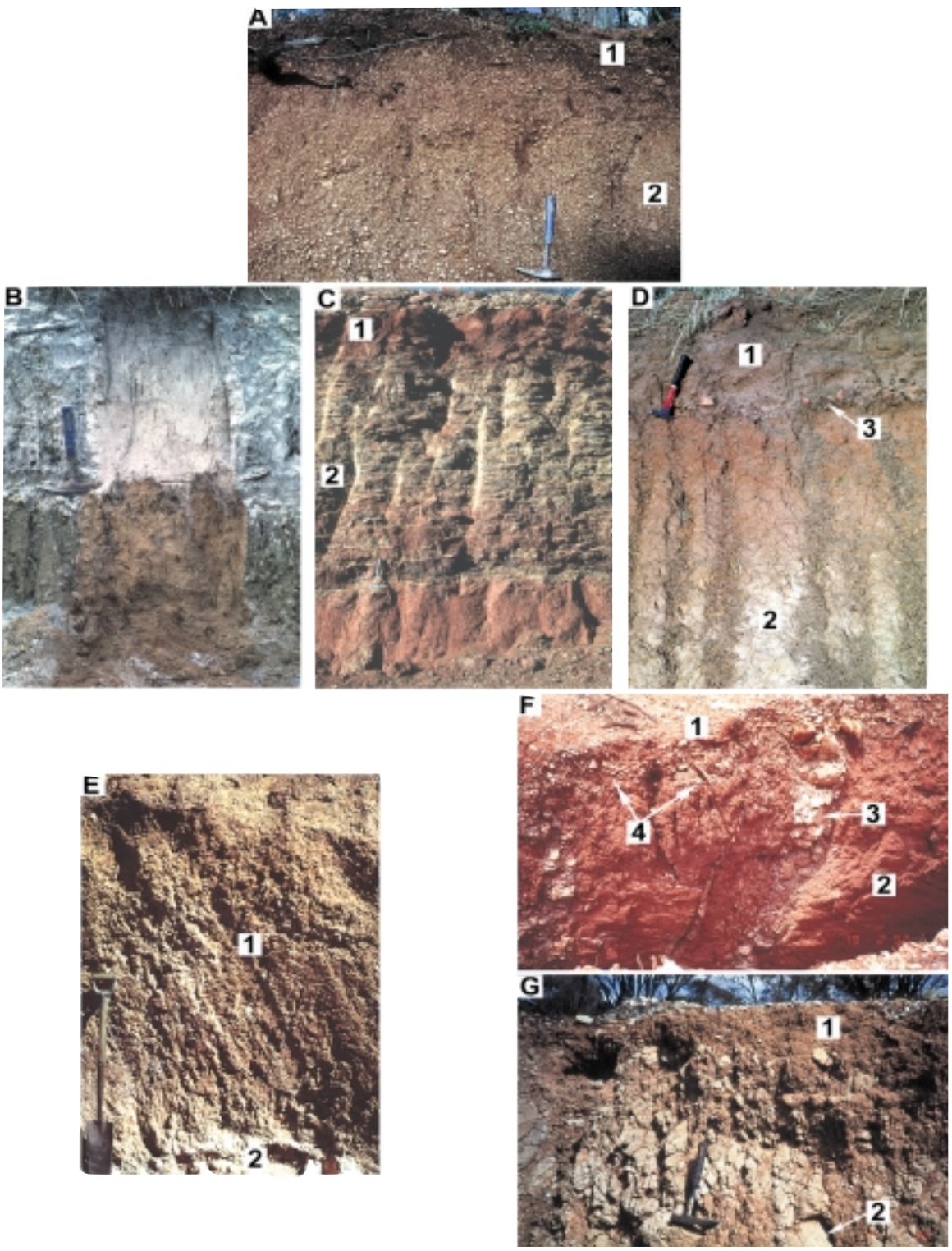

Figure 40 Examples of soil profiles formed on ferruginous duricrust, colluvium and alluvium, saprolite and bedrock. Soil type is related to the nature of the parent material and geomorphic processes. (a) Gravelly soil profile on ferruginous duricrust showing a thin organic horizon (1) over pisolitic horizon (2): Jarrahdale (approx. 411500mE, 6421000mN). Hammer for scale. (b) Podzols developed in deep uniform sand: Jarrahdale (approx. 411500mE, 6421000mN) (photo by H. M. Churchward). Hammer for scale. (c) Acid, red sandy clay in colluvium (1) over silicified colluvium (red-brown hardpan) (2): Lawlers (253850mE, 6902175mN). Hammer for scale. (d) Acid, red sandy clay in colluvium (1) over saprolite (2); stone line (3) marks the unconformity: Lawlers (259620mE, 6896850mN). Hammer for scale. (e) Acid, red clay (1) on saprolite (2): Mt Gibson (516065mE, 6707370mN). Spade for scale. (f) Thin layer of red clay (1) over mafic saprolite (2); erosion of a quartz vein (3) to form a stone line (4): Wombola (approx. 388000mE, 6570000mN). The profile is approximately 1 m high. (g) Lithosol (1) over an ultramafic bedrock (2): Wombola (approx. 388000mE, 6570000mN). Hammer for scale. Photographs by R. R. Anand unless otherwise specified.

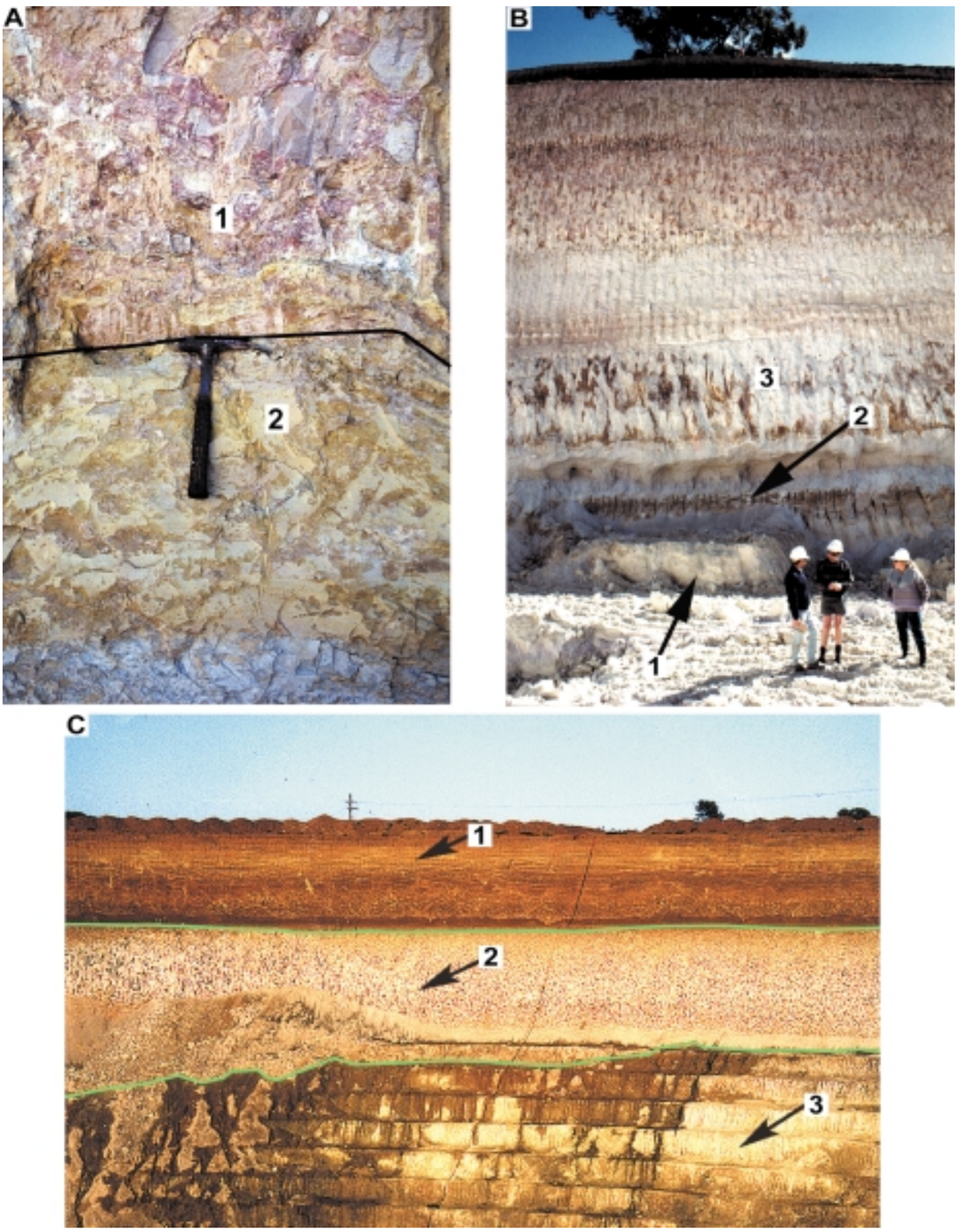

Figure 45 Field photographs of sediments. (a) Mine exposure at Lancefield South pit (approx. 432000mE, 6840000mN) shows saprolite of Permian conglomerate or till (1) (Group A) overlying saprolite formed on greenstone sequence (2). Both clasts and matrix are weathered to kaolinite. Hammer for scale. (b) Mine exposure at Lady Bountiful Extended (approx. 329000mE, 6625000mN) showing Group B sediments overlying saprolite. Saprolite of the residual profile (1), thick basal sands (2) and various layers of mottled clays (3) typical of palaeochannel sediments developed over granitic rocks. Figures for scale. (photo by C. R. M. Butt). (c) Mine exposure at Bronzewing (302200mE, 6969400mN) showing sediments (Group B and D) overlying saprolite. Silicified (hardpanised) sandy silty colluvium and alluvium of Group D (1) overlying mottled palaeochannel clays of Group B (2) and saprolite (3). The height of the section is approximately 30 m. Photographs by R. R. Anand unless otherwise specified.

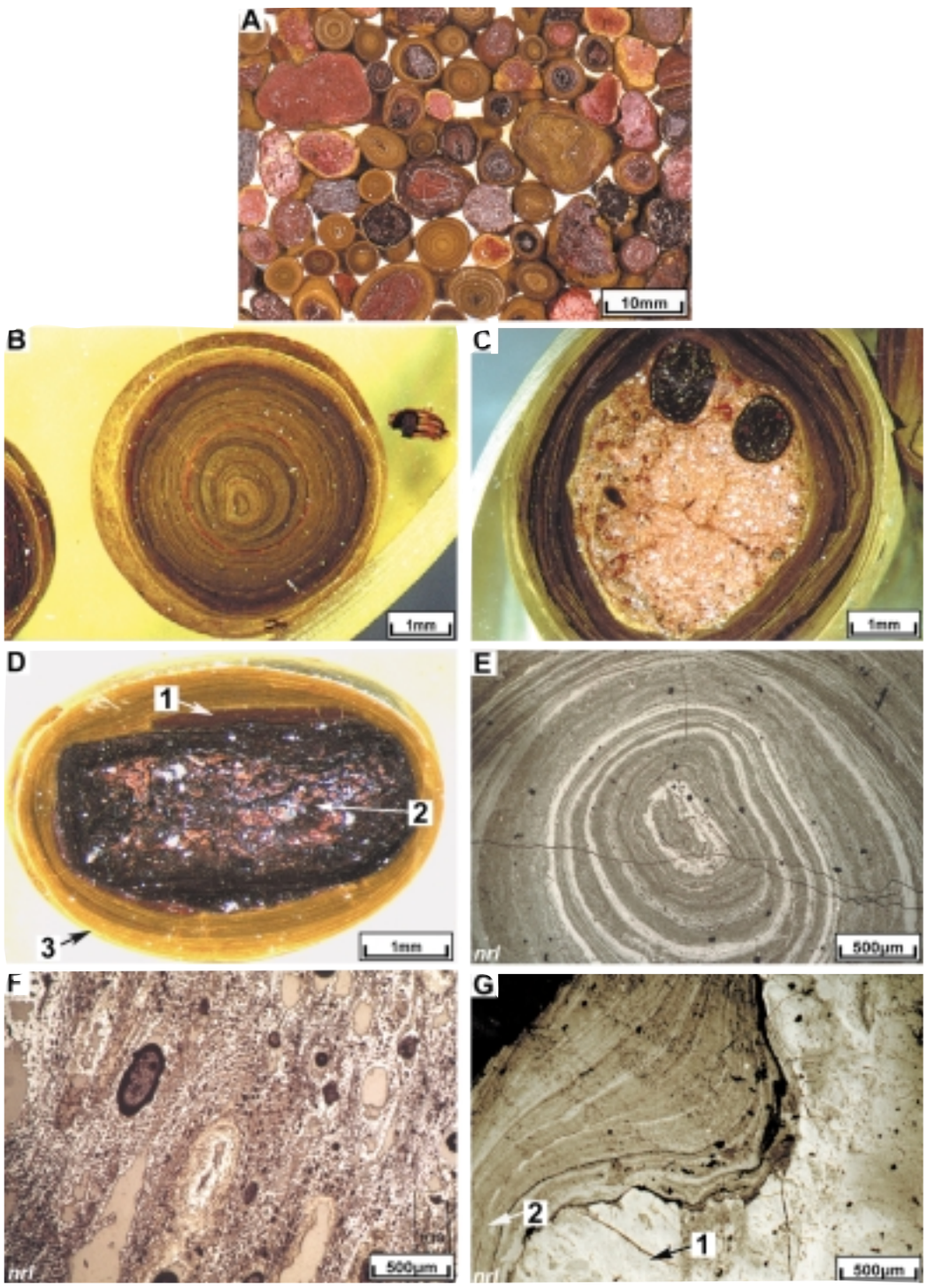

Figure 47 Photographs of pisoliths from palaeochannel sediments. (a) Concentric pisoliths with thick, finely laminated cutans around a variety of nuclei typical of palaeochannel sediments: Paddington (sample 07-0782). (b) Details of pisolith in (a) showing finely laminated cutans: Paddington (sample 07-0782). (c) Concentric pisolith with a compound nucleus and finely laminated cutans from palaeochannel sediments: Sundowner (sample 07-4329). (d) Concentric pisolith showing fragmented and truncated inner cutans (1) around ferruginised lithic nuclei (2) that have been subject to abrasion, encased by goethite-rich concentric cutan accretion (3), indicating a polyphase development: Paddington (sample 07-0782). (e) Photomicrograph of a polished block taken in nrl showing a concentric pisolith with well-developed finely laminated, accretionary cutans: Paddington (sample 07-0782). This type of layering is common in pisoliths developed in palaeochannel sediments. (f) Photomicrograph of a polished block taken in nrl showing a concentric pisolith with a core comprising a hematitic wood fragment: Paddington (sample 07-0782). (g) Photomicrograph of a polished block taken in nrl showing a concentric pisolith with an irregular core (1) surrounded by concentric goethitic cutans (2): Paddington (sample 07-0782). The first few cutans closely follow the small external irregularities of the core, the cutans become more and more regular and circular outwards. Photographs by the authors; nrl, normally reflected light.

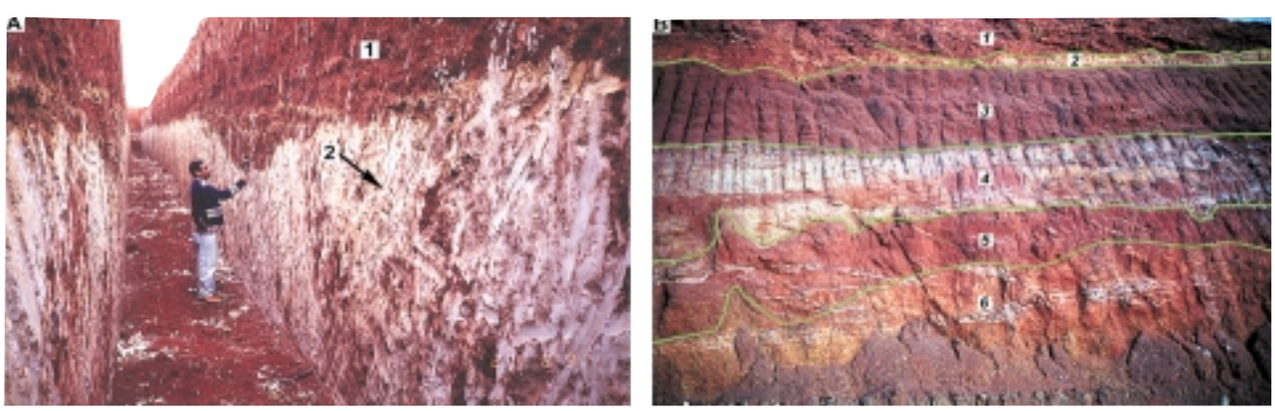

Figure 57 (a) Costean at Black Flag (333000mE, 6618000mN) showing red, massive plastic clays of Group C (1) overlying saprolite (2) (photo by H. M. Churchward). Figure for scale. (b) At Highway deposit, Mt Gibson (514233mE, 6717490mN), sediments comprise silicified (hardpanised) sandy silty colluvium and alluvium of Group D (1), calcrete developed in alluvium (2), massive red clays with lenses of ferruginous granules of Group C (3), slightly mottled palaeochannel clays of Group B (4). Sediments overlie palaeosols (5) and ferruginous nodules and pisoliths (6). Profile is approximately 10 m high (photo by J. E. Wildman).

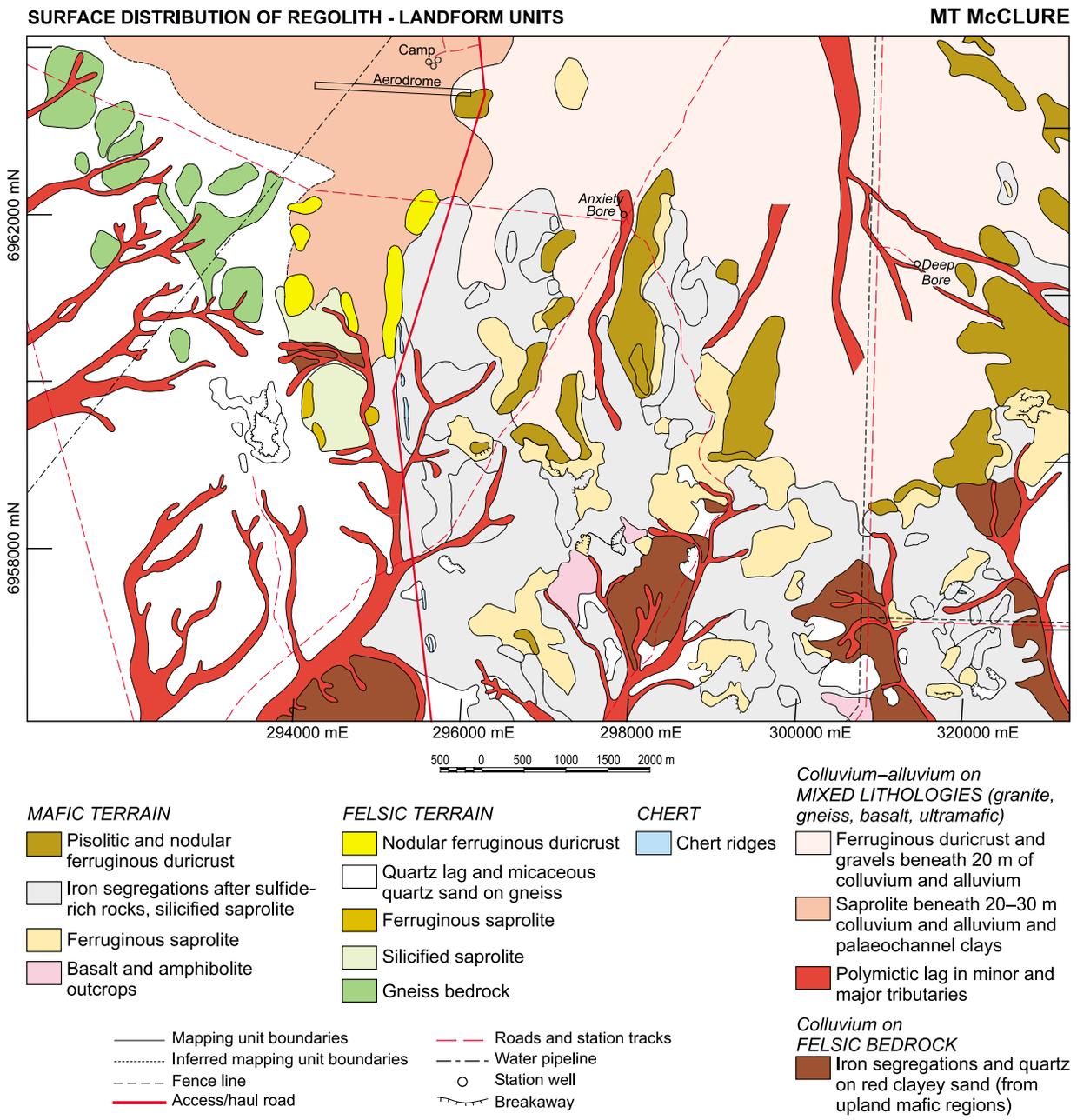

Figure 64 Distribution of ferruginous duricrust and gravel in the Mt McClure district, illustrating that duricrusts are more common on mafic and ultramafic bedrocks than on felsic rocks (after Williamson 1992).

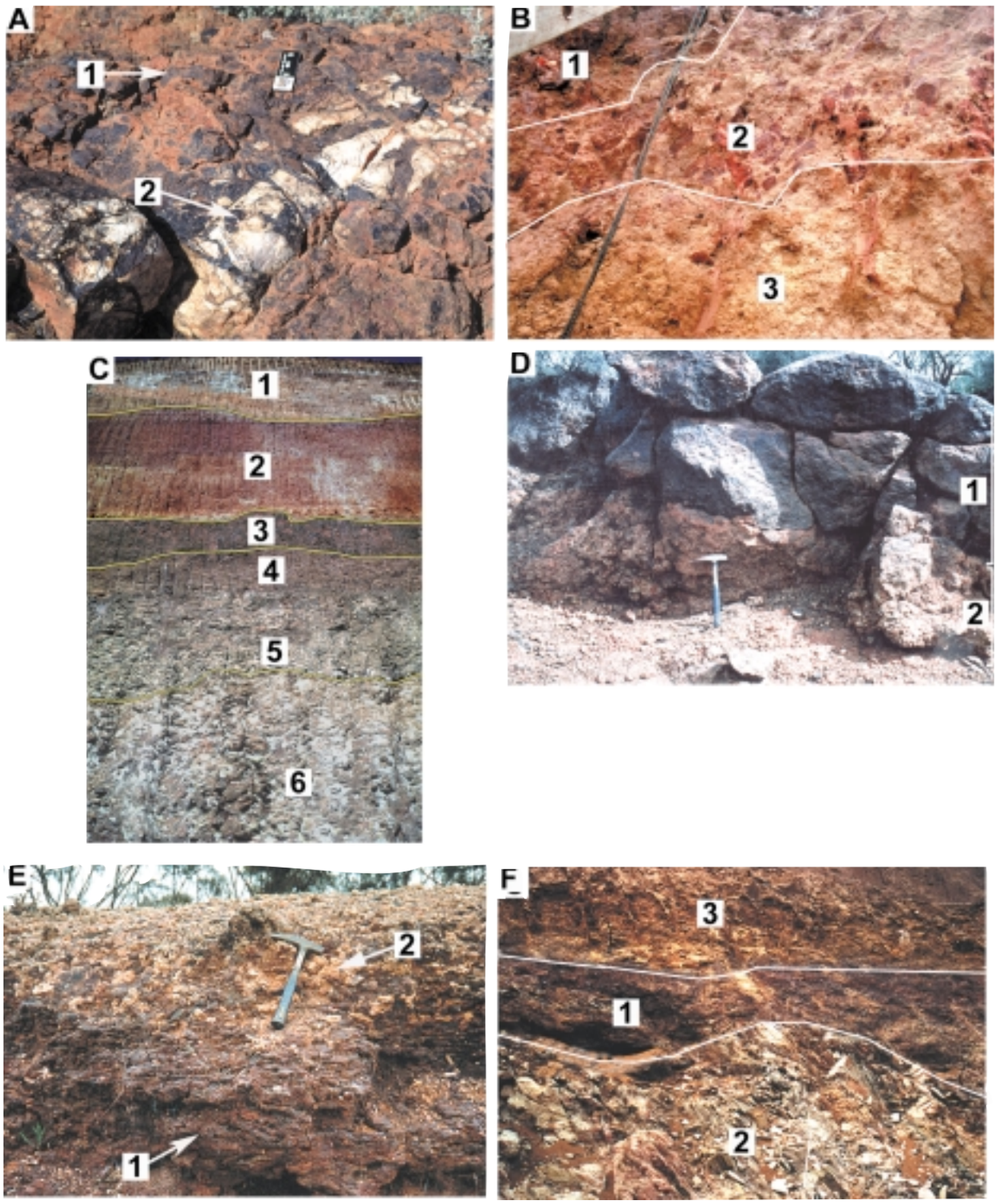

Figure 70 Field photographs of lateritic residuum (a–c) and ferricrete (d–f). (a) Massive ferruginous duricrust (1) on a crest; quartz vein (2) indicates that the duricrust has formed *in situ*: Mt Joel. Scale bar is 5 cm long. (b) Upper part of a profile at Boddington (439000mE, 6377000mN) showing residual massive duricrust (1) overlying fragmental duricrust (2) and bauxite zone (3). Exposure approximately 1 m high (c) Regolith profile showing sediments comprising silicified colluvium and alluvium (1), red palaeochannel clays (2) and ferricrete (3), overlying lateritic residuum (4), collapsed mottled saprolite (5) and mottled saprolite (6): Calista deposit (Mt McClure) 296020mE, 6965000mN. Profile approximately 15 m high. (d) Outcrop of pisolitic ferricrete (1) unconformably overlying mottled saprolite (2) on a crest at Grants Patch (approx. 320000mE, 6630000mN). The ferricrete has a marked pebbly/conglomeratic appearance and the hematite–maghemite-rich clasts are cemented by goethite. Hammer for scale. (e) Outcrop of slabby ferricrete (1) at the edges of a lake at Black Flag (approx. 333000mE, 6618000mN). The upper part of ferricrete is strongly infused with carbonates (2). Hammer for scale. (f) Mine exposure at the Wombat pit (Mt Gibson) (516250mE, 6707470mN) showing pisolitic ferricrete (1) unconformably overlying saprolite (2). The ferricrete is overlain by sand (3). Exposure approximately 1 m high. Photographs by R. R. Anand.

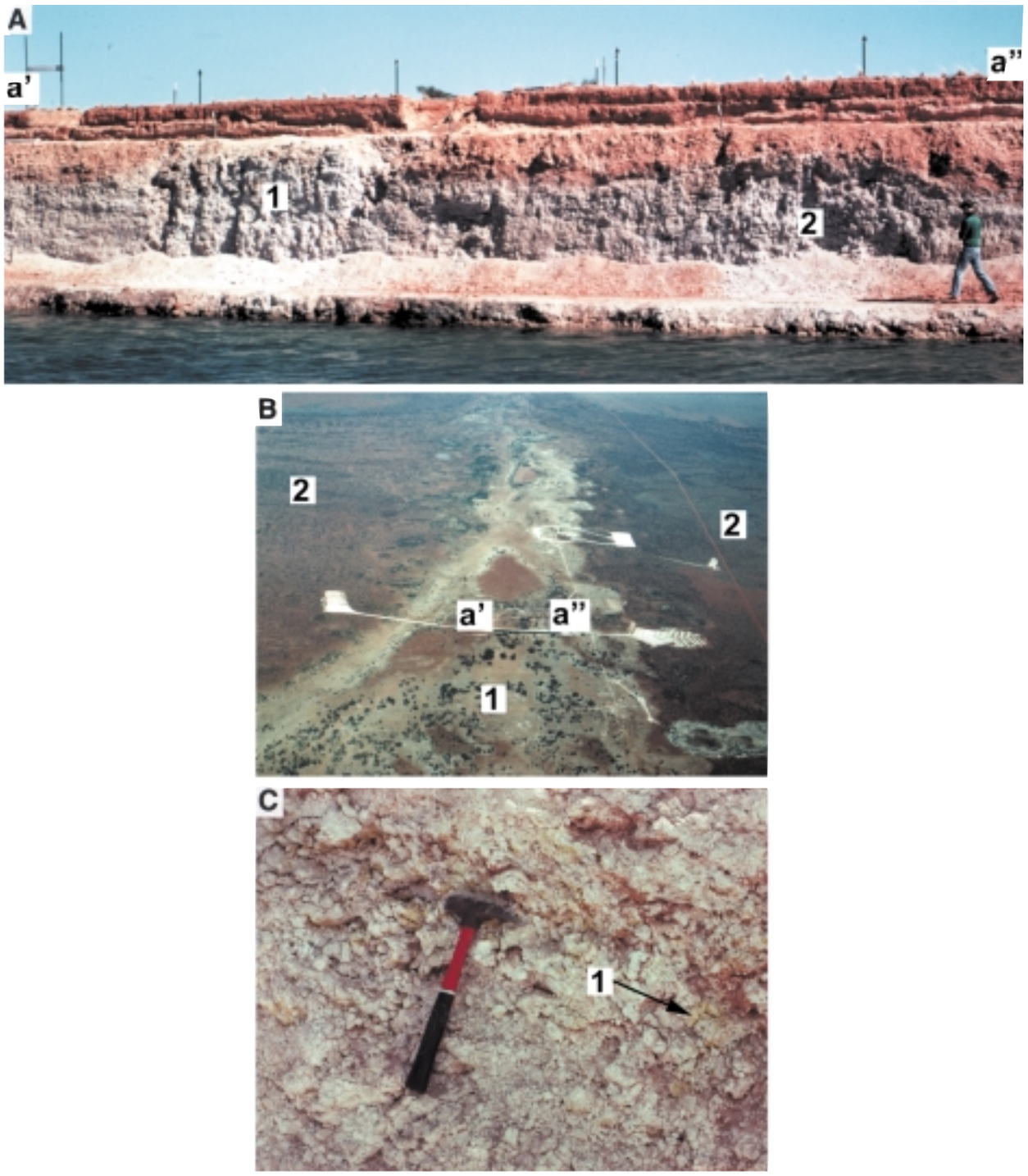

Figure 81 (a) Cross-section a'–a'' through groundwater calcrete and associated deposits (approx. 788000mE, 6990000mN). A diapir (1) and a mound (2) have developed by upward pressure due to active precipitation of carbonate at groundwater level. Figure for scale. (b) Aerial view of the Yeelirrie palaeodrainage with groundwater calcrete (1) surrounded by very gently sloping, red, sandy, alluvial plains (2). Cross-section a'–a'' is indicated as a cutting across the drainage. (c) Detailed photograph of the groundwater calcrete exposed in section a'–a''. The calcrete is porous and white with yellow carnotite mottles (1). Hammer for scale. Photographs by C. R. M. Butt.

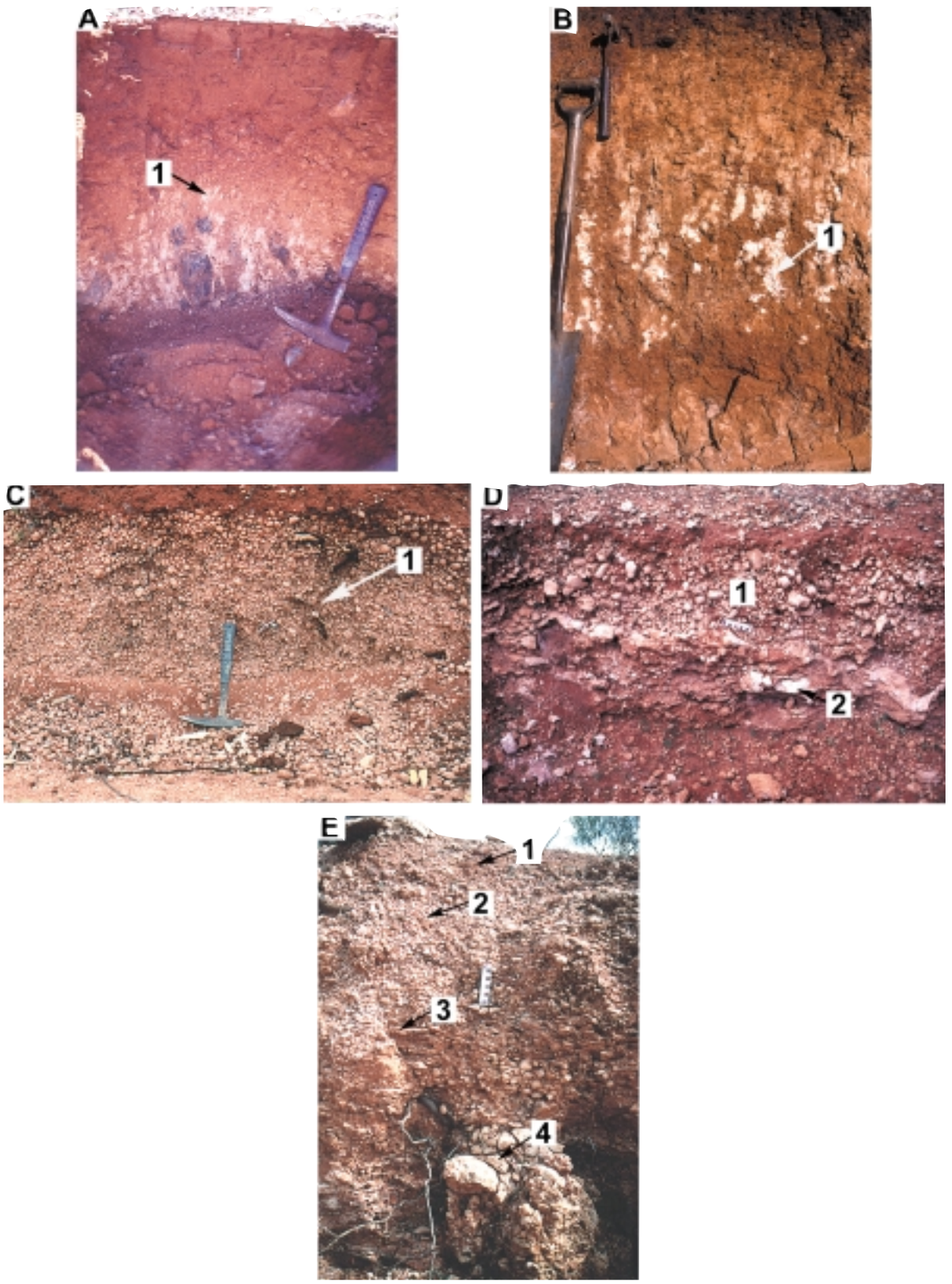

Figure 84 Morphological characteristics of calcrete profiles. (a) Calcrete on fresh gabbro at Menzies (300200mE, 6711800mN) and (b) on mafic saprolite at Mt Gibson (approx. 518000mE, 6712000mN) showing carbonate stringers (1). Hammer for scale. (c) Pisolitic calcrete (1) near Kalgoorlie. Hammer for scale. (d) Nodular calcrete (1) overlying laminated calcrete (2): Federal area, Kalgoorlie (345300mE, 6632800mN). Scale bar [below (1)] is 10 cm long. (e) Thin soil with powdery calcrete and lithoclasts (1) overlies pisolitic calcrete (2) which, in turn, overlies a thin layer of laminated calcrete (3) and brecciated hardpan calcrete (4): near Menzies (approx. 300200mE, 6711800mN). Scale bar is 10 cm long. Photographs by R. R. Anand.

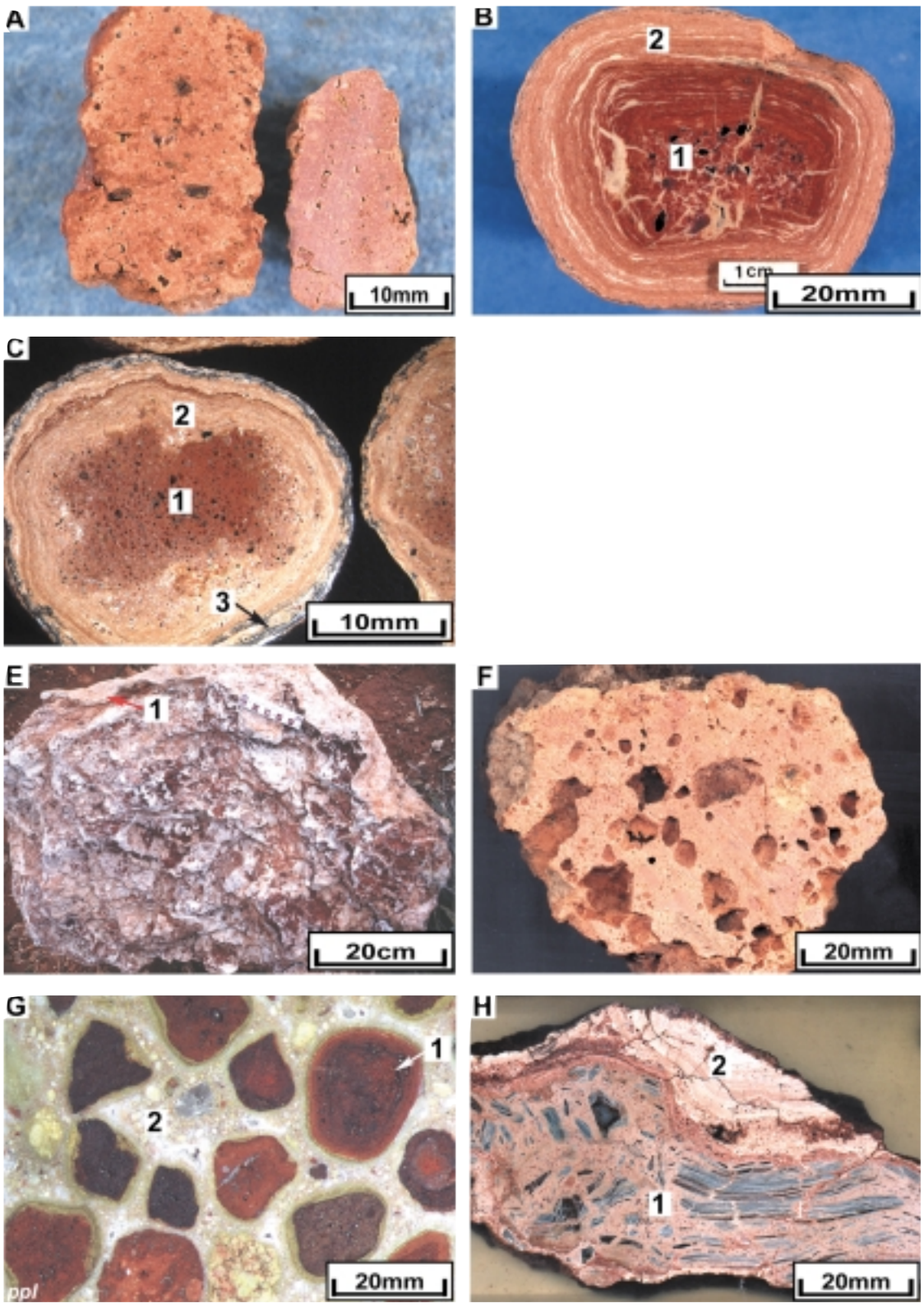

Figure 85 Details of calcrete forms. (a) Nodular calcrete: Mt Gibson. (b) Pisolitic calcrete at Mt Gibson and (c) at Matt Dam has a detrital hematitic core (1) surrounded by multiple cutans of calcite (2) and Mn oxides (3). (d) Laminar calcrete showing the fine-banded laminar zones: Mt Gibson. (e) Platy calcrete (1) encapsulating calcified hardpanised colluvium: Federal pit, Kalgoorlie. (f) Massive calcrete showing abundant voids: Kalgoorlie (specimen: M. Lintern). (g) Photomicrograph of a polished thin-section taken in ppl showing calcified ferruginous duricrust with ferruginous pisoliths (1) in a calcite matrix (2): Mt Gibson. (h) Brecciation of a schistose bedrock by calcite growth (1) and a laminar rind (2): Kalgoorlie (specimen: M. Lintern). Photographs by the authors; ppl, transmitted plane-polarised light.

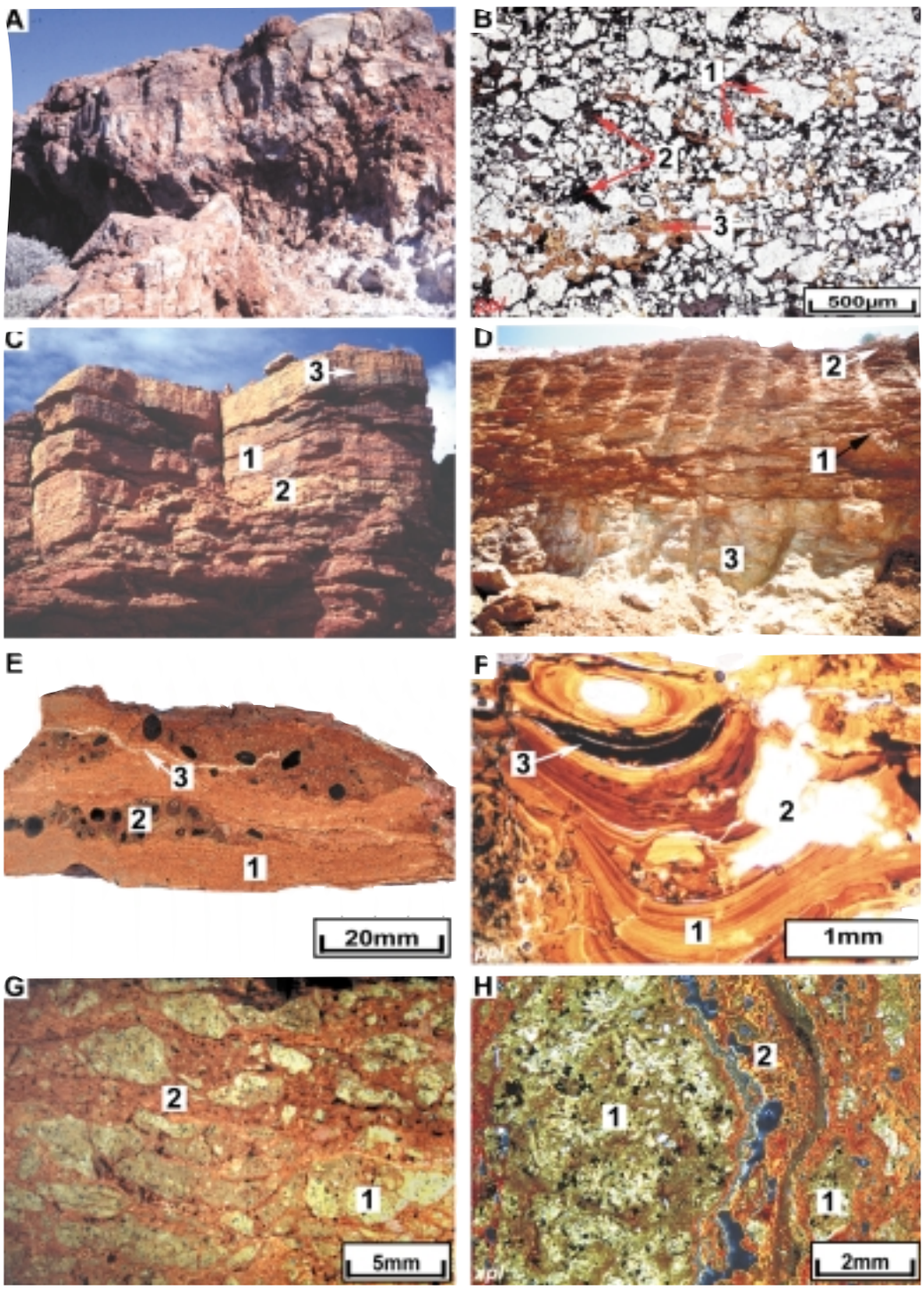

Figure 92 Photographs of silcrete and red-brown hardpan. (a) Massive silcrete, Dam Bore (photo by C. R. M. Butt). Profile is approximately 3 m high. (b) Photomicrograph of a thin-section taken in ppl showing angular quartz grains (1) in a black, quartz, anatase, zircon cement (2) and brown, amorphous aluminosilicates (3): Waterfall (thin-section 4993) (photo by C. R. M. Butt). (c) Red-brown hardpan developed in colluvium (hardpanised colluvium) has well-developed horizontal laminations (1), along which occurs powdery silica (2) and coatings of Mn oxides (3): Empire pit (293750mE, 7033000mN). Profile is approximately 2.5 m high. (d) Red-brown hardpan developed in saprolite, (hardpanised saprolite) (1) overlain by hardpanised colluvium (2); the unsilicified saprolite appears towards the base (3): Gourdis pit (282000mE, 7057000mN). Profile is approximately 3 m high (e) Details of hardpanised colluvium showing laminations (1), detrital ferruginous clasts (2) and carbonate veins (3): Mt Gibson. (f) Photomicrograph of a thin-section taken in ppl showing hardpanised colluvium with clay cutans (1), amorphous silica filling voids (2) and staining of Mn oxides (3): Mt Gibson. (g) Photomicrograph of a thin-section taken in xpl showing hardpanised saprolite with relic saprolite fragments (1) and hardpan matrix (2): Jundee (photo by C. Phang). (h) Photomicrograph of a polished thin-section taken in xpl showing relic saprolite (1) and a mixture of clay cutans and amorphous silica (2): Jundee (photo by C. Phang). Photographs by R. R. Anand unless otherwise specified; xpl, transmitted light with crossed polarisers; ppl, transmitted plane-polarised light.

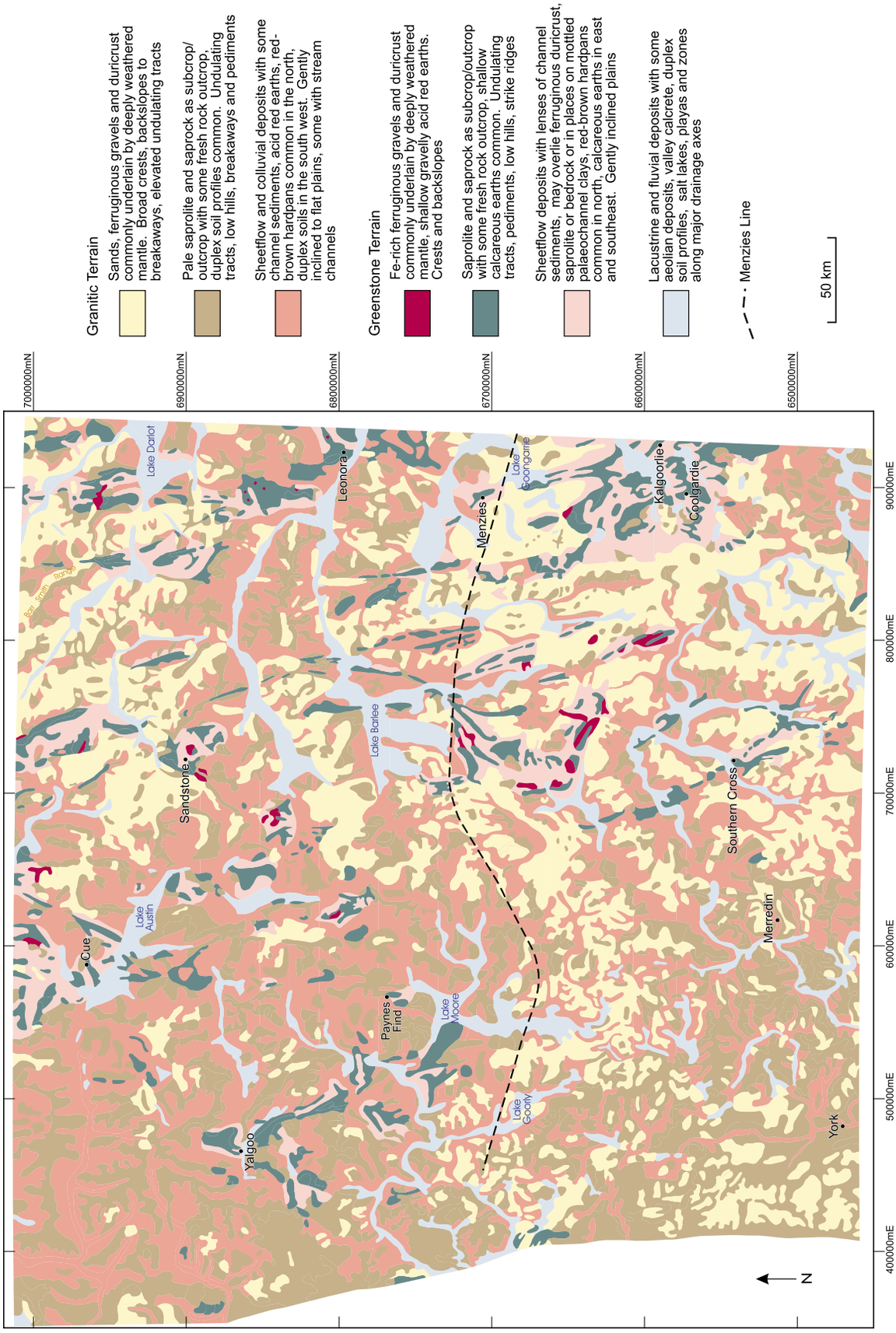

Figure 96 General regional distribution of regolith and landforms, Yilgarn Craton (simplified from Churchward & Anand 2000). The approximate position of the Menzies Line (after Butt *et al.* 1977) is also shown.

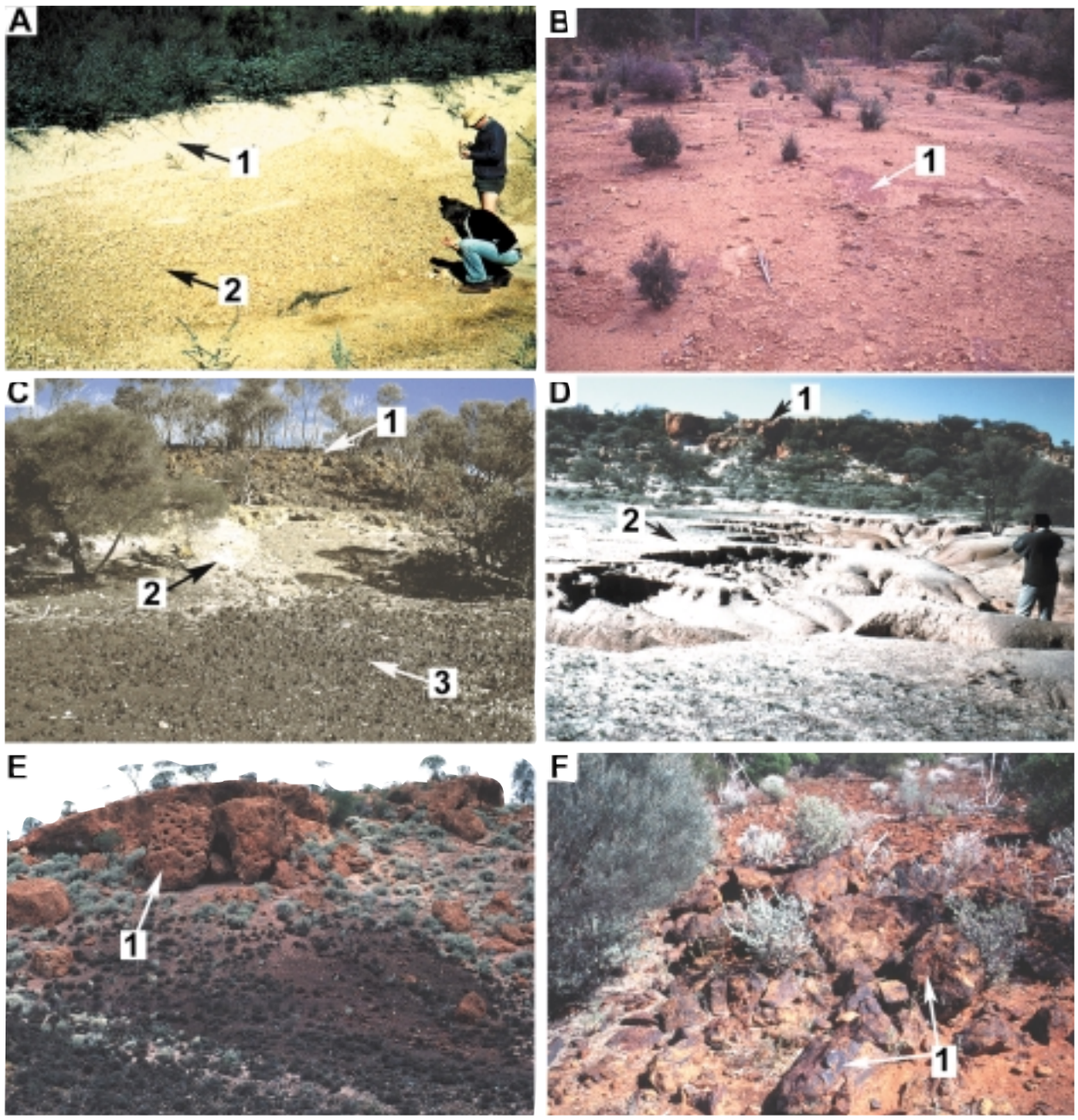

Figure 98 Field photographs of regolith materials and associated landforms. (a) Gravelly sandplains showing sands (1) on ferruginous gravel (2): Mt Gibson (513000mE, 6708000mN). Figures for scale. (b) Ferruginous duricrust (1) forms a continuous sheet on upper slopes at Jarrahdale (approx. 411500mE, 6421000mN). Bush in foreground approximately 0.5 m high. (c) A major breakaway comprising an erosional escarpment showing details of a weathering profile developed on ultramafic rock at Lawlers (260000mE, 6902500mN). Fe-rich duricrust (1) and saprolite (2) occur on face. A coarse lag of duricrust occurs on gently inclined pediments (3). Fe-rich duricrust at (1) is approximately 3 m high. (d) A major breakaway comprising an erosional escarpment showing details of a weathering profile developed on granite at Mt Magnet. The breakaway gives way to a steep debris slope below. Mottled saprolite (1) and saprolite (2) occur on the face. The scarp appears to still be active, indicated by erosional gullies (photo by H. M. Churchward). Figure for scale. (e) A major breakaway comprising an erosional escarpment capped by Fe-saprolite (1) that gives way to a steep debris slope below: Bottle Creek (252500mE, 6772000mN). Fe-saprolite block is approximately 2 m high. (f) Iron segregations after sulfide-rich rocks (1) capping low hills at Jundee (approx. 260000mE, 7078000mN). Fe-segregations shown at (1) are approximately 20 cm wide. Photographs by R. R. Anand unless otherwise specified.

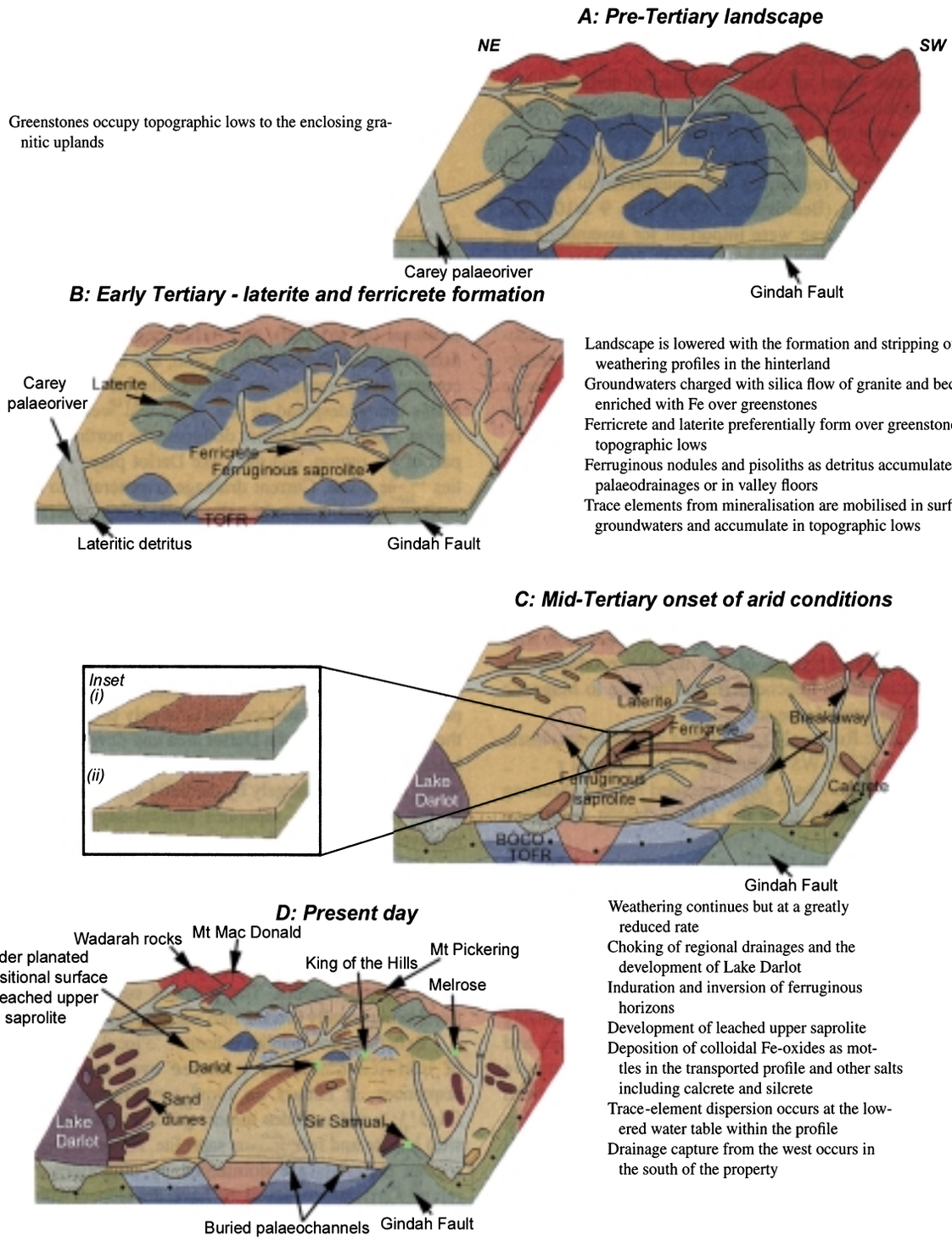

Figure 104 Interpreted history of landform evolution in the Darlot–Centenary region, Yilgarn Craton (after Krcmarov *et al.* 2000). Inset shows the principle of relief inversion (after Ollier 1994), whereby an old valley floor is partially covered with alluvium and colluvium, which is then cemented by Fe-rich groundwaters, thereby becoming more resistant to subsequent erosion and is consequently inverted in the landscape.

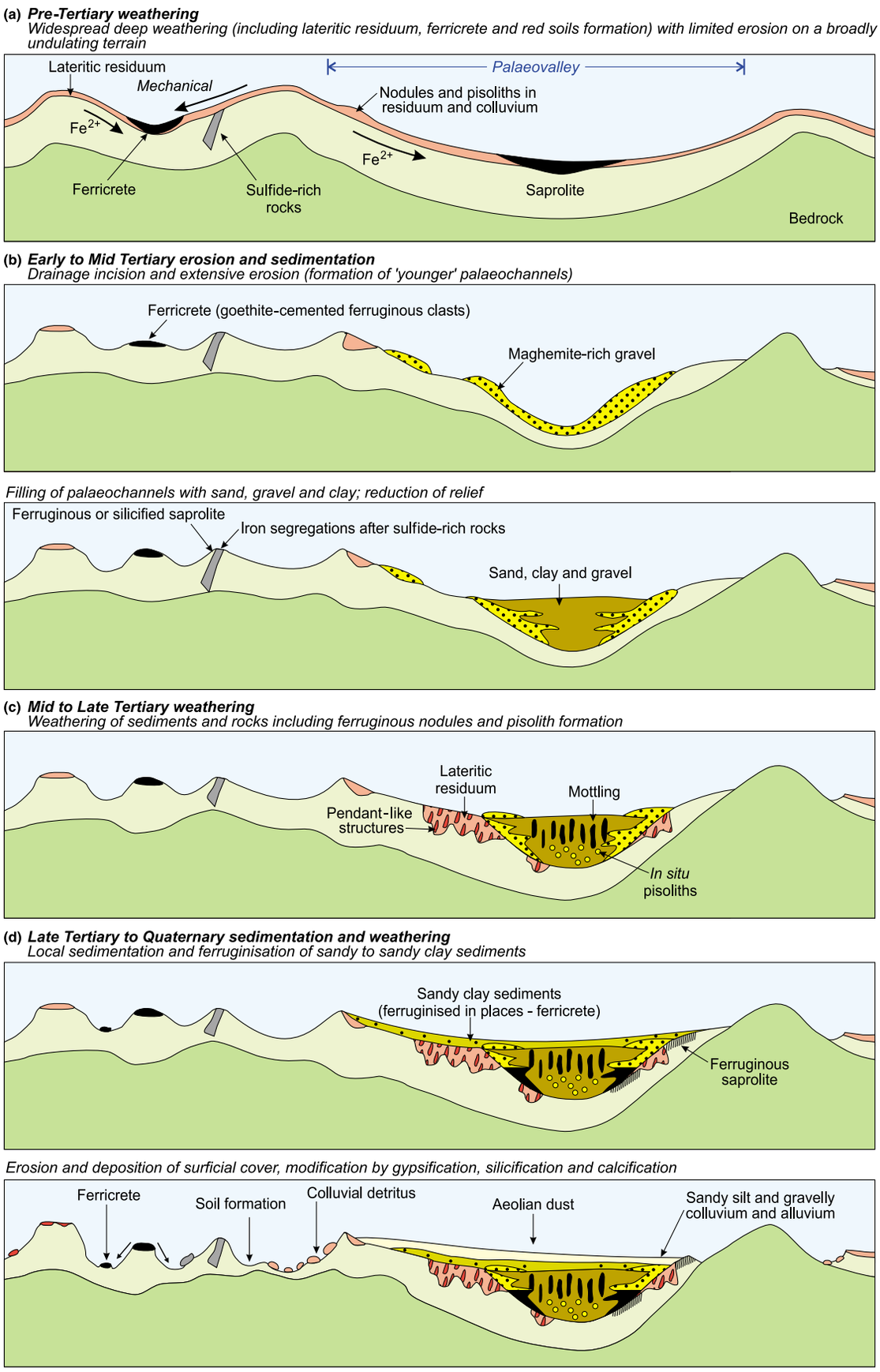

Figure 107 Interpreted regolith–landscape model showing general regolith-forming processes characteristic for parts of the inland Yilgarn Craton. Rates of weathering and erosion were continuous, but their relative importance would have changed over time (see text for details).

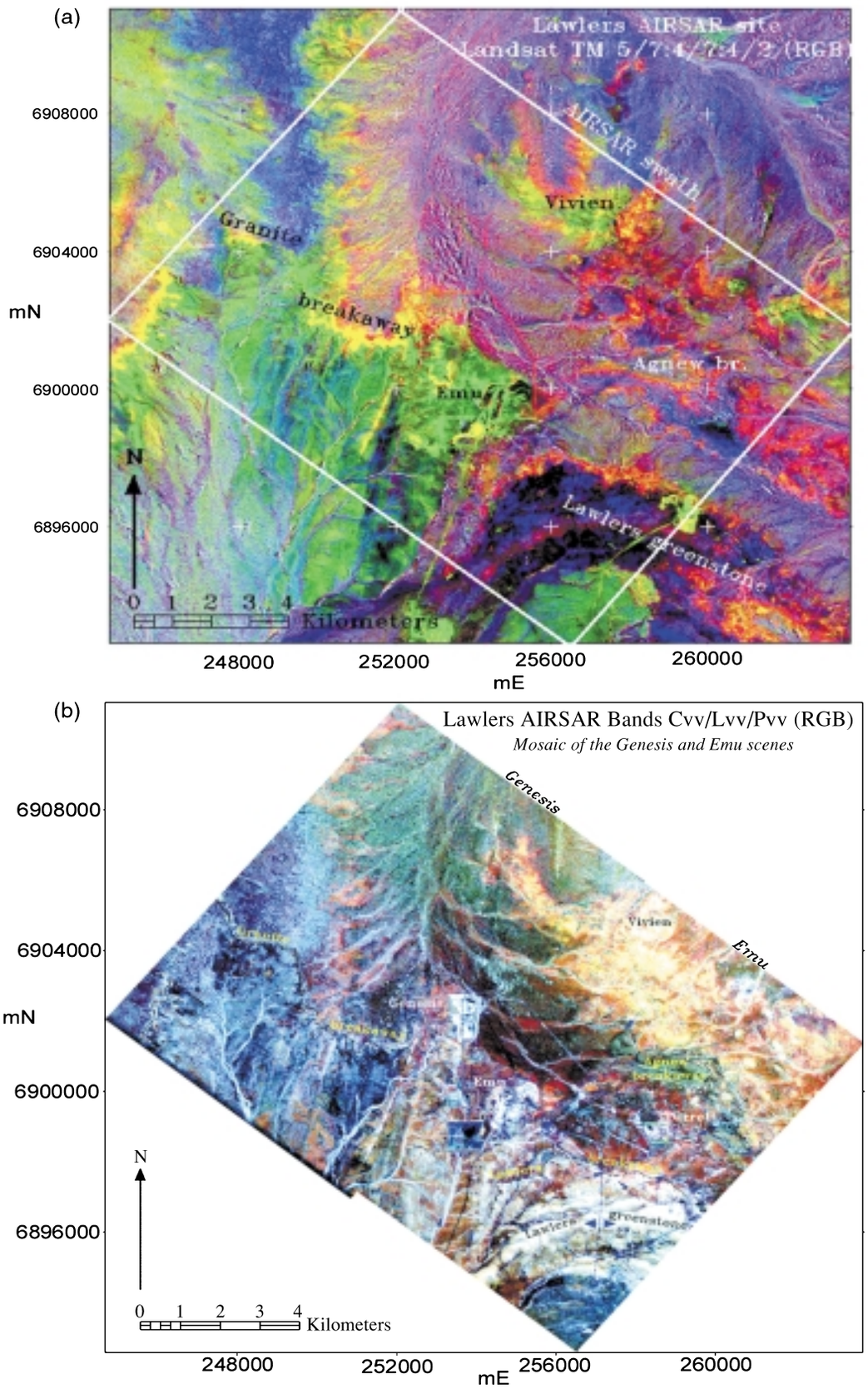

Figure 109 (a) Composite image of Landsat TM band ratios 5/7:4/7:4/2 (RGB) of the Lawlers district demonstrating the capability of these data to highlight spectral subdivision between the surficial materials principal regolith terrains occupying this region (after Tapley 1998). (b) Colour composite image of the Lawlers district comprising AIRSAR bands Cvv/Lvv/Pvv as RGB. The magnitude of radar backscatter is related directly to the abundance and texture of the surface regolith materials (after Tapley 1998).